Signal Processing Methods for Robust Heart Rate Estimation from Multimodal Physiological Signals

by

Shalini A. Rankawat

201121012

A thesis submitted in the partial fulfillment of the requirements for the degree of

DOCTOR OF PHILOSOPHY

in
Information and Communication Technology

to

Dhirubhai Ambani Institute of Information and Communication Technology

Gandhinagar, India

December 2017

Dedicated to my Parents, in-laws and loving family

Declaration

This is to certify that

i) the thesis comprises my original work towards the degree of Doctor of Philosophy in Information and Communication Technology at DA-IICT and has not been submitted elsewhere for a degree.

ii) due acknowledgment has been made in the text to all other material used.

Signature of Student

Shalini A. Rankawat

Certificate

This is to certify that the thesis work entitled "Signal Processing Methods for Robust Heart Rate Estimation from Multimodal Physiological Signals" has been carried out by Shalini A. Rankawat (201121012) for the degree of Doctor of Philosophy in Information and Communication Technology at this Institute under my supervision.

Thesis Supervisor

Prof. Rahul Dubey

Acknowledgements

First of all, I thank almighty God for giving me motivation to undertake the PhD course and providing me strength and perseverance to complete it. I would like to express my sincere gratitude to my supervisor Prof. Rahul Dubey for his advice, guidance, and support throughout the research work and for constant encouragement to complete the research work. I greatly appreciate the freedom and a wonderful working environment provided by him. I also thank my co-guide, Prof. Manjunath V. Joshi for his valuable guidance and suggestions. I am deeply grateful to my Research Progress Seminar Committee members Prof. Deepak Ghodgaonkar, Prof. M. V. Joshi, Prof. Amit Bhatt and Prof. Biswajit Mishra for their valuable suggestions, inputs and giving overall direction to the research work.

I would like to thank present director Prof. K.S Dasgupta and former director Prof. R. Nagaraj, of DA-IICT for providing excellent academic and research facilities in DA-IICT. It is an honour and privilege to study in such an excellent and reputed institute. I wish to thank all the professors of DA-IICT; especially Prof. Prabhat Ranjan, Prof. Chetan Parikh, Prof. Mazad Zaveri, Prof. Aditya Tatu and Prof. Samresh Chatterji for their guidance and help during the course work and research work. I express my gratitude to Prof. Suman K. Mitra, Dean (Academic Programs) for his encouragement and constant support through out my research work.

I thank my colleagues, friends and co-PhD students: Bhavesh Dharmani, Sai Nambiar, Shubham Jain, Nupur Jain, Anshu Chittroda, Ashish Phophalia and Gauri Joshi for technical discussion, suggestions, help and encouragement in completing the thesis. I would also like to thank all the staff of resource centre and help desk for promptly providing me technical research papers, Journals and necessary software whenever required. I would like to thank Mr. Jigar Yagnik and Mr. Jalpesh Pandya for providing necessary administrative information.

I thank Commissionerate of Technical education, Government of Gujarat Gandhinagar for providing me an opportunity to pursue PhD at DA-IICT. I also thank Prof. Chetan Bhatt, Principal and all the faculty members of IC department of Government Engineering College, sector 28, Gandhinagar for their patience and support.

Furthermore, I express my sincere thanks to Dr. S. K. Nigam for sparing his time for technical discussion and invaluable guidance on clinical aspect of the research work. I am

also grateful to Marcus Vollmer for always responding to my e-mails and generously sharing details of his published work. Special thanks to reviewers of my published journal paper for their valuable comments and advice that have shaped the course of this research work.

Finally, I would like to thank my family for being so supportive and helping; my daughters, Mansi for technical discussion and Anushree for bearing all the odds due to my busyness with the research work; my parents Dr. M.L Sharma and Mrs. Veena Sharma for constant encouragement, especially to my father for taking keen interest in the research work; my father in-law Mr. M.P Rankawat and particularly my mother-in-law late Rajrani Rankawat who had always encouraged me to pursue higher studies; my brothers Mr. Ashutosh Sharma, Mr. Anurag Sharma and their families for their understanding, encouragement, and support; my husband Mr. Ashutosh Rankawat has been perhaps the most patient and supportive witness to my academic journey over the past years and I thank him for being there all throughout for constant support and encouragement.

Shalini A.Rankawat

DA-IICT, Gandhinagar

Abstract

Cardiovascular diseases are the major cause of world–wide mortality. Heart rate (HR) and heart rate variability (HRV) are important health parameters to monitor functioning of heart of cardiac patients. Multimodal physiological signals namely; Electrocardiogram, Arterial Blood Pressure, Photoplethysmogram, Electroencephalogram, Electrooculogram, Electromyogram etc. are recorded in ICU for close monitoring of vital health parameters of critically ill patients.

However, Electrocardiogram (ECG), that provides direct measure of heart rate, is often corrupted by noise or is missing and the heart rate estimated from such signals would be erroneous. Thus, there is a need for development of methods for robust heart rate estimation especially when ECG is either noisy or missing. This thesis investigates the development of appropriate signal processing techniques for robust heart rate estimation from fusion of cardiovascular signals with non-cardiovascular (NC) signals that are not related to cardiac activities but contain some markers of heart beats. The signals used in proposed study are ECG, Arterial Blood Pressure (ABP), Electroencephalogram (EEG), Electro-oculogram (EOG) and Electromyogram (EMG).

A novel slope sum function and Teager-Kaiser Energy (SSF-TKE) method is developed for ECG artifacts detection in NC signals. It requires neither additional ECG channel nor a priori user input. Results from evaluation on standard databases have shown that SSF-TKE method is a highly effective technique for R-peak artifacts detection in non-cardiovascular signals contaminated with ECG artifacts.

The use of SSF-TKE method is then explored in R-peak detection in ECG signal. SSF-TKE is a simple method for R-peak detection that does not consider detail morphology of ECG, except steep slopes, amplitude and periodicity of QRS complex. This method has achieved excellent R-peak detection performance across a number of standard databases with variety of signal morphology. Experiments have demonstrated that SSF-TKE algorithm is highly resistance to different types of ECG noises and its beat detection performance is superior to well known QRS detectors, ‘gqrs’ and ‘epltd’ in noisy signals and in ECG signals with pacemaker beats.

A new statistical and rhythm based beat SQI method has been developed for assessment of signal quality of cardiovascular and non-cardiovascular signals. It is based on rhythm of

detected heart beats and probability of the beat being a matched beat. The proposed beat SQI is a simple method of signal quality assessment and it requires only one beat detector. It is shown that signal classification accuracy of beat SQI is better than that of bSQI, a well known SQI assessment method, which requires two independent QRS detectors. Beat SQI works satisfactorily on bradycardia, tachycardia and signals with different types of arrhythmias, except on certain types of arrhythmias like atrial fibrillation, ventricular bigeminy and atrial ectopic. Beat SQI has enabled effective participation of non-cardiovascular signals in the voting fusion process.

A novel voting fusion method is presented for robust heart beat detection and heart rate estimation from fusion of multimodal physiological signals i.e. cardiovascular signals and non-cardiovascular signals. The proposed fusion method is based on weighting the beats from each signal according to the corresponding SQI of the beats, assessed by the beat SQI method. The evaluation results of beat SQI based majority fusion method for robust heart beat detection on different standard databases are presented and compared with other methods. The results show that fusion improves overall score of beat detection as compared to that achieved by individual well known detectors. The proposed algorithm for beat detection has also been evaluated on PhysioNet/CinC Challenge 2014 hidden test dataset by submitting it in PhysioNet web server and presently the algorithm ranks fifth in results from the 2014 challenge.

The beat SQI based voting fusion method has been evaluated on standard databases for robust heart rate estimation from fusion of multimodal signals. The fusion method provides a significantly better estimate of heart rate than heart rate estimate derived from a single signal. The proposed method has been validated on concurrent noisy cardiovascular signals (ECG and ABP) of a synthetic noise dataset, generated by adding different types of calibrated noise in clean signals, to assess participation of non-cardiovascular signals in majority voting fusion for robust heart beat as well as heart rate estimation. The results on noise evaluation dataset show that proposed voting fusion method has significantly improved accuracy of heart rate estimate as compared to that obtained from single cardiovascular signal, even when both ECG and ABP signals are extremely noisy concurrently. It demonstrates effective participation of non-cardiovascular signals in voting fusion for robust heart rate estimation and NC signals have increased robustness of the system.

The proposed algorithm has been implemented on Raspberry Pi 3 and its computation time is 75 times faster than the required constraints for real time applications. The asymptotic runtime complexity analysis of our algorithm is O(N), where 'N' is the number of samples in the signal.

Contents

List of Figures

List of Tables

Chapter 1

Introduction

According to the World Health Organization (WHO), cardiovascular diseases are the leading cause of world-wide mortality representing about 31% of all global deaths in 2012. More than 40% of these deaths were premature i.e. under the age of 70 years [1]. Cardiovascular diseases have been identified as one of the major challenges of 21stcentury for health care and related diagnostic developments. WHO has set a global target of 25% reduction in overall mortality due to cardiovascular diseases, cancer, diabetes or chronic respiratory diseases by 2025. Hence, prevention and control of cardiovascular diseases has been accorded top priority by WHO.

Researchers world over have given significant importance to work in the field of cardiac health with strong focus on improving signal analysis techniques for cardiovascular diagnostics. In such studies, heart rate (HR) and heart rate variability (HRV) play an important role. HR and HRV may contain indicators of many cardiovascular and non-cardiovascular diseases namely, myocardial infarction, myocardial dysfunction, diabetic neuropathy, liver cirrhosis, sepsis etc. [2]. Hence, accurate estimation of HR is important requirement for patient's overall health monitoring. Robust sensor fusion of multimodal physiological signals improves heart rate estimation in clinical evaluation [3]. The present thesis is an attempt in this direction and objective of our study is to develop techniques for robust heart rate estimation from multimodal physiological signals by fusion of cardiovascular and non-cardiovascular signals.

1.1 Overview

Intelligent bed side monitors in ICU simultaneously record multimodal physiological signals namely; Electrocardiogram (ECG), Arterial Blood Pressure (ABP), Photoplethysmogram (PPG), Electroencephalogram (EEG), Electrooculogram (EOG), Electromyogram (EMG) etc. for close monitoring of vital health parameters of critically ill patients. Cardiovascular signals

(ECG, ABP and PPG) are directly related to cardiac activity and are normally used to detect heart beats. Heart rate is one of the most important health parameters, which can be estimated directly from ECG [4]. Non-cardiovascular signals are not directly related to cardiac activity; EEG, EOG and EMG are some of the non-cardiovascular signals.

The problem, however, is that ECG recorded in intensive care unit (ICU) is often missing or corrupted by intrinsic systematic noises like power line interference, baseline wander etc. and random noises caused by motion, muscle contractions, sweating, misplaced electrodes, and power failure that affects the detection of QRS complexes [5]. This leads to large errors in the estimation of heart rate [6, 7]. Pacemaker artifacts can also introduce large errors in the automatic estimation of heart rate [8]. If relatively high level of noise is present in the ECG signal, it will provide incorrect estimation of HR and errors in HRV analysis. In such cases, there may be large number of false alarms from ICU monitor that may reduce alertness level of clinical staff to real alarms affecting patient's overall care [9-12].

Other pulsatile cardiovascular signals that directly reflect cardiac activity, such as ABP and PPG, can also provide redundant and independent measures of HR with certain limitations [13-16]. Non-cardiovascular signals like EEG, EOG and EMG are though not directly related to cardiac activity, but are usually contaminated by ECG artifacts [17-19] as can be seen in Figure 1.1. All these signals contain HR information and it's detection from physiological signals other than ECG has been carried out by many researchers. The physiological signals containing markers of heart beats can be used for HR estimation, especially when ECG is noisy or missing, because various sources of measurement errors do not affect multimodal signals in the same way. For example, sweating affects ECG measurement but the quality of the BP signal measurement does not depend on it. The great advantage of using multimodal signals is that noise and artifacts that disrupt ECG may not influence other signals and hence different multimodal signals can be considered to be independent to a certain extent [3].

Robust HR estimation is essential for monitoring of ICU patients [20]. Medical practioners cannot rely on monitor's estimates without visual confirmation due to presence of noise and artifacts in signals. Researchers have used various techniques such as averaging [7], machine learning [21], Kalman filtering [3, 22-24] and signal quality assessment [6, 25-27] to improve upon the estimates of parameters derived from noisy physiological signals. Averaging methods smooth out true physiological changes and can also reduce the transient artifacts. Machine learning techniques detect artifacts efficiently, but it requires large amounts of physiological data to train the model. Kalman filter (KF) methods reliably detect abrupt changes and artifacts from physiological signals. Signal quality assessment methods provide an improved estimate of parameters identified from the recorded data.

This problem of inaccurate data from noisy signals can be handled by combining inputs

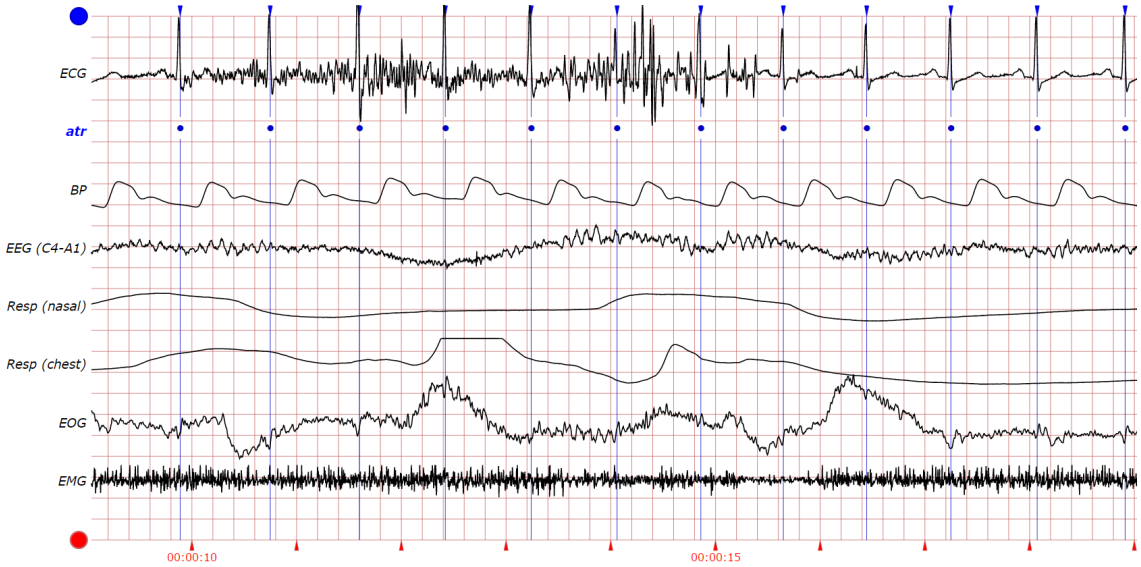

Figure 1.1: ECG artifacts in NC signals
(Source: Record no. 112 of PhysioNet/CinC 2014 training dataset)

from multiple independent sources [28]. Data fusion techniques combine data from multiple sensors and related information from associated databases to achieve improved accuracy and more specific inferences as compared to those from a single sensor [29]. The purpose of using data fusion in multi-sensor environments is to obtain a lower detection error probability and a higher reliability. The data fusion techniques can be classified into three categories: (i) data association, (ii) state estimation, and (iii) decision fusion [30]. Decision-level sensor fusion combines the detection results instead of raw data of different sensors and is most suitable when we have different types of sensors [31]. Naive Bayes method, Dempster-Shafer theory, fuzzy probabilities, rule-based method, and voting techniques are some of the applied fusion methods [32].

In the present study a decision-level sensor fusion technique based on majority voting fusion has been proposed where redundant HR information in NC signals is being used to improve the accuracy of HR estimation. The advantage of multimodal sensor fusion is that it can provide robust health parameter estimates even when data from only one signal is relatively noise free. We have observed that the fusion of cardiovascular with non-cardiovascular signals improves the accuracy of physiological parameters. The non-cardiovascular signals can fill in the gap of heartbeats when ECG and ABP signals are noisy. The fusion of sensor data has following advantages [33]:

1. Robustness and reliability: Redundancy in multiple sensors enables the system to provide reliable information even when one sensor is relatively noise free.

2. Extended spatial and temporal coverage: If measurement from one sensor is missing over a period of time then the information from the others can be utilized.

3. Increased confidence: Estimate of a parameter provided by one sensor can be confirmed by estimates of other sensors.

4. Reduced ambiguity and uncertainty: Ambiguous interpretation of measured parameter is reduced by fused estimate.

5. Robustness against interference: The system becomes less susceptible against noise and artifacts by increasing the mode of measurements of parameter.

6. Improved accuracy: Fusion of multiple independent measurements of a parameter provides better accuracy than from a single sensor.

Nevertheless, sensor fusion has certain limitations:

1. Quality of input data: The effectiveness of multi-sensor concept depends on quality of input data. If a lot of poor quality data is fused, it may not produce good quality output and may even reduce the quality of the output.

2. Extra equipment: Fusion requires more than one sensor, which increases effective cost of the system.

3. Time delays: If quality of input data is poor, fusion process introduces unnecessary time delays without any gain in the quality of output and confidence.

It has been theoretically proved that sensor fusion in specific cases for majority vote and maximum likelihood theory in decision fusion improves the performance [34]. The study by Dasarathy showed that performance gain or loss by increasing the number of inputs in a sensor fusion process depends on the sensor fusion algorithm [35, 36].

We have proposed a decision sensor fusion model based on majority voting fusion of cardiovascular and non-cardiovascular signals for robust heart rate estimation [37]. Fusion of multimodal physiological signals has increased redundancy and reliability of the system. Since, the measurement sensors are multimodal; it provides robustness against noise/interference in voting fusion. The major limitation of sensor fusion is degradation of output due to poor quality of input sensor data. This limitation has been taken care of in our study by assigning proper weights to the input data based on quality of the signal and its reliability. We have developed an algorithm based on beat SQI for signal quality index assessment that has improved the performance of the algorithm. Since, ICU monitor simultaneously records multiple physiological signals for clinical analysis purpose, and the same have been used for robust heart

rate estimation in our study, hence no extra equipment is required . Majority voting fusion method is simple and has low computational load.

There are two major steps in HR estimation. The first step is heart beat detection and second HR estimation. Cardiac activities generate strong electric field, which introduce ECG (R-peak) artifacts in NC signals. The quantum of ECG artifacts depends on the proximity of recording sensors to the heart and these artifacts may also occur inconsistently [38]. ECG artifacts pose problems in clinical interpretation and analysis of non-cardiovascular signals, which reduce their usefulness. ECG artifact removal from EEG, EOG and EMG is, therefore, one of the prominent areas of research in Biomedical Engineering. Automatic detection methods have been proposed in earlier studies. The ensemble average subtraction (EAS) method [39], independent component analysis (ICA), and adaptive noise canceling theory [40] have been developed to eliminate ECG artifacts for which an additional reference ECG channel is required [41].

We have developed a novel algorithm using Slope Sum Function (SSF) and Teager-Kaiser Energy (TKE) operator (SSF-TKE) for R-peak artifacts detection in NC signals [42]. This method is simple and does not require an additional reference ECG channel as is the case in previous studies. The algorithm has used redundant information of heart beat markers as ECG artifacts in NC signals for HR estimation. It was observed from the recordings of NC signals that ECG artifacts are present like periodic quasi-spikes with diminished amplitude. ECG artifact in NC signal is one type of noise which is of interest and is to be detected for HR estimation, but other noises present in the signal have to be removed. This has been done using Butterworth band-pass filter of first order of appropriate frequency range. The mathematical operator SSF distinguishes the true ECG artifact spikes while TKE enhances them for efficient detection using adaptive threshold.

This study on R-peak artifacts detection differs from the previous works in the sense that we have utilized the detected artifacts to fill the gaps when ECG signal is either noisy or missing. It has helped us in robust estimation of heart rate. The SSF-TKE algorithm has also been extended with some modifications for R-peak detection using morphological features of QRS complex of ECG waveform. There are various techniques available for R-peak detection like empirical mode decomposition (EMD), Hilbert transform, Wavelets Transform, Artificial neural network etc. [43]. All these techniques have certain limitations that have been discussed in chapter 4. After beat detection, it is necessary to find out signal quality of the beats because false beats may degrade the quality of outcome of fusion.

Signal quality is important for accurate assessment of health parameters extracted from physiological signals for clinical decisions. Fusion of detected heart beats from noisy signals with those from clean signals may degrade the quality of fused heart beats. Hence, correct

assessment of SQI is essential for efficient fusion of physiological signals. ECG and ABP signals are quite often corrupted by noise or may be missing. The R-peak artifacts in NC signals may also occur intermittently. It is essential to develop beat SQI rather than overall signal quality index for selection of clean parts of the signal with prominently detected true beats, excluding its noisy parts, for fusion. A statistical, probability and rhythm based beat SQI assessment technique is being proposed in this study [37]. A simple and rational approach has been used based on beat rhythm of the signal immediately preceding the beat and on the probability of the beat being matched or unmatched with respect to reference beat annotation.

Intensive care unit patients generally suffer from irregular heartbeats known as cardiac arrhythmia. The heart beats in arrhythmia can be irregular, too fast, or too slow. It is essential that the SQI should be able to correctly classify the ECG with different types of arrhythmias for accurate HR estimation. It has been observed that the performance of our beat SQI on arrhythmia signals is better than that of standard signal quality metric bSQI in classification of quality of signals. The novel probability and rhythm based beat SQI method is simple and assesses quality of signal without the need of an additional detector. A new beat SQI based majority voting fusion method for robust heart beat detection has also been proposed for fusion of heartbeats from cardiovascular and NC signals [37]. The fusion of NC signals with cardiovascular signals has improved the accuracy of HR estimation in records with noisy ECG or both noisy ECG and ABP signals.

The presence of noise in the ECG caused by power line interference, base line wander, movement, muscle contractions, sweating etc. seriously affects detection of QRS complexes. We have evaluated our algorithm on MIT-BIH noise stress test database containing signals with varying signal to noise ratio (SNR) from -6 to 24 dB. The proposed algorithm has also been experimentally validated on artificially corrupted synthetic noise dataset created by adding different types of noises in clean ECG and ABP signals. Baseline wander ('bw'), muscle artifact ('ma'), and electrode motion artifact ('em') noises of different SNR levels are added to clean ECG signal of record no. 123 of Physionet/CinC Challenge 2014 training dataset. MIT-BIH noise stress test database and UNIX shell script for generating sample noise stress test records (nstdbgen) are used for generating the 'bw', 'em' and 'ma' types of noise models in ECG. Six types of ABP noises; saturation to ABP maximum artifact (a_{smax}), saturation to ABP minimum artifact (a_{smin}), Linear attenuation to BP mean (a_{lamean}), square wave artifact (a_{sw}), high frequency artifact (a_{hf}) and Sinc function impulse artifact (a_{imp}) of different SNR levels have been separately added to clean ABP signal of record no. 123 of Physionet/CinC Challenge 2014 training dataset using Matlab source code. The synthetic noise evaluation dataset has been created to assess the contribution of NC signals in robust HR estimation. Noises have been added beginning after the first 2 minutes of each record, during

two-minute segments alternating with two-minute clean segments. The SNR during the noisy segments was set to a value of 12, 9, 6, 3, 0, -3, -6, -9, -12 dB separately, generating 162 noisy signals. The performance of majority voting fusion algorithm is excellent even when both ECG and ABP are noisy, which demonstrates participation of NC signals in voting fusion.

Finally, the algorithm has been tested on Raspberry Pi to see if it can be implemented for real time applications. It has been found that the computation time achieved by our algorithm is 72 to 138 times faster than the required constraints for real time applications depending upon the no. of signals in the record.

We have carried out this physiological signal processing study using several databases like PhysioNet/CinC Challenge 2011 training set-a, PhysioNet/CinC Challenge 2014 public training dataset, PhysioNet/CinC Challenge 2014 test dataset, MIT-BIH Arrhythmia database, MIT-BIH polysomnographic database, MIT-BIH noise stress test database and MGH-MF waveform database. All the databases have been discussed in section 2.9.

1.2 Motivation for the work

It has already been stated that cardiovascular diseases are one of the major global health challenges. It is observed that the last three decades have seen extensive research activities in the field to combat the menace of such diseases through improved diagnostic techniques and related patient care. This has motivated us to undertake research work in the field of cardiovascular health monitoring. The health parameters of critically ill patients are monitored by bedside monitors in ICU. Missing or noisy ECG signals give incorrect HR estimate that may lead to wrong clinical decisions. Sometimes the support staff too, due to false alarm caused by noise or motion artifacts in the monitoring unit, becomes insensitive to true alarms and that may be fatal to the patients [20]. Hence, reliable beat detection and HR estimation is a necessary prerequisite for accurate monitoring of HRV.

In some of the recent studies, it has been pointed out that ECG R-peaks are present as artifacts in non-cardiovascular signals (EEG, EOG and EMG) and as such they can be used for the beat detection especially, when more reliable cardiovascular signals i.e., ECG and ABP are missing or noisy. We observed that ECG artifacts are clearly visible in some NC signals but in other records they are obscured or absent. Hence, detection of ECG artifacts in EEG, EOG and EMG signals is very challenging. We have been motivated to work on ECG artifact detection from non-cardiovascular signals. A new algorithm has been developed for detection of R-peak artifacts. Recently, the focus of research has shifted towards development of fast and efficient algorithms for beat detection in ECG and determination of quality of ECG signal for portable devices. Since, the results of our algorithm in artifact detection in NC signals

were encouraging, we implemented the same algorithm with some modifications for R-peaks detection in ECG. We have also developed an algorithm for determining the quality of ECG signals.

Cardiovascular signals i.e. ECG and ABP may be corrupted by noise. In NC signals also ECG artifacts may be entirely absent or even when they are present their presence may be inconsistent. Therefore the presence of R-peak in ECG and ECG artifacts in NC signals is an important criterion for determining the signal quality for the purpose of HR estimation. It is essential that only good quality signals are fused together to get accurate and robust heart rate. There are several standard signal quality metrics to find ECG signal quality but most of them are based on the principle of agreement level between two independent detectors. To assess signal quality of NC signals, generally containing obscured R-peak artifacts, was another challenging task. We have addressed the challenge by developing statistical and probabilistic based beat SQI method that works on single detector.

In previous research studies, it was found that fusion of multiple sensors with redundant heart rate information can be used to improve the heart rate. Taking clue from all these studies, we were motivated to work on fusion of non-cardiovascular (NC) signals with cardiovascular for robust heart rate estimation to reduce the number of false and missed alarms for ICU patients.

1.3 Scope and accomplishment of research work

This thesis explores signal processing methods to improve HR estimation from fusion of multimodal physiological signals. The study considers signal extraction, removal of errors introduced at each processing stage and fusion of cardiovascular signals with NC signals. The majority voting fusion method has yielded HR estimates in clinical situations when both ECG and ABP are noisy. The main objective of the thesis is to obtain robust heart rate estimation from fusion of cardiovascular signals (ECG and ABP) with non-cardiovascular signals (EEG, EOG and EMG). To achieve this goal, new indigenous algorithms have been developed for beat detection, beat signal quality index and majority voting fusion.

Although there are many published works related to the task of deriving HR from fusion of cardiovascular signals specifically from ECG, ABP and PPG, mentioned in chapter 7. HR estimation from fusion of cardiovascular and non-cardiovascular signals is yet an unexplored area. Another objective of this study is to develop a method for combining beats obtained from multiple signals using majority voting fusion technique to get a more accurate estimate of heart rate than that is available from any individual signal.

We have also validated our algorithm experimentally on a synthetic noise dataset generated

by adding different types of calibrated noises in clean ECG and ABP signals. The performance of the algorithms on such a dataset has shown that the inclusion of NC signals in fusion gives accurate results for HR estimation even in the worst scenario, when both ECG and ABP are noisy. This establishes the robustness of our algorithm.

1.3.1 Related work constraints

From the existing literature survey on beat detection, signal quality index and fusion for HR estimation, we have observed following constraints in the existing studies:

1. Most of the previous studies on robust heart rate estimation are based on fusion of multiple signals, but they have used only cardiovascular signals; that too ECG and ABP signals. It has been observed that sometimes both ECG and ABP signals are simultaneously noisy and HR estimation in such cases would be erroneous.

2. There are very few existing studies that have used multimodal signals i.e., NC signals along with cardiovascular signals for robust heart beat detection. But they have not extended their studies to robust HR estimation.

3. One study on robust heart beat detectiom has used adaptive filter for detection of R-peak artifacts in EEG signal, which required an additional ECG signal. In other studies, initial annotations obtained from cardiovascular signals were used to train EEG and EOG detector. Hence, these methods heavily depended on availability of ECG signal.

4. Most of the existing techniques of R-peak artifact detection in NC signals have one or all of the following limitations: requirement of a priori user input, real time implementation and more than one channel to operate.

5. To the best of our knowledge, one of the studies on robust HR estimation from cardiovascular signals has used bSQI; but bSQI requires two independent detectors for SQI assessment.

6. The previous studies on fusion of cardiovascular and NC signals for robust heart beat detection have not used beat SQI. One of the studies has used overall signal quality, that too for selection/rejection of the entire signal for voting fusion; whereas other studies have used window wise average for fusion. The R-peak artifacts may be present inconsistently in NC signals; hence beat SQI is essential for effective participation of NC signals in fusion for robust HR estimation.

7. Most of the fusion studies using multimodal signals for robust heart beat detection have not assigned weights to the signals based on SQI; NC signals are either assigned predetermined fixed lower weights or given lower priority in voting.

8. Well known existing open source QRS detector algorithms are sensitive to noise therefore, they do not perform efficiently on noisy signals.

9. Most of the existing QRS detectors are not able to detect paced beats introduced by pacemaker. Hence, their beat detection performance drops down on signals with paced beats.

10. Many studies on robust heart beat detection did not use window based approach, hence abrupt changes in HR may give erroneous results.

1.3.2 Salient features of the present study

The salient features of the study are listed as follows:

1. We have carried out the study of robust heart rate estimation from fusion of multimodal signals namely cardiovascular signals and NC signals using various signal processing methods.

2. Slope Sum Function combined with Teager Kaiser Energy operator (SSF-TKE) method has been developed for R-peak artifacts in NC signals. The proposed algorithm selects adaptive optimal value of threshold 'T' window wise, which minimizes missed beats (FNs) and false detection (FPs). The method has yielded better R-peak artifacts detection as compared to that of TKE alone.

3. SSF-TKE method does not require additional ECG channel as well as any a priori input for R-peak artifacts detection. It operates on single channel and can be implemented in real time.

4. A novel statistical and rhythm based beat SQI algorithm has been developed for signal quality assessment, which works on single QRS detector. The performance of beat SQI in the classification of ECG signal quality has been found to be better than that of bSQI. Apart from excellent performance in assessment of signal quality, the proposed beat SQI method works satisfactorily on bradycardia, tachycardia and different types of arrhythmias.

5. SSF-TKE method has also been implemented for R-peak detection in ECG. It considers prominent morphological feature of ECG i.e., slopes and amplitude of QRS waveform. The method has demonstrated excellent R-peak detection performance across a large number of standard databases with variety of signal morphology. It is also highly resistant against different types of ECG noises in the signals and performs quite well in signals with pacemaker beats.

6. Beat SQI based majority voting fusion technique has been proposed for the fusion of heart beats of multimodal physiological signals. The weights to the signals for fusion are assigned based on beat SQI. This has enabled reliable and effective participation of NC signals in the fusion process.

7. The performance of beat SQI based voting fusion method has been excellent on number of standard databases. It has achieved score of 91.76% on hidden test dataset of PhysioNet/CinC/Challenge- 2014 and is presently ranked in top five. Our algorithm has outperformed other studies that have used cardiovascular signals along with NC signals.

8. Since, robust heart beat detection would not necessarily give robust heart rate estimation, study of robust heart beat detection has been further extended to robust heart rate estimation to check for the effectiveness of beat SQI based majority fusion method in HR estimation. The method has yielded excellent HR estimation results within clinical acceptable limits, even in records with noisy ECG and noisy ABP signals.

9. Experimentally, the proposed majority voting fusion algorithm has been validated on artificially created noise dataset by mixing different types of ECG and ABP noises of different SNR levels separately in clean ECG and ABP signals in a record of standard dataset.

10. The proposed algorithm was implemented on Raspberry Pi 3 and computation time is estimated. It is 72 to 138 times faster than the required constraints for real time applications depending upon the no. of signals in the record.

11. Asymptotic run time complexity analysis of the proposed algorithm has been carried out. The asymptotic complexity of the algorithm is O(N), where 'N' is the number of samples in the signal.

1.3.3 Layout of proposed work:

The broad layout of the research work is shown in Figure 1.2. The first step is beat detection from cardiovascular and non-cardiovascular signals. The proposed SSF-TKE method has been

used for R-peak detection in ECG and R-peak artifacts detection in NC signals. Open source 'gqrs' and 'epltd' algorithms have also been used for R-peak detection in ECG. A well known open source algorithm 'wabp' has been used for pulse detection in ABP and heart beat is located by adjusting for pulse transit time. The HR has been estimated directly from detected R-R peak interval in ECG, EOG, EEG, EMG signals and ABP peaks (onset of the ABP pulse adjusted with pulse transit time) interval. A new beat SQI method is used for assessment of quality of detected beats in signals. Weights are assigned to individual beats based on its beat SQI value and the detected beats of multimodal signals are fused by majority voting fusion method. The HR is estimated from R-R interval of fused beats and compared with reference HR and HR estimates from individual signals.

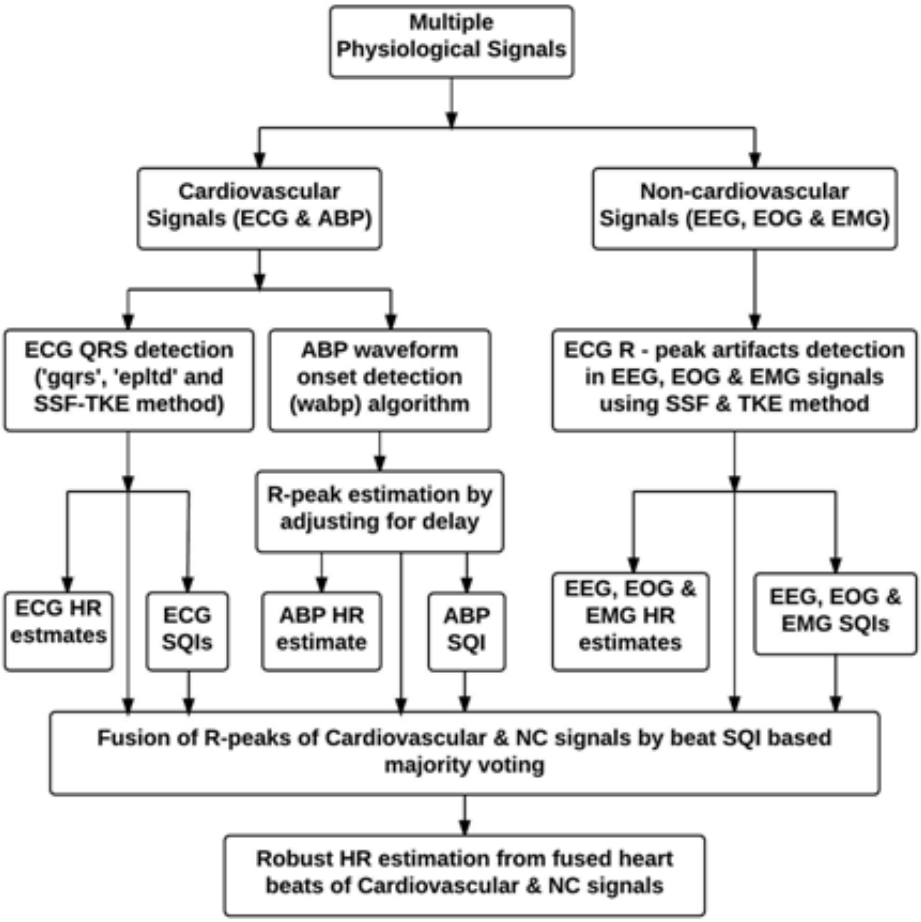

Figure 1.2: Layout of proposed work for ECG artifacts detection and majority voting fusion for robust HR estimation

1.4 Organization of Thesis

This thesis is organized in following eight chapters:

- Chapter 1 has presented overview of the research work on robust heart rate estimation with related work constraints and salient features. It highlights the global health challenges of cardiovascular diseases and the motivation to contribute towards the world wide efforts in the field of cardiovascular research.

- Chapter 2 briefly discusses about functioning of heart, lead arrangement and data acquisition from ECG, ABP, EEG, EOG and EMG. It also contains a brief description of different types of noises in ECG and ABP. Various standard databases of PhysioNet that have been used in this work are also discussed.

- Chapter 3 is related to our proposed algorithm on "ECG artifacts detection in non-cardiovascular signals using slope sum function and Teager Kaiser energy (SSF-TKE)". The proposed SSF-TKE algorithm along with its flow chart has been discussed in detail. It also contains a brief review of the related previous works. The performance evaluation of algorithm on different standard databases, results and discussion thereof have also been given.

- Chapter 4 explores heart beat detection from cardiovascular signals. The proposed algorithm along with flow chart have been discussed. Various techniques used for QRS detection and related works have also been discussed briefly. The relationship of ABP with R-peak is also given. Performance analyses of SSF-TKE method in R-peak detection on standard databases and synthetic dataset have been compared with performance of well known QRS detectors and discussed.

- Chapter 5 briefly discusses SQI assessment methods for different physiological signals. A novel statistical and rhythm based beat SQI assessment method has been proposed and its performance is evaluated on standard databases and compared with standard metric of signal quality bSQI.

- Chapter 6 presents robust heart beat detection from fusion of multimodal signals. A brief literature survey of existing works is given. A beat SQI based majority voting fusion method is proposed for fusion of cardiovascular and NC signals. The performance of the proposed method have been evaluated on no. of standard databases and compared with other methods. Its performance has also been validated on noisy synthetic dataset.

- Chapter 7 is on robust heart rate estimation and it presents review of related works. The performance of the proposed method on standard databases containing NC signals has been presented. The algorithm is experimentally validated on the synthetic noise dataset and the results are discussed. The other experimental validation of our algorithm on Raspberry Pi 3 for real time implementation is also included. Asymptotic runtime complexity analysis of our algorithms have been estimated.
- Chapter 8 summarizes the research work and presents the final conclusion. It also provides direction for future research in this area.

Chapter 2

Multimodal physiological signals and data acquisition

2.1 Introduction

The main objective of this research is to estimate robust heart rate using multimodal physiological signals. The signals of primary interest are ECG, ABP, EEG, EOG, and EMG. These signals are chosen because they are generally recorded simultaneously in ICU to monitor vital health parameters of a patient. All signals are measured non-invasively, except ABP. The physiology of human heart, multimodal physiological signal generation, their acquisition and different types of noises are briefly discussed in this chapter.

2.2 Physiology of the human heart

The heart is a four-chambered muscular organ that pumps blood for circulation in the body. The specialized pacemaker cells in the sinoatrial (SA) node located at the junction of the superior vena cava and the right atrium, determines rhythm of the blood pumping or heart rate (HR). There are two upper atria which receive blood and two lower ventricles for pumping it out. A diagram of the heart showing its anatomy is shown in Figure 2.1.

The cardiac cycle refers to a complete heart beat that includes systole and diastole and the intervening pause. The cycle begins with contraction of the atria and ends with relaxation of the ventricles. Systole refers to contraction of the atria or ventricles of the heart while in case of diastole, the atria or ventricles relaxes and is filled with blood. The atria and ventricle work in co-ordination. The deoxygenated blood is collected in right atrium from the superior and inferior vena cava and during atrial contraction it is passed from the right atrium to the right

ventricle through the tricuspid valve. The deoxygenated blood in the right ventricle is pumped to the lungs for oxygenation through pulmonary valve. The oxygenated blood from lungs is received in the left atrium and during atrial contraction it is passed to the left ventricle via the mitral valve.

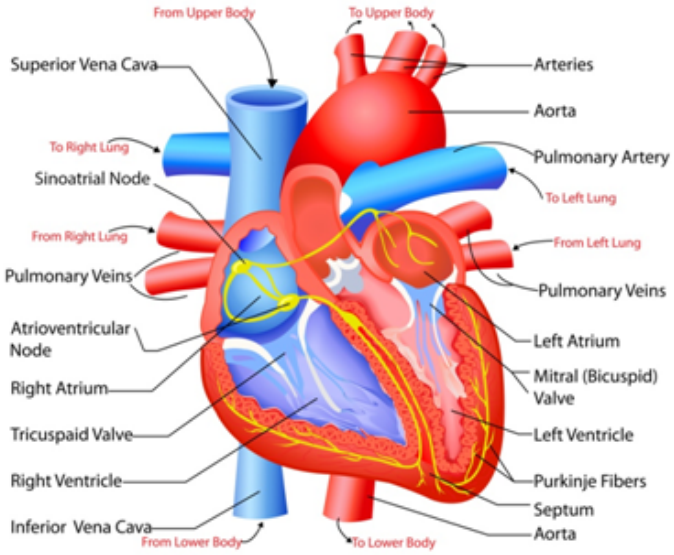

Figure 2.1: Anatomy of heart
(Source: Website https://www.shutterstock.com/image-vector/easy-edit-vector-illustration-anatomy-heart-139537109)

The SA node is the basic, natural cardiac pacemaker that triggers its own train of action potentials. The action potential of the SA node propagates through the rest of the heart, causing a particular pattern of excitation and contraction [44]. The cardiac activities in a cardiac cycle and corresponding ECG wave generation are briefly described.

The firing of SA node generates electrical activity causing contraction of atria generating P wave in the ECG. Due to small change in voltage, the P wave is a slow and low-amplitude wave of 0.1-0.2 mV and 60-80 ms duration. There is a propagation delay in the excitation wave at the atrio-ventricular (AV) node and complete blood is transferred from the atria to the ventricles during this period. This results into an isoelectric segment of about 60- 80 ms after the P wave in the ECG known as PQ segment. The stimulus is then propagated to the ventricles at a high rate by firing of AV node, His bundle and purkinje system. The time duration between the onset of atrial depolarization (P wave) and the onset of ventricular depolarization (beginning of QRS complex) is termed as P-R interval in ECG, which normally

ranges from 0.12 to 0.20 seconds. The rapid spread of stimulus wave upwards from the apex of the heart cause rapid depolarization of the ventricles. It generates a sharp biphasic or triphasic wave of the largest amplitude in the ECG of about 1 mV amplitude over a relatively short duration of 80-100 ms known as QRS wave depending upon the position of recording electrodes. The impaired conduction in the ventricles causes prolongation of QRS complex (greater than 100 ms). Atrial repolarization also occurs simultaneously but it is not seen due to the low amplitude of the signal. The abnormal conduction of electrical impulses within the ventricles may also change the shape of QRS complex. An isoelectric ST segment of about 100-120 ms duration is generated due to relatively long action potential of ventricular muscle cells after the QRS complex. Ventricular repolarization produces T wave in ECG with an amplitude of 0.1-0.3 mV and of 120-160 ms duration [45].

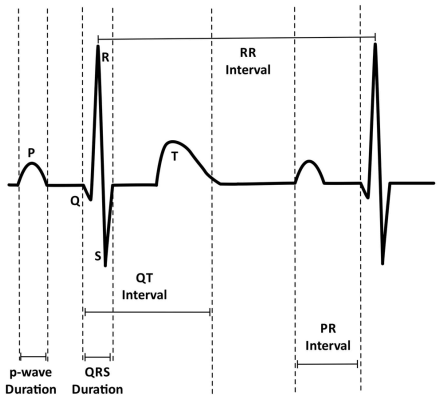

Figure 2.2: Cardiac cycle in an ECG signal
(Source: https://www.ubqo.com/Content/images/Products/CardioZ/ecg-measure.png)

A typical ECG waveform is shown in Figure 2.2. Normally the value of ECG signal peak is about 1 mV and amplifier gain of 1000 is used. Sampling rate of 500 Hz is recommended for recording diagnostic ECG. Bandpass filter of about 0.05-100 Hz is used for filtering clinical ECG. Lower sampling rate of 100 Hz and reduced bandwidth of 0.5-50 Hz may be used for ECG recordings for heart rate monitoring.

2.2.1 Cardiac Arrhythmia

An electrical system of heart controls the rhythm and rate of the heart beats. The electrical signal is triggered by sinoatrial (SA) node that generates heart beat at regular intervals. This electrical signal spreads and it causes the heart to contract for pumping blood to the lungs and body. The regular rhythm of heart beat is 60-100 times a minute for healthy human at rest.

The problem in electrical conduction system of heart disturbs normal sinus rhythm resulting in irregular heart beats known as arrhythmia. The heart can beat too fast, too slow, or with an irregular rhythm during an arrhythmia. Tachycardia is a heart rate higher than normal whereas it is lower than normal in bradycardia. In these conditions the heart may not be able to pump out blood properly to all parts of body and that can damage body parts. There are many reasons of cardiac arrhythmia like irregular firing patterns from the SA node or abnormal and additional pacing activity from other parts of the heart. There are different types of cardiac arrhythmias like ventricular arrhythmias, supraventricular tachycardias, bradyarrhythmias and extra beats.Ventricular arrhythmias contain ventricular fibrillation and ventricular tachycardia. Supraventricular tachycardias contain atrial flutter, paroxysmal supraventricular tachycardia and atrial fibrillation. Premature junctional contractions, premature ventricular contractions and premature atrial contractions are types of extra beats.

Premature ventricular complex (PVC) generally have wide QRS complex. The wave shapes of PVCs are usually different from those of the normal beats of the same person due to the different conduction paths of the ectopic impulses [46]. ECG signal with a few normal beats and PVCs are shown in Figure 2.3.

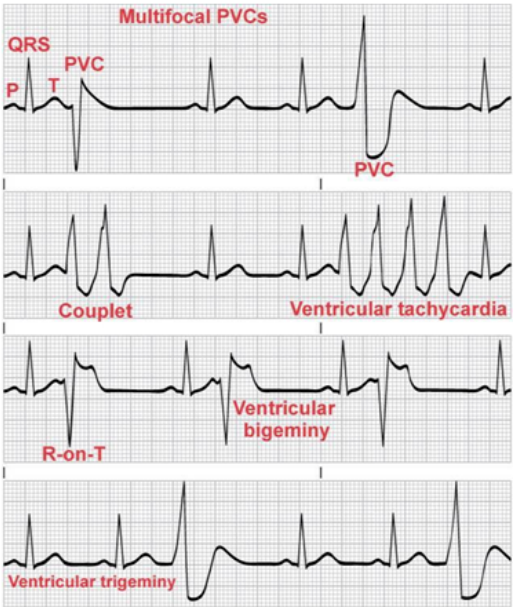

Figure 2.3: ECG signals with PVCs
(Source: Basic dysrhythmias : interpretation & management by Robert J. Huszar)

Premature Ventricular Complex generates disturbance in rhythm of R-R interval as shown in Figure 2.4.

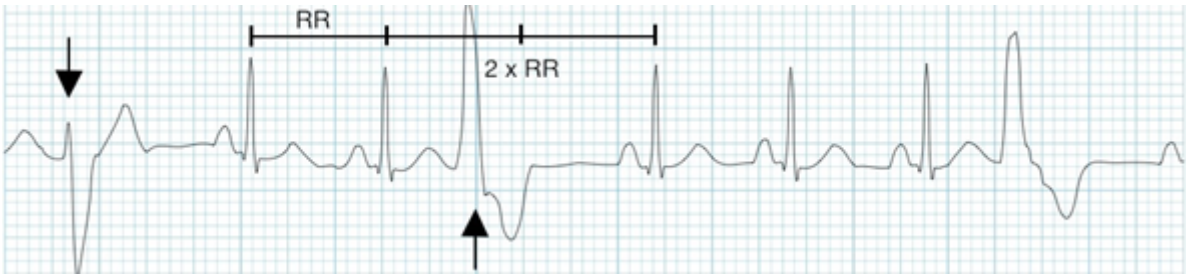

Figure 2.4: Error in HR estimation due to PVC
(Source: Life in the fast lane - Premature Ventricular Complex (PVC) by Edward Burns; website https://lifeinthefastlane.com/ecg-library/basics/pvc/)

2.3 Cardiovascular Signals

2.3.1 Electrocardiography

Electrocardiography is the process of recording of electrical activity of heart with limb and chest electrodes. The heart rate in terms of beats per minute (bpm) may be easily estimated by counting the R-R interval. Some of the cardiovascular diseases such as myocardial ischemia and infarction, ventricular hypertrophy, and conduction problems alter the shape of ECG wave. Therefore, clinical diagnosis of the heart functioning is done by ECG analysis.

2.3.2 Lead Configuration

An electrical activity of heart can be analyzed from 12 lead ECG that gives a tracing from twelve different electrical positions of the heart. Each lead pick up the signal at different position of the heart. The12-lead ECG contains three bipolar limb leads (I, II, III), three unipolar limb leads (IV, V, and VI) and six precordial unipolar leads (V1, V2, V3, V4, V5 and V6). Lead IV, V, and VI is also known as AVR, AVL and AVF respectively. Reference electrode is placed on right leg. The left arm, right arm, and left leg are used to obtain leads I, II, and III respectively. The combined reference for chest leads is formed by combining the left arm, right arm, and left leg leads known as Wilson's central terminal. The augmented limb leads known as AVR, AVL, and AVF are known as AV for the augmented lead, R for the right arm, L for the left arm, and F for the left leg. These electrodes are placed on the limb indicated by the name of the lead, with the reference being Wilson's central terminal. The directions of the axes formed by the six limb leads are shown in Figure 2.5. The equilateral triangle formed by leads I, II, and III is known as Einthoven's triangle. The center of the triangle represents

Wilson's central terminal. The heart is supposed to be placed at the center of the triangle [44-47].

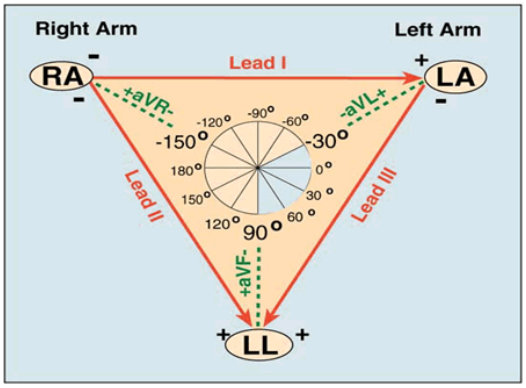

Figure 2.5: Einthoven's triangle and the axes of the six ECG leads
(Source: Cardiovascular dynamics by Robert F. Rushmer)

The six chest leads V1-V6 are also known as precordial leads. Each precordial lead consists of a positive electrode which is placed at six standardized positions on the chest with Wilson's central terminal as the reference. The positions for placement of the chest leads are indicated in Figure 2.6. The positions of the positive electrode for the six precordial leads are very important as it can view the cardiac electrical vector from different orientations in a cross-sectional plane. The right half of the heart activity is reflected by V1 and V2, septal activity can be seen by V3 and V4 whereas left ventricular activity can be viewed by V5 and V6. The 12-lead system serves as the basis of the standard clinical ECG.

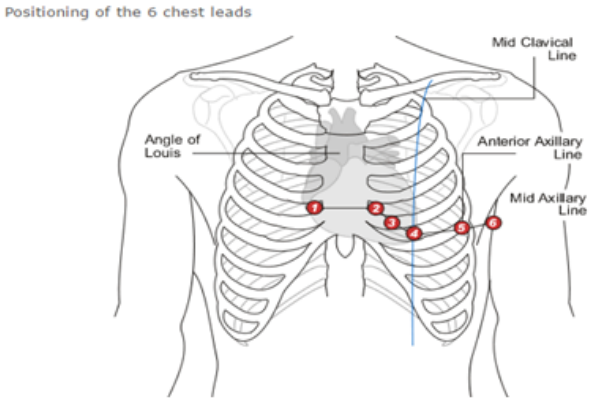

Figure 2.6: Placement of the pre-cordial (chest) leads V1-V6 for ECG
(Source: Website
http://www.nottingham.ac.uk/nursing/practice/resources/cardiology/images/6_lead_placement.gif)

2.3.3 Types of ECG Noise

Electrocardiogram signal may be contaminated by various types of noises. The actual value of signal is very low in the range of 0.5-1 millivolt in an offset environment of 300 mV. Signal acquisition becomes a big challenge because frequency band in which ECG signals lie overlaps with the frequency band of noises. The main sources of noise in ECG are briefly described below:

- Power Line Interference:- Power line interference has 50/60 Hz pickup. The amplitude of power line noise is very large and system gets affected. This noise is removed by implementing a notch filter at 50/60 Hz.
- Baseline wander:- This noise is due to respiration, offset voltages in the electrode and body movement. It resides in lower frequency range. It can be removed by high pass filter with a cut- off frequency of 0.05 Hz so that ECG signal remains undistorted.
- Motion artifact:- Motion artifacts are transient baseline changes caused by changes in the electrode-skin impedance with electrode motion. The motion artifact is due to vibrations or movement of the subject. It is around 500 percent of peak-to-peak ECG amplitude with duration of 100-500 ms.
- Muscle artifact:- Contraction of muscle generates potentials and creates artifact at millivolt level. The baseline electromyogram is usually in the microvolt range and therefore, it is insignificant. Typical parameters: amplitude Standard Deviation-10 percent of peak-to-peak, ECG Duration-50 ms, Frequency Content- dc to 10,000 Hz.
- Electrode contact noise:- Electrode contact noise is transient interference caused by loss of contact between the electrode and skin. The loss of contact can be permanent, or intermittent, when a loose electrode is brought in contact with the skin during movements and vibration. This switching action at the measurement system input can result in large artifacts.
- Instrumentation Noise:- Artifacts generated by electronic devices in the instrumentation system.
- Electrosurgical Noise:- Electrosurgical noise completely destroys the ECG. It contains large amplitude sinusoid with frequencies approximately between 100 kHz and 1 MHz. The sampling rate of an ECG signal is 250 to 1000 Hz, therefore an aliased version of this signal will be added to the ECG. The variable parameters are amplitude, the duration and the aliased frequency. Typical parameters of the noise are: Amplitude -

200 percent of peak-to-peak ECG amplitude, Frequency Content - Aliased 100 kHz to 1 MHz, Duration- 1-10 s [5].

2.3.4 Arterial Blood Pressure

Arterial blood pressure is the pressure exerted by blood within brachial artery in the upper arm. It can be determined by the cardiac output (CO), systemic vascular resistance (SVR) and central venous pressure (CVP) over a cardiac cycle. In normal resting heart rate condition, it can be approximately determined from measurements of systolic pressure and diastolic pressure. The blood pressure is measured using a sphygmomanometer and it fluctuates between systolic pressure level of 120 mm Hg and a diastolic pressure level of 80 mm Hg for a healthy human at resting state. The variation in blood pressure values in various chambers of the heart system helps the physician to determine health of cardiovascular system [48].

2.3.5 BP recording and measurement

The blood pressure is measured by direct (invasive) and indirect (noninvasive) methods. The indirect methods consist of simple equipment and cause very little discomfort to the patient whereas the direct method provides continuous and much more reliable information about the absolute vascular pressure from probe inserted directly into the blood stream. The direct method of pressure measurement is used when the highest degree of absolute accuracy, dynamic response and continuous monitoring is required [49]. The arterial blood pressure is directly measured by inserting a cannula needle in an artery. The advantage of this system is that blood pressure is constantly monitored beat-by-beat. The waveform of arterial blood pressure is depicted in Figure 2.7 [50].

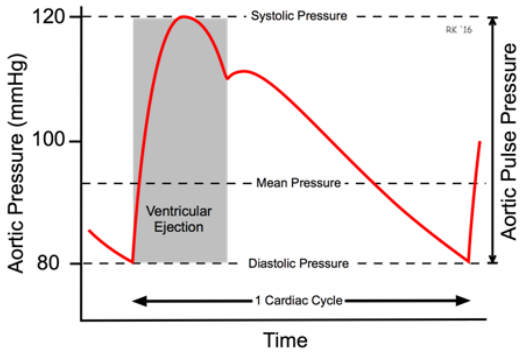

Figure 2.7: Arterial blood pressure across a Cardiac cycle
(Source: Cardiovascular Physiology Concepts by Richard E. Klabunde; website: http://www.cvphysiology.com/Blood%20Pressure/BP002)

2.3.6 Correlation of ABP with ECG

Heart contraction ejects blood from the left ventricle that creates onset in ABP pulse. There exists a delay between the onset of ABP pulse and the R peak that is referred as the Pulse Transit Time (PTT). This time varies from patient to patient and even between successive heart contractions and therefore it should be estimated on individual patients basis [51].

Measurement of ECG and ABP are taken from different sources, therefore the same type of noise may not affect both the signals concurrently. It may be possible that when ECG signal is noisy, BP signal is clean and vice-versa. The BP signal can locate heartbeats based on an association model between ECG R peak and ABP pulse as shown in Figure 2.8 [52]. The main advantage of the association model of ECG and BP is that it can reliably estimate location of heartbeat with relatively high sensitivity and specificity by adjusting the location of onset of ABP pulse with PTT in case of noisy ECG signal. However, this approach cannot work if sufficient physiological information is not available. There is a limitation for correlation when both ABP and ECG signals are noisy simultaneously.

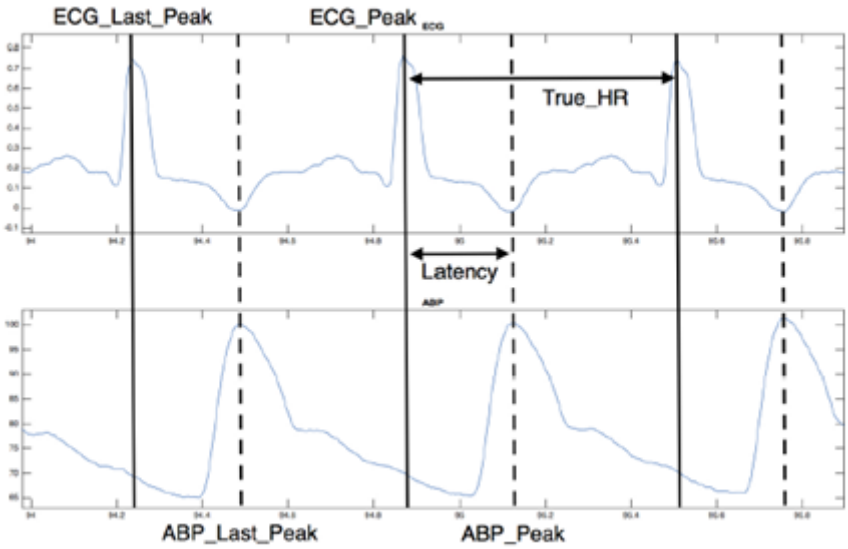

Figure 2.8: Correlation of ECG R-peak with ABP Pulse
(Source: H. Chen et al., Phsiological Measurement 37, no. 9, pp 1404 - 1421, 2016)

2.3.7 Types of Arterial Blood Pressure noise

ABP is often corrupted by different types of noise and artifacts such as transducer flushing, catheter clotting, movement artifacts, and non-invasive cuff inflations. These artifacts are generally non-Gaussian, nonlinear and non-stationary [53]. In a previous study six generic artifact types were identified after extensive searches through the MIMIC II database. These

are: (i) rapid saturation (over a period of 5 to 20 seconds) to some maximal ABP, (ii) rapid saturation to some ABP minimum, (iii) rapid saturation to the current mean ABP, (iv) high amplitude square wave artifact, (v) high frequency noise and (vi) highly transient impulse-like artifact [54]. These artifacts are briefly described:

1. **Saturation to ABP maximum artifact (a_{smax}):** This type of artifact is created due to the flushing of the arterial line caused by a blood clot or thrombosis of the arterial line to reduce damping. This artifact manifests itself as a rapid saturation from a normal ABP to a maximum value (ABPmax), which is set to be equal to 200 mm Hg ± 10 mm Hg, with an exponential-like curve.

2. **Saturation to ABP minimum artifact (a_{smin}):** It is due to transient constriction in the arterial line such as pinching from arm movement. It consists of four consecutive parts: (a) a rapid exponential diastolic saturation, (b) a rapid saturation from a normal ABP to a minimum value (ABPmin) with an exponential decay, (c) an exponential increase from ABPmin to some ABP value, and (d) a gradual transition back to the normal blood pressure. An artifact boundary is created with these four parts and then applied to the ABP.

3. **Reduced pulse pressure artifact (a_{pp}):** The main cause of this artifact can be attributed to damping caused by thrombus in the arterial line. It is similar to the systolic and diastolic ABP saturation artifact gradually decreasing the pulse pressure.

4. **Square wave artifact (a_{sw}):** This type of artifact consists of a series of square waves with varying random duty cycles.

5. **High frequency artifact (a_{hf}):** This band-pass filtering phenomenon may be due to movement artifact and disturbance of the transducer. High frequency noise is simulated by differentiating the signal.

6. **Impulse artifact (a_{imp}):** This type of artifact could be due to motion, or a sharp mechanical artifact such as crimping of the tubing. It is simulated by the Sinc function. The central lobe of the Sinc function has been used as a_{imp} artifact [54].

2.4 Non-Cardiovascular Signals

2.4.1 Electroencephalogram (EEG)

Electroencephalography is an electrophysiological and noninvasive monitoring method to record electrical activity of the brain (EEG) with placement of electrodes on the scalp. Sometimes

invasive electrodes are used in specific applications. EEG measures voltage fluctuations resulting from ionic current within the neurons of the brain [55]. Different types of neural oscillations, also known as brain waves, are used for diagnostic applications of epilepsy, sleep disorders, coma, and brain death. EEG can also be used in ICU for monitoring of brain function for non-convulsive seizures, the effect of anesthesia on patients in coma and for secondary brain damage in conditions such as subarachnoid hemorrhage [56].

2.4.2 Electrooculogram (EOG)

Electro-oculography is a technique for measuring the corneo-retinal standing potential that exists between the front and the back of the human eye. This potential is created from the metabolic activity of the retina. The cornea of the eye is electrically positive with a resting potential of the order of 1 mV relative to the back of the eye. The eye can be considered as an electric dipole due to this potential difference. The movement of dipole causes changes in electric field that can be observed. Eyes movement from left to right or up and down, creates an electrical deflection called an electrooculogram (EOG) signal. It allows detection of eye rotations by measuring electric bio-potentials from the eyes by surface electrodes as shown in Figure 2.9 [57-59]. EOG signals are mainly used in ophthalmological diagnosis and in recording eye movements.

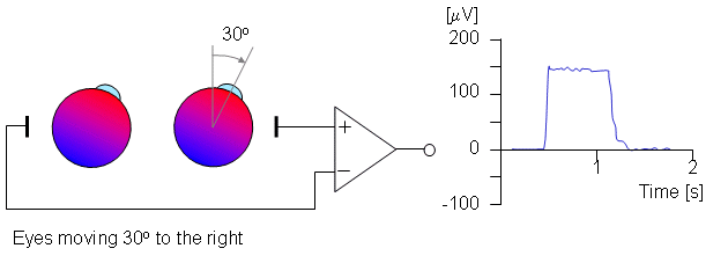

Figure 2.9: Bioelectric potentials of EOG signal
(Source: Bioelectromagnetism:- principles and apllications of bio-electric and bio-magnetic fields, by J. Malmivuo and R. Plonsey, 1995)

2.4.3 Electromyogram (EMG)

Electromyogram (EMG) is generated by the bioelectric potentials associated with muscle activity. There are mainly two types of EMG: (i) Intramuscular EMG and (ii) Surface EMG (sEMG). sEMG is measured at the body surface near a muscle while the intramuscular EMG is measured from the needle electrode penetrating the skin of muscle. sEMG is used for the diagnosis of neuromuscular disorder and for rehabilitation. It is also used for device control

applications such as prosthetic devices, robots, and human-machine interface. Needle electrodes are inserted directly when there is problem in measurement of potentials from surface of muscle [60].

The amplitude of the measured EMG waveform is the instantaneous sum of all the action potentials generated at any given time. The EMG waveform appears like a random-noise waveform because action potentials occur in both positive and negative polarities that sometimes add and sometimes cancel at a given pair of electrodes. EMG is used as a diagnostics tool for identifying neuromuscular diseases and disorders of motor control. It is also used as a control signal for prosthetic devices such as prosthetic hands, arms, and lower limbs [61].

2.5 Noise and Artifacts in NC Signals

The artifact in NC signals may be either patient-related or technical. Patient related artifacts are unwanted physiological signals that may significantly disturb the NC signals. AC power line noise, too much electrode paste/jelly or dried pieces, broken wire contacts, impedance fluctuation etc. are few technical artifacts present in EEG. Patient related artifacts in EEG are motion artifact, muscle artifact, ECG artifact, eye movements and sweating [56]. Electrical fields of the heart extend to the base of skull and ECG artifacts are picked up by EEG with wide inter electrode distance (ear electrodes). Therefore, ECG artifacts may be prominent on ear referential montages and they pose major problem in clinical interpretation of EEG [62].

EOG signal is always mixed with many unwanted signals like facial muscle movements that can cause the upward or downward drift of the baseline of eye signal [63]. Signals from other parts of the body like ECG, EEG, EMG and breathing can introduce interference in eye signal. Other sources of interference in EOG are technical artifacts like power line interference, noise due to skin contact impedance etc.

Surface EMG signals are contaminated by several intrinsic and extrinsic sources of low frequency noise. The two intrinsic noise sources originate in the electronics of the amplification system and at the skin-electrode interface [64]. These noise sources together form the baseline noise that is detected whenever a sensor is attached to the skin. An additional noise source, the movement artifact noise also originates at the electrode-skin interface. It is generated when: (a) the muscle moves underneath the skin, and (b) when a force impulse travels through the muscle and skin underlying the sensor causing a movement at the electrode-skin interface. The resulting time-varying voltage produced across the two electrodes can be the most troublesome of noise sources and requires the utmost attention [65-66]. Since electrical activities of heart propagate through out the body threfore, EMG is also contaminated by ECG artifacts.

2.6 Data acquisition system for cardiovascular signals

Medical data acquisition system faces a challenge of measuring a very small voltage electrical signal in the presence of much larger common-mode voltages and noise. Bioelectrical signal measurements from the heart (ECG), muscles (EMG), skin (GSR), scalp (EEG), eyes (EOG) and pulse (PPG) are typically very small in amplitude and require amplification to accurately record, display and analyze the signals. The typical amplitude and frequency range for ECG, EEG, EOG, and EMG signals are given in Table 2.1 [67-68].

Table 2.1: Frequency and amplitude ranges for ECG, EEG, EOG and EMG

Signal	Frequency Range (Hz)	Amplitude (mV)
ECG	0.05 – 150 Hz (diagnostic) 0.5 – 40 Hz (monitoring)	0.1-5
EEG	0.1-100	0.025 – 0.1
EOG [68]	0.1 – 100	0.05 – 3.5 For eye movement up to 70 degree
EMG	25 – 5,000 Hz	0.1-100

2.6.1 ECG data acquisition

Electrical potential, generated by the heart is sensed by the electrodes on the skin surface using biological transducers. This electrical potential captured by sensor is an AC signal with bandwidth of 0.05Hz to 100Hz and amplitude around ± 0.5 mV peak-to-peak. These ECG signals have low amplitude voltage in the presence of high offsets and noise. Ag/AgCl is the common electrode used in the acquisition of the signals and has a maximum offset voltage of ± 300 mV. The ECG signal to be recorded is in the range of ± 0.5 mV, superimposed on electrode offset of ± 300 mV. The system also picks up 50/60 Hz noise from power lines. Amplitude of power line noise may be very high and needs to be filtered. A block diagram of data acquisition system for ECG signal is shown in Fig. 2.10 [69].

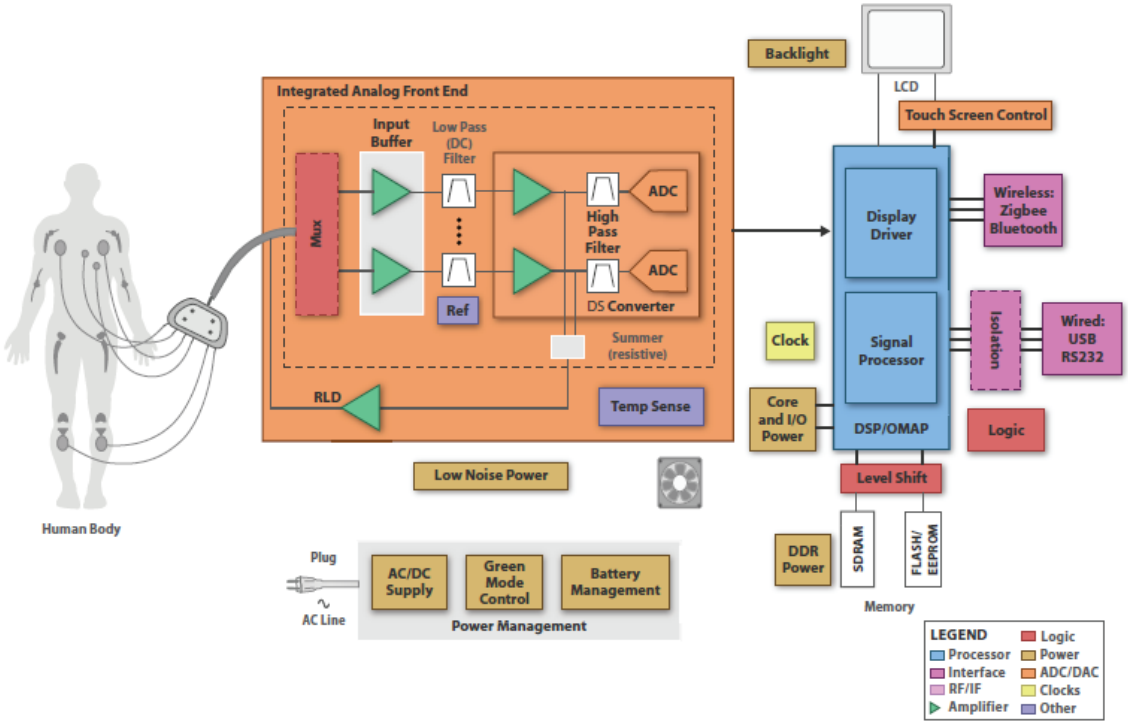

Figure 2.10: ECG data acquisition system
(Source: Diagnostic, Patient Monitoring and Therapy Applications Giude by Texas Instruments; website http://www.ti.com/lit/sg/slyb147a/slyb147a.pdf)

An analog signal is converted to a digital signal by data acquisition unit (DAQ). The digital signal is sampled at regular intervals using a software which stores and display the data on the computer screen. Appropriate sampling rate for data acquisition depends on the signal to be measured. The minimum rate at which digital sampling can accurately record an analog signal is chosen according to the Nyquist frequency criteria, which is double the highest expected signal frequency [70]. The aliasing is not supposed to be a problem as there is always a low pass analog filtering. The signal band width should be selected based upon the chosen sampling frequency in any ADC system. However, for a signal of given frequency content, the fidelity of signal does not increase significantly by increasing the sampling rate beyond a certain point. The cost of an ADC increases for higher sampling rates, because it requires more computer processing time and storage space in memory to process the larger number of data points when the sampling rate is increased [71]. According to previous findings, the optimal range of sampling rate for spectral analysis of HRV parameters should be between 250 and 500 Hz or even higher [72].

Modern multichannel ECG machines capture heart signals from a standard 12 lead configuration sequencing the lead selector. The lead selection operations are stored in ROM.

The selected ECG signal is amplified, filtered and sent to A/D converter [49]. Amplifier is important for proper signal amplification because it has a direct effect on resolution. If amplification is reduced too much, it can cut off peaks and troughs and that can result in loss of input signal information. Analog front-end processing unit forms an important part of data acquisition system, since it needs to distinguish between noise and the desired signal, which is of small amplitude. It consists of a high input impedance instrumentation amplifier to remove the AC line noise, which is common to both inputs and amplifies the remaining unequal signals present. An operational amplifier is used to remove common-mode voltages. The analog front end must be AC coupled to remove artifacts from the electrode offset potential. The requirements of Instrumentation Amplifier are: stability in low gain (1to10), high common-mode rejection, low input bias current (IB), good swing to the output rail, very low offset and drift; while the requirements of Operational Amplifier are low noise in high gain (Gain = 10 to 1000) and rail-to-rail output [69].

2.6.2 ABP data acquisition

Arterial Blood Pressure is a direct method of blood pressure measurement in which a catheter or a needle type probe is inserted through a vein or artery. A simplified circuit diagram commonly used for processing the electrical signals received from the pressure transducer for the measurement of arterial pressure is given in Fig. 2.11 [49].

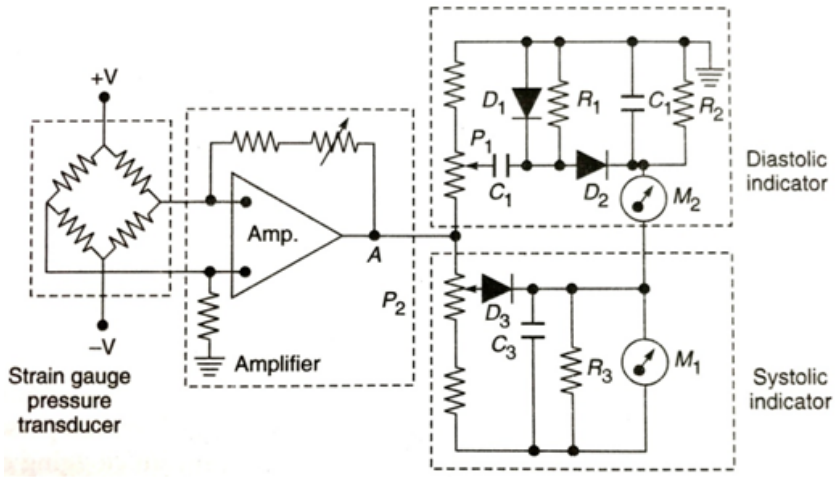

Figure 2.11: Circuit diagram for measurement of arterial blood pressure
(Source: Handbook of Biomedical Instrumentation by R. S. Khandpur)

2.7 Data acquisition system for non-cardiovascular signals

2.7.1 EEG signal acquisition

The EEG recording electrodes and their proper functioning are crucial for acquiring high quality data. Different types of electrodes commonly used in the EEG recording systems are (i) disposable (gel-less, and pre-gelled types), (ii) Reusable disc electrodes (gold, silver, stainless steel, or tin), (iii) Headbands and electrode caps, (iv) Saline-based electrodes, and (v) Needle electrodes. International Federation in Electroencephalography and Clinical neurophysiology has adopted standard way for electrode placement called 10-20 electrode placement system. Electrode placement is labeled according to brain areas like Fm (frontal), C (central), T (temporal), P (posterior), and O (occipital) is shown in Figure 2.12 [56].

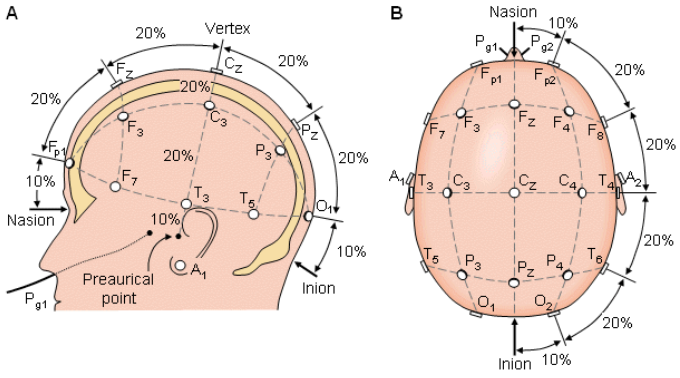

Figure 2.12: Standard 10 - 20 EEG electrode positioning system
(Source: H. H. Jasper, "The ten-twenty electrode system of the International Federation," Electroencephalography and Clinical Neurophysiology, pp. 371-375)

Electroencephalograph (EEG) signals picked up by the surface electrodes are small in amplitude as compared to ECG signal. The brain waves are not periodic like ECG. Every channel has an individual multistage, AC coupled, very sensitive amplifier with differential input and adjustable gain in a wide range. The preamplifier used in EEG recording must have high gain and low noise characteristics, because the EEG potentials are small in amplitude. The amplifier must also have very high common mode rejection to minimize stray interferences from power line and other electrical signals. EEG recorded by surface electrode may contain numerous artifacts like power line interference, muscle artifacts, ECG artifacts, EOG artifacts etc. These artifacts are large and sharp causing great difficulty in EEG signal analysis and are generally removed using low pass filter and high pass filter and many a times by using band pass filter. The filtered signal is passed through A-D converter for display.

2.7.2 EOG signal acquisition

EOG potentials are picked up by Ag-AgCl surface electrodes placed on the skin near the eye. Five electrodes are used to measure the EOG signal of an eye. One pair of electrode is placed above and below the eye to pick up the voltages corresponding to the vertical movement of the eyeball. Another pair of electrode is placed to the left and right of the eye to measure horizontal movement. The reference electrode is either placed on the forehead or at earlobe. The impedance between any pair of electrodes should not exceed 5 kΩ. The electrodes should not be placed too close to the lateral canthi because this sometimes causes frequent blinking and thereby increases artifacts. Microelectrodes have a small measurement surface that allows much smaller skin movement artifacts in the recordings as compared to conventional electrodes [73].

The frequency range of EOG signal is 0.1-20 Hz and the amplitude lies between 0.05-3.5 mV. Hence a voltage gain of minimum 2000 is needed for further processing the raw signal. The collected signal from the electrodes is fed to an instrumentation amplifier having high input impedance and Common mode rejection ratio (CMRR) more than 90 dB, followed by a band pass filter with a cut off frequency band of 0.1-30 Hz to eliminate unwanted data. A 12 bit Analog to Digital Converter is used for conversion of the signal in digital format for displaying it on LCD or display unit.

2.7.3 EMG signal acquisition

The EMG signal is a summation of all the action potentials within the range of the electrodes, each weighted by its distance from the electrodes. Since the overall strength of muscular contraction depends on the number of fibers energized and the time of contraction, there is a correlation between the overall amount of EMG activity for the whole muscle and the strength of muscular contraction. The EMG potentials from a muscle or group of muscles produce a noise like waveform that varies in amplitude with the amount of muscular activity. Peak amplitudes vary from 25 μV to about 5 mV, depending on the location of the measuring electrodes with respect to the muscle and the activity of the muscle. A frequency response from about 5 Hz to well over 15000 Hz is required for faithful reproduction.

The amplifier for EMG measurements, like that for ECG and EEG, must have high gain, high input impedance and a differential input with good common-mode rejection. However, the EMG amplifier must accommodate the higher frequency band. In many commercial electromyograms, the upper-frequency response can be varied by use of switchable low pass filters [74-75].

EMG is usually recorded by using surface electrodes or by using needle electrodes, which

are directly inserted in to the muscles. A ground electrode is necessary for providing common reference for measurement. Full bandwidth of the surface EMG signal spans up to 500 Hz. The signal acquired from the electrode is amplified using differential type amplifier with good band width and higher input impedance of 1012 ohms in parallel with 5 pf capacitor. The common mode rejection should be greater than 90 dB up to 5 kHz. Then low frequency and high frequency filters are used to select the pass band on incoming signal. Since Butterworth filter preserves amplitude linearity in the pass band region, it is generally used for filtering the EMG signal. To select an appropriate ADC for digitizing EMG signals, it is important to consider three interacting factors: (a) gain of the system, (b) input noise of the system, and (c) maximum voltage output of the system.

We have not done any data acquisition for our research work contained in this thesis but have used several standard databases which are available on PhysioNet [76] for the research. We are giving a brief summary of the PhysioNet data acquisition.

2.8 PhysioNet Database acquisition

A dataset in PhysioBank has number of records and each record contains one or more signals with header and annotations information. Signal is a finite sequence of integer samples usually obtained by digitizing a continuous observed function of time at a fixed sampling frequency expressed in Hz. All sample intervals for a given signal are equal. These samples are represented by 8, 12, 16, 24 or 32 bit integers. Generally, all signals in a record have the same sampling frequency. In a multi-frequency record, the least common multiple of various sampling intervals used in the record is defined as frame interval and the frame frequency is the number of frame intervals per second. Annotations are commonly used to label heartbeats.

The standard PhysioNet MIT format databases from PhysioNet have been used in this research. MIT signal file are binary files containing samples of digitized signals and are in the form: Recordname.dat. It cannot be interpreted properly without their corresponding header files. MIT header file are short text files that describe the contents of associated signal files and are in the form: Recordname.header. MIT annotation files are binary files containing annotations and are in the form Recordname.atr. Annotation files should be read with their associated header files. The integer value of each sample is usually interpreted as a voltage, and the units are called analog-to-digital converter units, or adu. All signals in a given record are usually sampled at the same frequency, but not necessarily at the same gain. The gain for each signal is specified in 'adu' corresponds to one physical unit usually one millivolt, the nominal amplitude of a normal QRS complex. Most PhysioBank databases and their annotations are stored in a Waveform Database (WFDB) format. PhysioNet provides the

WFDB software package that is highly useful for reading, writing and processing the WFDB files. The WFDB Software produces digital values by default.

ECG signal is digitized using a sampling frequency of at least 120 Hz with at least 8 bit resolution over ± 5mv range. Ideally sampling frequency should be in the range of 250 Hz to 1 KHz with 12 bit or higher resolution over a ± 10mv range. An appropriate low-pass filter with a cutoff of about 40% or less of the sampling frequency is used as an anti-aliasing filter. Now these samples are written into text file form as a column of decimal numbers. Here, we have digitized more than one signals, therefore a separate column for each signal has been used. The functions from WFDB library are used to prepare a binary signal file and a header file from the text file.

2.9 Standard Databases

In the present work reported in this thesis, we have used several dataset, namely PhysioNet/CinC Challenge 2011 training set-a, PhysioNet/CinC Challenge 2014 training dataset (set p and set p2), PhysioNet/CinC Challenge 2014 hidden test dataset, MIT-BIH Polysomnographic database, MIT-BIH Arrhythmia database, MGH/MF waveform database and MIT-BIH noise stress test database. To validate the performance of our algorithm on noisy cardiovascular signals, a synthetic noise dataset has been generated by adding calibrated amount of different types of noises in clean ECG and ABP signals separately. A brief description of the above mentioned dataset/database is given below.

2.9.1 PhysioNet/CinC Challenge 2011 training set-a

The dataset is a collection of 1000 standard 12-lead simultaneous recordings of ECG of minimum 10 s duration with full diagnostic bandwidth (0.05-100 Hz). The signals are sampled at 500 Hz with 16-bit resolution. Signal quality is assigned to each ECG in a record in the form of letter and numerical rating i.e. A (0.95): excellent, B (0.85): good, C (0.75): adequate, D (0.60): poor, or F (0): unacceptable. The average grade was calculated for each record and it was assigned to one of 3 groups namely; acceptable, indeterminate and unacceptable. The dataset contains 773 acceptable records, 225 unacceptable records and 2 indeterminate records [77].

2.9.2 PhysioNet/CinC Challenge 2014 datasets

PhysioNet/CinC Challenge-2014 training dataset (set-p) [78] and extended training dataset (set-p2) [79], together known as public training set contains 200 records of human adults. The

hidden test data set of PhysioNet/CinC Challenge-2014 also contains 200 records but of a wider variety of signals than in the training set. Each record contains four to eight signals; an ECG signal along with a variety of simultaneously recorded physiologic signals. The duration of each record in set-p dataset is 10 minutes; some records are of shorter duration. The sampling frequency of signals in public training set is either 250 Hz or 360 Hz whereas signals in the test dataset have been sampled at rates between 120 Hz and 1000 Hz. Reference beat annotations of records of the training dataset have also been given.

2.9.3 MIT-BIH Polysomnographic database (slpdb)

This database contains multiple physiological signals of 16 adult males during sleep for evaluation of chronic obstructive sleep apnea syndrome and to test the effects of constant positive airway pressure (CPAP). Database has 18 records of four to seven-channel polysomnographic recordings of 80 hours. Each record of database contains ECG, invasive blood pressure, EEG, oxygen saturation, two respiration signals, and cardiac volume. Five records contain an EOG signal and an EMG signal also. The recording time of records is between 2h and 7h. These physiological signals are digitized at a sampling interval of 250 Hz and 12 bits/sample [80].

2.9.4 MIT-BIH Arrhythmia database (mitdb)

The MIT-BIH Arrhythmia database contains 48 two-channel ambulatory ECG recordings, each of half-hour duration, obtained from 47 subjects. Twenty-three recordings were chosen at random from a set of 4000, 24-hour ambulatory ECG recordings whereas the remaining 25 selected recordings include less common but clinically significant arrhythmias. The sampling frequency of recordings was 360 samples per second per channel with 11-bit resolution. The digitization rate of 360 samples/second per channel was chosen so that simple digital notch filter can be used to remove 60 Hz interference. The analog signals were filtered to limit saturation in A/D conversion and for anti-aliasing using a pass band of 0.1-100 Hz relative to real time during digitization [81].

2.9.5 MIT-BIH noise stress test database (nstdb)

This database includes 12 half-hour ECG recordings and 3 half-hour recordings of noise typical in ambulatory ECG recordings. The noise recordings were made using physically active volunteers with standard ECG recorders, leads, and electrodes. The three noise records are baseline wander (bw), muscle artifact (ma), and electrode motion artifact (em). 'nstdbgen' script has been used to create the ECG recordings by adding calibrated amounts of noise from

record 'em', using 'nst' in two clean recordings viz.118 and 119 of MIT-BIH Arrhythmia database. Noise was added beginning after the first 5 minutes of each record, during two-minute segments alternating with two-minute clean segments. The noise levels during the noisy segments of these records are signal-to-noise ratios (SNRs) of 24 dB, 18 dB, 12 dB, 6 dB, 0 dB and -6 dB [82].

2.9.6 MGH/MF waveform database (mghdb)

The MGH/MF waveform database contains 250 electronic recordings of hemodynamic and ECG waveforms of stable and unstable patients in operating room, critical care units, and cardiac catheterization laboratories. These recordings from 250 patients represent a broad spectrum of physiologic and pathophysiologic states and a typical record has three ECG leads, arterial pressure, pulmonary arterial pressure, central venous pressure, respiratory impedance, and airway CO2 waveforms. The length of individual record varies from 12 to 86 minutes; most of the records are of about an hour duration. The sampling rate is 360 samples per second per signal relative to real time. Each record includes an annotation file, which contains beat and event labels [83].

2.9.7 Synthetic noise dataset

The presence of noise in the ECG caused by power line interference, base line wander, movement, muscle contractions, sweating etc. seriously affects detection of QRS complexes and heart rate estimation. To validate the ECG beat detection performance of proposed SSF-TKE method and heart rate estimation performance of proposed beat SQI based majority fusion method in noisy ECG and ABP signals, a synthetic noise evaluation dataset has been created by adding different types of real ECG and realistic artificial ABP noises in clean ECG and ABP signals respectively. The standard MIT-BIH noise stress database contains ECG signals with electrode motion 'em' noise only. Synthetic noisy ECG signals are generated by adding calibrated amounts of baseline wander (bw), electrode motion (em) and muscle artifact (ma) noise from records 'bw', 'em' and 'ma' of MIT-BIH noise stress database in clean ECG signal of record 123 of PhysioNet challenge 2014 training dataset using 'nstdbgen' script from WFDB software package. Noise has been added beginning after the first 2 minutes of each record, during two-minute segments alternating with two-minute clean segments. The SNR during the noisy segments was set to a value of 12, 9, 6, 3, 0, -3, -6, -9 and -12 dB separately, giving a total of nine different noise levels for each type of ECG noise. The ECG signal with 'bw', 'em' and 'ma' noises of -12 dB SNR are shown in Figure 2.13.

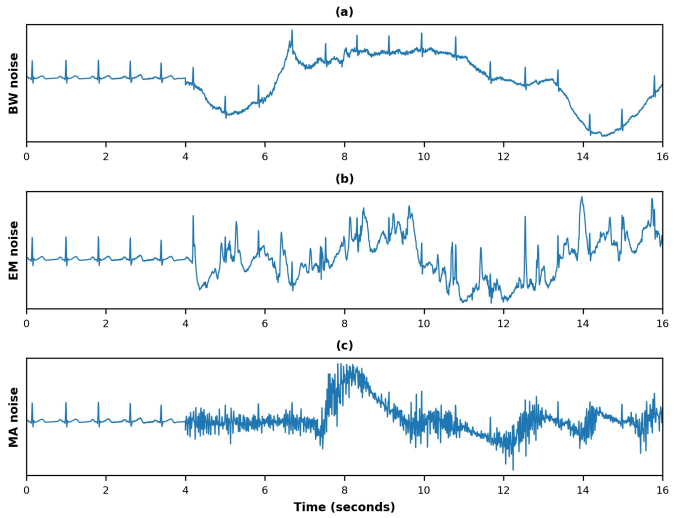

Figure 2.13: Types of noise in ECG: (a) Baseline wander (bw') noise, (b) Electrode motion (em) artifact noise and (c) muscle artifact (ma) noise

Since no standard database exists for real ABP noise, six artificial ABP noises namely, saturation to ABP maximum artifact (a_{smax}), saturation to ABP minimum artifact (a_{smin}), Linear attenuation to BP mean (a_{lamean}), square wave artifact (a_{sw}), high frequency artifact (a_{hf}) and Sinc function impulse artifact (a_{imp}) have been added to clean ABP signal of record no. 123 of PhysioNet challenge 2014 training dataset.

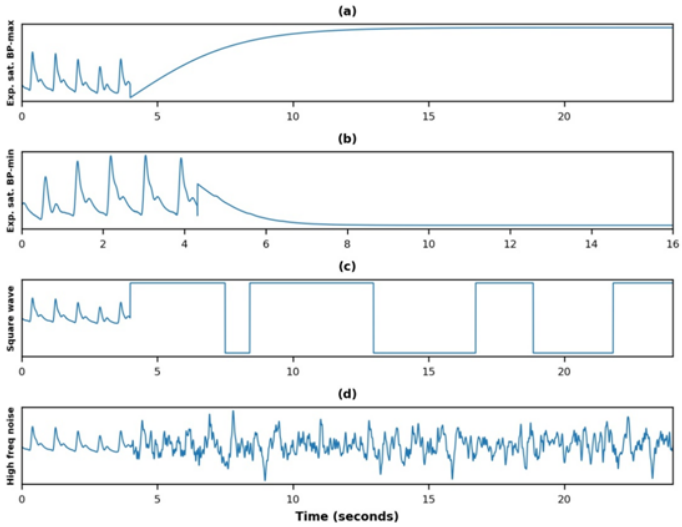

Figure 2.14: Artificially corrupted ABP signal obtained from adding (a) saturation to ABP maximum noise, (b) saturation to ABP minimum noise, (c) square wave noise, and (d) high frequency noise.

The six types of ABP noises have been added separately to ABP signal using Matlab source code. Noise has been added beginning after the first 2 minutes of each record, during two-minute segments alternating with two-minute clean segments. The SNR during the noisy segments was set to a value of 12, 9, 6, 3, 0, -3, -6, -9, -12 dB separately, giving a total of nine different noise levels for each type of ABP noise. Different types of ABP noises each of -12 dB SNR are shown in Figure 2.14.

Thus, the synthetic noise dataset contains three different types of noisy ECG signals and six different types of noisy ABP signals, each with nine different noise levels.

Chapter 3

Heart beat detection from Non-cardiovascular Signals

3.1 ECG artifact detection in Non-cardiovascular signals

3.1.1 Introduction

Artifacts are undesirable signals arising from environmental, experimental and physiological factors. The presence of artifacts in signal degrades signal quality and that makes the analysis of physiological signals difficult for diagnostic purposes. Therefore, artifact detection and its removal from the signals has been an important area of research for the last couple of decades. Physiological artifacts are variations in the desired signals due to other physiological processes in the body [84]. The heart generates strong electrical field that affects the surface potentials on the scalp, muscles and near the eyes. It introduces ECG artifacts in EEG, EMG and EOG signals [85].

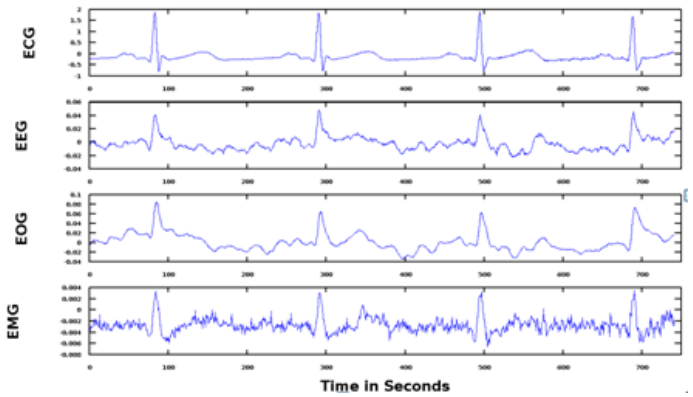

Figure 3.1: ECG Artifacts in Non-cardiovascular signals

.

Frequency band of ECG artifacts overlaps on the spectra of the various physiological NC signals, hence it becomes difficult to remove them using a filter. Majority of the artifacts in a signal have to be removed in such a way that minimizes the data loss. Basic filtering technique like low pass and high pass cannot be adopted for removing artifacts with overlapping spectra. ECG artifacts can be clearly seen in EEG, EOG and EMG signals shown in Figure 3.1

3.1.2 Related Works

Advancement in signal processing methods have brought significant improvement in artifact detection and removal in the past several years. There had been various techniques proposed for artifact separation and their removal.

Nakamura and Shibasaki [39] developed ensemble average subtraction (EAS) method for elimination of ECG artifacts from EEG signal. In this method, ECG contaminated EEG signal is segmented with respect to the timing of synchronous ECG R-peaks and the ensemble average is subtracted from EEG segments. The limitation of this method is that it requires a simultaneously recorded ECG channel to find the locations of the peaks of the induced spikes. It is also sensitive to noise. Sahul et al. [86] introduced artifact cancellation technique in EEG by adaptive filtering using an ECG as reference channel. Strobach et al. [87] developed a two-pass adaptive filtering algorithm, where they first generated an artificial reference by ensemble averaging, which was more related to the real interference. Cho et al. [40] used a least square acceleration filter for detection of R-peak artifacts from EEG signal. Benesty et al. [88] used recursive least square method for artifact removal in physiological signals. The choice of algorithm dictates the computational cost and accuracy of the adaptive filter. Least mean-square (LMS) algorithm has a computational complexity of O (L) (L is the filter length). Adaptive filtering based on the recursive least square (RLS) algorithm has higher accuracy but it is computationally more complex with a complexity of O (L^2). The method is easy to implement but an additional sensor is required to provide a reference input which adds to the complexity of the hardware system and it also has an ability to operate on-line without preprocessing or calibration. It can operate on single channels as well as on non-linear domain [84].

R. Everson et al. [89], A. Hyvarinen et al. [90], R. Vigario et al. [91], W. Zhou [92], J. Iriarte et al. [93] and C. J. James et al. [94] have used Independent Component Analysis (ICA) for ECG artifacts detection and elimination in EEG. Independent component analysis (ICA) is a blind source separation technique in which recorded multi-channel signals are separated into their independent constituent components [95]. One of the major limitations of ICA is the requirement of the independent sources to be non-Gaussian. ICA has a major advantage

that a priori information is not required for the algorithm to function. Therefore, no reference signals are required. It reduces the number of sensors and makes it more suitable for portable devices. James and Gibson [96] introduced the concept of temporally constrained ICA, which used a reference signal to separate only the component of interest (e.g., ECG-related component). It eliminates the need for detecting the artifact component, but requires a peak detection algorithm to find the ECG artifact peaks and to generate the reference signal. Stephanie Devuyst et al. [85] introduced a new automatic method to eliminate ECG noise in an EEG or EOG. It is based on a modified independent component analysis (ICA) algorithm which gives promising results while using only a single-channel EEG or EOG and the ECG. Hae-Jong Park et al. [17] proposed Energy Interval Histogram (EIH) method for ECG artifacts detection using smoothed nonlinear energy operator and optimal threshold. Ali Akber Dewan [97] has also used energy function and adaptive threshold for R-peak artifact detection in EEG. Zhou W. D. et al. [92] and J. A. Jiang et al. [41] used Wavelet Transform (WT) and Independent component analysis (ICA) method for ECG artifact removal in EEG signal and developed an automated method for detecting and eliminating ECG artifacts from EEG without an additional synchronous ECG. A suitable wavelet basis and scales used in the process are developed considering the properties of wavelet filters and the relationship between wavelet basis and characteristics of ECG artifacts. The selection of a proper scale is relative with respect to the sampling frequency of the EEG signal.

Morphological filters were used by Lanquart et al. [98] for removal of ECG artifacts. Artifact templates are defined and contaminated EEG signals is searched for artifacts parts of the signal that matches with the templates. Sung Pil Cho et al. [40] used least square acceleration based filter for ECG artifacts elimination in EEG signal. The method consisted of emphasizing ECG R-peak artifacts in EEG using LSA based filter, detection of R-peaks, generation of R-peak synchronized pulse, and ECG artifacts estimation and elimination using synchronous adaptive noise canceller (ES-ANC). G. Inuso et al. [99] developed a new combinational technique which combined Wavelet transform and Independent Component Analysis (WICA) and compared it with two other techniques based on ICA and wavelet de-noising. This technique has better artifact separation performance. WICA technique improves the performance of ICA because it projects the data onto a new space where the redundancy is higher and the artifacts features in frequency domain are fully explored. Moreover, WICA allows minimum information loss. Bogdan et al. [19] used Ensemble EMD and ICA method for ECG artifacts detection in EMG signals. In the matching pursuit (MP) based algorithm proposed by Yan-Bo Zhou et al. [100], the EEG signal is decomposed in to atoms using mixed over complete dictionary. The atoms that have similar morphological characteristics as of R-wave are detected and eliminated.

M. B. Hamaneh et al. [95] developed an automated algorithm for removal of ECG artifact. This method combines independent component analysis and continuous wavelet transformation, to identify and remove the ECG artifacts. The method outperforms algorithms that use general statistical features such as entropy and kurtosis for artifact rejection. Xavier Navarro et al. [101] developed a combination of empirical mode decomposition and adaptive filtering to cancel ECG noise in EEG montage for infants. C. Kezi Selva Vijilal et al. [102] developed a hybrid soft computing technique called Adaptive Neuro-Fuzzy Inference System (ANFIS) to estimate the interference and to separate the EEG signal from EOG, ECG and EMG artifacts. Here adaptive noise cancellation using ANFIS is performed on EEG signal with various interferences. ANFIS Neural network recognize patterns and adapt themselves to cope with changing environments. Neuro Fuzzy takes the advantages of the combination of neural network and fuzzy logic.

Aysa Jafarifarmanda [103] developed a new adaptive functional link neural network and adaptive radial basis function network (FLN–RBFN) based filter to remove ocular, muscular and cardiac artifacts from EEG signal using adaptive noise cancellation (ANC). It is a process by which the interference signal can be filtered out by identifying a linear model between artifact and the corresponding immeasurable interference. S. Femilin et al. [104] developed a method called adaptive neuro fuzzy inference system tuned by differential evolution algorithm (ANFIS-DE) to estimate artifacts. ANFIS has the advantage of easy implementation and learning ability. ANFIS-DE has better artifacts removal performance and simpler structure as compared to the existing approaches. The advantages of DE approach are simple structure, ease of use, speed, and robustness. ANFIS-DE produces high SNR when compared with ANFIS technique. In some of the studies only Teager Kaiser Energy (TKE) operator has been used for the detection of artifacts because of its sensitivity to instantaneous changes in frequency dependent energy. In this sense it is regarded as an efficient tool for detecting spike like signal. However, our approach is different as we have implemented two mathematical operators, Slope Sum Function and Teager-Kaiser energy together for efficient artifact detection.

3.2 Proposed Slope Sum Function and Teager-Kaiser Energy method for ECG Artifacts Detection in NC Signals

A new method for ECG artifacts detection from noncardiovascular physiological signals (EEG, EOG and EMG) is being proposed. The proposed algorithm for ECG artifacts detection in non-cardiovascular (NC) signals uses Slope Sum Function (SSF) and Teager-Kaiser energy (TKE) operator with an adaptive threshold [42]. It does not require any additional synchronous

ECG channel. Performance of the algorithm has been evaluated on PhysioNet/CinC Challenge 2014 public training set [78-79] and MIT- BIH polysomnographic database [80]. Various techniques proposed in previous studies for ECG artifacts detection in NC signals and their removal have already been discussed in section 3.1.2. The objective of our study is to utilize detected ECG artifacts differs for filling the gap where ECG signal is corrupt or missing.

3.2.1 Proposed Algorithm

In this method, we have implemented two mathematical operators i.e. Slope sum function and Teager-Kaiser energy to enhance diminished ECG artifacts present in NC signals. It is essential to remove noise present in the signal in low and high frequency regions and to pass it from that frequency band in which the ECG artifact lies. Therefore, band pass filter and selection of its frequency band of interest is essentially first step to remove noises like baseline wander, motion artifacts, power line interference etc. Optimal pass-band for R-peak artifact have been investigated. An adaptive threshold is necessary for reliable peak detection. Therefore, we have incorporated it in the proposed algorithm. The block diagram of SSF-TKE method is shown in Figure 3.2.

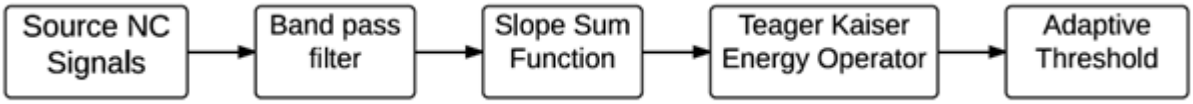

Figure 3.2: Block Diagram of ECG R-peak artifacts detection

ECG artifact detection consists of two major steps: Data pre-processing and R peak artifact detection using adaptive threshold. Firstly data pre-processing is done with a band pass filter of appropriate frequency range and then slope sum function is applied to highlight the R-peaks artifacts followed by application of TKE operator for enhancing these peaks. Finally, a moving average adaptive threshold is applied window wise for detection of R- peaks artifacts. The detected R-peaks artifacts have been validated with the given reference beat annotations.

The method is based on three features of ECG artifacts: the morphology (spike like sharp waves which are strongly correlated with the QRS complex of ECG), periodicity and its lack of correlation with the non-cardiovascular signals. The algorithm is executed as follows:

- **STEP-1:** (Data pre-processing): It involves filtering of NC signals through band pass filter of appropriate frequency range. The signal is passed through first order Butterworth band pass filter of frequency band in which energy of QRS complex (R-peak artifact) lies. This filter is best suited for applications requiring preservation of amplitude

linearity in the pass band region. It is precisely this feature that makes the Butterworth filter an ideal choice for conditioning the NC signals. The filter attenuates higher frequency noises like power line interference, electrosurgical noise etc. and also lower frequency noises like baseline wander, motion artifacts etc. The Butterworth band pass filter has also been chosen as its magnitude response is maximally flat in the pass band and monotonic overall. The band pass frequencies of 10-50 Hz, 5-45 Hz and 5-15 Hz yielded optimum R-peak artifact detection in EEG, EOG and EMG respectively.

- **STEP-2:** ECG artifacts in NC signals appear as poorly formed QRS complex as shown in Figure 3.1. Slope sum function has been implemented to enhance the slope of ECG (R-peak) artifacts and to suppress base NC signal. SSF is a cumulative sum of slopes that helps to enhance them.

  The ECG artifacts usually have steep slope similar to that of QRS complex with same temporal duration but with diminished amplitude. The window wise SSF is calculated as:

$$SSF(k) = \sum_{i=k}^{k} \Delta y_i, \Delta y_i = y_i - y_{i-1} \tag{3.1}$$

  Where, $'k'$ is the current sample number and 'w' is the window length. The window length $'w'$ is taken approximately equal to the duration of the ascending portion of R-peak artifact. The duration of rising slope of QRS complex is about 20 ms, hence we have chosen $'w' = 5$ samples or 20 ms at 250 Hz sampling rate. SSF transformed NC signals are depicted in Figure 3.3.

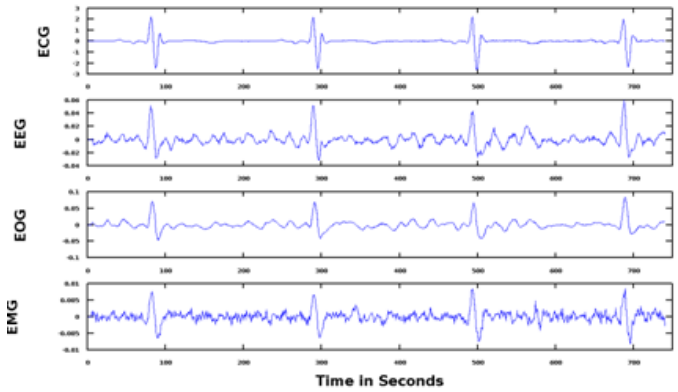

Figure 3.3: SSF transformed NC signals

- **STEP-3:** The implementation of TKE follows that of SSF. The TKE is an efficient tool for detecting spike like signals because of its sensitivity to instantaneous changes in

frequency dependent energy. For a discrete time series, the nonlinear energy operator Ψ and Smoothed nonlinear energy operator (SNEO) can be defined as follows [105]:

$$\Psi[x(n)] = x^2(n) - x(n+1)x(n-1) \tag{3.2}$$

$$\Psi_s[x(n)] = \Psi[x(n)] \otimes w(n) \tag{3.3}$$

where $\otimes$ is the convolution operator and $'w(n)'$ is Barthannwin window, a smoothing window function, of sample length 25. The reason for choosing Barthannwin window for convolving with the signal is that it has a main lobe at the origin and asymptotically decaying side lobes on both sides. For a linear combination of source signal 'x' and spike artifact 's', i.e., $y(n) = x(n) + s(n)$, where 'x' and 's' are uncorrelated. Operating $y(n)$ with non-linear energy operator 's' gives:

$$sy(n) = \Psi_s[y(n)] = \Psi_s[x(n)] + \Psi_s[s(n)] \tag{3.4}$$

For spike-dominant positions,$\Psi_s[x(n)] \approx 0$, $sy(n) \approx \Psi_s[s(n)]$, while for non-spike positions, $\Psi_s[s(n)] \approx 0$, $sy(n) \approx \Psi_s[x(n)]$. Using this property of SNEO, an ECG R-peak artifact is detected in the transformed SSF NC signals by finding an appropriate threshold 'T' that separates the spike regions from the background SSF signal with the condition $sy(n) > T$.

TKE operator further amplifies the enhanced R-peak artifacts in SSF transformed NC signal, resulting in excellent artifact detection. The normalized TKE of SSF of NC signals are shown in Figure 3.4.

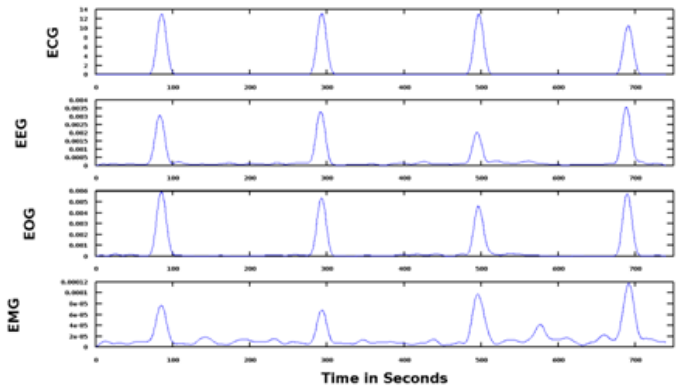

Figure 3.4: Normalized TKE of SSF transformed NC signals

- **STEP-4:** The threshold 'T' of TKE is defined as the mean energy multiplied by a scaling factor as follows:

$$T = C(\frac{1}{N}) \sum_{n=1}^{N} \Psi_s[y(n)] \tag{3.5}$$

Where 'N' is the number of samples in the signal and 'C' is scaling factor and its value is determined by experiment. We have heuristically set the value of 'C' as 1.4, 2.3 and 1.3 for EEG, EOG and EMG respectively. A single threshold cannot be applied to continuously varying physiological signals where spike energy of ECG artifacts in NC signals is variable and no prior precise knowledge on energy distribution of the spikes and background signal is available. Hence, we have developed an automated threshold adjustment method by dividing the normalized Teager Energy of transformed SSF NC signal into windows of 10 s duration (with 2 s overlap) and calculating window wise mean energy and threshold 'T'. Although the value of 'C' is empirically set, the value of threshold 'T' automatically adopts optimal value for each window depending upon the mean TKE of the window.

- **STEP-5**: Now R-Peak artifacts are detected from all the detected smoothed signal energy (sy) peaks of non-cardiovascular signals by following detection rules. First sample (peak) at position 'k' from N samples of the signal is selected and it's $\Psi_s[k]$ is compared with the threshold 'T'. If $\Psi_s[k] > T$, it will give 1st ECG R-peak artifact at position k_1, then go to step 6. Otherwise, select next sample and compare it's smoothed signal energy with 'T' and continue the procedure until the condition $\Psi_s[k] > T$ is satisfied.

- **STEP-6:** The 2nd R-peak artifact is detected using the periodicity characteristics of heart-beats. The expected position of 2nd R-peak, $k_{2exp.}$, will be

$$k_{2exp.} = k_1 + I_H \tag{3.6}$$

Where k_1 is the position of 1st R-peak artifact and I_H is the mean heart-beat interval.

The algorithm detects those peaks whose$\Psi_s[k] > T$ and are located within 0.20 s to 1.4 s from the 1st R-peak artifact, as candidate peaks for 2nd R-peak artifact. The peak nearest to the expected position $k_{2exp.}$ is selected as 2nd R-peak artifact. The procedure is repeated to detect subsequent R-peaks artifacts for which I_H will be a moving weighted average heart beat interval.

The flow chart of the proposed algorithm is given in Figure 3.5.

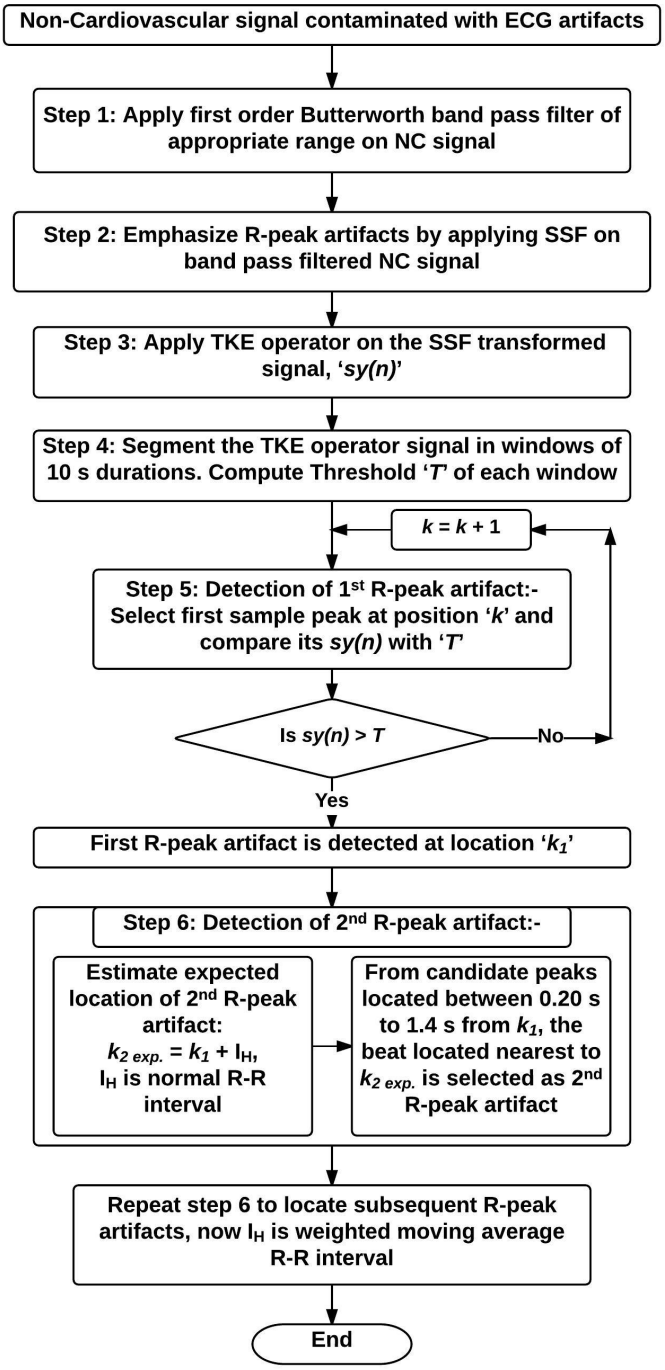

Figure 3.5: Flow chart of SSF-TKE method for ECG artifacts detection in non-cardiovascular signals

3.3 Performance Evaluation

The performance of the proposed algorithm has been evaluated on PhysioNet/CinC Challenge 2014 public training dataset and MIT-BIH polysomnographic database. The public training set contains 200 records, out of which (i) 110 records have EEG signals and (ii) 44 records have EOG and EMG signals. All the 18 records of MIT-BIH polysomnographic database contain EEG, whereas 5 of them have EOG and EMG signals as well.

The performance of beat detection has been evaluated in terms of statistical measures of sensitivity (Se), positive predictivity (PPV) and overall score which are given below:

$$Se_{gross} = 100 \cdot TP/(TP+FN) \tag{3.7}$$

$$PPV_{gross} = 100 \cdot TP/(TP+FP) \tag{3.8}$$

$$Se_{avg} = \frac{100}{n} \sum_{i=1}^{n} \frac{TP_i}{TP_i+FN_i} \tag{3.9}$$

$$PPV_{avg} = \frac{100}{n} \sum_{i=1}^{n} \frac{TP_i}{TP_i+FP_i} \tag{3.10}$$

where TP, FN, and FP denote true positive (matched beat; a detected beat located within 150 ms of the reference beat annotation), false negative (missed beat), and false positive (detection of false beat) respectively. TP_i, FN_i, and FP_i denote the statics for an individual record. 'n' are total number records in the dataset. The overall score is average of Se_{gross}, PPV_{gross} , $Se_{average}$, and $PPV_{average}$. The annotations were compared to the reference annotation using beat by beat algorithm defined by ANSI/AAMI EC38 and EC57 standards as implemented by the 'bxb' and 'sumstats' tool from the WFDB software package. The F_1 measure, which is a harmonic mean, has also been used to measure the accuracy of the algorithm:

$$F_1 = \frac{2 \cdot PPV \cdot S_e}{(PPV+S_e)} \tag{3.11}$$

The R-peak artifacts detection performance of SSF-TKE method on NC signals in PhysioNet/CinC Challenge 2014 public training dataset has been reported in appendix Table A.1. However, the results on EEG, EOG and EMG signals of PhysioNet/CinC Challenge 2014

training dataset containing significant number of artifacts (subsets of the dataset) are presented through Tables 3.1, 3.2 and 3.3 respectively.

Table 3.1: ECG artifacts detection performance of SSF-TKE method on PhysioNet/CinC Challenge 2014 training dataset (signals with significant number of artifacts) in EEG signals

Record No.	Total No. of beats	Total detected beats	Matched beats	EEG		
				Sensitivity (%)	Predictivity (%)	F_1 Score (%)
102	685	681	673	98.25	98.83	98.54
108	907	868	805	88.75	92.74	90.70
114	631	633	631	100.00	99.68	99.84
119	741	738	723	97.57	97.97	97.77
121	883	832	740	83.81	88.94	86.30
122	631	627	585	92.71	93.30	93.00
123	734	742	730	99.46	98.38	98.92
129	685	690	581	84.82	84.20	84.51
130	838	813	771	92.00	94.83	93.39
136	695	681	654	94.10	96.04	95.06
141	702	706	655	93.30	92.78	93.04
145	708	687	611	86.30	88.94	87.60
147	872	863	855	98.05	99.07	98.56
149	727	723	708	97.39	97.93	97.66
151	806	784	749	92.93	95.54	94.22
154	920	849	782	85.00	92.11	88.41
159	710	722	635	89.44	87.95	88.69
163	884	843	790	89.37	93.71	91.49
164	872	823	764	87.61	92.83	90.14
180	884	805	734	83.03	91.18	86.91
182	791	778	732	92.54	94.09	93.31
193	597	605	585	97.99	96.69	97.34
197	681	690	662	97.21	95.94	96.57
199	666	652	642	96.47	96.34	96.40
Total	**18250**	**17835**	**16797**			
Average				**92.42**	**94.17**	**93.27**
Gross				**92.04**	**94.18**	**93.10**

Table 3.2: ECG artifacts detection performance of SSF-TKE method on PhysioNet/CinC Challenge 2014 training dataset (signals with significant no. of artifacts) in EOG signals

Record No.	Total No. of beats	Total detected beats	Matched beats	EOG		
				Sensitivity (%)	Predictivity (%)	F_1 Score (%)
103	707	705	684	96.75	97.02	96.88
106	888	820	764	86.04	93.17	89.46
108	907	832	675	74.42	81.13	77.63
111	690	696	667	96.67	95.83	96.25
112	707	707	641	90.66	90.66	90.66
113	665	688	556	83.61	80.81	82.19
117	868	816	751	86.52	92.03	89.19
119	741	742	740	99.87	99.73	99.80
123	734	741	731	99.59	98.65	99.12
124	787	770	717	91.11	93.12	92.10
126	635	663	518	81.57	78.13	79.81
132	869	853	822	94.59	96.37	95.47
138	740	737	723	97.70	98.10	97.90
143	920	830	675	73.37	81.33	77.15
144	527	526	523	99.24	99.43	99.33
146	794	778	739	93.07	94.99	94.02
149	727	720	615	84.59	85.42	85.00
155	745	729	708	95.03	97.12	96.06
161	670	703	580	86.57	82.50	84.49
162	690	681	560	81.16	82.23	81.69
164	872	822	691	79.24	84.06	81.58
175	723	723	694	95.99	95.99	95.99
177	689	704	601	87.23	85.37	86.29
178	774	772	765	98.84	99.09	98.96
179	861	820	753	87.46	91.83	89.59
181	655	685	541	82.60	78.98	80.75
183	697	701	695	99.71	99.14	99.42
189	721	703	642	89.04	91.32	90.17
190	698	703	624	89.40	88.76	89.08
198	699	692	638	91.27	92.20	91.73
1023	635	663	518	81.57	78.13	79.81
1503	751	730	656	87.35	89.86	88.59
Total	**23786**	**23455**	**21207**			
Average				**89.43**	**90.39**	**89.88**
Gross				**89.16**	**90.42**	**89.78**

Table 3.3: ECG artifacts detection performance of SSF-TKE method on PhysioNet/CinC Challenge 2014 training dataset (signals with significant no. of artifacts) in EMG signals

Record No.	Total No. of beats	Total detected beats	Matched beats	EMG		
				Sensitivity (%)	Predictivity (%)	F_1 Score (%)
111	690	702	609	88.26	86.75	87.50
119	741	741	726	97.98	97.98	97.98
123	734	736	727	99.05	98.78	98.91
124	787	741	579	73.57	78.14	75.79
138	740	726	695	93.92	95.73	94.82
144	527	502	377	71.54	75.10	73.28
146	794	774	655	82.49	84.63	83.55
149	727	627	427	74.69	73.98	74.33
153	566	627	427	75.44	68.10	71.58
155	745	719	607	81.48	84.42	82.92
161	670	681	649	96.87	95.30	96.08
175	723	729	532	73.58	72.98	73.28
178	774	770	755	97.55	98.05	97.80
182	791	772	609	76.99	78.89	77.93
183	697	729	572	82.07	78.46	80.22
Total	**10706**	**10683**	**9062**			
Average				**84.37**	**84.49**	
Gross				**84.64**	**84.83**	**84.74**

Looking at the results of Table 3.1 to Table 3.3 on PhysioNet/CinC Challenge 2014 public training dataset, one can observe that average sensitivity and average predictivity for signals having large quantum of artifacts is quite high. For example in the EEG signal of record numbers 114, 123 and 147 (Table 3.1), average sensitivity and average predictivity of artifact detection lie in the range of 98 to 100%, whereas EOG and EMG signals of record no. 119, 123 and 178 also show almost the same trend, which can be seen in Tables 3.2 and 3.3 respectively. This can be considered as an excellent artifact detection performance of the proposed algorithm. We have compared our results with those of other studies in Table 3.4. It is seen that proposed SSF-TKE results have outperformed other studies. To the best of our knowledge artifact detection in EMG signals of PhysioNet/CinC Challenge 2014 public training dataset have not been reported by any researcher.

Table 3.4: ECG artifacts detection performance comparison of SSF-TKE method on PhysioNet/CinC Challenge 2014 training dataset in NC signals

Signal Type	Algorithm	Total No. of beats	Average (%)		Gross (%)		
			Sensitivity (%)	Predictivity (%)	Sensitivity (%)	Predictivity (%)	F_1Score (%)
EEG	**SSF-TKE**	18250 beats (24 records)	**92.42**	**94.17**	**92.04**	**94.18**	**93.10**
	Galeotti et al. [106]	NR (24 records)	62.49	90.42	61.72	90.73	73.46
EOG	**SSF-TKE**	32035 (All 44 records)	82.76	83.09	82.73	83.40	83.06
		23786 (32 records)	**89.43**	**90.39**	**89.16**	**90.42**	**89.78**
	Galeotti et al.	NR (32 records)	58.50	85.31	59.39	87.40	70.72
EMG	**SSF-TKE**	32035 (All 44 records)	**62.45**	**62.71**	**62.15**	**62.54**	**62.34**

Table 3.5: ECG artifacts detection performance of SSF-TKE method on MIT-BIH Polysomnographic database (signals with significant no. of artifacts) in EEG signals

Record No.	Total No. of beats	Total detected beats	Matched beats	Sensitivity (%)	Predictivity (%)	F_1 Score (%)
slp01a	7806	7807	7707	98.73	98.72	98.73
slp01b	11467	11532	10923	95.26	94.72	94.99
slp02a	16145	15252	14374	89.03	94.24	91.56
slp02b	11317	10397	9262	81.86	89.08	85.32
slp37	30611	27186	22887	74.76	84.19	79.20
slp45	27686	27170	22802	82.36	83.92	83.13
slp66	15775	15458	11403	72.29	73.77	73.02
slp67x	5374	5294	4454	82.88	84.13	83.50
Total	**126181**	**120096**	**103812**			
Average				**84.65**	**87.85**	**86.18**
Gross				**82.27**	**86.44**	**84.31**

The R-peak artifacts detection performance of SSF-TKE method on NC signals in MIT-BIH Polysomnographic database has been reported in appendix Table A.2. However, ECG artifact detection performance of SSF-TKE method on EEG, EOG and EMG signals of the database with significant amount of ECG artifacts are shown in Table 3.5 and Table 3.6 respectively.

Table 3.6: Performance of SSF-TKE method for ECG artifact detection on MIT-BIH Polysomnographic database (signals with significant no. of artifacts) in EOG and EMG signals

Record No.	Total No. of beats	Total detected beats	Matched beats	Sensitivity (%)	Predictivity (%)	F_1 Score (%)
			EOG			
slp32	21718	22088	17189	79.14	77.82	78.48
slp37	30611	27114	21874	71.46	80.67	75.79
slp41	25884	26394	21252	82.10	80.52	81.30
slp45	27686	27480	26084	94.21	94.92	94.56
slp48	24711	26101	19414	78.56	74.38	76.42
Total	**130610**	**129177**	**105813**			
Average				**81.09**	**81.66**	**81.31**
Gross				**81.01**	**81.91**	**81.46**
			EMG			
slp41	25884	27043	18226	70.41	67.40	68.87
slp45	27686	27585	24208	87.43	87.76	87.60
Total	**53570**	**54628**	**42434**			
Average				**78.92**	**77.58**	**78.24**
Gross				**79.21**	**77.68**	**78.44**

It is observed that efficiency of beat detection is quite high in some of the records namely EEG (slp 01 a), EOG and EMG (slp 45). The performance of our method may be considered comparable or even better than those of other studies included in the Table 3.7, in view of the fact that these studies have excluded a large no. of records from the dataset and even in the selected records, they have reported results only on part of the records (on selected no. of beats) as is evident by the number of beats, we have mentioned in the Table 3.7 against each study. It appears that they may have taken into account only those beats where the performance of their methods is higher and their reported results do not reflect the real performance of their algorithms. To the best of our knowledge we have not found any other similar works in case of EOG and EMG to compare with.

Table 3.7: Performance comparison of SSF-TKE method on MIT-BIH Polysomnographic database for ECG artifacts detection in NC signals

Signal Type	Algorithm	Record No.	Total No. of beats	Average (%)		Gross (%)		
				Sensitiv -ity	Predictiv -ity	Sensiti -vity	Predicti -vity	F_1 Score
EEG	Jiang et al. (CWT) [41]	Part of 3 records slp01, slp02 and slp67	16690	98.34	99.40	98.41	99.47	98.94
	SSF-TKE	Full records slp01a, slp01b, slp02a	35418	**94.34**	**95.89**	**93.18**	**95.41**	**94.29**
	Zhou et al. (MP based algorithm) [100]	Part of 2 records slp01 and slp02	17054	-	-	98.83	99.47	99.15
	SSF-TKE	Full records slp01a and slp02a	23951	**93.88**	**96.48**	**92.20**	**95.76**	**93.94**
	SSF-TKE	All 18 records	368364	64.94	67.06	60.79	62.74	61.75
EOG	**SSF-TKE**	All 5 records	130610	**81.10**	**81.66**	**81.01**	**81.91**	**81.46**
EMG	**SSF-TKE**	All 5 records	130610	61.57	60.83	61.94	61.22	61.58

3.4 Discussion

Our ECG artifacts detection algorithm is based on detection of the most prominent part of the QRS complex using slope sum function and Teager Kaiser energy. The algorithm is very simple, yet effective for ECG artifact detection. ECG artifact in NC signals appears as poorly formed QRS complex and more often it appears diphasic than triphasic. It usually has steep slopes similar to that of QRS complex with same temporal duration but with diminished amplitude [107]. SSF enhances the slope of ECG R-peak artifacts in NC signals from the background base signal and noise. TKE operator further amplifies the enhanced R-peak artifacts in SSF transformed NC signal, resulting in excellent artifacts detection. It operates on single

channel and can be implemented in real time.

The selection of threshold plays an important role in efficiency of ECG artifacts detection. A new adaptive threshold algorithm has been developed, which optimizes the threshold 'T' from the mean TKE of each 10 s window length, instead of calculating one value of threshold 'T' for the whole signal from mean energy of entire signal. Thus, the algorithm automatically adjusts the value of threshold 'T' depending on the mean energy of signal over the window length. When the mean TKE of the signal is low over a period, the algorithm adopts lower value of threshold 'T' and vice-versa. Thereby the algorithm selects window wise optimal value of threshold 'T', which has increased accuracy of artifacts detection and minimized missed beats (FNs) and false detection (FPs).

The performance of SSF-TKE method has been evaluated on NC signals by applying two methods of ECG artifacts detection, namely (i) applying TKE operator directly on the band pass filtered signal, and (ii) applying TKE on the SSF transformed signal on EEG, EOG and EMG signals. The performance comparison of our proposed SSF-TKE algorithm on EOG signal, contaminated with R-peak artifacts, with that of direct TKE method is shown in Figure 3.6.

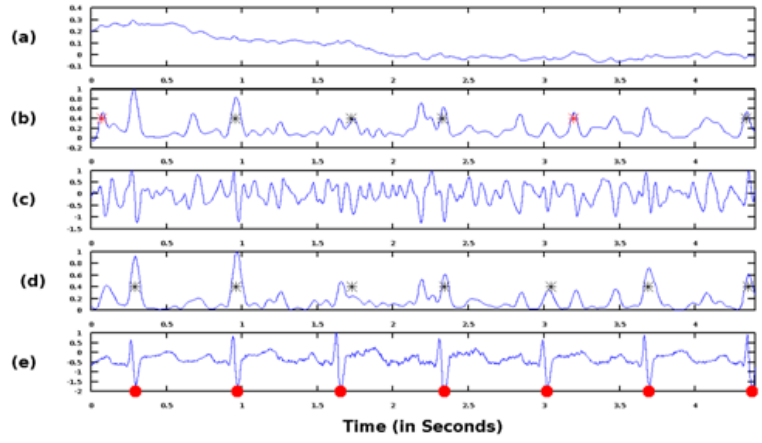

Figure 3.6: (a) EOG signal contaminated with ECG artifacts; (b) Teager Kaiser Energy operator directly applied on band pass filtered EOG signals (direct TKE method); (c) SSF transformed band pass filtered EOG signal; (d) TKE operator applied on the SSF transformed EOG signal (SSF-TKE method); (e) Reference ECG beat annotations are shown as (●). Matched beats are shown as (*) and missed beats by (*)

It can be seen in Figure 3.6 (b) that first and fifth detected beats are unmatched beats and ECG artifact corresponding to sixth reference beat annotation is not detected by direct TKE method; whereas all the ECG artifacts have been correctly detected by SSF -TKE method as shown in Figure 3.6 (d). Thus, R-peak artifacts detection performance of SSF-TKE method

in NC signals is better than that of TKE method. The comparison of most commonly used techniques in ECG artifacts detection with SSF-TKE method on a number of factors is given in Table 3.8 [84].

Table 3.8: A comparison of various artifact detection techniques with the proposed algorithm

Features	No additional sensor required	No a priori user input required	Automatic artifact removal	Can operate on line	Can operate on single channels	Can operate in the non-linear domain
Adaptive filter	X	X	√	√	√	√
Wiener filter	√	X	√	X	√	√
Kalman filter	√	X	√	√	√	√
Particle filter	√	X	√	√	√	√
Independent Component Analysis	√	√	X	√	X	√
Canonical Correlation Analysis	√	√	X	X	X	√
Single Channel ICA	√	√	X	X	√	√
Dynamical Embedding ICA	√	√	X	X	√	√
Dynamical Embedding SSA	√	√	√	X	√	X
Morphological Component Analysis	√	X	√	X	√	X
Wavelet ICA	√	√	X	X	√	√
Empirical Mode Decomposition ICA	√	√	X	X	√	√
Proposed SSF-TKE	√	√	NA	√	√	√

All the previous studies have been carried out for detection and elimination of ECG artifacts to get clean NC signals for diagnostic purpose i.e. from EEG for studies of epilepsy and sleep disorder, and from EMG for study of Parkinson diseases and control of prosthesis.

It can be seen from Table 3.8 that SSF-TKE algorithm has the advantages of operating on line and on single channel. It also does not require a priori user input and can operate on non-linear domain. Furthermore, no additional channels are required for artifact detection. The performance of proposed algorithm relies on the quantum of ECG artifacts present in NC signals, which depends on the proximity of recording sensors to the heart. ECG artifacts may also occur inconsistently in NC signals. Since validation of detected beats is done with reference beat annotations, FN beats will be erroneously higher as compared to the actual missed beats (FN) by the algorithm and thereby calculated detection rate will be erroneously lower as compared to the actual detection rate in such signals. In EEG signal of record no. 114, the proposed method has achieved sensitivity and predictivity of 100% and 99.68% respectively with F1 score of 99.84%. In EOG signal of record no. 119, SSF-TKE method has achieved sensitivity and predictivity of 99.87% and 99.73% respectively. Similarly in record no. 123, the method has achieved F_1 score of 98.10%, 98.77% and 99.52% for EEG, EOG and EMG respectively. This proves the effectiveness of the proposed method in R-peak artifacts detection in NC signal contaminated with ECG artifacts.

3.5 Conclusion

SSF-TKE method is an efficient method for detecting ECG artifacts in non-cardiovascular signals without the need of an additional ECG channel. The method uses Slope Sum Function and Teager-Kaiser Energy operator with adaptive threshold algorithm to detect ECG R-peak artifacts in NC signals. The performance of SSF-TKE method on NC signals of PhysioNet/CinC Challenge 2014 public training dataset and MIT-BIH Polysomnographic database has shown that it is efficient in ECG artifact detection. The quantum of ECG artifacts in NC signals depends on the proximity of recording sensors to the heart, that's why the R-peak artifacts detection may be higher in EOG signal as compared to that in EEG and EMG signals. The SSF-TKE method has shown improved ECG artifacts detection results as compared to those of direct application of Teager energy operator on non-cardiovascular signals. The proposed novel algorithm of ECG artifacts detection in EEG, EOG and EMG physiological signals have demonstrated that the method can be efficiently implemented for biomedical signal processing with accurate analysis.

Chapter 4

Heart beat detection from cardiovascular signal

4.1 QRS (R-peak) detection in ECG

4.1.1 Introduction

The human heart generates strong electric field that induces skin potential at the surface of body. These bio-potentials are picked up by surface electrodes and recorded as ECG which reveals information about atrial and ventricular activities of heart. Readily recognizable features of ECG wave pattern are designated by letters P-QRS-T. However, QRS complex is the most prominent feature in the ECG because of its high amplitude compared to the P and T waves. In addition to the significance of various features of the QRS complex, the timing of the sequence of QRS complexes over long period of time is also very important. These inter-complex timings are readily measured by recording the occurrences of the peaks of the large R waves. Fluctuations in the sequence of inter-beat intervals can be used to assess the presence or likelihood of cardiovascular disease [108]. Any cardiac dysfunction associated with excitation from ectopic centers in the myocardium may lead to premature complexes (atrial or ventricular), which change the morphology of the waveform and the duration of the R-R interval. The occurrence of multiple premature complexes is considered clinically important, as it indicates disorders in the de-polarization process preceding the critical cardiac arrhythmia. The energy of heart beats is mainly located in the QRS complex, therefore, an accurate QRS detector is one of the most important components of ECG analysis. It is very important to accurately detect heartbeats, because it gives information about the heart rate [4] and heart rate variability. Physicians all over the world are using ECG to diagnose cardiac diseases which are one of the main causes of mortality in our society.

We got very promising results in our earlier work on ECG artifact detection in NC signals using SSF-TKE method, which is reported in chapter 3, and that encouraged us to use it in our further work on QRS detection. The motivation behind this work is to increase the accuracy of QRS detection in multimodal physiological signals for robust heart rate estimation for ICU patients. In this chapter, a modified version of SSF-TKE is being proposed that is simple and computationally fast QRS detection algorithm.

4.1.2 Related Works

Analysis of ECG provides important and relevant information about the state of heart. Advancement in technology has digitized ECG information enabling it to be processed by computers. In the last three decades many software algorithms have been developed for QRS detection. It is difficult to detect the R-peak because different sources of noise may be present in the same frequency band. QRS beat detection algorithms have two important steps: QRS enhancement and QRS detection. The QRS enhancement is used to enlarge the QRS complex relative to other ECG features (P wave, T wave and noise) and is referred to as pre-processing or feature extraction. The QRS detection is used to demarcate QRS complex by providing the onset and offset points of the QRS complex, especially, the location of the prominent R peak. There are several signal processing techniques that have been used to emphasis the QRS segment in time, frequency and time-frequency domain. Kohler et al. [4] and Elgendi et al. [109] have given an overall review of QRS detection methods based on the principles used for the detection, as summarized below:

1. **Algorithms based upon amplitude and first derivative**: Frisen et al. [5], Fraden J. et al [110], Moriet-Mahoudeaux P. [111] and Gustafson [112] have used this technique for QRS detection. In this technique, amplitude threshold is applied to the ECG signal usually followed by its first derivative to enhance the slope of the QRS complex, followed by a second threshold. The algorithm is simple and usually contains a threshold and firsts derivative equation for feature extraction. However, main drawback of this method is that signal noise is not removed properly.

2. **First derivative QRS detection algorithm:** In this beat detection technique, a first order differentiator is commonly used as a high pass filter to eliminate base line wander and to create zero crossing in the location of the R peaks. Okada et al. [113] used first derivative of ECG signal followed by threshold. Pan J. Tompkins et al. [114] applied digital filter to ECG signal followed by first derivative and threshold. Arzeno et al. [115] and Benitez et al. [116] used first derivative before applying Hilbert transform followed by threshold. Zhang et al. [117] used it before applying wavelet transform followed

by threshold. First derivative based methods are often used in real time analysis for large dataset since they do not require extensive computations. The first derivative does not remove high frequency noise but it reduces motion artifacts and base line wander. First derivative class of algorithm is simple and contains one equation for feature extraction. Complexity increases with segmentation. One of the most popular single lead first derivative based QRS detection methods is the Hamilton-Tompkins algorithm which is an improved version of the originally proposed Pan-Tompkins method in 1985 that used patient specific threshold for QRS peak detection.

3. **First and second derivative method:** QRS enhancement algorithms compute the first and second derivatives of the measured ECG signal independently. A linear combination of the magnitude of these derivatives is then used to emphasis the QRS complex area relative to other ECG features. However, the signal noise is not removed properly. First and second derivative classes of algorithms are simple and contain only up to four equations for feature extraction. The complexity of this class of algorithms derives from the number of equations used and segmentation, if applied. Balda et al. [118], Ahlstrom et al. [119] calculated first and second derivatives of the ECG signal and a threshold criterion for QRS detection was applied for the linear combination of the derivatives in the algorithms.

4. **Digital Filters:** Many sophisticated digital filters have been used for QRS enhancement. Engelse et al. [120] used first derivative of ECG signal followed by digital filters and threshold. Pan J. et al. [114] used first derivative after applying band-pass filter to the ECG signals. The band-pass filtered signal was differentiated to emphasis high signal slopes, suppressing smooth ECG waves and baseline wander. Ulusar et al. [121] applied band-pass filter before Hilbert transform followed by threshold. Zhang et al. also used band pass filter followed by first derivative before applying wavelet transform then followed by threshold. The digital filter can increase signal to noise ratio (SNR) depending on the nature of the filter and its order.

5. **Mathematical morphology:** The use of mathematical morphology operators for QRS detection was introduced by Trahanias [122]. Yongli et al. [123] applied mathematical morphology filtering to ECG signals followed by threshold. Zhang et al. [124] used the first derivative after multiscale mathematical morphology, followed by threshold in order to remove motion artifacts and base line drift. The signal noise is partially addressed by the mathematical morphology class of algorithms. The use of low pass filter improves SNR.

6. **Empirical mode decomposition (EMD):** It was introduced by Xing et al. [125] for nonlinear and non-stationary signal analysis. In this method any complex data set can be decomposed into finite and often small number of intrinsic mode functions (IMF) which admit well behaved Hilbert transforms. Usually when raw ECG signals are decomposed into number of IMFs, the combination of IMFs produces a resulting signal where the QRS complex is more pronounced. The complexity increases with the number of processed ECG segments. Arafat et al. [126] applied high pass filter followed by EMD filtering and threshold.

7. **Hilbert transform:** The use of the Hilbert transform for QRS detection was proposed by Zhou et al. [127] and also by Nygards et al. [128] independently. The Hilbert transform does not improve the SNR itself. Therefore, some investigators filter the signal before applying the Hilbert transform. Benitez et al. [116] used a band-pass filter of 8–20 Hz to remove muscular noise and maximize the QRS. The primary disadvantage of this method is the increased computational burden required for FFT calculations compared to the time domain approaches. Hilbert transform techniques generally have a large computation overhead [129]. Hilbert transform method is sensitive to noise, baseline wander and heart rate variation [130].

8. **Filter banks:** It is another technique of QRS detection, which decomposes the bandwidth of the input ECG signal into sub-band signals with uniform frequency bandwidths, each of constant length. The sub-bands can be down sampled, since the sub-band bandwidth is much lower than the input signal. The sub-bands provide information from various frequency ranges; thus, it is possible to perform time- and frequency-dependent processing of the input signal. Afonso et al. [131] and Zhang et al. [132] applied filter banks to ECG signal followed by threshold. The filter banks significantly improve the SNR for Gaussian noise compared to the mean and median averaging methods [133]. The drawback of using filter banks is relatively high computational cost due to the involvement of a large amount of multipliers in the FIR filters [132].

9. **Wavelets Transform:** Dinh et al. [134] and Szilagyi et al. [135] applied wavelet transform (WT) to ECG signal followed by threshold. [136-138] also primarily used wavelet transform for QRS detection. WT does not increase the SNR, but the SNR can be improved by selecting the coefficients with the largest amplitude [138]. Choice of the wavelet scale varies throughout the literature. Szilagyi [139] used wavelet scales of 2^3 and 2^4, while Xiaomin et al. [140] used from scales of 2^2 to 2^4 to detect QRS complexes. Martinez et al. [141] recommended re-sampling of the signal at 250 Hz.

10. **Artificial neural network:** ANN has been widely applied in non-linear signal classification and optimization. In many applications, their performance was shown to be superior to classical linear approaches. It has been used by [146-148]. Liyang et al. [136] applied wavelet transform to ECG followed by neural networks. Xue et al. [142] applied NNs, as a filter, to ECG signal followed by a matched filter. NN are highly sensitive to noise [143]. In the context of QRS detection, NN has been used as adaptive non-linear predictor (Hu and Tompkin) [142, 144, and 145]. It often needs a considerable amount of memory to store the neuron weights.

11. **Matched filtering approach:** After some analog preprocessing steps such as automatic gain control, the ECG signal is digitized and further processed by a comb filter (low pass) with a notch at 50 Hz and a band pass filter with cut-off frequencies at 15 Hz and 40 Hz. This digital filter stage is followed by a matched filter for further improvement of the signal-to-noise ratio (SNR). The match filter improves SNR [149], however, it is computationally expensive because of the sample-by-sample moving comparison with the template along the ECG signals.

12. **Syntactic algorithm:** It detects a QRS complex by itself [150–152]. The signal to be analyzed by a syntactic method is assumed to be a concatenation of linguistically represented primitive patterns; i.e., strings. The method is sensitive to noise and has a high computational cost compared to other approaches.

13. **Zero Crossing Method:** Kohler et al. [4], Mallat et al. [153] and Zheng et al. [137] have primarily used zero crossing method for QRS detection. The method is simple but computationally inefficient and is sensitive to noise.

14. **Singularity Method:** Xing H. et al. [125] have used singularity technique along with other techniques for QRS detection. The singularity approach load is more complex than the zero- crossing approach. It is computationally inefficient and sensitive to noise.

15. **Genetic algorithm:** R. Poli et al. [154] have applied genetic algorithms to a combined design of optimal polynomial filters for preprocessing of the ECG and the parameters of a decision stage.

16. **Length and energy transforms:** F. Gritzali [155] and Kohler [4] have applied length and energy transforms for QRS detection. The transforms are defined for multichannel ECG signals but may also be used for single-channel ECG analysis. The authors state that both transforms are superior to conventional transforms for feature extraction, whereas the length transform works particularly good in cases of small QRS complexes

17. **Area estimation and window averaging :** R. S. Anand et al. [156] have used 3-sample area estimation and M-sample window averaging with threshold for QRS segment detection.

4.2 Beat detection from ABP

The ABP waveform contains rich information about the cardiovascular system such as heart rate, systolic, mean, and diastolic arterial pressures to estimate location of heart beats. Reliable and accurate ABP pulse detection is crucial for beat-by-beat extraction. The 'wabp' algorithm given by Zong et al. [13] consists of three components: a low-pass filter, a windowed and weighted slope sum function, and a decision rule for detecting onset of ABP pulse. The algorithm employs a windowed and weighted slope sum function (SSF) to extract ABP waveform features. Adaptive threshold and search strategies are applied to the SSF signal to detect ABP pulses and to determine their onsets.

There is a delay between onset of ABP pulse and R-peak of ECG. This delay is known as pulse wave transit time (PWTT). The ECG-ABP PWTT includes the pulse wave transmission time from arota to redial artery as well as pre-ejection (PEP) of the heart. PWTT is closely related to pulse wave velocity (PWV). Zong W. et al. [26], Gosse P. et al. [157] and Franchi D. et al. [158] have studied ECG – ABP pulse delay/transit time (PTT). The duration of PTT varies from 15 ms to 40 ms.

'wabp' locate arterial blood pressure (ABP) pulse waveforms in a continuous ABP signal. The detector algorithm is based on analysis of the first derivative of the ABP waveform. This program detects heart beats (pulse waveforms) in a continuous arterial blood pressure (ABP) signal. This version of wabp works best with ABP signals sampled at 125 Hz, but it can analyze ABPs sampled at any frequency using on-the-fly re-sampling provided by the WFDB library. 'wabp' has been optimized for adult human ABPs. The output of 'wabp' is an annotation file in which all detected beats are labelled normal. 'wabp' can process records containing any number of signals, but it uses only one signal for ABP pulse detection.

4.3 Proposed algorithm for R-peak detection

The good performance of SSF-TKE method in R-peak artifact detection in NC signals motivated us to implement the algorithm in R-peak detection in ECG signals as well. SSF-TKE is a simple and fast algorithm for QRS detection that uses only one morphological feature of ECG i.e. QRS waveform; its steep QR and RS slopes and periodicity. Slope sum function (SSF) calculate cumulative sum of the first difference of signal across a window and amplifies

steep slopes of QRS and TKE operator further amplifies QRS spikes. The algorithm uses eye-closing period of 200 ms and moving average R-R interval of previous eight beats to select the next beat among candidate beats that have reduced FP beats even in noisy signals. The algorithm selects window wise optimal value of adaptive threshold, which has increased accuracy of beat detection and minimized missed beats (FNs) and false detection (FPs). Some modifications have been made in SSF-TKE method in preprocessing stage and selection of 'C' value in adaptive threshold as described below. QRS complex is the most distinct and visible morphological feature of ECG. However, ECG signals are sometimes contaminated by different sources of noise. These artifacts often have similar shape as that of QRS complex that makes QRS detection difficult. Hence preprocessing of signals is necessary to reduce the noise and enhance QRS complexes for proper beat detection.

The flow chart of modified SSF-TKE method is given in Figure 4.1.

4.3.1 Pre-processing

Removal of pacemaker beats: Paced beats are high frequency spikes in ECG recording produced by electrical activity of pacemaker implanted in the patients. Filtering of the signal widens paced peaks making it difficult to distinguish them from normal QRS complex, hence ideally paced beats should be detected and removed at the analog level itself before any filtering of the signal. Since, we are using databases in digital form, the following method has been used to detect and remove paced beats. The ECG signal is segmented into windows of 256 ms length for paced beat detection. The absolute values of first derivative of the signal are found for each window. Since the frequency of paced beat is high, the amplitude of its slope will also be high. It is observed that if the value of amplitude exceeds the threshold value of 2 then the location corresponds to paced beat is removed.

Application of band pass filter: Most of the energy of QRS complex in ECG lies between frequency range of 3 Hz-40 Hz. The SSF-TKE method uses third order Butterworth filter of 5–40 Hz to suppress high frequency noise and remove baseline wander in R-peak detection.

4.3.2 Adaptive threshold

Adaptive threshold has been calculated on 10 s window with overlap of 2 s and the mean value is scaled by a factor 'C' of 1.4 for QRS detection.

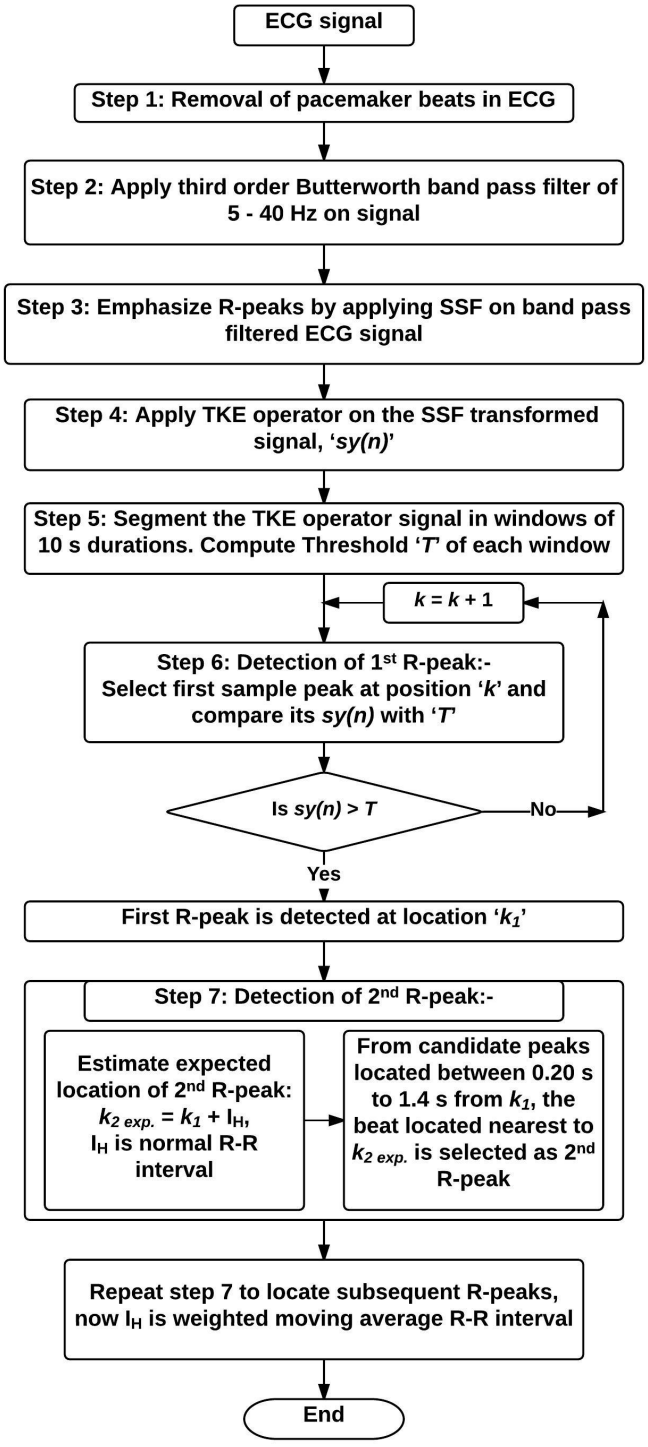

Figure 4.1: Flow chart of modified SSF-TKE method for R-peak detection in ECG signal

4.4 Performance analysis

The proposed SSF-TKE method has been implemented on different standard datasets namely, PhysioNet/CinC 2014 Challenge training dataset, MIT-BIH Polysomnographic database, MIT-BIH noise stress test database, MIT-BIH Arrhythmia database and MGH/MF waveform database.The SSF-TKE method has achieved overall scores of 99.79% and 93.76% in beat detection on MIT-BIH Polysomnographic database and MIT-BIH noise stress test database respectively, which are better than the results of other well-known individual detectors. In PhysioNet/CinC Challenge 2014 public training dataset and MGH/MF waveform database, SSF-TKE has achieved overall scores of 92.53% and 90.05% respectively that are comparable with the scores of other detectors. The performance of our method in ECGs with variable cardiac rhythm in MIT-BIH Arrhythmia database and MGH/MF waveform database is slightly lower than those of other QRS detectors. The R-peak detection results of SSF-TKE method on PhysioNet/CinC Challenge 2014 public training dataset, MIT-BIH Polysomnographic database, MIT-BIH Arrhythmia database and MGH/MF waveform databases are given in appendix Table A.3, Table A.4, Table A.5 and Table A.6 respectively.

It can be seen from Table 4.1 that SSF-TKE method has achieved higher predictivity in PhysioNet/CinC Challenge 2014 training dataset, MIT-BIH Polysomnographic database and MIT-BIH noise stress test database as compared to those of other QRS detectors, whereas in MGH/MF waveform database it is comparable with the top predictivity achieved by other detectors. This is because we have designed our algorithm to keep false detections (FPs) low to reduce errors in heart rate estimation.

However, in MIT-BIH Arrhythmia database the beat detection performance of SSF-TKE method is slightly lower than that of other detectors. Since SSF-TKE method considers only one morphological feature of ECG i.e., QRS waveform and its rhythm, its performance is slightly lower in ECGs with variable cardiac rhythm; particularly in atrial premature beats (APB) and/or ventricular premature beats (VPB). There are 13 records with atrial premature beats and/or ventricular premature beats in MIT-BIH Arrhythmia database. SSF-TKE method has achieved gross sensitivity, predictivity and F1 score of 99.69%, 99.56% and 99.62% respectively on 35 records of MIT-BIH Arrhythmia database (excluding 13 records of ECGs with APB and VPB).

The performance of modified SSF-TKE method in R-peak detection on different standard databases and comparison of its performance with that of other QRS detectors has been reported in Table 4.1.

Table 4.1: Performance comparison of SSF-TKE method in heart beat detection in ECG

Database	Algorithm	Number. of beats	Accuracy (%)		Gross (%)			Score (%)
			Se	PPV	Se	PPV	F1	
PhysioNet/CinC Challenge 2014 public training dataset*	epltd [12]	150102	**94.30**	92.30	**94.50**	91.00	**92.72**	**93.03**
	gqrs [12]	150102	94.00	92.60	94.10	91.00	92.52	92.93
	SSF-TKE	150102	90.83	**94.46**	89.62	**95.21**	92.33	92.53
	jqrs [12]	150102	90.50	93.20	90.90	92.30	91.60	91.70
	wavelet [12]	150102	90.10	91.80	90.30	91.70	91.00	91.00
	coqrs [12]	150102	91.60	90.80	91.80	89.50	90.60	90.90
MIT-BIH Polysomnographic database (slpdb)	**SSF-TKE**	368364	99.86	**99.74**	99.86	**99.69**	**99.77**	**99.79**
	gqrs	368364	99.94	99.46	99.94	99.38	99.66	99.68
	epltd	368364	**99.96**	99.17	**99.96**	99.02	99.49	99.53
MIT-BIH noise stress test database (nstdb)	**SSF-TKE**	26370	93.02	**94.36**	93.19	**94.47**	**93.82**	**93.76**
	elgendi [30]	26370			95.39	90.25	92.75	
	epltd	26370	95.66	89.61	95.75	88.06	91.75	92.27
	gqrs	26370	**96.33**	86.89	**96.43**	83.32	89.40	90.74
	Benitez et al. [30]	N/A			93.48	90.60	92.02	
	Pan and Tompkins [30]	26370			74.46	93.67	82.97	
MIT-BIH Arrhythmia database (mitdb)	Martinez et al. [31]	109428			**99.80**	99.86	**99.83**	
	Elgendi [30]	109985			99.78	**99.87**	99.82	
	epltd [25]	109267			99.69	99.77	99.73	
	Pan and Tompkins [32]	109809			99.75	99.54	99.64	
	gqrs	109464	97.99	98.57	97.71	98.55	98.12	98.20
	SSF-TKE	109464	97.14	98.45	96.63	98.59	97.60	97.70
MGH/MF waveform database (mghdb)	epltd	1542273	**89.46**	90.06	**91.44**	**95.59**	**93.47**	**91.64**
	gqrs [16]	N/A	87.25	**93.97**	88.16	92.19	90.13	90.39
	SSF-TKE	1542273	86.76	93.75	84.61	95.06	89.53	90.05

* One record namely 42878 in PhysioNet/CinC Challenge 2014 training dataset does not have ECG signal

4.4.1 Experiment on Standard noise test database

To validate our algorithm on noisy ECG signals, experiments have been carried out on standard MIT-BIH noise stress test database. In this dataset, ECG recordings have been created by adding 'em' noise varying from 24 dB to – 6 dB in two clean records (118 and 119) of the MIT-BIH Arrhythmia Database.

Experiment 1: The proposed SSF-TKE method has been validated on MIT-BIH noise stress test database to assess noise tolerance of the method. The detailed comparison of performance of SSF-TKE method on MIT-BIH noise stress test database with that of two other well known QRS detectors, gqrs and epltd is given in Table 4.2.

Table 4.2: Performance comparison of SSF-TKE method with 'gqrs' and 'epltd' on MIT-BIH noise stress test database

Signal	Total	gqrs			epltd			SSF-TKE		
No.	beats	Se (%)	PPV (%)	F_1 (%)	Se (%)	PPV (%)	F_1 (%)	Se (%)	PPV (%)	F_1 (%)
118 e24	2301	99.00	99.96	99.48	99.00	100.00	99.50	99.00	99.61	99.30
118 e18	2301	99.00	99.96	99.48	99.00	100.00	99.50	99.00	99.61	99.30
118 e12	2301	99.00	99.43	99.21	99.00	99.91	99.45	99.00	99.61	99.30
118 e06	2301	98.91	90.71	94.63	98.96	93.21	96.00	98.91	99.13	99.02
118 e00	2301	97.70	67.65	79.94	97.61	78.72	87.15	96.35	96.27	96.31
118 e-06	2301	96.96	57.99	72.57	92.00	70.52	79.84	87.22	87.72	87.47
119 e24	2094	94.84	99.7	97.21	94.84	100.00	97.35	94.51	98.02	96.23
119 e18	2094	94.84	99.7	97.21	94.84	100.00	97.35	94.51	98.02	96.23
119 e12	2094	94.84	99.4	97.07	94.84	99.80	97.26	94.32	97.63	95.95
119 e06	2094	94.70	94.93	94.81	94.84	90.73	92.74	89.35	91.67	90.50
119 e00	2094	94.08	74.26	83.00	94.13	75.32	83.68	85.10	85.67	85.38
119 e-06	2094	92.12	59.03	71.95	88.87	67.16	76.50	78.99	79.4	79.19
Average		96.33	86.89	90.55	95.66	89.61	92.19	93.02	94.36	93.68
Gross	26370	96.43	83.32	89.40	95.75	88.06	91.74	93.19	94.47	93.83
Score	**(%)**			**90.74**			**92.27**			**93.76**

It can be seen from Table 4.2 that SSF-TKE method has achieved gross F_1 score of 93.82% as against 89.40% and 91.57% by 'gqrs' and 'epltd' respectively representing overall better performance as compared to that of 'epltd' and 'gqrs'. The beat detection performance com-

parison of 'gqrs', 'epltd' and SSF-TKE method on signals with SNR of 24 dB (clean signals) and on signals with SNR of – 6 dB (most noisy signals) is given in Table 4.3.

Table 4.3: Performance comparison of SSF-TKE method for noise tolerance (on MIT-BIH noise stress test database)

Signal No.	SNR (dB)	gqrs			epltd			SSF-TKE		
		Se (%)	PPV (%)	F1 (%)	Se (%)	PPV (%)	F1 (%)	Se (%)	PPV (%)	F1 (%)
(i) 118 e 24	24	99.00	99.96	99.48	99.00	100.00	99.50	99.00	99.61	99.30
(ii) 118 e-06	-6	96.96	57.99	72.57	92.00	70.52	79.84	87.22	87.72	87.47
(A) Difference [(i)-(ii)]		2.04	41.97	26.90	7.00	29.48	19.66	11.78	11.89	11.83
(iii) 119 e 24	24	94.84	99.7	97.21	94.84	100.00	97.35	94.51	98.02	96.23
(iv) 119 e-06	-6	92.12	59.03	71.95	88.87	67.16	76.51	78.99	79.4	79.19
(B) Difference [(iii)-(iv)]		2.72	40.67	25.26	5.97	32.84	20.85	15.52	18.62	17.04
Average difference [(A, B)]		**2.38**	**41.32**	**26.08**	**6.48**	**31.16**	**20.25**	**13.65**	**15.26**	**14.44**

It can be seen from Table 4.3 that in SSF-TKE method, the average drop in F1 score for clean signals to most noisy signals is 14.44%; whereas the corresponding drop in 'epltd' and 'gqrs' is 20.25% and 26.08% respectively.

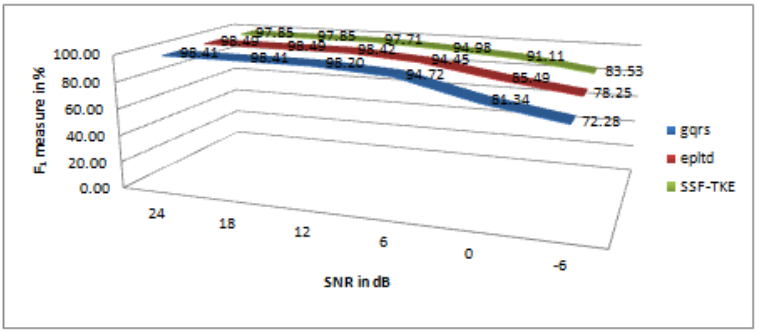

Figure 4.2: Plot of gross F1 measure on signals with different SNR

The average F1 measure achieved by 'gqrs', 'epltd' and 'SSF-TKE' algorithms at different SNR levels on MIT-BIH noise stress test database are plotted in Figure 4.2. It can be seen from the figure that at lower noise levels (24dB, 18dB, 12dB), the F1 measures across gqrs, epltd and SSF-TKE are 98.41%, 98.49%, 97.85% respectively, which shows very low variance. However, at higher noise levels (6dB, 0dB, -6dB), the F1 scores drop steeply from 94.45 % to 78.25 % for epltd, and 94.72% to 72.28 % for gqrs whereas in SSF-TKE method, F1 measure

drops gradually i.e from 94.98% to 83.53%. Thus, SSF-TKE is more resistant to noise as compared to well known 'gqrs' & 'epltd' detectors.

4.4.2 Experiment on Standard dataset for paced beat detection

Experiment 2

The electrical activity of pacemaker produce high frequency spikes in ECG signal. These beats should be removed for accurate beat detection and HR estimation. In pre-processing stage if the ECG signal with paced beats is passed through low pass filter, the original morphology of paced beats gets distorted and it makes detection of QRS beats very difficult. We have taken care of paced beat detection and their removal in our algorithm. It is applied before pre-processing the signal. There are ten records with paced beats in PhysioNet/CinC Challenge 2014 public training set, however six such records, namely 1033, 1195, 1242, 1354, 1858 and 2277 contain incorrect beat annotations [188]. The detail beat detection performance results of gqrs, SSF-TKE method and epltd on ECG signals with paced beats on four records (with correct beat annotations) of PhysioNet/CinC Challenge 2014 public training dataset are given in Appendix (Table A.7) and the summarized results are compared in Table 4.4.

Table 4.4: Performance comparison of SSF-TKE method in heart beat detection in ECG signals with paced beats in PhysioNet/CinC Challenge-2014 training dataset

Database	Algorithm	No. of beats	Average (%)		Gross (%)			Score (%)
			Se	PPV	Se	PPV	F1	
PhysioNet/CinC Challenge 2014 training dataset	**SSF-TKE**	3887	95.00	96.35	94.96	96.42	95.67	**95.67**
	epltd	3887	98.30	59.01	98.28	55.60	71.02	77.79
	gqrs	3887	99.95	49.99	99.95	49.99	66.65	74.97

The SSF-TKE method has achieved a score of 95.67% on ECG signals with paced beats in PhysioNet/CinC Challenge 2014 public training set, which is better than the scores of 'epltd' and 'gqrs' algorithms. The performance of proposed algorithm is quite efficient for paced beat detection and their removal. It may be one of the reasons for efficient beat detection by SSF-TKE method in most of the dataset.

4.5 Experiment on synthetic noise dataset

MIT-BIH noise stress database used for noise evaluation in the earlier experiment contain ECG signals with only 'em' noise. To evaluate the performance of SSF-TKE method on

Table 4.5: Beat detection performance comparison of gqrs, epltd and SSF-TKE on noisy ECG signals of synthetic noise dataset

ECG Noise	Noise level (dB)	Total beats	gqrs			epltd			SSF-TKE		
			Se (%)	PPV (%)	F1 (%)	Se (%)	PPV (%)	F1 (%)	Se (%)	PPV (%)	F1 (%)
Baseline wander noise	24	734	100.00	100.00	100.00	100.00	100.00	100.00	100.00	100.00	100.00
	18	734	100.00	100.00	100.00	100.00	100.00	100.00	100.00	100.00	100.00
	12	734	100.00	100.00	100.00	100.00	100.00	100.00	100.00	100.00	100.00
	9	734	100.00	100.00	100.00	100.00	100.00	100.00	100.00	100.00	100.00
	6	734	100.00	100.00	100.00	100.00	100.00	100.00	100.00	100.00	100.00
	3	734	100.00	99.86	99.93	100.00	100.00	100.00	100.00	100.00	100.00
	0	734	100.00	99.73	99.86	100.00	100.00	100.00	100.00	100.00	100.00
	-3	734	100.00	99.19	99.59	100.00	100.00	100.00	100.00	100.00	100.00
	-6	734	100.00	98.00	98.99	100.00	100.00	100.00	100.00	100.00	100.00
	-9	734	100.00	94.10	96.96	100.00	99.73	99.86	100.00	100.00	100.00
	-12	734	100.00	87.38	93.27	100.00	99.19	99.59	100.00	100.00	100.00
Diff b/w 24 dB and - 12 dB			**0.00**	**12.62**	**6.73**	**0.00**	**0.81**	**0.41**	**0.00**	**0.00**	**0.00**
Electrode motion artifact	24	734	100.00	100.00	100.00	100.00	100.00	100.00	100.00	100.00	100.00
	18	734	100.00	100.00	100.00	100.00	100.00	100.00	100.00	100.00	100.00
	12	734	100.00	100.00	100.00	100.00	100.00	100.00	100.00	100.00	100.00
	9	734	100.00	99.86	99.93	100.00	100.00	100.00	100.00	100.00	100.00
	6	734	100.00	99.19	99.59	100.00	100.00	100.00	100.00	100.00	100.00
	3	734	100.00	94.22	97.02	100.00	100.00	100.00	100.00	100.00	100.00
	0	734	99.86	84.06	91.28	100.00	99.59	99.79	100.00	100.00	100.00
	-3	734	99.59	74.97	85.54	100.00	96.71	98.33	100.00	100.00	100.00
	-6	734	99.59	71.18	83.02	99.73	88.41	93.73	100.00	99.86	99.93
	-9	734	99.59	66.82	79.98	98.50	77.99	87.05	100.00	99.59	99.79
	-12	734	99.32	63.50	77.47	97.41	75.98	85.37	98.91	98.24	98.57
Diff b/w 24 dB and - 12 dB			**0.68**	**36.50**	**22.53**	**2.59**	**24.02**	**14.63**	**1.09**	**1.76**	**1.43**
Muscle artifact noise	24	734	100.00	100.00	100.00	100.00	100.00	100.00	100.00	100.00	100.00
	18	734	100.00	100.00	100.00	100.00	100.00	100.00	100.00	100.00	100.00
	12	734	100.00	99.59	99.79	100.00	100.00	100.00	100.00	100.00	100.00
	9	734	100.00	97.35	98.66	100.00	100.00	100.00	100.00	100.00	100.00
	6	734	99.86	90.72	95.07	100.00	100.00	100.00	100.00	100.00	100.00
	3	734	100.00	85.55	92.21	100.00	99.73	99.86	100.00	99.86	99.93
	0	734	99.73	78.96	88.14	100.00	95.57	97.73	99.86	99.73	99.79
	-3	734	99.46	74.04	84.89	99.18	89.00	93.81	99.86	99.73	99.79
	-6	734	99.18	68.61	81.11	98.77	85.60	91.71	99.05	98.38	98.71
	-9	734	99.46	65.24	78.80	97.96	80.16	88.17	96.87	96.21	96.54
	-12	734	99.05	62.40	76.57	96.73	76.76	85.60	89.51	89.51	89.51
Diff b/w 24 dB and - 12 dB			**0.95**	**37.60**	**23.43**	**3.27**	**23.24**	**14.40**	**10.49**	**10.49**	**10.49**

baseline wander, electrode motion and muscle artifact noises, a synthetic noise evaluation dataset has been created by adding calibrated amounts of noise from records ‘bw’, ‘em’ and ‘ma’ of MIT-BIH noise stress database in clean ECG signal of record 123 of set p of PhysioNet/CinC Challenge 2014 training dataset using ‘nstdbgen’ script from WFDB software package. Synthetic noise has been added beginning after the first 2 minutes of each record, during two-minute segments alternating with two-minute clean segments. The SNR during the noisy segments was set to a value of 24, 18, 12, 9, 6, 3, 0, -3, -6, -9 and -12 dB separately, giving a total of eleven different noise levels for each type of noise. The ECG signal with ’bw’, ’em’ and ’ma’ noises are shown in Figure 2.13.

The beat detection performance of SSF-TKE method on ECG signals with ‘bw’, ‘em’ and ‘ma’ noises of different SNR levels along with its comparison with the performance of ’gqrs’ and ’epltd’ algorithms is given in Table 4.5. The beat detection performance, in terms of F1 score, of gqrs, epltd and SSF-TKE on ECG baseline wander, electrode motion artifact and muscle artifact noises are plotted in Figure 4.3, Figure 4.4 and Figure 4.5 respectively for different noise levels.

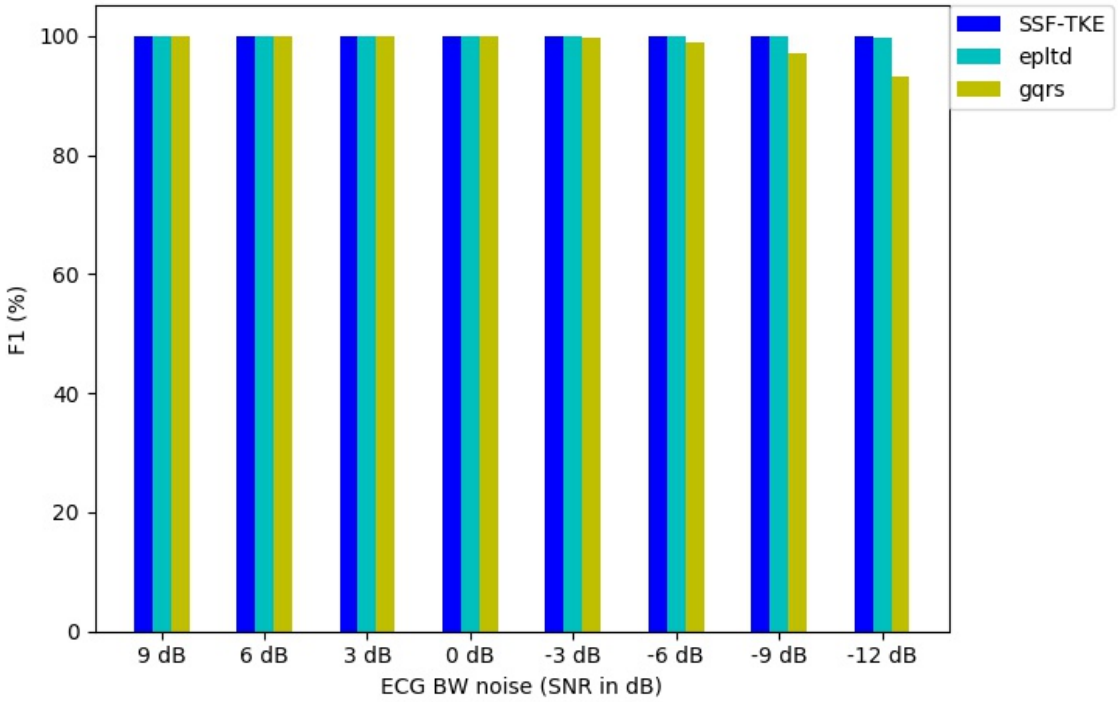

Figure 4.3: Beat detection performance of single detectors at various ’bw’ noise levels

Figure 4.3 shows that there is no effect of ‘bw’ noise on beat detection performance of SSF-TKE method, whereas in gqrs (from 3 dB and below) and epltd (from -9 dB and below) there is drop in the F1 score for lower values of SNR. Hence, SSF-TKE is highly resistant to

baseline wander noise and its beat detection performance in baseline wander noise is better than that of 'epltd' and 'gqrs'.

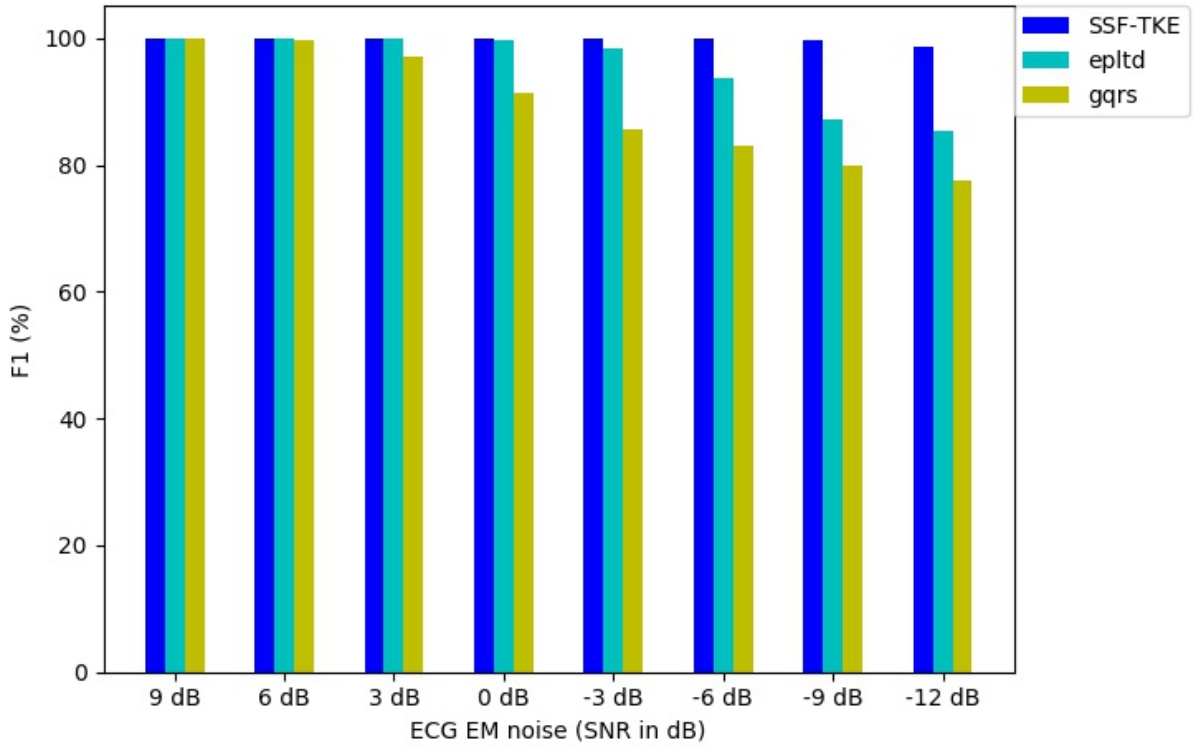

Figure 4.4: Beat detection performance of single detectors at various 'em' noise levels

It can be seen from Figure 4.4 that electrode motion artifact noise affected the beat detection performance of SSF-TKE method from SNR level of -6 dB and below. This noise has also affected the detection as well as F1 scores of 'gqrs' & epltd' from noise levels of 9 dB to 0 dB. It can be seen in Table 4.5 that drop in F1 score of SSF-TKE method from SNR of 24 dB to -12 dB is 1.43% only; whereas the corresponding drop in F1 scores in 'gqrs' and 'epltd' is 22.53% and 14.63% respectively. Thus it is evident that SSF-TKE is highly resistant to 'em' noise level.

Muscle artifact noise is the most troublesome amongst ECG noises and it starts affecting all the detectors from relatively lower noise levels (higher SNR values). In SSF-TKE method, the drop in F1 score from SNR of 24 dB to -12 dB is 10.49% and the corresponding drop of F1 score in gqrs and epltd is 23.43% and 14.40% respectively (Table 4.5). Hence SSF-TKE method is more resistant to ECG 'ma' noise as compared to 'gqrs' and 'epltd' algorithms.

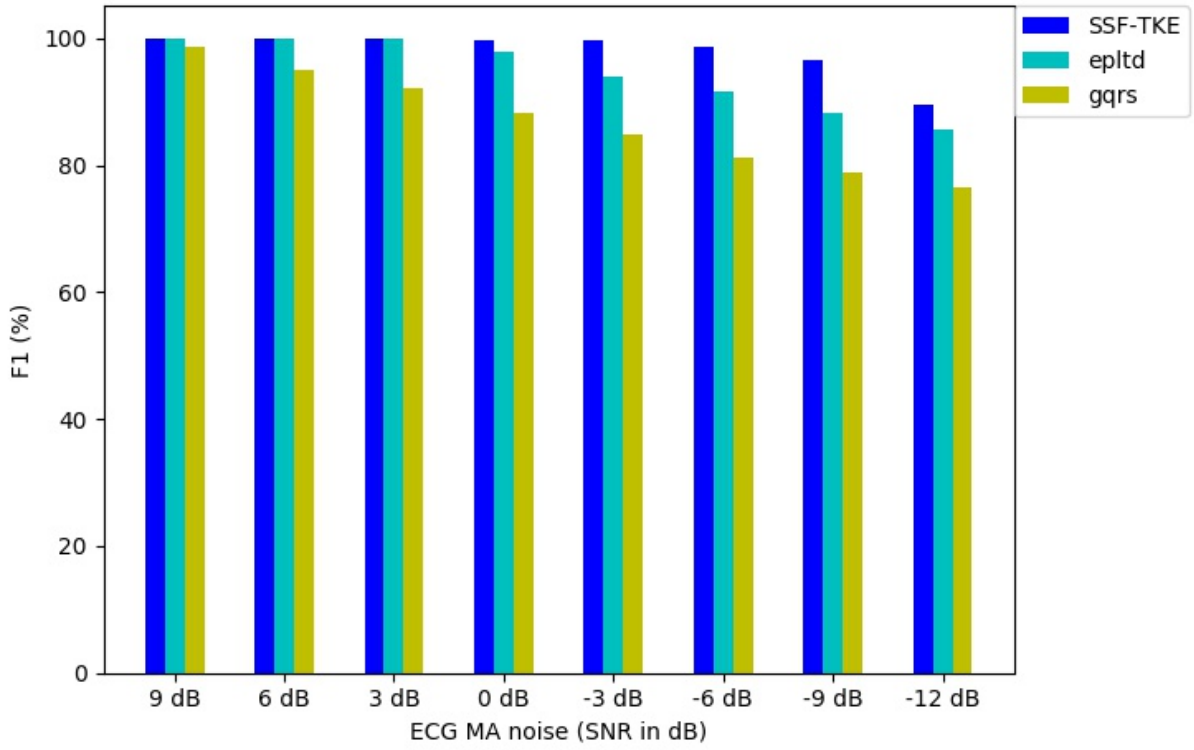

Figure 4.5: Beat detection performance of single detectors at various 'ma' noise levels

The validation of proposed SSF-TKE method on noise evaluation dataset has further established that the proposed method is more resistant to 'bw', 'em' and 'ma' noise as compared well known detectors 'gqrs' and 'epltd'. There is no effect of 'bw' noise on SSF-TKE method on the range of noise levels selected for the noise experiment. The drop in beat detection performance of SSF-TKE method for increase in noise levels of 'em' and 'ma' noise is gradual as compared to that of 'gqrs' and 'epltd'.

4.6 Discussion

SSF-TKE is a simple QRS detection that uses only one morphological feature of ECG i.e. QRS waveform; its steep QR and RS slopes and periodicity. Slope sum function (SSF) calculates cumulative sum of the first difference of signal across a window, which amplifies steep slopes of QRS. TKE operator further amplifies QRS spikes in SSF transformed signals resulting in excellent beat detection. SSF-TKE algorithm uses eye-closing period of 200 ms and moving average R-R interval of previous eight beats to select the next beat among candidate beats, which have enabled excellent beat detection in noisy signals. The detection threshold has been set to minimize the number of false detections (FPs), this has resulted in achieving excellent

predictivity for all the databases (except MIT-BIH Arrhythmia database). The use of window wise adaptive threshold 'T' has also increased accuracy of beat detection and minimized false detections (FPs). Search back operation for missed beats has not been used in SSF-TKE method to allow its use for real time beat detection, but this is at the cost of slightly lower sensitivity.

SSF-TKE method has performed quite well in ECG beat detection. It has outperformed other QRS detectors in MIT-BIH Polysomnographic database and MIT-BIH noise stress test database, whereas its performance on PhysioNet/CinC Challenge 2014 training dataset and MGH/MF waveform database is comparable with that of other well-known detectors. SSF-TKE method is more resistant against 'bw', 'em' and 'ma' noises as compared to 'epltd' and 'gqrs'. This method has excellent beat detection performance in ECG with pace maker beats in PhysioNet/CinC Challenge 2014 training dataset; better than that of gqrs and epltd (Table 4.4). Some of the other advantages of this method are its computational simplicity and faster run time. SSF-TKE method can be used for on line detection with minimum memory requirements.

However, in MIT-BIH Arrhythmia database, the beat detection performance of SSF-TKE method is slightly lower than that of other detectors. MIT-BIH Arrhythmia database contains records of normal ECG as well as records of ECG signals that are affected by premature atrial complexes, premature ventricular complexes, paced beats, left bundle branch blocks (LBBB) and right bundle branch blocks (RBBB). The analysis of bxb report has revealed that beat detection performance of SSF-TKE method has been excellent in normal beats, RBBB, LBBB and paced beats; whereas its detection performance is slightly lower in ventricular premature beats, atrial premature beats and fused ventricular/normal beats. Since, SSF-TKE method considers only QRS waveform and its rhythm, hence it's performance is slightly lower in ECGs with variable cardiac rhythm; particularly in those ECGs that contain atrial premature beats (APB) and ventricular premature beats (VPB).

4.7 Conclusion

The proposed SSF-TKE method has demonstrated excellent R-peak detection performance across a number of standard databases with variety of signal morphologies. The beat detection performance of SSF-TKE has been excellent on MIT-BIH Polysomnographic database and set p of PhysioNet /CinC Challenge 2014 dataset, which contain predominantly ECGs with normal sinus rhythm, and the performance is better than that of 'epltd' and 'gqrs'. SSF-TKE method has outperformed all other individual QRS detectors in MIT-BIH noise stress test database. The method has been validated on synthetic noise evaluation dataset containing

different types of ECG noises and it is found that SSF-TKE method is highly resistant against noises and its performance on different types of ECG noises is better than well known QRS detectors 'gqrs' and 'epltd'. SSF-TKE has also performed quite well in the signals with paced beats as compared to 'gqrs' and 'epltd'. However, it has some limitation in beat detection of ECGs with atrial premature beats and/or ventricular premature beats. The proposed method can be used for real time application due to its computational simplicity and absence of search back operation.

Chapter 5

Beat Signal Quality Index

5.1 Introduction

Multiple sensors are widely used to monitor health status due to the rapid development of sensing and computing technologies. In clinical environment these multiple sensors provide data-rich environment for better estimation of physiological parameters. Data collected from multiple sensors are corrupted from different sources of noise and health parameters extracted from such noisy signals would be inaccurate. Data fusion methodologies that integrate the data from multiple sensors provide an essential tool for degradation modeling and prognostics. To achieve this goal, the first and foremost step is to measure signal quality of a degraded signal. The data fusion approach can be simplified if we are able to measure signal quality index. Signal quality index (SQI) is used to identify trustworthiness of segments of data for clinical use. Therefore, estimation of signal quality is important for accurate assessment of health parameters for clinical decisions. Fusion of heart beats detected from noisy signals with those from clean signals may degrade the detection of fused heart beats also. Hence, correct assessment of SQI is essential to assign proper weights to physiological signals for fusion depending upon level of noise. Artifacts in ECG, ABP, EEG, EOG, and EMG signals do not always manifest simultaneously. Signal quality index helps to choose trustworthy signals for fusion. We can achieve reliable and accurate estimation of heart rate from fusion of multimodal physiological signals using SQI. In this study, a new beat signal quality index has been proposed.

5.2 Related Works

Several studies have been carried out for assessment of signal quality of physiological signals.

5.2.1 SQI assessment of ECG

Estimation of signal quality of ECG waveform has been explored by several studies. J. Allen et al. [6] mainly used ECG power spectra over predefined frequency bands and a preset limit on the ECG amplitude (bandwidths are chosen based on typical monitoring conditions). T. He et al. [159] used independent component analysis (ICA) to enhance ECG signal quality by reducing the noise or artifacts. Moody and Mark [160] used the residual after projecting a QRS complex onto the first five principal components (PCs) of an ensemble of QRS complexes, or the Karhunen–Lo'eve transform (KLT). Other approaches include amplitude thresholds and heuristically derived decision trees [161, 162], auto and cross-co-relational analysis [163], QRS features (such as amplitude to baseline ratio) [164, 165], and comparison across multiple QRS detectors along with general signal statistics [165].

Standard noise measurement methods for ECG, which can be used as individual signal quality metrics, were reviewed by Clifford et al. (2006), including root mean square (RMS) power in the iso-electric region, the ratio of R-peak to noise amplitude in the iso-electric region, the Crest factor or peak-to-RMS ratio and the ratio between in-band (5-40 Hz) and out-of-band spectral power. Redmond et al. (2008) used signal masking methods to determine artifacts and the degree of missing in the ECG. Three feature mask were described in their work: (1) a rail contact mask was used to mark the saturation to 0 or rail voltage; (2) a high-frequency mask was obtained by using a fifth-order high-pass elliptic forward-backward filter with a cut-off of 40 Hz (with a fixed threshold in order to detect muscle and electrode–tissue contact noise) and (3) a low power mask was employed using an IIR filter with a pass band of 0.7-33 Hz and a fixed threshold to locate low power sections in the ECG signal. Wang [166] used the normalized area differences from successive QRS wavelets to generate a quality index. Relying on beat-by-beat analysis, Bartolo et al. [167] used weighted cross correlation with a QRS template for estimation of noise level in the signal.

Ikaro Silva et al. [168] proposed a SQI estimation method based on adaptive filtering of all available signal channels from multi-channel waveform records. Their SQI algorithm works on multichannel records based on the coupling information estimated from concurrent waveforms. To estimate the degree of coupling between the desired channel and other concurrent waveforms, they used the multichannel adaptive filter (MCAF). Li et al. [165] developed signal quality metrics based on the degree of agreement between beat detection on different leads, the degree of agreement between different QRS detectors (bSQI), the relative power in QRS complex, the relative power in base line, the third moment (skewness) of distribution, the kurtosis, and the percentage of flat line signal. G. D. Clifford et al. [169] used support vector machine (SVM) and multilayer perceptron artificial neural network classifiers to identify quality of ECG using different combinations of seven SQIs developed earlier by Li et al..

Joachim Behar et al. [170] used machine learning approach for SQI estimation based on a combination of several basic SQIs. These basic SQIs are given below.

The bSQI of an ECG lead is defined as the ratio of beats detected synchronously, within an interval of 150 ms, by both R-peak detectors to all the detected beats (by either R-peak detector) within the window length of 10 s [24]. It is based upon the agreement level between two distinct R-peak detectors. Two well documented open-source QRS detection algorithms with different noise sensitivities were used. One is based on digital filtering (DF) and integration [171] and other is based on a length transform (LT) after filtering [172]. (These routines are known as 'eplimited' and 'wqrs' respectively.) A consensus beat detection signal quality index ($bSQI$) was defined for the k^{th} beat as:

$$bSQI(k) = \frac{N_{matched}(k,w)}{N_{all}(k,w)}$$

where $N_{matched}$ is the number of beats that both algorithms agreed upon (within $\gamma = 150$ ms) and N_{all} is the number of all beats detected by either algorithm (without double counting the matched beats). In other words,$N_{all} = NDF + NLT - N_{matched}$, where NDF is the number of beats detected by the DF method and NLT is the number of beats detected by the LT method. The length of window $'w'$ is set to 10 s long, centered at ± 5 s around the $'k'^{th}$ beat.

Seven SQIs introduced in previous works [170], [165], [173] were calculated for every single-lead separately as follows:

1. kSQI: The fourth moment (kurtosis) of the signal is defined as $kSQI = E\{X-\mu\}^4/\sigma^4$, where 'X' is the signal vector considered as the random variable, μ is the mean of 'X', 'σ' is the standard deviation of 'X', and $E\{X-\mu\}$ is the expected value of the quantity $X-\mu$. A good ECG is expected to be highly non-Gaussian since it is not very random.

2. Spectral distribution of ECG, sSQI: Since the QRS energy is mainly concentrated in a 10 Hz wide frequency band, centered around 10 Hz (Murthy et al. 1978), the ratio of the power spectral density (PSD) in this band compared to the PSD in the overall signal provides a measure of the signal quality. The spectral distribution ratio (SDR) of an ECG segment was defined to be the ratio of the sum of the power P, of the ECG between frequencies f, of 5 Hz and 14 Hz to the power between 5 Hz and 50 Hz as follows: $SDR(k) = \frac{\int_{5Hz}^{14Hz} P(k,w)df}{\int_{5Hz}^{50Hz} P(k,w)df}$

   Moderate values of SDR indicate good ECG quality. Thus, the spectral distribution signal quality index ($sSQI$) is defined as:

   (a) $sSQI(k) = 1$, if $0.5 \leq SDR \leq 0.8$

   (b) $sSQI(k) = 0$, if $SDR < 0.5$ or > 0.8

3. pSQI: The relative power in the QRS complex: $\frac{\int_{5Hz}^{15Hz} P(f)df}{\int_{5Hz}^{40Hz} P(f)df}$ Most of the power of QRS is expected to be in the 5-15-Hz band.

4. basSQI: The relative power in the baseline: $\frac{\int_{1Hz}^{40Hz} P(f)df}{\int_{0Hz}^{40Hz} P(f)df}$. A sudden "low frequency ($\leq$ 1 Hz) bump" will result in low basSQI.

5. bSQI: The fraction of beats detected by wqrs that matched with beats detected by eplimited.

6. rSQI: The ratio of the number of beats detected by eplimited and wqrs.

7. pcaSQI: A ratio comprising of the sum of the eigenvalues associated with the five principal components over the sum of all eigenvalues obtained by principal component analysis applied to the time-aligned ECG cycles detected in the window by the eplimited algorithm, segmented at 100 ms on either side of the R-peak.

8. iSQI: An inter-channel signal quality index (iSQI) is the ratio of the number of matched beats ($N_{matched}$) to all detected beats (N_{all}) between a given lead and all other synchronous ECG leads, using only eplimited method. Subsequently, the maximum value over each 10 s epoch (± 5 s around the current beat) is calculated for each beat.

9. fSQI: The ratio of power P (5-20Hz)/P (0-fn Hz), where fn = 62.5 Hz is the Nyquist frequency.

Pimentel et al. [174] used an estimate of signal quality as a 'confidence' measure in the input of a hidden semi-Markov model, down weighting the impact of peaks detected on the ECG or ABP if the signal quality was low. Vollmer [175] used the difference between a smoothed windowed maximum and a smoothed windowed minimum: if this difference was too low then the signal was considered of bad quality, equivalently considered as a check on the amplitude of pulses on the waveform. Johannesen et al. [176] used physiological constraints to filter waveforms: there should be at least 10 beats per 60 s of recording. De Cooman et al. [177] and Vollmer [175] used the regularity of the resultant R-R series for signal quality.

5.2.2 Signal quality assessment of ABP signals

Zong et al. [26] used a beat-by beat fuzzy implementation based on ABP pulse detection and ABP features such as systolic, diastolic, mean, and maximum blood pressures for SQI assessment. Sun et al. used systolic, diastolic, and mean blood pressures to generate an abnormality index based on a priori physiological bounds. The algorithm identifies a series

of features in each ABP pulse. Plausible heuristic constraints are set on the ABP amplitudes, slopes and beat to beat variations in each pulse in order to generate a signal abnormality index, 'jSQI'.

5.3 Proposed Beat Signal Quality Index

ECG and ABP signals are often found corrupted by noise and some times missing. In NC signals, quantum of R-peak artifacts and their amplitude depends on the proximity of recording sensor of the NC signals to the heart. Beat SQI assumes greater importance in fusion of heart beats extracted from NC signals because ECG artifacts may occur inconsistently or may be absent altogether. Hence, SQI should ensure that such NC signals might not degrade the quality of heart beat fusion. Thus it is essential to develop beat SQI, rather than overall signal quality index, to enable participation of clean parts of a signal with prominently detected true beats in the beat fusion process and excluding its noisy parts.

We have proposed a statistical and probability based beat SQI assessment technique [37]. The method uses a simple and rational approach, based on beat rhythm of the signal immediately preceding the beat and on the probability of the beat being matched or unmatched with respect to the reference beat annotation. The beat SQI thus depends on the deviation of the beat from rhythm of heart beats as well as on the probability of the beat being matched beat with the given deviation.

R-R interval is a continuous random variable when a person is in the state of rest and it follows normal distribution. A random variable, i.e., R-R interval 'x', distributed normally with 'μ' and variance σ^2, is given by Eq. (5.1):

$$x = \mu \pm K\sigma \tag{5.1}$$

$$\frac{\sigma}{\mu} = \frac{1}{K}\frac{|x-\mu|}{\mu} \tag{5.2}$$

where μ is mean/median R-R interval, and σ is standard deviation. Value of 'K' depends upon the probability of the variable 'x' lying around mean/median value. σ/μ is a measure of dispersion of a probability distribution and gives dispersion $|x-\mu|$ of a random variable about mean/median value $'\mu'$, as given in Eq. (5.2). σ/μ is also a statistical measure and it is inverse of signal to noise ratio (SNR) [178].

The beat SQI is assessed from following two factors; (i) beat rhythm of the signal, and (ii) deviation of the beat from rhythm.

1. Beat rhythm factor 'C_{bri}': It gives a measure of beat rhythm of the signal. The coefficient

of variation CV_{si} of previous eight beats is used to calculate beat rhythm factor 'C_{bri}' as given in Eqs. (5.3) and (5.4):

$$CV_{si} = \frac{\sigma_{si}}{\mu_{si}} \tag{5.3}$$

$$C_{bri} = 1 - CV_{si} \tag{5.4}$$

where σ_{si} is standard deviation and μ_{si} is median of R-R interval of eight beats of the signal preceding i^{th} beat. μ_{si} is taken as 0.83 s for the first beat; corresponding to normal HR (72 bpm). For 2^{nd} to 8^{th} beats, μ_{si} is taken as average of all R-R intervals preceding the beat. Higher values of σ_{si} with respect to μ_{si} indicate presence of high level of noise and absence of beat rhythm in the signal. In such cases, coefficient of variation CV_{si} would be high and beat rhythm factor C_{bri} will be low.

1. Beat deviation factor 'C_{bdi}': It is a measure of deviation of an individual beat from the beat rhythm. The beat rhythm is assessed from median μ_i of eight R-R intervals preceding the R-R interval of 'i^{th}' beat. The deviation 'D_i' for 'i^{th}' beat is calculated from R-R interval 'x_i' and median μ_i as given in Eqs. (5.5) and (5.6):

$$x_i = t_i - t_{i-1} \tag{5.5}$$

where t_i and t_{i-1} are temporal locations of 'i^{th}' and '$(i-1)^{th}$' beats respectively.

$$D_i = |x_i - \mu_i| \tag{5.6}$$

Low values of D_i indicate that the detected beat is in synchronization with the rhythm of beat occurrence. Values of beat deviation factor C_{bdi} are assigned based on deviation D_i as given below in Eqs. (5.7), (5.8) and (5.9):

$$D_i \leq 250ms, C_{bdi} = 1 \tag{5.7}$$

$$250ms \leq D_i \leq 300ms, C_{bdi} = 0.9 \tag{5.8}$$

$$D_i > 300ms, C_{bdi} = 0.8 \tag{5.9}$$

A detected beat is considered as matched beat if it is located within 150 ms of the reference beat annotation [179]. Hence, if D_i is within 250 ms, there is higher probability that the detected beat is a matched beat and therefore for $D_i \leq 250ms$, beat deviation factor C_{bdi} is

assigned a value of 1. For values of D_i higher than 250 ms, the probability of detected beat being a matched beat decreases progressively, hence lower values of beat deviation factor, C_{bdi} are assigned for higher values of deviation D_i.

The SQI of 'i^{th}' beat is a product of beat rhythm factor 'C_{bri}' and beat deviation factor 'C_{bdi}' as given in Eqs (5.10):

$$SQI_i = C_{bri} * C_{bdi} \tag{5.10}$$

Median value has been used in the calculations of Coefficient of Variation CV_{si} and deviation D_i, instead of mean, because missed beats or false detected beats introduce lower variation in median R-R interval as compared to that in mean R-R interval. The flow chart of proposed SQI assessment method is given in Figure 5.1.

5.4 Performance Analysis of Beat SQI

The performance of proposed beat SQI method has been evaluated on PhysioNet/CinC Challenge 2011 training database (set-a) [77]. The dataset contains 1000 standard 12-lead ECG recordings (leads I, II, III, aVR, aVL, aVF, V1, V2, V3, V4, V5, and V6) each of 10 seconds duration, out of which 773 records are acceptable, 225 records unacceptable and 2 records are indeterminate (which are not considered for evaluation). Beat SQI method, using 'gqrs' detector, is evaluated on the above mentioned database to classify ECG signals and its performance is compared with that of bSQI metrics. We have used two R-peak detectors 'gqrs' and 'wqrs' for calculating the bSQI. The average SQI of a record is average of SQI values of all the 12 leads in the record.

As per classification criterion given in PhysioNet/CinC Challenge-2011 (set-a), a record is classified as:

1. Acceptable, if average SQI $\geq$ 0.70 and not more than one lead has 'zero' SQI value

2. Intermediate, if average SQI $\geq$ 0.70 but more than two leads have 'zero' SQI value

3. Unacceptable, if average SQI < 0.7.

A threshold value of 0.7 is taken for evaluation of bSQI and beat SQI on set-a of PhysioNet/CinC Challenge-2011 training database.

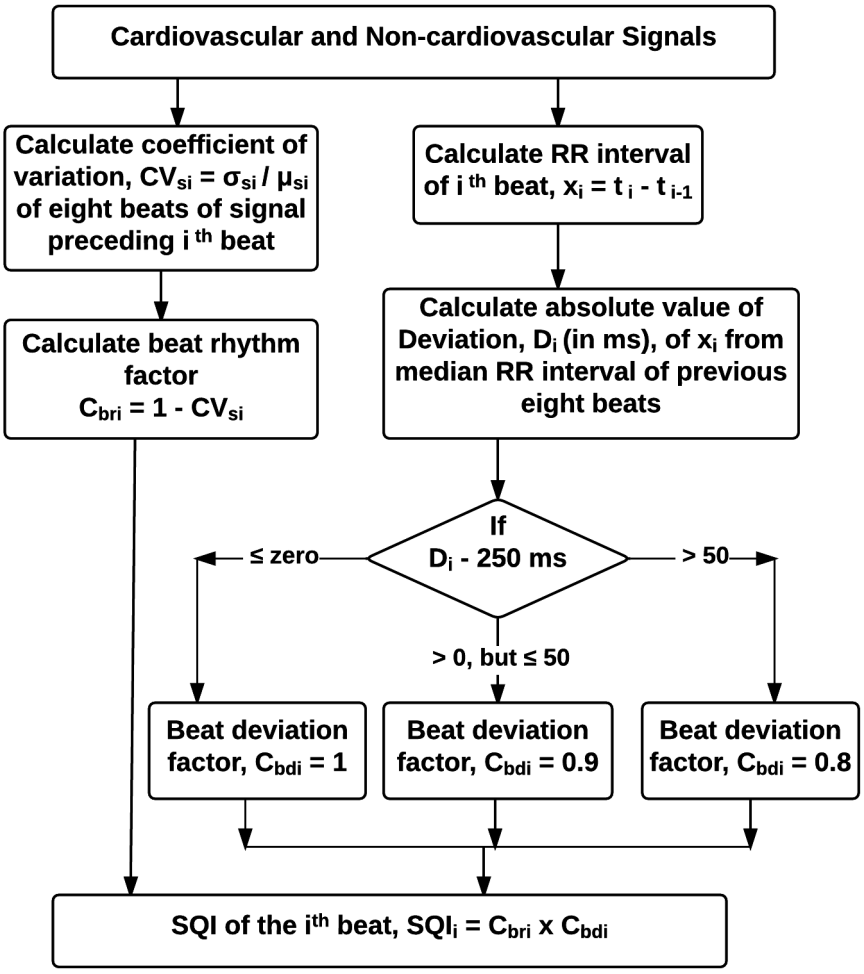

Figure 5.1: Flow chart of beat SQI assessment

5.4.1 Performance of beat SQI method on ECG

The performance of SQI assessment methods is evaluated in terms of sensitivity (Se_{sqi}), specificity (Sp) and accuracy (Ac). Sensitivity (Se_{sqi}) measures proportion of truly identified poor quality signals from unacceptable records, specificity (Sp) is proportion of truly identified good quality records from acceptable records, and accuracy (Ac) measures the proportion of truly identified ECG records. Performance of beat SQI method on PhysioNet/CinC Challenge-2011 training database (set-a) and its comparison with signal quality metric bSQI is given in Table 5.1.

The beat SQI method has achieved sensitivity, specificity, and accuracy of 0.853, 0.928 and 0.911 respectively and its performance is comparable or better than that of bSQI.

Table 5.1: Performance comparison of the proposed beat SQI with bSQI on 12 leads of set-a of PhysioNet/CinC Challenge-2011 training database

SQI	Performance Indices		
	Se_{sqi}	Sp	Ac
bSQI	0.738	0.948	0.901
Proposed Beat SQI	**0.853**	**0.928**	**0.911**

5.4.2 Performance of beat SQI method on ECG with arrhythmias

The ICU patients generally suffer from irregular heart beats known as cardiac arrhythmia. The heart beats in arrhythmia can be irregular, too fast, or too slow. Some of the main types of arrhythmias are extra beats, supraventricular tachycardias, ventricular arrhythmias, and brad-yarrhythmias.

Table 5.2: Performance comparison of beat SQI with bSQI for classification of arrhythmia signals of set-a of PhysioNet/CinC Challenge-2011 training database

SQI	Accuracy in different Arrhythmias			
	Tachycardia	Bradycardia	Other Arrhythmias	Overall
bSQI	0.810	0.919	0.873	0.872
Proposed beat SQI	0.896	0.926	0.873	0.904

It is essential that the SQI should be able to correctly classify the ECG with different type of arrhythmias for accurate HR estimation of ICU patients. Out of 1000 records in PhysioNet/CinC Challenge-2011 training database (set-a), 655 records have normal sinus rhythm, 343 records have arrhythmias and 2 records are indeterminate. The performance of beat SQI on arrhythmia signals in PhysioNet/CinC Challenge-2011 training database (set-a) is given in above Table 5.2.

The performance of beat SQI on arrhythmia signals is better than that of bSQI. It can be seen from Table 5.2 that beat SQI achieved overall classification accuracy of 0.904 for arrhythmias, which is slightly lower than the overall accuracy of 0.911 achieved on all signals (Table 5.1). The performance of beat SQI varied on different types of arrhythmia.

ECG and simultaneously recorded EOG signals of record no. 1503 of PhysioNet/CinC Challenge 2014 training database along with their beat SQIs are shown in Figure 5.2. It can be seen in Figure 5.2 (a) and 5.2 (b) that as the ECG becomes noisy, rhythm of detected beats becomes quite irregular and corresponding beat SQI value decreases. Beat SQI values in EOG signal increase gradually as rhythm of detected beats improves as seen in Figure 5.2 (c) and 5.2 (d). It establishes that the beat SQI assessment method is efficient in proper assessment of signal quality. The beat SQI method has enabled participation of clean parts of a signal in the

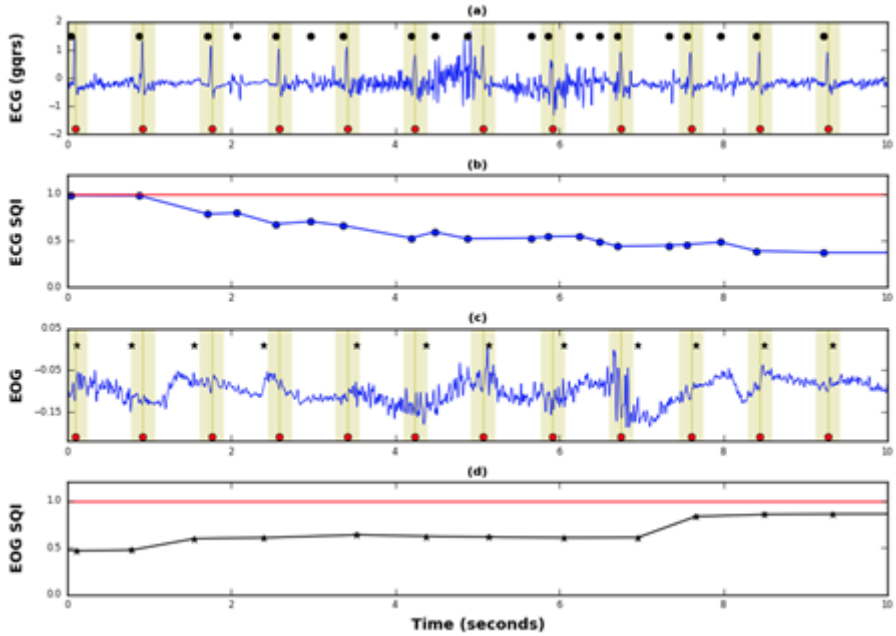

Figure 5.2: (a) Detected beats in ECG by gqrs (●); (b) Beat SQI values of ECG; (c) Detected beats by modified SSF-TKE method in EOG (*); (d) Beat SQI values of EOG. Reference beat annotations (●).

beat fusion process, excluding the noisy parts.

5.5 Discussion

SQI plays an important role in selection of good quality signals for fusion. It assumes greater importance in fusion of heart beats extracted from NC signals because ECG artifacts may occur inconsistently or may be absent altogether. Hence, SQI should ensure that such NC signals might not degrade the quality of heart beat fusion. The beat SQI assesses the quality of signal based on a very short range of previous eight beats of the signal; hence it changes rapidly with change in signal quality with minimum time lag. This has enabled participation of those NC signals in the fusion where presence of ECG artifacts is intermittent. The proposed beat SQI is simple method of signal quality assessment because it requires only one beat detector; whereas bSQI assessment needs two independent detectors. Although the beat SQI is based on signal rhythm, beat deviation factor C_{bdi} accounts for signals with HRV and arrhythmias. It works satisfactorily on bradycardia, tachycardia and different types of arrhythmias. However, its performance was lower on certain arrhythmias like atrial fibrillation, ventricular bigeminy, irregular atrial tachycardia and atrial ectopic because beat SQI is predominantly rhythm dependent. We have used combination of beat SQI and kSQI in majority voting fusion method

for further improving ECG signal quality assessment. For signal quality assessment of ABP and NC signals, only beat SQI has been used.

5.6 Conclusion

The performance of proposed statistical and probability based beat SQI assessment method has been excellent in assessing signal quality and it has achieved accuracy of 0.91 on PhysioNet/CinC Challenge-2011 (set-a) dataset, which is better than that of bSQI. The performance of beat SQI in classification of ECG signals with arrhythmias is also better than that of bSQI. It works satisfactorily on ECGs with bradycardia, tachycardia and different types of arrhythmias. However, performance of beat SQI is slightly lower on certain arrhythmias like atrial fibrillation, ventricular bigeminy, irregular atrial tachycardia and atrial ectopic beats, because it is predominantly rhythm dependent.

Chapter 6

Robust heart beat detection

6.1 Introduction

The rapid development in biomedical monitoring technologies has enabled modern intensive care units to employ multiple bed side monitors to track the health of the patients. The effectiveness of the systems critically depends upon quality of signal acquisition. However, the utility of monitoring system is compromised by the fact that the signals are often severely corrupted by noise, artifacts and missing data. On the other hand, multimodal physiological signals recorded simultaneously in ICU carry redundant information. For example, heart beat information is contained in ABP and PPG that are directly related to cardiac activity. NC signals like EEG, EOG and EMG are often contaminated by ECG artifacts. The sensors responsible for measuring these multimodal signals are independent and their sources of noise and artifacts do not affect each sensor in the same way. The redundant heart beat information in these signals can be detected and used to fill in the gaps when ECG is corrupt or missing. Medical practitioners are increasingly using robust parameters extracted from data fusion for supporting clinical decisions of ICU patients [20].

Over the past years, several large databases have been developed with concurrent recordings of multiple physiological signals, including ECG, BP, EEG, respiration, photoplethysmogram (PPG) etc. by Goldberger et al. [76], Welch [83], Moody and Mark [81], Terzano [180] and Saeed [181]. Researchers have discovered optimal methods for reliable heart beat detection by combining information from simultaneously recorded physiological waveform. Fusion of multiple sensors has many advantages; increased reliability, enhanced performance efficiency and better control [182].

Heart beats can be directly detected from cardiovascular signals that are related with functioning of heart such as ECG and ABP. However, ECG and ABP are sometimes contaminated or may be missing due to measurement errors leading to inaccurate estimation of heart beat

position causing false alarms in ICU. Accurate beat detection is required for correct estimation of heart rate and heart rate variability for clinical diagnosis. In this study a beat SQI based majority voting fusion method has been proposed for robust heart beat detection from cardiovascular and non-cardiovascular signals.

6.2 Related Works

Robust heart beat detection using NC signals along with cardiovascular signals is a new area of research. There have been some studies on robust heart beat detection from multiple physiological signals. In most of these studies, only cardiovascular signals have been used. However, there are few studies where both cardiovascular and NC signals have been used and they are:

Lars Johannesen et al. proposed a robust heart beat detection method by fusion of multiple signals using voting technique [106]. They used modified versions of U3 detector for beat detections in ECG, EEG and EOG signals and a second derivative-based approach for heart beats detection in ABP, Stroke Volume (SV) and Photoplethysmogram (PPG) signals. The detector used in the study for EEG and EOG signals was trained with initial annotations obtained from voting of cardiovascular signals namely ECG, ABP and SV. Hence, the method will give erroneous beat detection when ECG and ABP signals are corrupt. In voting, predetermined fixed lower weights are assigned to SV, EEG and EOG signals as compared to weights of ECG and ABP signals irrespective of quality of signals, which does not seem to be an appropriate way of weight assignment.

In the method proposed by Jan J. Gieraltowski et al. [183], beat annotations detected in ECG, ABP, EEG, EOG and EMG signals are fine-tuned and joined using signal quality. RS slope and amplitude method has been used for detection of heart beat annotations. A signal is rejected, if annotations detected are less than 1/6th of total annotations, which is one of the constraints in this study. Secondly, ECG and ABP signals are given more importance in joining the annotations. The algorithm does not use window wise analysis hence abrupt changes in HR may give erroneous results.

Jongmin Yu et al. [184] proposed a heart beat detection method from multimodal physiological signals using voting fusion technique. Adaptive filter in cascade has been used for detection of ECG artifacts in EEG, EOG and EMG signals, using EEG as a primary signal in the filter. Three candidate locations of heart beat; one from ECG, one from other group of cardiovascular signals (BP, SV, and SpO2), and one from NC signals (EEG, EOG and EMG) are merged through voting for majority. If ECG artifacts in EEG signal are either absent or not detectable, beat detection in all the NC signals will be erroneous. The method does not take signal quality in to consideration for voting. Further more, if ECG section is missing, the

method may occasionally loose the anchor points as pointed out by the authors.

Some of the studies in which only cardiovascular signals have been used for robust heart beat detection are:

Johnson A. et al. [51] used two approaches for fusion of heartbeats of cardiovascular signals: the first based on signal quality for ECG and ABP signals and the second on the regularity of the derived R-R intervals between successive detected beats in ECG, ABP, SV and PPG signals . They used "gqrs", "coqrs" and "jqrs" methods for QRS detection in ECG and "wabp" open-source algorithm for detection of onset of the pulses in ABP signal. The peaks were extracted using a zero-crossing procedure in SV signal and a peak energy technique in PPG signals. Only cardiovascular signals have been used for robust beat detection.

Thomas De. Cooman et al. [177] proposed a procedure containing majority voting, location estimation and Hjorth's mobility for combining beats of ECG, ABP, SV and PPG signals. The selection of a signal for voting in a record was done on the basis of value of normalized correlation coefficient between the power spectral density (PSD) values of the ECG signal and the other signal calculated around average HR frequency (Avg. HR obtained from one minute segment of ECG). Thus the proposed method essentially needs one reference ECG signal.

Using information from pulsatile ABP signal, Quang Ding et al. [185] inserted missing beats and removed false detected beats in ECG signal for robust beat location. Roman Schulte et al. [186] proposed a Signal Quality index based fusion of ECG, ABP and SV signals for robust beat location. They divided each signal in to sub-segments and SQI of each sub-segment was calculated based on signal statistics, number of peaks and their location. The signal with highest SQI was considered for the final peak detection in the sub-segment. We have proposed a novel beat SQI based majority voting fusion method for robust heart beat detection from cardiovascular and NC signals.

6.3 Proposed Beat SQI based majority voting fusion method

The beat SQI based majority voting fusion (MVF) method for robust heart beat detection involves following three steps:

1) R-peak detection in ECG, ABP signals and R-peak artifacts detection in NC signals,

2) Estimation of beat SQIs of signals, and

3) Fusion of heart beats using beat SQI based majority voting fusion method.

The layout of proposed work is given in Figure 6.1.

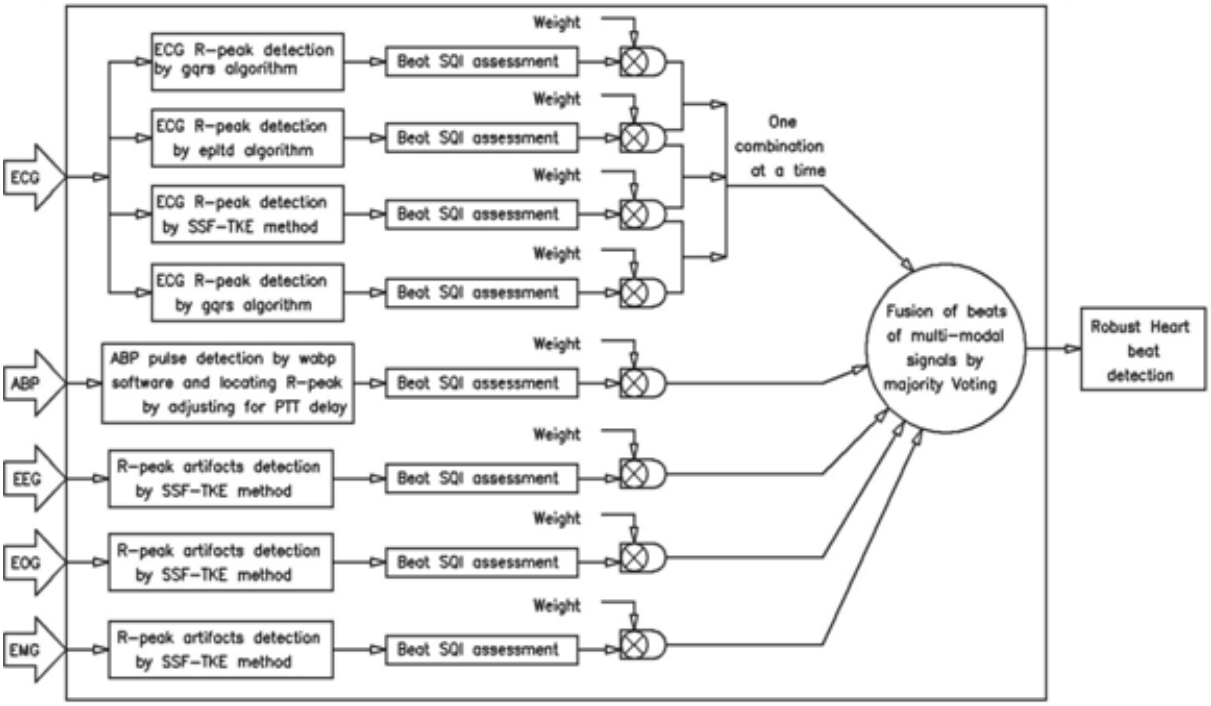

Figure 6.1: Layout of proposed method

6.3.1 R-peak detection in multimodal physiological signals

Three QRS detectors; 'gqrs', 'epltd', and SSF-TKE method have been used for R-peak detection in ECG signals. Open source algorithm, 'wabp' has been used for detection of onset of ABP pulses in ABP signals [26].

We have estimated the delay between onset of ABP pulse and R-peak of ECG (Pulse Transit Time) by calculating average delay between R-peaks of ECG and ABP pulses of ABP for the first 50 beats of record and used it to adjust the lag for remaining ABP pulses. A default pulse transit time (PTT) of 200 ms is used when either initial ECG/ABP signal is noisy or ECG signal is absent in the record. SSF-TKE method is used for R-peak artifacts detection in NC signals and with some modifications for R-peak detection in ECG.

6.3.2 Beat SQI based majority voting fusion method

A new majority voting fusion method based on beat SQI is being proposed for fusion of heartbeats from cardiovascular and NC signals. Two beats of ECG signals (in pairs of different combinations of gqrs, epltd and SSF-TKE method), one beat of ABP signal (ABP pulse detected by wabp and adjusted by PTT) and one beat each of EEG, EOG and EMG signals have

been fused for robust HR estimation.

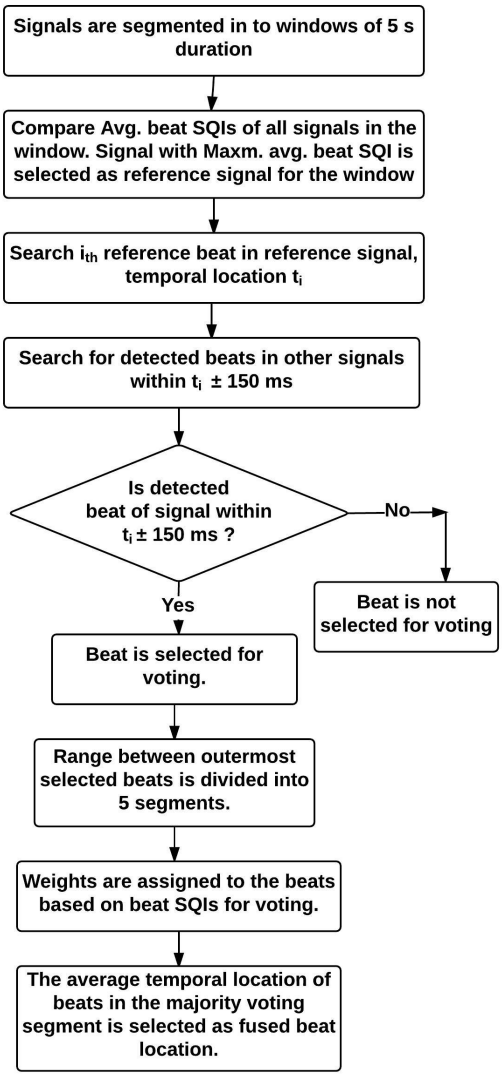

Figure 6.2: Flow chart of beat SQI based fusion method

The flow chart of proposed algorithm is shown in Figure 6.2. It involves the following steps:

1. Signals are segmented in to windows of 5 seconds duration with 2 s overlap to identify reference signal.

2. Average beat SQIs of all signals in the window are compared and the signal with highest average beat SQI is selected as reference signal for the window, to search for candidate beats for voting.

3. The i^{th} beat is located in the reference signal at temporal location 't_i'. R-R interval, $RR_i = t_i - t_{i-1}$ is calculated, where t_{i-1} is temporal location of $(i-1)^{th}$ beat:

   - If RR_i is within $\mu_{i-1} \pm 150ms$, where μ_{i-1} is median of eight R-R intervals preceding $(i-1)^{th}$ beat, the located beat is true positive (TP) and selected as i^{th} reference beat at location 't_i'.
   - If $RR_i > \mu_{i-1} + 150ms$, i^{th} beat is missed in the reference signal and the i^{th} reference beat is assumed at the expected location, $t_{exp} = t_{i-1} + \mu_{i-1}$.
   - If $RR_i < \mu_{i-1} - 150ms$, the located beat is false positive (FP) beat. Detected beats are searched in the temporal duration of $t_{exp} \pm 150ms$. If a beat is located in this duration then it is probable TP beat and is selected as i^{th} reference beat at location 't_i', otherwise the i^{th} initial reference beat is assumed at the expected location, $t_{exp} = t_{i-1} + \mu_{i-1}$.

4. Detected beats of other signals are searched for within time interval of t_i ± 150 ms.

5. All beats detected within t_i ± 150 ms, except assumed reference beat, are eligible beats for voting.

6. The temporal range of outermost eligible beats is divided into 5 segments for voting. The eligible beats have been assigned weights for voting based on beat SQI and type of signal as shown in Table 6.1 below:

Table 6.1: Weights assigned to multimodal signals for voting based on beat SQI

Signal	$SQI_i \geq 0.9$	$0.9 > SQI_i \geq 0.8$	$0.8 > SQI_i \geq 0.7$
ECG (gqrs), ECG (Modified SSF-TKE) and ABP	5	3	1
EEG, EOG and EMG	3	2	0

Higher values of weights have been assigned to cardiovascular signals as compared to NC signals for the same value of beat SQI because cardiovascular signals are directly related to cardiac activities whereas in NC signals the heart activities appear as artifacts. Signal is considered noisy for beat SQI values less than 0.7.

7. The mean temporal location of beats in the segment with majority voting is selected as fused beat location.

8. The procedure is repeated for next beat.

6.4 Performance Evaluation

The voting fusion algorithm has been evaluated on PhysioNet Challenge 2014 training dataset, MIT-BIH Polysomnographic database, MGH/MF waveform database, MIT-BIH noise stress test database, and MIT-BIH Arrhythmia database with three different combinations of QRS detectors namely epltd/SSF-TKE, gqrs/SSF-TKE and epltd/gqrs. The detailed results on these databases are tabulated in Table A.8, Table A.9, Table A.10, Table A.11 and Table A.12 respectively. The algorithm has also been validated on PhysioNet/CinC Challenge 2014 test dataset.

Table 6.2: Performance comparison of beat SQI based majority voting fusion method in heart beat detection with other studies on PhysioNet/CinC Challenge 2014 training dataset

	Algorithm	No. of beats	Average (%)		Gross (%)			Score (%)
			Se	PPV	Se	PPV	F_1	
Single detectors	epltd [171]	150102*	94.30	92.30	94.50	91.00	92.72	93.03
	gqrs [76]	150102*	94.00	92.60	94.10	91.00	92.52	92.93
	SSF-TKE	150102*	90.83	94.46	89.62	95.21	92.33	92.53
Other algorithms	Pangerc et al. [187]	151032	**97.84**	**97.21**	**98.10**	**97.54**	**97.82**	**97.67**
	Johnson et al. [51]	151032	96.50	95.10	96.90	94.20	95.50	95.60
	Johannesen et al. [176]	151032	95.67	92.28	95.85	91.44	93.59	93.81
	Marcus Vollmer [175]	151032	92.60	94.30	92.90	94.50	93.69	93.58
	Thomas De Cooman et al. [177]	151032	94.20	93.50	94.50	91.90	93.18	93.53
	Gieraltowski et al. [183]	151032	93.20	93.80	92.90	92.90	92.90	93.20
Voting fusion method (Present work)	(epltd/SSF-TKE)	151032	96.04	95.48	96.35	95.83	96.09	95.93
	(gqrs/SSF-TKE)	151032	94.76	94.62	95.28	95.04	95.16	94.93
	(gqrs/epltd)	151032	95.56	94.17	96.01	93.36	94.66	94.78

* One record namely 42878 in PhysioNet/CinC Challenge-2014 training set does not have ECG signal

The beat detection performance of the voting fusion method on PhysioNet/CinC Challenge 2014 training dataset has been compared with those of other studies in Table 6.2. It can be seen from the table that our voting fusion method (epltd/SSF-TKE combination) has achieved overall score of 95.93%, which is second after the best score of 97.67% by Pangerc et al. [187]. The voting fusion with epltd/SSF-TKE combination has improved overall score by 2.90% over the score of well known best single detector 'epltd'. Therefore, fusion of multiple signals increases the accuracy of beat detection and also improves the robustness of system. Our algorithm has also performed well on records containing ECG with paced beats.

Table 6.3: Performance comparison of beat SQI based majority voting fusion method in heart beat detection with other studies on PhysioNet/CinC Challenge 2014 hidden test dataset

	Algorithm	No. of beats	Average (%)		Gross (%)			Score (%)
			Se	PPV	Se	PPV	F_1	
Single Detectors	epltd [171]	152478	87.82	86.29	91.02	84.72	87.76	87.46
	gqrs (C-code sample entry) [51]	152478	87.34	87.03	89.74	85.41	87.52	87.38
Other Detectors	Pangerc et al.	152478	**93.86**	**91.57**	**95.65**	**93.48**	**94.55**	**93.64**
	S. Vernekar (unpublished)	152478	-	-	-	-	-	92.24
	Johnson et al.	152478	92.61	89.03	95.07	89.30	92.09	91.50
	Joachim Behar et al. [170]	152478	91.63	88.79	94.02	88.78	91.33	90.80
	Johannesen et al.	152478	91.27	87.21	92.80	87.48	90.06	89.73
	Marcus Vollmer	152478	-	-	90.51	88.47	89.48	89.55
	Mollakazemi et al.	152478	88.87	87.34	91.15	88.07	89.58	88.85
	Gieraltowski et al.	152478	87.97	87.46	88.55	88.32	88.43	88.07
Voting fusion method (Present work)	(epltd/SSF-TKE)	152478	92.40	89.48	93.65	91.51	92.57	91.76
	(gqrs/SSF-TKE)	152478	91.60	88.85	92.74	90.39	91.55	90.89
	(gqrs/epltd)	152478	92.35	88.46	93.77	88.11	90.85	90.67

The MVF algorithm with three different combinations was also submitted on PhysioNet web server to run on hidden test dataset of PhysioNet/CinC Challenge 2014. The challenge

has set a limit of 6*10^10 CPU instructions per record for the entries. The automatic scoring engine generated the scores for different voting fusion combinations. The beat detection performance of the voting fusion method on PhysioNet/CinC Challenge 2014 hidden test dataset has been compared with those of other studies in Table 6.3.

The voting fusion method (epltd/SSF-TKE) has scored 91.76% on PhysioNet/CinC Challenge 2014 test dataset. Our algorithm was ranked third at the time of submission in PhysioNet web server on 29/12/2016 and currently it is ranked 5th. The snapshots of the PhysioNet website displaying the results from the 2014 Challenge at the relevant point of time are given in Figure B.1 and Figure B.2 (Annexure B). gqrs/SSF-TKE and gqrs/epltd combinations have also achieved excellent scores of 90.89% and 90.67% respectively and these scores are within the top ten scores of the challenge. The run time statistics of the algorithm on PhysioNet web server are: (i) Average running time (training set): 6.89e+09 instructions, (ii) Maximum running time (training set): 9.68e+09 instructions, (iii) Average running time (test set): 6.18e+09 instructions, and (iv) Maximum running time (test set): 9.92e+09 instructions. The average and maximum run time of the algorithm are very low and are well within the limit set by the challenge. The voting fusion with epltd/SSF-TKE combination has improved overall score by 4.30% over the score of best single detector 'epltd'. The hidden test dataset is not available to the public and the results are obtained by submitting the algorithm online to PhysioNet. This dataset contains more difficult records therefore the overall performance of fusion methods are lower as compared to training set.

The training and test datasets of PhysioNet/CinC Challenge 2014 contain ECG waveform with wide variety of unusual beats corresponding to pacemaker activity, supraventricular Tachycardia, cardiac massage, electrocautery interference, premature ectopic beats, defribillation, fusion of paced and normal beats, flutter, and ventricular fibrillation [188]. The voting fusion algorithm has also performed well on test dataset that contains more noisy, frequent missing ECG signals and arrhythmias.

The beat detection performance of the voting fusion method on MIT-BIH polysomnographic database has been compared with those of other studies in Table 6.4. The performance of all the single QRS detectors on the database is excellent. Hence there is very little scope of improvement of results after fusion. It can be seen from the table that proposed voting fusion method (epltd/SSF-TKE) has obtained score of 99.85% which is comparable to best reported result of Pangerc et al. with score of 99.87%. The performance of all the single QRS detectors on the database is excellent. Hence there is very little scope of improvement of results after fusion. Still the majority voting fusion method (epltd/SSF-TKE) has improved overall score by 0.17% over the score of well known best single detector 'gqrs'.

Table 6.4: Performance comparison of beat SQI based majority voting fusion method in heart beat detection with other studies on MIT-BIH Polysomnographic database

	Algorithm	No. of beats	Average (%)		Gross (%)			Score (%)
			Se	PPV	Se	PPV	F_1	
Single Detectors	SSF-TKE	368364	99.86	99.74	99.86	99.69	99.77	99.79
	gqrs	368364	99.94	99.46	99.94	99.38	99.66	99.68
	epltd	368364	99.96	99.17	99.96	99.02	99.49	99.53
Other Detectors	Pangerc et al.		**99.98**	99.74	**99.98**	**99.76**	**99.87**	**99.87**
	Vollmer M.	368364			99.90	99.70	99.80	
	Chen H. et al.							99.66
	Johannesen et al.				99.98	98.85	99.41	
Voting fusion method	(epltd/SSF-TKE)	368364	99.93	**99.79**	99.94	99.75	99.84	99.85
	(gqrs/epltd)	368364	99.93	99.77	99.95	99.72	99.84	99.84
	(gqrs/SSF-TKE)	368364	99.83	99.78	99.82	99.74	99.78	99.79

Table 6.5: Performance comparison of beat SQI based majority voting fusion method in heart beat detection with other studies on MGH/MF waveform database

	Algorithm	No. of beats	Average (%)		Gross (%)			Score (%)
			Se	PPV	Se	PPV	F_1	
Single Detectors	epltd	1542273	89.46	90.06	91.44	95.59	93.47	91.64
	gqrs [16]	N/A	87.25	93.97	88.16	92.19	90.13	90.39
	SSF-TKE	1542273	86.76	93.75	84.61	95.06	89.53	90.05
Other Detectors	Chen H. et al.							95.53
	Pangerc et al.		**95.96**	93.95	**96.53**	94.11	95.30	95.14
	De Cooman T. et al.							94.40
	Liu N. T. et al.	1526672			90.60	96.70	93.55	
Voting fusion method	(gqrs/epltd)	1542273	95.35	**95.47**	95.68	**95.89**	**95.78**	**95.60**
	(gqrs/SSF-TKE)	1542273	94.61	95.22	94.87	95.99	95.42	95.17
	(epltd/SSF-TKE)	1542273	91.31	92.22	91.60	92.65	92.12	91.94

MGH/MF database is a collection of hemodynamic and ECG waveforms of stable and unstable patients in critical care units, operating rooms and cardiac catheterization laboratories representing a broad spectrum of physiologic and patho-physiologic states. This provides

an opportunity to test the robustness of beat detection fusion method. The performance of beat SQI based majority voting fusion method in heart beat detection on MGH/MF waveform database has been compared with other studies in Table 6.5.

The new voting fusion algorithm (gqrs/epltd) has achieved excellent result with overall score of 95.60% which is the best reported result so far on this database. The gqrs/SSF-TKE combination has also achieved excellent score of 95.17%. Fusion algorithm (gqrs/epltd) has improved the overall score by 3.96% over the score of well known best single detector 'epltd'. Thus, the proposed voting fusion method has performed extremely well on long records with wide variety of ECG wave morphology and rhythm.

This method has also been implemented on standard MIT-BIH noise stress test database that contains ECG signals with 'em' noise of different SNR levels to assess it's performance on noisy signals. The beat detection performance of the voting fusion method on MIT-BIH noise stress test database has been compared with those of other studies in Table 6.6.

Table 6.6: Performance comparison of beat SQI based majority voting fusion method in heart beat detection with other studies on MIT-BIH noise stress test database (nstdb)

	Algorithm	No. of beats	Average (%)		Gross (%)			Score (%)
			Se	PPV	Se	PPV	F_1	
Single Detector	epltd	26370	95.66	89.61	95.75	88.06	91.75	92.27
	gqrs	26370	96.33	86.89	96.43	83.32	89.40	90.74
Other algorithms	Marcus Vollmer	N/A			94.90	92.02	93.44	
Voting fusion method (Present work)	(epltd/SSF-TKE)	26370	93.09	93.79	93.25	93.89	93.57	93.50
	(gqrs/SSF-TKE)	26370	93.71	92.44	93.87	92.07	92.96	93.02
	(gqrs/epltd)	26370	95.92	85.80	96.03	82.60	88.81	90.09

It can be seen from the Table 6.6 that voting fusion algorithm epltd/SSF-TKE and gqrs/SSF-TKE combinations have improved overall score 1.23% and 0.75% respectively over the score of well known best single detector 'epltd'. The excellent results of the proposed majority voting fusion algorithm on standard MIT-BIH noise stress test database proves its robustness against noise.

The performance of proposed algorithm has been evaluated on benchmark MIT-BIH Arrhythmia database, which contains records of normal ECG signals as well as ECG signals that are affected by non-stationary effects, low signal to noise ratio, premature atrial complexes,

premature ventricular complex, left bundle blocks and right bundle blocks. The beat detection performance of the voting fusion method on MIT-BIH Arrhythmia database has been compared with those of other studies in Table 6.7.

Table 6.7: Performance comparison of beat SQI based majority voting fusion method in robust heart beat detection with other studies on MIT-BIH Arrhythmia database

	Algorithm	No. of beats	Average (%)		Gross (%)			Score (%)
			Se	PPV	Se	PPV	F_1	
Single detectors	epltd	109267			99.69	99.77	99.73	
	gqrs	109494	97.99	98.57	97.71	98.55	98.12	98.20
	SSF-TKE	109494	97.14	98.45	96.63	98.59	97.60	97.70
Other algorithms	Pangerc et al.	N/A			**99.90**	**99.92**	**99.91**	**99.91**
	Mollakazemi et al	47721			99.07	99.76	99.41	
	Plesinger et al	107230			99.77	98.99	99.38	
	Marcus Vollmer	109494			98.59	99.68	99.13	
Voting fusion method Present work	(gqrs/epltd)	109494	99.56	99.67	99.54	99.65	99.60	99.61
	(gqrs/SSF-TKE)	109494	98.81	99.08	99.44	99.18	99.31	99.12

The majority voting fusion (gqrs/epltd combination) has increased the gross F1 measure by 1.19% over the F1 measure achieved by individual QRS detector 'gqrs'. However, there is a minor drop in F1 measure achieved by voting fusion method (gqrs/epltd combinations) as compared to that of best single QRS detector (epltd). It can be seen from the table that the performance of other fusion algorithms on MIT-BIH arrhythmia database are also relatively low except that of Pangerc et al. [187]. F1 measure of 99.60% achieved by our algorithm (gqrs/epltd) is better than that of other studies, except Pangerc et al. [187]. The performance of our algorithm on MIT-BIH arrhythmia database that includes uncommon but clinically important arrhythmia signals, has been satisfactory.

The beat detection performance of majority voting fusion method in noisy part of ECG signal of record no. 1503 of set-p2 of PhysioNet/CinC Challenge 2014 is depicted in Figure 6.3. The beats detected in ECG by 'gqrs' and in ABP by wabp (pulse adjusted by PTT) are shown in Figure 6.3 (a) and 6.3 (c) respectively. The beats detected by modified SSF-TKE in

EOG and EMG signals are shown in Figure 6.3 (d) and 6.3 (e) respectively. It can be seen in the Figure 6.3 that there are number of false detections by 'gqrs' in noisy part of ECG, whereas the detected beats in EOG and EMG signals are matching with reference beats when ECG is noisy. It is evident from Figure 6.3 (f) that beat SQI based majority fusion method has achieved excellent beat detection from fusion of multimodal signals, when ECG is noisy.

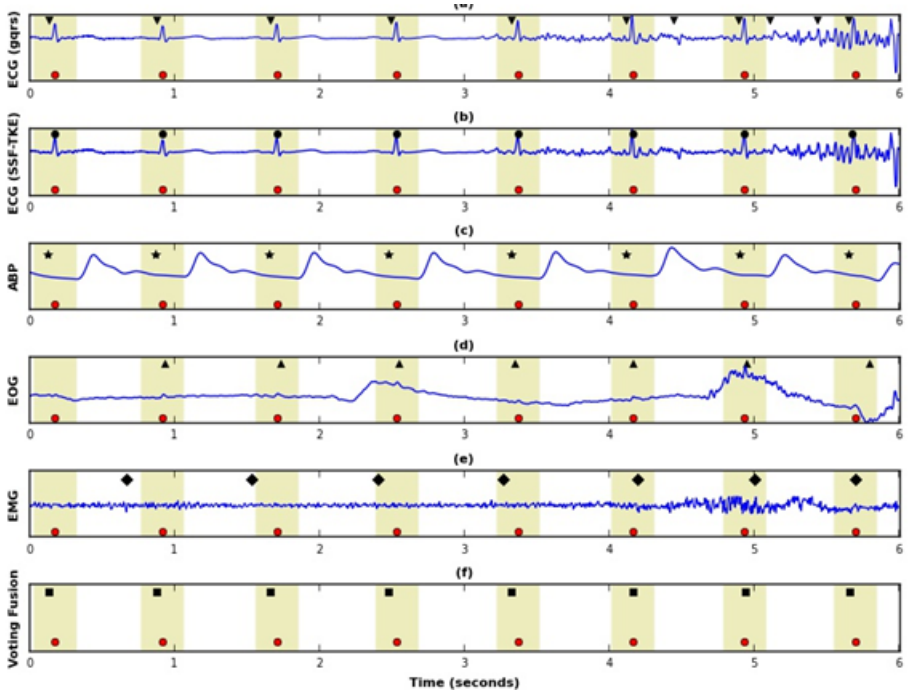

Figure 6.3: (a) ECG beats by gqrs (▼); (b) ECG beats by SSF-TKE (●); (c) Beats from ABP pulse by 'wabp' (*); (d) EOG beats by modified SSF-TKE (▲); (e) EMG beats by modified SSF-TKE (♦); and (f) Beats from voting fusion method (■). Reference beat annotations (●)

6.4.1 Experimental validation of the proposed method on simultaneously noisy ECG and ABP signals

The beat detection performance of MVF algorithm is validated on the synthetic noise dataset. The results of majority voting fusion method with different combinations of QRS detectors on ECG 'bw', 'em' and 'ma' noises along with different types of ABP noises are tabulated in Table A.13, Table A.14 and Table A.15 of appendix A respectively. It can be seen from the Table A.13, Table A.14 and Table A.15 that majority voting fusion method has achieved excellent beat detection results in all types of ECG and ABP noises, except high frequency ABP noise in combination with ECG 'em' and 'ma' noises in which there is minor drop in F1 scores (less than 1%) for higher noise levels (SNR of -3 dB and below). Table A.13, Table

A.14 and Table A.15 in appendix 'A' show that all the three combinations of majority voting fusion have substantially increased F1 scores (from 0.14% to 23.16%) over the score of well known QRS detectors in concurrently extremely noisy (SNR levels of 0 dB to -12 dB) ECG and ABP signals. It has been observed that the increase in F1 score over well known single detectors is higher for higher noise levels in the ECG and ABP signals. However, in ECG 'bw' noise the increase in F1 score is only at higher noise level of -12 dB (Table A.13).

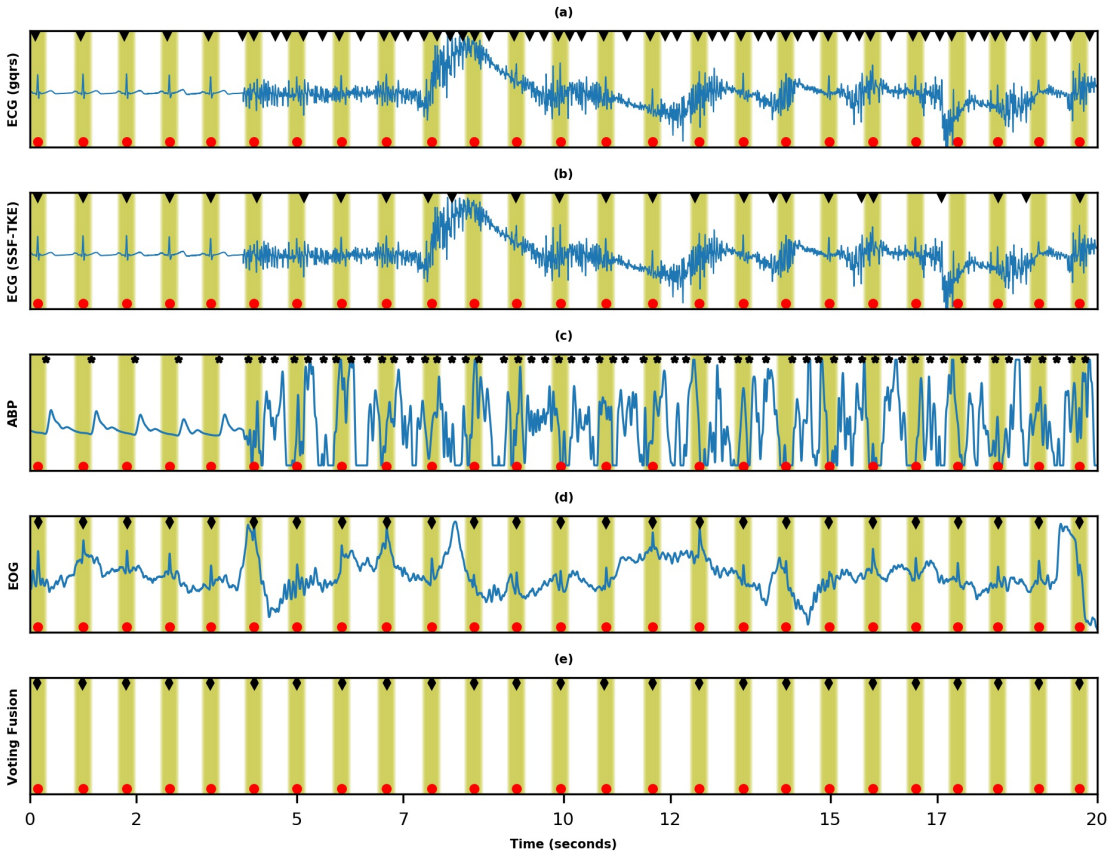

Figure 6.4: Beat detection performance of majority voting fusion method on noisy ECG and noisy ABP signals: (a) ECG beats by gqrs (▼), (b) ECG beats by modified SSF-TKE, (▼) (c) Beats from ABP pulse by 'wabp' (*), (d) EOG beats by modified SSF-TKE (♦), and (e) Beats from voting fusion method (♦). Reference beat annotations (●)

The validation of majority voting fusion method on ECG with 'ma' noise and ABP with 'high frequency' noise each of -12 dB mixed in clean ECG and ABP signals of record no. 123 of set-p dataset of PhysioNet/CinC Challenge 2014 is depicted in Figure 6.4. It can be seen in Figure 6.4 (a) and Figure 6.4 (c) that both ECG and ABP signals are concurrently

noisy and there are large no. false positive detection by 'gqrs' in noisy ECG as well as by 'wabp' in noisy ABP signal. SSF-TKE has also some false positive as well as false negative detection as shown in Figure 6.4 (b). ECG artifacts detected by SSF-TKE in EOG are true positive beats as can be seen in Figure 6.4 (d). The MVF algorithm has efficiently selected final fused beats that are matching with reference beat annotations as can be seen in Figure 6.4 (e). The above analysis shows that when both cardiovascular signals are simultaneously noisy, non-cardiovascular signals participate in voting fusion algorithm for robust beat detection. It validates excellent beat detection performance of our MVF algorithm in worst case of concurrently noisy cardiovascular signals.

6.5 Discussion

The majority voting fusion method uses statistical and probabilistic based beat SQI that selects the beats of multimodal signal for fusion based on their quality. The best quality signal in the window is selected as reference signal for that window and the reference signal plays critical role in selection of other signal beats for voting fusion to locate final fused beat. The advantage of window based selection of reference signal is that it keeps on switching according to the relative quality of signals and ensures that the voting process, i.e. selection of candidate beats for voting is always governed by the best quality signal among the participating signals in fusion. In records with multiple ECG leads, the voting fusion method make use of all the ECG leads and selects the ECG lead with highest SQI for fusion.

The beat SQI based majority voting fusion (MVF) method (with different combinations of QRS detectors) has achieved scores of 91.76%, 95.93%, 95.60%, 93.50% and 99.85% in beat detection on PhysioNet/CinC Challenge 2014 hidden test dataset, PhysioNet/CinC Challenge 2014 training dataset, MGH/MF waveform database, MIT-BIH noise stress test database and MIT-BIH Polysomnographic database and it has improved overall score by 4.30%, 2.90%, 3.96%, 1.23% and 0.17% respectively over the score of single ECG QRS detector (gqrs or epltd) in these databases. The MVF method has demonstrated excellent R-peak detection performance across a number of standard databases with wide variety of signal morphologies. In PhysioNet/CinC Challenge 2014 public training dataset, there are seven records with incorrect beat annotations viz. 1033, 1195, 1242, 1354, 1858, 2277 and 42511 [188]. If these seven records are excluded, the scores achieved by epltd/SSF-TKE and gqrs/SSF-TKE combination would be 97.07% and 96.47% respectively. The proposed fusion algorithm removes pacemaker beats from ECG efficiently, it may be one of the reason for achievement of high score in PhysioNet/CinC Challenge 2014 test dataset. The improvement in overall score by the MVF method over the scores of individual QRS detectors on number of standard databases

have established effective participation of NC signals in the voting fusion process. The minor drop in F1 measure achieved by voting fusion method (gqrs/epltd combinations) in MIT-BIH arrhythmia database as compared to that of single detector 'epltd' may be due to relatively lower F1 measure of 'gqrs' in the arrhythmia database. Excellent performance of majority fusion method on MIT-BIH noise stress test database shows that the algorithm is resistant against noise.

The proposed method has achieved excellent beat detection performance in experimental validation on the synthetic noise dataset in which both ECG and ABP are concurrently noisy. Thus, MVF method is able to fill in the gaps of heart beats during the periods of concurrently noisy cardiovascular signals using redundant heart beat information from NC signals.

SSF-TKE, 'gqrs' and 'epltd' detectors have been used for R-peak detection in ECG and their combinational pair are also used. Performance of 'gqrs' is excellent in signals with normal sinus rhythm (NSR) but has serious limitation on noisy signals. 'epltd' algorithm performs well on signals with NSR, arrhythmias and complex wave morphology but its performance degrades on noisy signals. SSF-TKE method performs exceedingly well on signals with NSR and on noisy signals but has limitation on signals with varying cardiac rhythm. These QRS detectors complement each other in fusion, which has contributed in excellent performance of MVF method on large no. of standard databases. The performance of different combinations of beat SQI based majority fusion method varied on different datasets; 'epltd/SSF-TKE' combination performed best on PhysioNet/CinC Challenge 2014 training and test dataset, MIT-BIH Polysomnographic database and MIT-BIH noise stress test database. This may be because performance of SSF-TKE method and 'epltd' is better than that of 'gqrs' on ECG signals with normal sinus rhythm and on noisy ECGs. 'gqrs/epltd' combination performed best on MIT-BIH Arrhythmia database and MGH/MF waveform database, possibly because 'epltd' and 'gqrs' performed better than SSF-TKE method on ECGs with cardiac arrhythmias.

Our beat SQI based voting fusion method is one of the few multichannel algorithms that have used five multimodal signals i.e. ECG, BP, EEG, EOG and EMG for robust heart beat detection. The majority voting fusion method using NC signals along with cardiovascular signals has achieved better beat detection performance in PhysioNet Challenge 2014 training dataset, PhysioNet Challenge 2014 hidden test dataset, MIT-BIH Polysomnographic database as compared to other studies by Johannesen et al. [106], Gieraltowski et al. [183] and Jongmin Yu et al. [184] that have used similar combination of signals.

6.6 Conclusion

The majority voting fusion method has achieved excellent performance in robust heart beat detection by fusion of multimodal physiological signals on number of standard databases. The fusion is based on beat signal quality of each of the signals that reflects the level of trust in the peaks detected on these signals. It has improved the scores over the single ECG QRS detector in these databases. The majority voting fusion method has achieved highest score among the results of reported studies on MGH/MF waveform database and MIT-BIH noise stress test database. The beat detection score of 91.76% achieved by voting fusion method (epltd/SSF-TKE combination) on PhysioNet/CinC Challenge 2014 hidden test dataset presently ranks 5th on the results of the Challenge. The scores achieved by the other two combinations i.e. gqrs/SSF-TKE (90.89%) and epltd/gqrs (90.67%) on hidden test dataset of PhysioNet/CinC Challenge 2014 are also within the top 10 scores of the challenge. The validation of majority voting fusion method on synthetic noise dataset has demonstrated that use of NC signals in majority voting fusion has substantially increased the accuracy of heart beat detection in concurrenly noisy ECG and ABP signals. Thus, majority voting fusion method has achieved robust heart beat detection from fusion of multimodal physiological signals.

Chapter 7

Robust heart rate estimation

7.1 Introduction

In continuation of our previous works as reported earlier, where we have applied majority voting fusion method on multimodal signals and obtained very good results for heart beat detection, even in noisy ECG and ABP signals, we have implemented the MVF algorithm for estimating robust heart rate from multimodal signals. We were encouraged to see in the study of robust heart beat detection that implementation of the fusion algorithm on multimodal signals has increased true beats and reduced false positive beats detections as compared to the detections by single detectors, especially in noisy cardiovascular signals. This has motivated us to study HR estimation from multimodal signals where higher true beats and lower false positive beats play an important role towards the accuracy of HR estimation. The essence of fusion method is to discriminate a true positive beat from false positive beat in different signals using signal quality index to obtain a series of TP beats for optimal heart rate estimation. This may also be useful in decreasing false alarms in patient monitoring system triggered by incorrect assessment of HR from noisy or missing ECG recordings in ICUs. A reliable heart rate estimation system is important for diagnosis of heart disease, monitoring cardiac health of ICU patients and also to avoid false alarms in ICUs. Our majority voting fusion (MVF) method has used redundant heart beat information in cardiovascular signals and non-cardiovascular signals for robust heart rate estimation. The method relies on the extraction of heart beat information from ECG, ABP, EEG, EOG and EMG to make a more robust estimation about the heart rhythm.

Non-stationary signals of HR may contain indications of some current or future cardiac problem. HR has an important role in the analysis and assessment of HRV which is used for an assessment of overall cardiac health and that of the state of automatic nervous system. As per a previous study, R-R interval can also be used to detect diabetes [189]. The nervous system

is also responsible to regulate cardiac activities. Huge data on the work related to cardiac diseases, their diagnostic techniques and related studies has piled up in the literature and it's analysis has become a time consuming and tedious job for both men and machine. Hence, studies on HR and HRV versus time have become a challenging task for the researchers in the field. Any method/technique which is simple and takes lesser computation time is a welcome addition to the current literature in the field.

ICU patients with severe and life-threatening diseases and injuries require constant and close monitoring to ensure normal bodily functions. Heart rate is one of the important vital parameter which should be monitored closely and precisely. Therefore, it is important to create systems for reliable heart rate estimation. The fusion of different signals gives more information about the health of the patient, and in addition can be more efficient and accurate for HR estimation. [190].

The MVF method has been evaluated for robust HR estimation on records of PhysioNet/CinC Challenge 2014 public training dataset containing NC signal along with cardiovascular and on all the records of MIT-BIH polysomnographic database. The proposed algorithm has been validated on the 'synthetic noise dataset' generated by adding different types of real noise to a clean ECG and ABP signals. Furthermore, we have also validated our algorithm on single board microcomputer i.e. Raspberry Pi 3. Practically the algorithm takes a very small computation time, which is important for real time application requirements of the algorithm.

7.2 Related Works

Heart rate information can be obtained easily by beat detection from the ECG [4], pulsatile waveforms such as the ABP [13] and pulse oximetry waveforms recorded from the photoplethysmogram [191]. For reliable HR estimation, Ebrahim et al. [190], Feldman et al. [3] and Tarassenko et al. [23] have used fusion of data from multiple sensors. Sensor fusion can provide robust cardiovascular parameter estimates even when only one channel of data is relatively noise free. However, if data from an untrustworthy signal is used, the resultant estimate may be degraded. Ebrahim et al. [190] have used a statistical robust sensor fusion (RSF) method for HR estimation from fusion of ECG, pulse oximeter and intra-arterial catheter using Kalman filter. Q. Li et al. developed a robust HR estimation method based on signal quality analysis, Kalman filtering and data fusion from ECG and ABP signals. They have used SQI to adjust Kalman gain in Kalman filter. A.V. Gribok et al. proposed an algorithm for reliable estimation of instantaneous heart rate (HR) from noisy ECG using weighted regularized least squares [192]. The advantage of the method is that least squares problem allows analytical

computation of statistical confidence intervals on the estimated heart rate. G. Borges and V. Brusamarello [28] have applied Bayesian fusion for HR estimation from ECG, ABP and PPG. They have used a simple heart beat detection algorithm using a moving window of 0.3 seconds and a peak is selected when the maximum value of the window is in the middle of the overall window.

To the best of our knowledge, all the previous studies have used only cardiovascular signals for robust heart rate estimation. Lars Johannesen et al., Gieraltowski et al. and Jongmin Yu et al. have proposed robust heart beat detection methods by fusion of multimodal signals i.e. cardiovascular signals and non-cardiovascular signals and that too on a limited number of signals in a dataset. They have reported the results in terms of sensitivity and predictivity of beat detection only and have not extended their work to heart rate estimation.

The basic objective of heart beat detection is heart rate estimation and HRV analysis. Accurate R-peak detection is a necessary, but not sufficient condition for accurate heart rate estimation. It can be seen in Eq. (7.1) that R-R interval or equivalently HR are not a directly measured quantity; rather, they are indirectly obtained by computing the difference of the directly observable cummulative R peak occurrence times. Computing the difference of an observable quantity containing some measurement noise (or errors) amplifies the noise and significantly contaminates the computed differences [192]. The right-hand side of Eq. (7.1) contains measurement noise because cumulative R peak occurrence times cannot be determined with absolute certainty regardless of which QRS detection algorithm is used. Further, ANSI recommends a time window of 150 ms for considering the synchronization between a beat detected by QRS algorithm and a reference annotation, hence a beat is considered as matched beat, if it is located within 150 ms on either side of the reference beat annotation. Thus a matched beat may not be located exactly at the location of its corresponding reference beat and HR estimated from such matched beats would be in variance with actual heart rate (from reference beat annotations). In addition, false positive (FP) and false negative (FN) beats add more noise to the determination of the cumulative beat occurrence times. The sensitivity of such determinations to the slightest misidentification of peaks in ECG waveforms is significantly amplified in the computation of R-R interval. Hence, accurate heart beat detection may not necessarily give accurate heart rate estimation. Alistair Johnson et al. have also reported that sensitivity and predictivity may not be a good evaluation parameter of fusion technique for clinical application of accurate HR estimation, which can be better assessed by absolute error or rMSE of R-R interval [51].

We have proposed a beat SQI based majority voting fusion algorithm for robust HR estimation from fusion of NC signals and cardiovascular signals.

7.3 Proposed method

The term "heart rate" normally refers to the rate of ventricular contractions. It is important to determine both atrial and ventricular rates because there are some conditions in which the atrial and ventricular rates differ (second and third degree AV block). These rates can be estimated from ECG strip chart. Ventricular rate can be determined by measuring the time intervals between R waves (R-R intervals) whereas atrial rate can be determined by measuring the time intervals between P waves (P-P intervals). QRS complex is the most visible feature in ECG, therefore R- R interval is generally used to determine heart rate.

The heart rate is estimated over a window length of 10 s duration as given in Eq. (7.1):

$$HR(bpm) = 60/[MeanR - R_{interval(seconds)}] = 1 \tag{7.1}$$

The HR can be estimated directly from detected R-R peak interval in ECG, EOG, EEG and EMG signals and by adjusting ABP pulse peaks with pulse transit time in ABP signals. In the proposed beat SQI based majority fusion method, the HR has been estimated from R-R interval of fused beats obtained from fusion of multimodal physiological signals. The estimated HR is validated from reference beat annotation HR. The root mean square error (rMSE) of the estimated HR ($HR_{i\ signal}$) and reference beat annotation HR ($HR_{i\ ref}$), as given in Eq. (7.2), has been used to evaluate the HR estimation performance of the algorithm.

$$HRrMSE = \sqrt{\frac{1}{N}\sum_{i=1}^{N}(HR_{isignal} - HR_{iref})^2} \tag{7.2}$$

Where, N is total number of beats in a signal.

7.4 Performance Evaluation

PhysioNet/CinC Challenge 2014 public training dataset and MIT-BIH Polysomnographic database are being used for performance evaluation of the proposed algorithm. We have calculated rMSE of HR estimates obtained from R-R interval of fused beats using Eq. (7.2). The beat SQI based majority voting fusion method has been evaluated for robust heart rate estimation on all 110 records of PhysioNet/CinC Challenge 2014 training dataset and all the 18 records of MIT-BIH Polysomnographic database that contain either one or all the three NC signals. The results on both the datasets have been reported into different groups based on HR rMSE of ECG and ABP signals.

7.4.1 Experiment 1: Performance evaluation of robust heart rate estimation on the standard PhysioNet/CinC Challenge 2014 public training database.

The proposed beat SQI based majority voting fusion algorithm is implemented on 110 records of PhysioNet/CinC Challenge 2014 public training dataset that contain either one or all the three NC signals. The detail results on entire dataset are given in Table A.16 of appendix A. To evaluate HR estimation performance of majority voting fusion, the results are classified into three groups based on rMSE of estimated HR from ECG and ABP signals;

(i) noisy ECG and good ABP signals

(ii) noisy ECG and noisy ABP signals

(iii) good ECG and good ABP signals

The HR estimation results for the above three groups are given in Tables 7.1, 7.2 and 7.3 respectively. It can be seen from Table 7.1 that majority voting fusion method has substantially improved accuracy of HR estimates over that of well known single QRS detector 'gqrs' (i.e. substantial reduction in rMSE of HR estimate) in records with noisy ECG and clean ABP signal. In record no. 188 and 199, the majority voting fusion has reduced the rMSE of HR estimates from 35.10 bpm & 30.39 bpm to 1.58 bpm and 0.25 bpm respectively. The majority voting fusion has substantially reduced estimation error of ECG heart rate (more than 95%) in all the records of this group and the maximum reduction of 99.56% is in record no. 148. The majority voting fusion method has reduced average rMSE of HR estimate of noisy ECG signals from 15.54 bpm to 0.24 bpm i.e. 98.46% reduction in HR estimation error for noisy ECG and good ABP signals (Table 7.1).

It can be seen from the Table 7.2 that the proposed MVF method has also substantially improved accuracy of HR estimates over that of well known single QRS detector 'gqrs' (i.e. substantial reduction in rMSE of HR estimate) in records with noisy ECG and noisy ABP signals. The HR rMSE of ECG (by gqrs) of record no. 2800 and 3188 is 41.87 bpm and 39.78 bpm respectively; whereas the rMSE of HR estimate derived from ABP signals of these records is 16.78 bpm and 14.76 bpm respectively. The MVF method has reduced rMSE of HR estimates from 41.87 bpm and 39.78 bpm to 4.02 bpm and 1.48 bpm respectively. It has substantially reduced estimation error of ECG heart rate (from 55.18% to 98.74%) in all the records of this group and the maximum reduction is in record no. 2800. The proposed fusion method has yielded accurate HR estimates with low average rMSE of 0.84 bpm, even when both ECG (avg. rMSE of 11.68 bpm) and ABP (avg. rMSE of 9.01 bpm) signals are noisy (Table 7.2). There is an average 92.81% reduction in HR estimation error in records with noisy ECG and noisy ABP signals.

Table 7.1: Sensitivity, Predictivity and HR rMSE by Majority voting fusion method (for noisy ECG and good ABP signals of PhysioNet Challenge 2014 training dataset)

Record No.	Voting		HR rMSE (bpm)					
	Sensitivity (%)	Predictivity (%)	ECG	ABP	EEG	EOG	EMG	Voting
112	100.00	100.00	19.52	0.86	5.99	2.62	6.36	0.14
146	100.00	100.00	22.53	0.10	9.22	6.20	7.99	0.15
148	100.00	100.00	18.26	0.06	10.59	-	-	0.08
156	100.00	100.00	8.88	1.74	19.58	-	-	0.08
168	100.00	100.00	15.68	0.90	18.77	-	-	0.08
169	100.00	100.00	30.39	0.14	13.25	-	-	0.25
175	100.00	100.00	6.24	0.09	11.35	2.30	8.44	0.28
188	99.64	99.64	35.10	1.67	13.88	-	-	1.58
189	99.72	99.72	20.01	0.96	7.83	6.37	7.55	0.34
190	100.00	100.00	4.28	0.05	7.48	4.69	9.16	0.10
191	100.00	100.00	5.68	0.13	10.06	-	-	0.15
192	100.00	100.00	4.14	0.44	6.32	-	-	0.04
198	100.00	100.00	19.71	0.96	8.26	3.53	9.61	0.14
1020	100.00	99.83	5.10	0.57	13.42	-	-	0.07
2527	99.71	99.86	17.55	0.12	14.12	8.42	8.87	0.11
Average	**99.94**	**99.94**	**15.54**	**0.59**	**11.34**	**4.88**	**8.28**	**0.24**

Table 7.2: Sensitivity, Predictivity and HR rMSE by Majority voting fusion method (for noisy ECG and noisy ABP signals of PhysioNet Challenge 2014 training dataset)

Record No.	Voting		HR rMSE (bpm.)					
	Sensitivity (%)	Predictivity (%)	ECG	ABP	EEG	EOG	EMG	Voting
107	99.87	100.00	2.99	1.60	12.76	-	-	1.34
113	99.85	99.85	4.98	27.9	9.16	8.24	10.86	0.16
117	100.00	100.00	1.24	5.51	15.41	12.08	16.79	0.17
122	99.84	100.00	1.84	3.75	4.88	-	-	0.18
124	99.87	99.87	18.08	8.70	9.88	5.06	8.03	0.25
131	99.86	99.86	12.08	37.32	9.47	-	-	0.24
132	99.88	100.00	1.81	3.52	12.43	7.34	16.67	0.15
133	99.62	99.50	26.66	2.76	14.22	-	-	1.89
143	100.00	100.00	1.50	2.94	9.55	13.36	16.23	0.10
145	100.00	100.00	1.15	2.99	3.31	7.99	9.94	0.04
153	99.82	100.00	3.80	7.90	15.21	12.96	12.18	1.04
176	100.00	100.00	2.45	2.31	8.35	6.18	9.12	0.17
177	99.71	100.00	6.92	2.20	7.80	7.30	8.25	1.88
1503	99.87	99.87	19.79	3.22	10.54	7.25	9.68	0.25
2800	74.47	74.17	41.87	16.78	13.41	-	-	4.02
3188	99.88	99.64	39.78	14.76	18.16	-	-	1.48
Average	**98.28**	**98.30**	**11.68**	**9.01**	**10.91**	**8.78**	**11.78**	**0.84**

Table 7.3: Average Sensitivity, Average Predictivity and Average HR rMSE by Majority voting fusion method (for good ECG and good ABP signals of PhysioNet Challenge 2014 training dataset).

No. of Records	Voting		Average HR rMSE (bpm.)					
	Avg. Sensitivity (%)	Avg. Predictivity (%)	ECG	ABP	EEG	EOG	EMG	Voting
79	**99.15**	**99.15**	**1.50**	**1.53**	**10.03**	**8.16**	**10.47**	**0.53**

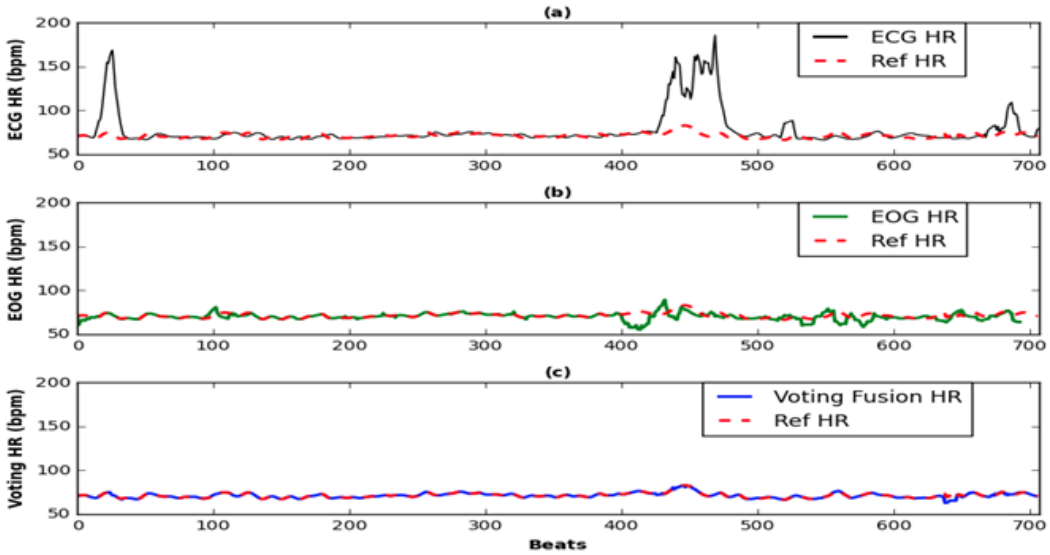

Figure 7.1: HR estimates (bpm) for signal no. 112 of PhysioNet challenge 2014 training dataset from: (a) ECG (gqrs); (b) EOG signal (SSF-TKE); (c) Majority Voting Fusion (gqrs/SSF-TKE) method.

In records with good ECG and good ABP signals also, the majority voting fusion method has achieved accurate HR estimates with average rMSE of 0.53 bpm as against average rMSE of 1.50 bpm achieved by gqrs in ECG and 1.53 bpm by wabp in ABP (Table 7.3). Thus, the majority voting fusion has improved accuracy of HR estimates over that of well known QRS detector 'gqrs' (64.67% reduction in HR estimation error) in records with clean ECG and clean ABP signals of PhysioNet/CinC Challenge 2014 training dataset.

The results are well within clinical acceptable limit of ± 5 bpm. In this context, one can say that our method has yielded excellent results for HR estimation even when both the cardiovascular signals are noisy. This also confirms the participation of NC signals in fusion process for robust HR estimation.

HR estimates from ECG (gqrs), EOG signal (SSF-TKE), majority voting fusion (gqrs/SSF-TKE) method for record no. 112 of PhysioNet/CinC Challenge 2014 public training dataset

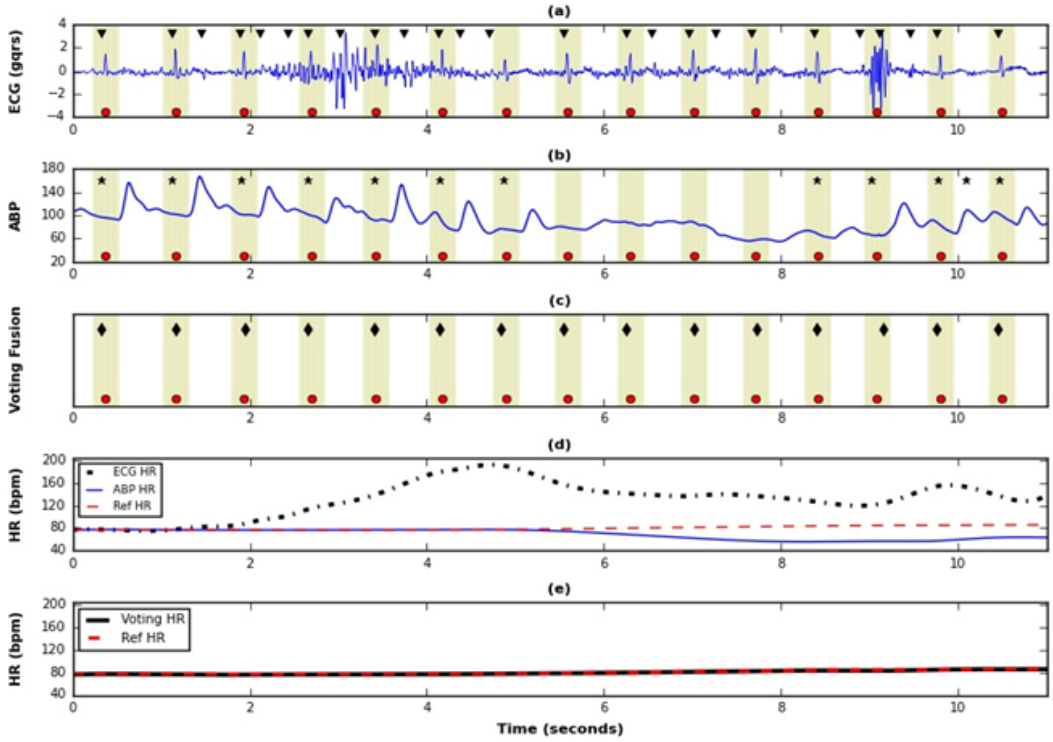

Figure 7.2: (a) ECG signal with detected beats (gqrs) (▼); (b) ABP signal with detected beats (*) (pulse adjusted by PTT); (c) Beat detection (♦) by voting fusion method; (d) HR estimates from ECG (gqrs), ABP and reference beats; (e) Voting fusion HR estimate.

are plotted in Figure 7.1 to validate our algorithm when ECG signal is noisy. The HR estimates obtained from ECG signal by gqrs are in large variance from reference beat HR at some places as shown in Figure 7.1 (a), whereas HR estimates from simultaneously recorded EOG signals in Figure 7.1 (b) have very small variance from reference HR. The estimated HR from voting fusion method closely follows reference beat HR as can be seen in Fig. 7.1 (c). This clearly shows the efficiency of voting fusion method in accurate HR estimation in noisy ECG signals and participation of NC signals in it.

It can be seen from Fig. 7.2 (a) and 7.2 (b) that both ECG and ABP of record no. 1503 of PhysioNet Challenge 2014 training dataset are noisy concurrently. The detected beats in ECG (by gqrs) and ABP (pulse adjusted by PTT) are quite irregular and there are number of FP beats in ECG and FN beats in ABP. As seen in Fig. 7.2 (d), HR estimates for ECG and ABP are in large variance with reference beat HR. However, it can be seen in Fig. 7.2 (c) and 7.2 (e) that the fusion method has achieved excellent beat detection and voting HR estimate is perfectly matching with reference beat HR. Thus, the majority voting fusion can give accurate HR estimate from fusion of NC signals with cardiovascular signals, even when both ECG and ABP signals are simultaneously noisy.

Table 7.4: Sensitivity, Predictivity and HR rMSE by Majority voting fusion method (for noisy ECG and noisy ABP signals of MIT-BIH Polysomnographic database).

Record No.	Voting		HR rMSE (bpm.)					
	Sensitivity (%)	Predictivity (%)	ECG	ABP	EEG	EOG	EMG	Voting
slp 02a	99.61	99.87	4.65	5.90	9.79	-	-	3.14
slp 02b	99.45	99.64	6.78	4.33	12.90	-	-	4.56
slp 03	99.97	97.76	4.28	2.11	10.79	-	-	1.23
slp 04	99.77	99.85	6.57	4.18	11.13	-	-	1.27
slp 14	99.77	99.74	2.07	6.98	12.17	-	-	1.77
slp 16	99.65	99.83	7.20	1.98	14.83	-	-	1.68
slp 32	99.85	99.88	5.08	1.30	10.70	6.71	9.98	1.01
slp 41	99.95	99.86	1.44	7.62	9.80	8.61	9.11	0.75
slp 45	99.94	99.96	3.12	1.28	7.75	4.78	5.90	0.77
Average	**99.77**	**99.60**	**4.58**	**3.96**	**11.10**	**6.70**	**8.33**	**1.80**

7.4.2 Experiment 2: Performance evaluation of robust heart rate estimation on standard MIT-BIH Polysomnographic database.

The proposed majority voting fusion method with all the three different combinations of QRS detectors is further implemented on all the 18 records of MIT-BIH Polysomnographic database and the detail results are given in Table A.17 of appendix A. It can be seen from the Table A.17 that HR estimation performance of epltd/SSF-TKE combination of MVF is better than those of gqrs/SSF-TKE and gqrs/epltd combinations. The results of HR estimation of gqrs/SSF-TKE combination have been classified into two groups based on rMSE of estimated HR of ECG and ABP signals;

(i) noisy ECG and noisy ABP signals, and

(ii) good ECG and good / noisy ABP signals.

HR estimation performance of the majority voting fusion method is compared with that of gqrs in Tables 7.4 and 7.5. It can be seen from the Table 7.4 that the proposed majority fusion method has improved accuracy of HR estimates over that of well known single QRS detector 'gqrs' (i.e. reduction in rMSE of HR estimate) in records with noisy ECG and noisy ABP signals. The HR rMSE of ECG (by gqrs) of record no. slp 04 and slp 16 is 6.57 bpm and 7.20 bpm respectively; whereas the rMSE of HR estimate derived from ABP signals of these records is 4.18 bpm and 1.98 bpm respectively. The majority voting fusion has reduced the rMSE of HR estimates from 6.57 bpm and 7.20 bpm to 1.27 bpm and 1.68 bpm respectively. The majority voting fusion has substantially reduced estimation error of ECG heart rate (from 14.49% to 80.67%) in all the records of this group and the maximum reduction is in record no. slp 04. The majority voting fusion method has yielded accurate HR estimates with low

Table 7.5: Average Sensitivity, Average Predictivity and Average HR rMSE by Majority voting fusion method (for good ECG and good / noisy ABP signals of MIT-BIH polysomnographic database)

No. of Records	Voting		Average HR rMSE (bpm.)					
	Avg. Sensitivity (%)	Avg. Predictivity (%)	ECG	ABP	EEG	EOG	EMG	Voting
09	**99.88**	**99.95**	**0.69**	**1.96**	**10.46**	**11.80**	**14.52**	**0.40**

average rMSE of 1.80 bpm, even when both ECG (avg. rMSE of 4.58 bpm) and ABP (avg. rMSE of 3.96 bpm) signals of MIT-BIH polysomnographic database are noisy (Table 7.2). There is an average 60.70% reduction in HR estimation error in records with noisy ECG and noisy ABP signals.

In records with good ECG and good ABP signals also the majority voting fusion method has achieved accurate HR estimates with average rMSE of 0.40 bpm as against average rMSE of 0.69 bpm achieved by gqrs in ECG and 1.96 bpm by 'wabp' in ABP (Table 7.5). Thus, the majority voting fusion has improved accuracy of HR estimates over that of well known QRS detector 'gqrs' (42.03% reduction in HR estimation error) in records with clean ECG and clean ABP signals of MIT-BIH polysomnographic database. Again the HR estimation results of our algorithm are very promising and demonstrates the utility of the algorithm in robust HR estimation using NC signals in case of noisy cardiovascular signals.

7.4.3 Experiment 3: Experimental validation of the proposed method on synthetic noise dataset

The proposed HR estimation method is experimentally validated on a synthetic noise dataset to evaluate its performance on noisy cardiovascular signals. This will also assess the contribution of NC signals in voting fusion for robust HR estimation when both the cardiovascular signals are noisy. The synthetic noise evaluation dataset is generated by adding different types of real ECG and artificial ABP noises in clean ECG and ABP signals as discussed in section 2.9.7. ECG is corrupted by simulating real time noises like base line wander (bw), electrode motion artifact (em), muscle artifact (ma) and power line interference noise. Since above mentioned ECG noises are electrical in nature, they do not affect ABP, which is a mechanical signal. ABP is recorded by different types of sensors and is often corrupted by other type of noises that are often non-Gaussian, nonlinear and nonstationary [54]. ABP waveforms are frequently corrupted by transducer flushing, catheter clotting, movement artifacts, and non-invasive cuff inflations noises [53]. Q. Li identified six different types of artifacts similar to those described

by Mc Ghee et al. These are: (i) saturation to ABP maximum artifact, ii) saturation to ABP minimum artifact, (iii) reduced pulse pressure artifact, (iv) high amplitude square wave artifact, (v) high frequency noise, and (vi) highly transient impulse artifact. Since no database of real ABP noise exists, Q. Li et al. developed a number of ABP artifact simulation algorithms to create realistic artificial ABP noises. Six types of ABP noise; a_{smax}, a_{smin}, a_{lamean}, a_{sw}, a_{hf} and a_{imp} have been added separately to ABP signal of record no. 123 of set-p dataset from Physionet/CinC challenge 2014 using Matlab source code [193].

In this experiment, we have validated HR estimation performance of the proposed method on synthetic noise evaluation dataset containing ECG signals with 'bw', 'em' and 'ma' noises of different SNR levels in combination with different types of ABP noises with varying noise levels. It has been observed that the effect of Sinc function impulse artifact (a_{imp}) has very little impact on HR estimation performance for all combinations of ECG and ABP noises. The HR rMSE results of the experiment for single QRS detectors and voting fusion methods on ECG 'bw', 'em' and 'ma' noises with different combinations of ABP noises of SNR levels from 12 dB to -12 dB are given in Table 7.6, Table 7.7 and Table 7.8 respectively.

It is evident from the Table 7.6 that all the three combinations of majority voting fusion method has shown excellent HR estimation performance on different SNR levels of ECG 'bw' noise and different types of ABP noise, except for gqrs/epltd combination on high frequency (brown) ABP noise of -9 dB level. Amongst the three combinations of majority voting fusion (MVF), epltd/SSF-TKE combination has shown consistently the best results. The HR rMSE of single detectors 'gqrs' and 'epltd' increases for higher levels of ECG 'bw' noise. All the combinations of majority voting fusion method, except gqrs/epltd combination, on high frequency ABP noise, have significantly improved HR estimates as compared to well known individual QRS detector (gqrs and epltd) for ECG 'bw' noise and all types of ABP noises at higher SNR levels (-9 and -12 dB). In ECG 'bw' noise at -12 dB noise level, 'gqrs' and 'epltd' has HR rMSE of 35.68 bpm and 4.79 bpm respectively. In the worst noise combination of ECG 'bw' noise with ABP high frequency noise each of SNR -12 dB, majority voting fusion (gqrs/epltd) combination has achieved HR rMSE of 0.27 bpm. Thus, majority voting fusion (gqrs/epltd) combination has increased the accuracy of HR estimation as compared to that of individual QRS detector in extremely concurrently noisy ECG and ABP signals and has reduced the HR estimate error by 94.36% with respect to that of 'epltd'. We have plotted the HR estimation performance of single QRS detectors and all the three combinations of majority voting fusion method on ECG 'bw' noise and ABP square wave noise in Figure 7.3.

It can be seen from Figure 7.3 that there is no effect of 'bw' noise on HR estimation performance of SSF-TKE; whereas the performance of gqrs and epltd starts deteriorating from noise level of 3 dB and - 9 dB respectively. The performance of all the three combinations of

Table 7.6: HR estimation performance of MVF on noise dataset (ECG 'bw' and ABP noises)

ABP Noise	Noise levels in ECG and ABP (dB)	HR rMSE (bpm)						
		gqrs	epltd	SSF-TKE	ABP	Voting Fusion		
						gqrs/SSF-TKE	epltd/SSF-TKE	gqrs/epltd
Exponential saturation to ABP maximum	12	0.04	0.06	0.03	14.29	0.19	0.16	0.20
	9	0.04	0.06	0.03	14.29	0.19	0.16	0.20
	6	0.04	0.06	0.03	14.29	0.19	0.16	0.20
	3	1.06	0.06	0.03	14.30	0.22	0.16	0.22
	0	1.57	0.06	0.03	14.30	0.26	0.12	0.24
	-3	3.75	0.07	0.03	14.30	0.26	0.13	0.26
	-6	7.82	0.08	0.03	14.30	0.27	0.13	0.27
	-9	16.62	1.60	0.03	14.61	0.28	0.14	0.27
	-12	35.68	4.79	0.04	15.92	0.25	0.16	0.24
Exponential saturation to ABP minimum	12	0.04	0.06	0.03	12.84	0.19	0.16	0.20
	9	0.04	0.06	0.03	12.84	0.19	0.16	0.20
	6	0.04	0.06	0.03	12.98	0.19	0.16	0.20
	3	1.06	0.06	0.03	13.09	0.22	0.16	0.22
	0	1.57	0.06	0.03	13.04	0.26	0.12	0.24
	-3	3.75	0.07	0.03	13.11	0.26	0.13	0.26
	-6	7.82	0.08	0.03	13.27	0.27	0.13	0.27
	-9	16.62	1.60	0.03	13.35	0.28	0.14	0.27
	-12	35.68	4.79	0.04	13.42	0.25	0.16	0.24
Linear saturation to ABP mean	12	0.04	0.06	0.03	1.58	0.19	0.16	0.20
	9	0.04	0.06	0.03	2.21	0.19	0.16	0.20
	6	0.04	0.06	0.03	2.20	0.26	0.22	0.26
	3	1.06	0.06	0.03	2.20	0.30	0.26	0.30
	0	1.57	0.06	0.03	2.44	0.36	0.28	0.33
	-3	3.75	0.07	0.03	4.49	0.34	0.27	0.35
	-6	7.82	0.08	0.03	4.68	0.34	0.24	0.33
	-9	16.62	1.60	0.03	14.27	0.38	0.25	0.36
	-12	35.68	4.79	0.04	14.27	0.39	0.25	0.37
Square Wave	12	0.04	0.06	0.03	20.17	0.19	0.16	0.20
	9	0.04	0.06	0.03	20.10	0.19	0.16	0.20
	6	0.04	0.06	0.03	20.18	0.19	0.16	0.20
	3	1.06	0.06	0.03	20.17	0.22	0.16	0.22
	0	1.57	0.06	0.03	20.22	0.26	0.12	0.24
	-3	3.75	0.07	0.03	20.33	0.26	0.13	0.26
	-6	7.82	0.08	0.03	20.45	0.27	0.13	0.27
	-9	16.62	1.60	0.03	23.34	0.28	0.14	0.27
	-12	35.68	4.79	0.04	25.60	0.25	0.16	0.24
High Frequency Noise	12	0.04	0.06	0.03	39.43	0.19	0.16	0.19
	9	0.04	0.06	0.03	76.42	0.19	0.16	0.20
	6	0.04	0.06	0.03	94.70	0.20	0.16	0.20
	3	1.06	0.06	0.03	104.01	0.24	0.17	0.25
	0	1.57	0.06	0.03	104.86	0.29	0.15	0.27
	-3	3.75	0.07	0.03	105.43	0.27	0.16	0.28
	-6	7.82	0.08	0.03	109.67	0.28	0.19	0.28
	-9	16.62	1.60	0.03	110.61	0.32	0.22	17.08
	-12	35.68	4.79	0.04	115.19	0.26	0.17	0.27

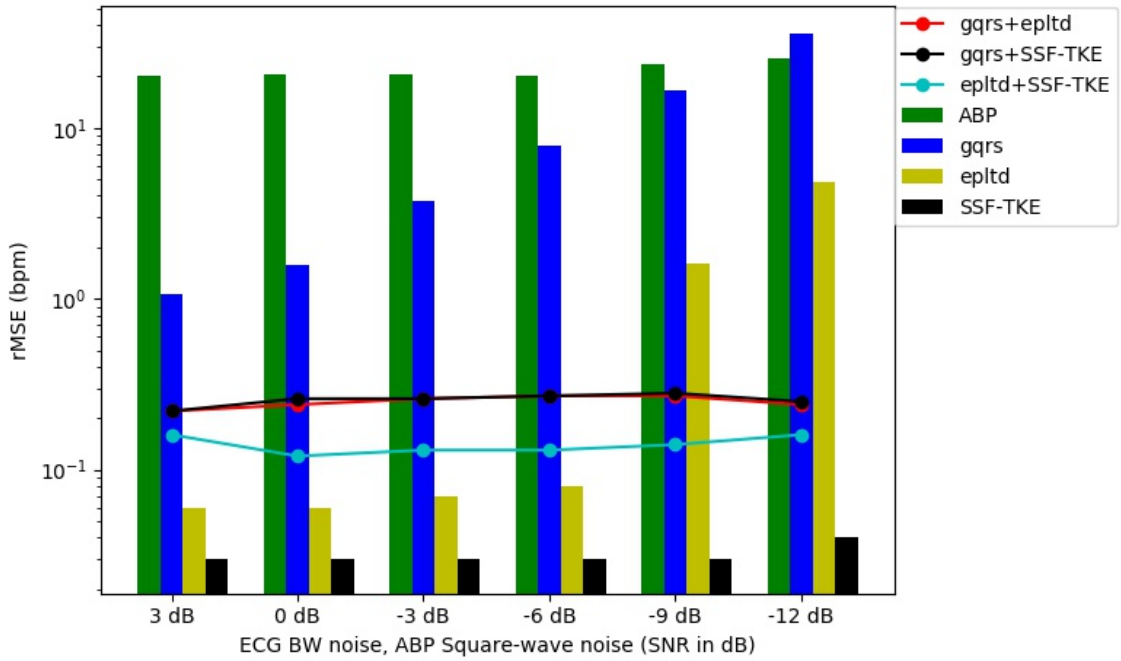

Figure 7.3: HR rMSE of individual ECG detectors and majority voting fusion with different combinations of detectors for different levels of 'bw' noise in ECG and square wave noise in ABP

voting fusion method is almost consistent at all noise levels, with epltd/SSF-TKE combination giving the best results among the three.

HR estimation performance of different combinations of voting fusion method on noise evaluation dataset i.e. ECG with 'em' noise and different types of ABP noises of different SNR levels is given in Table 7.7. It can be seen from the Table 7.7 that at higher noise levels (-9 and -12 dB), the majority voting fusion method has significantly improved accuracy of HR estimation as compared to individual single detectors, except high frequency noise of ABP signal. All the three combinations of voting fusion have shown noise resistant trend beyond -3 dB noise level. Amongst different combinations of MVF, the performance of gqrs/SSF-TKE is better than that of other two combinations for all types of ABP noises at higher noise levels, except for linear saturation to ABP mean noise, in which performance of epltd/SSF-TKE combination is better as compared to others. In ECG 'em' noise at -12 dB noise level, 'gqrs' and 'epltd' has HR rMSE of 78.24 bpm and 43.25 bpm respectively. In the worst noise combination of ECG 'em' noise with ABP high frequency noise each of SNR -12 dB, majority voting fusion (gqrs/epltd) combination has achieved HR rMSE of 1.27 bpm. Thus, majority voting fusion (gqrs/epltd) combination has increased the accuracy of HR estimation as compared to that of individual QRS detector in extremely concurrently noisy ECG and ABP

Table 7.7: HR estimation performance of MVF on noise dataset (ECG 'em' and ABP noises)

ABP Noise	Noise levels in ECG and ABP (dB)	HR rMSE (bpm)						
		gqrs	epltd	SSF-TKE	ABP	Voting Fusion		
						gqrs/SSF-TKE	epltd/SSF-TKE	gqrs/epltd
Exponential saturation to ABP maximum.	12	0.04	0.07	0.03	14.29	0.19	0.16	0.20
	9	1.18	0.07	0.03	14.29	0.20	0.16	0.20
	6	3.07	0.07	0.03	14.29	0.24	0.16	0.23
	3	12.47	0.08	0.03	14.30	0.26	0.17	0.25
	0	31.44	2.35	0.03	14.30	0.22	0.17	1.24
	-3	49.63	9.66	0.03	14.30	0.20	1.26	1.24
	-6	60.38	25.02	1.08	14.30	0.18	1.26	1.26
	-9	70.59	40.82	1.98	14.61	0.18	1.26	1.26
	-12	78.24	43.25	3.36	15.92	0.18	1.26	1.26
Exponential saturation to ABP minimum	12	0.04	0.07	0.03	12.84	0.19	0.16	0.20
	9	1.18	0.07	0.03	12.84	0.20	0.16	0.20
	6	3.07	0.07	0.03	12.98	0.24	0.16	0.23
	3	12.47	0.08	0.03	13.09	0.25	0.17	0.25
	0	31.44	2.35	0.03	13.04	0.22	0.17	1.24
	-3	49.63	9.66	0.03	13.11	0.20	1.26	1.25
	-6	60.38	25.02	1.08	13.27	0.19	1.26	1.26
	-9	70.59	40.82	1.98	13.35	0.19	1.26	1.26
	-12	78.24	43.25	3.36	13.42	0.19	1.26	1.26
Linear Saturation to ABP mean	12	0.04	0.07	0.03	1.58	0.19	0.16	0.20
	9	1.18	0.07	0.03	2.21	0.20	0.16	0.20
	6	3.07	0.07	0.03	2.20	0.29	0.22	0.28
	3	12.47	0.08	0.03	2.20	0.34	0.25	0.34
	0	31.44	2.35	0.03	2.44	0.46	0.29	0.42
	-3	49.63	9.66	0.03	4.49	0.43	0.29	0.40
	-6	60.38	25.02	1.08	4.68	0.43	0.28	0.40
	-9	70.59	40.82	1.98	14.27	0.41	0.27	0.39
	-12	78.24	43.25	3.36	14.27	0.41	0.28	0.40
Square Wave	12	0.04	0.07	0.03	20.17	0.19	0.16	0.20
	9	1.18	0.07	0.03	20.10	0.20	0.16	0.20
	6	3.07	0.07	0.03	20.18	0.24	0.16	0.23
	3	12.47	0.08	0.03	20.33	0.25	0.17	0.25
	0	31.44	2.35	0.03	20.22	0.22	0.17	1.24
	-3	49.63	9.66	0.03	20.45	0.20	1.26	1.24
	-6	60.38	25.02	1.08	20.17	0.18	1.26	1.26
	-9	70.59	40.82	1.98	23.34	0.18	1.26	1.26
	-12	78.24	43.25	3.36	25.60	0.18	1.26	1.26
High Frequency noise	12	0.04	0.07	0.03	39.43	0.19	0.16	0.19
	9	1.18	0.07	0.03	76.42	0.20	0.16	0.20
	6	3.07	0.07	0.03	94.70	0.25	0.17	0.23
	3	12.47	0.08	0.03	104.01	0.26	0.17	0.28
	0	31.44	2.35	0.03	104.86	0.23	0.21	19.08
	-3	49.63	9.66	0.03	105.43	0.24	20.92	20.83
	-6	60.38	25.02	1.08	109.67	0.30	29.17	29.20
	-9	70.59	40.82	1.98	110.61	21.62	21.62	21.72
	-12	78.24	43.25	3.36	115.19	0.25	1.26	1.27

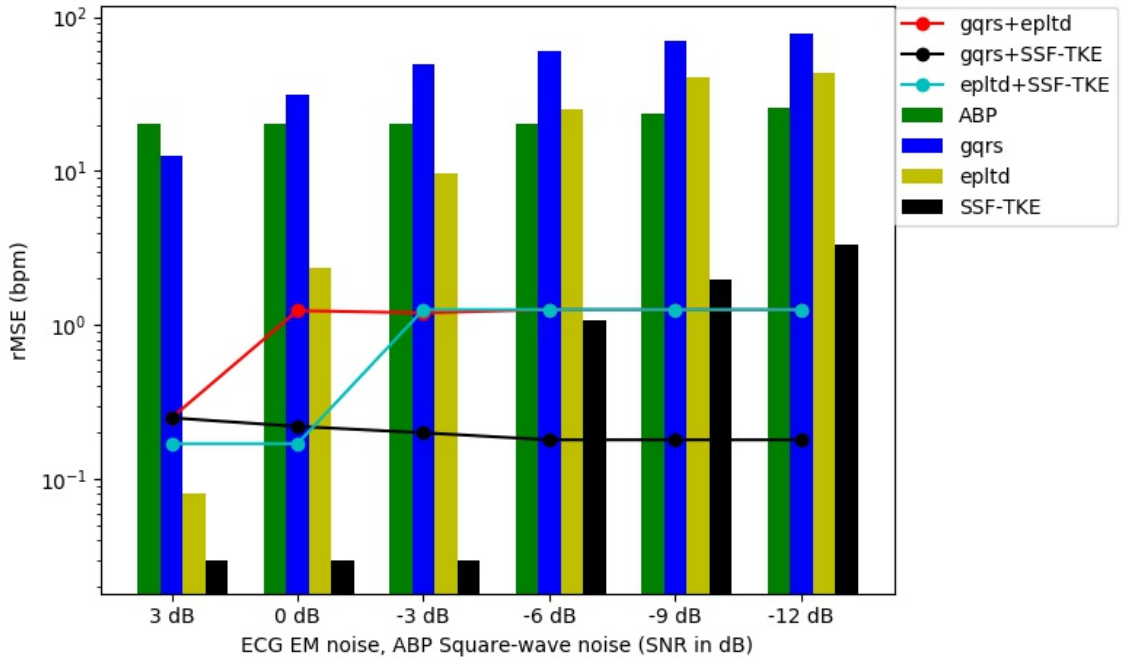

Figure 7.4: HR rMSE of individual ECG detectors and majority voting fusion with different combinations of detectors for different levels of 'em' noise in ECG and square wave noise in ABP

signals and has reduced the HR estimate error by 97.06% with respect to that of 'epltd'. The HR rMSE of individual ECG detectors and majority voting fusion with different combinations of detectors for different levels of 'em' noise in ECG and square wave noise in ABP is plotted in Figure 7.4.

SSF-TKE has minimum HR rMSE at all noise levels of ECG 'em' noise followed by epltd and gqrs. 'gqrs' is highly sensitive to ECG 'em' noise; whereas epltd and SSF-TKE method are noise resistant up to noise levels of 3 dB and -3 dB respectively. The performance of all the three combinations of voting fusion is excellent, with gqrs/SSF-TKE combination performing the best. There is substantial improvement in HR estimation performance of gqrs/SSF-TKE combination as compared to individual detectors for noisy ECG and ABP signals (for -6 dB to -12 dB); whereas for gqrs/epltd and epltd/SSF-TKE combinations such improvement is at noise levels of -9 dB and -12 dB. It can be seen that the HR estimation performance of individual ECG detectors is excellent in relatively clean signals, but proposed voting fusion method is effective when the noise level in cardiovascular signals is high.

It can be observed from the above Table 7.8 that in ECG 'ma' noise also, the performance of SSF-TKE is better than that of gqrs and epltd at all noise levels. The HR rMSE from majority voting fusion of gqrs/SSF-TKE combination is giving better performance in the more

Table 7.8: HR estimation performance of MVF on noise dataset (ECG 'ma' and ABP noises)

ABP Noise	Noise levels in ECG and ABP (dB)	HR rMSE (bpm)						
		gqrs	epltd	SSF-TKE	ABP	Voting Fusion		
						gqrs/SSF-TKE	epltd/SSF-TKE	gqrs/epltd
Exponential saturation to ABP maximum	12	2.10	0.06	0.03	14.29	0.22	0.16	0.22
	9	7.15	0.06	0.03	14.29	0.24	0.16	0.23
	6	19.18	0.08	0.03	14.29	0.23	0.16	0.22
	3	32.13	1.81	1.17	14.30	0.22	0.17	0.23
	0	49.02	11.30	1.19	14.30	0.23	0.17	0.24
	-3	60.51	21.98	1.19	14.30	0.22	0.18	1.25
	-6	75.40	28.73	2.64	14.30	0.22	1.26	1.25
	-9	85.41	40.33	3.77	14.61	0.22	1.26	1.25
	-12	91.34	47.59	3.92	15.92	0.19	1.26	1.26
Exponential saturation to ABP minimum	12	2.10	0.06	0.03	12.84	0.22	0.16	0.22
	9	7.15	0.06	0.03	12.84	0.25	0.16	0.23
	6	19.18	0.08	0.03	12.98	0.23	0.16	0.22
	3	32.13	1.81	1.17	13.09	0.22	0.17	0.23
	0	49.02	11.30	1.19	13.04	0.23	0.17	0.23
	-3	60.51	21.98	1.19	13.11	0.22	0.18	1.25
	-6	75.40	28.73	2.64	13.27	0.22	1.26	1.25
	-9	85.41	40.33	3.77	13.35	0.22	1.26	1.25
	-12	91.34	47.59	3.92	13.42	0.20	1.26	1.26
Linear Saturation to ABP mean	12	2.10	0.06	0.03	1.58	0.22	0.16	0.22
	9	7.15	0.06	0.03	2.21	0.25	0.16	0.23
	6	19.18	0.08	0.03	2.20	0.34	0.22	0.32
	3	32.13	1.81	1.17	2.20	0.43	0.28	0.41
	0	49.02	11.30	1.19	2.44	0.46	0.31	0.43
	-3	60.51	21.98	1.19	4.49	0.46	0.31	0.41
	-6	75.40	28.73	2.64	4.68	0.44	0.31	0.39
	-9	85.41	40.33	3.77	14.27	0.40	0.29	0.39
	-12	91.34	47.59	3.92	14.27	0.44	0.29	0.43
Square Wave	12	2.10	0.06	0.03	20.17	0.22	0.16	0.22
	9	7.15	0.06	0.03	20.10	0.25	0.16	0.23
	6	19.18	0.08	0.03	20.18	0.23	0.16	0.22
	3	32.13	1.81	1.17	20.33	0.22	0.17	0.23
	0	49.02	11.30	1.19	20.22	0.23	0.17	0.24
	-3	60.51	21.98	1.19	20.45	0.22	0.18	1.25
	-6	75.40	28.73	2.64	20.17	0.22	1.26	1.25
	-9	85.41	40.33	3.77	23.34	0.22	1.26	1.25
	-12	91.34	47.59	3.92	25.60	0.19	1.26	1.26
High Frequency noise	12	2.10	0.06	0.03	39.43	0.22	0.16	0.22
	9	7.15	0.06	0.03	76.42	0.25	0.16	0.23
	6	19.18	0.08	0.03	94.70	0.24	0.16	0.23
	3	32.13	1.81	1.17	104.01	0.24	0.20	0.24
	0	49.02	11.30	1.19	104.86	0.22	0.15	14.08
	-3	60.51	21.98	1.19	105.43	0.22	17.05	31.16
	-6	75.40	28.73	2.64	109.67	18.32	25.73	34.14
	-9	85.41	40.33	3.77	110.61	0.29	19.33	20.29
	-12	91.34	47.59	3.92	115.19	0.26	18.33	16.97

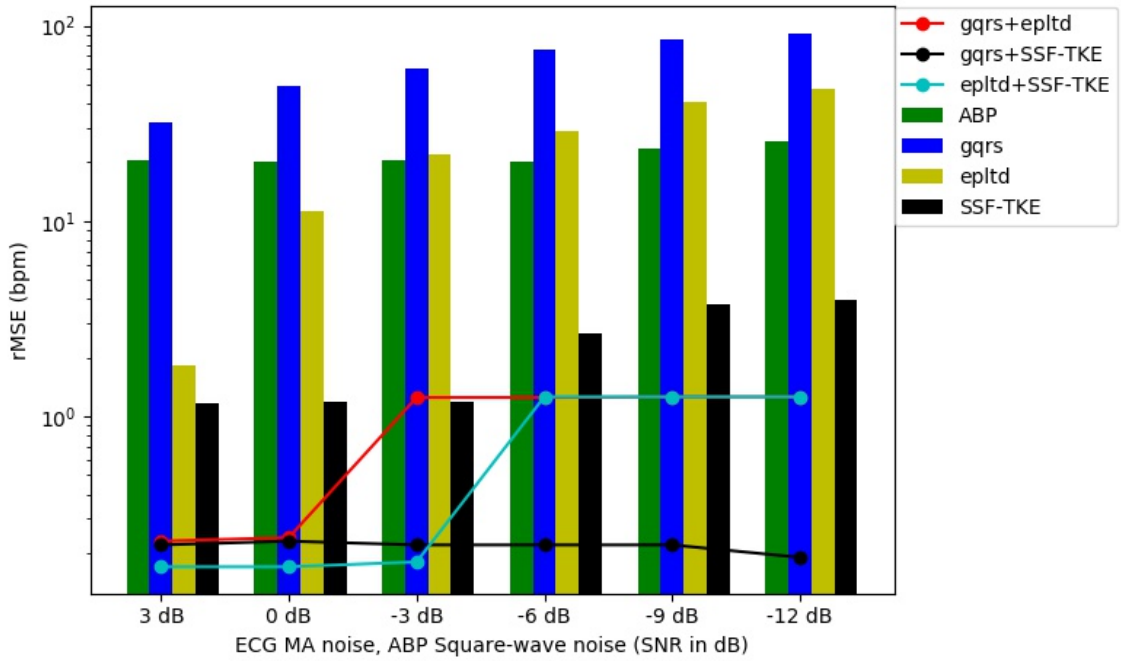

Figure 7.5: HR rMSE of individual ECG detectors and majority voting fusion with different combinations of detectors for different levels of 'ma' noise in ECG and square wave noise in ABP

noisy signals as compared to other two combinations, except in linear saturation to ABP mean noise, in which the performance of epltd/SSF-TKE is better. MVF method has limitation on high frequency ABP noise at some noise levels. ECG 'ma' noise along with ABP square wave noise at different noise levels is plotted against HR rMSE in Figure 7.5. It can be seen that the combination of gqrs and SSF-TKE have lesser rMSE or more accuracy in HR estimation as compared to other two combinations. In ECG 'ma' noise at -12 dB noise level, 'gqrs' and 'epltd' has HR rMSE of 91.34 bpm and 47.59 bpm respectively. In the worst noise combination of ECG 'ma' noise with ABP square wave noise each of SNR -12 dB, majority voting fusion (gqrs/epltd) combination has achieved HR rMSE of 1.26 bpm. Thus, majority voting fusion (gqrs/epltd) combination has increased the accuracy of HR estimation as compared to that of individual QRS detector in extremely concurrently noisy ECG and ABP signals and has reduced the HR estimate error by 97.35% with respect to that of 'epltd'. The MVF method works effectively in HR estimation on different types of noisy signals especially at higher noise levels as shown in Figure 7.5.

Figure 7.6 shows that majority voting fusion method provides an accurate HR estimation in noisy ECG with 'ma' noise and noisy ABP with 'high frequency' noise each of -12 dB of

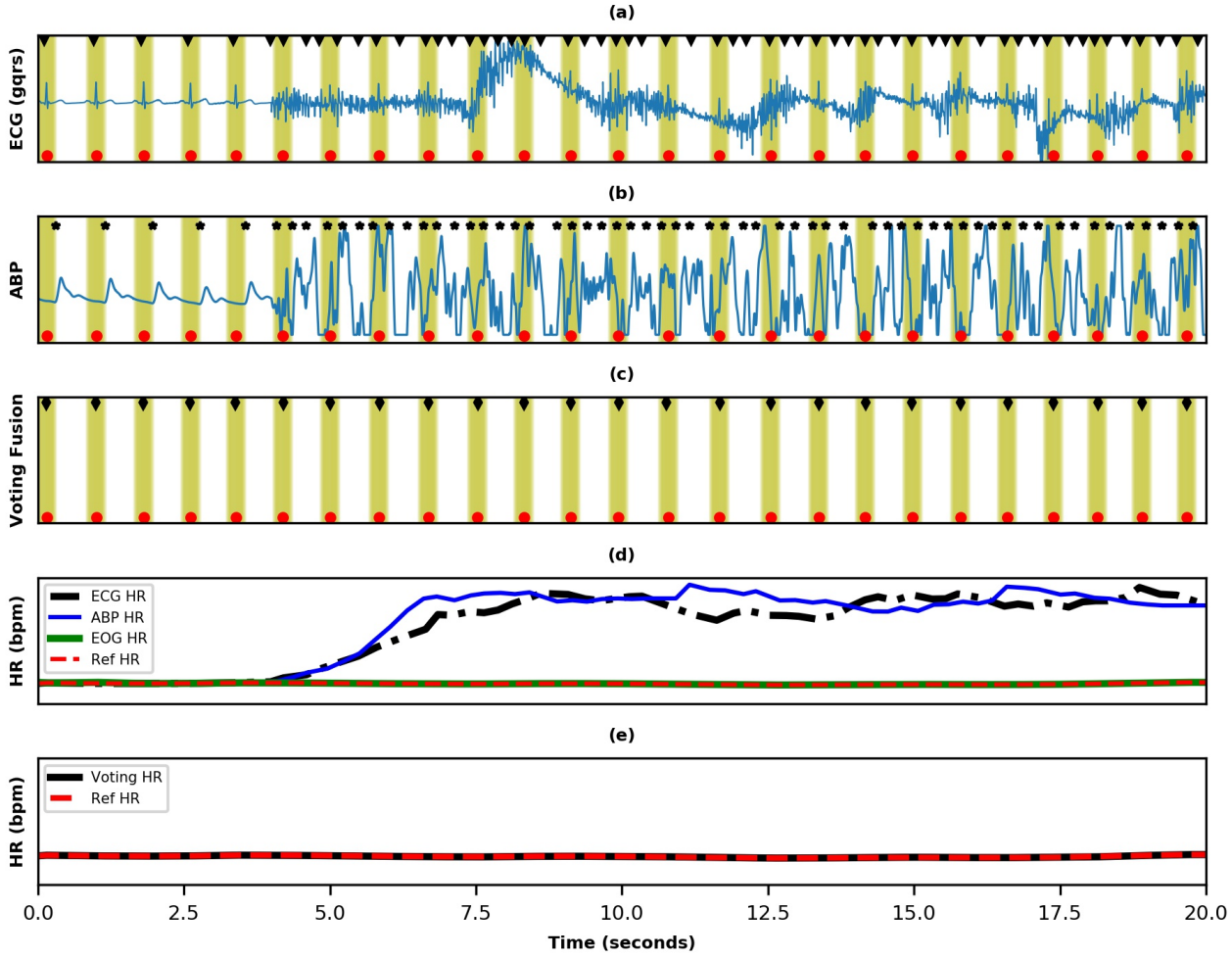

Figure 7.6: HR estimation from multimodal physiological signals in record no. 123 synthetic noise generated in ECG and ABP (a) ECG signal with detected beats (gqrs) (▼); (b) ABP signal with detected beats (*) (pulse adjusted by PTT); (c) Beat detection (♦) by voting fusion method; (d) HR estimates from ECG (gqrs), ABP, EOG and reference beats; (e) Voting fusion HR estimate.

the synthetic noise dataset by fusing them with simultaneously recorded NC signals. There are large numbers of false beat detection in noisy ECG by 'gqrs' as seen in Figure 7.6 (a) resulting in large variation in estimated HR from reference HR as can be seen in Figure 7.6 (d). Similarly, 'wabp' detects large number of false positive in noisy ABP [Figure 7.6 (b)] and HR estimated from ABP is also highly erroneous as shown in Figure 7.6 (d). In such condition the HR estimation from fusion of noisy cardiovascular signals, with large no. of false detections, will be inaccurate. The beat detections by SSF-TKE method in EOG signal are matching with reference beat annotations as can be seen in Figure 6.4 (d) and correspondingly the HR estimated from EOG is matching with the reference beat HR [Figure 7.6 (d)]. The final string of fused beats produced by MVF method by fusion of cardiovascular signals with non-cardiovascular signals are matching with reference beat annotations as seen in Figure 7.6 (c). The HR estimated independently from ECG, ABP and EOG signals along with that from reference beat annotations are shown in Figure 7.6 (d). The HR obtained from voting fusion of noisy cardiovascular signals and NC signals is plotted in Figure 7.6 (e) and it is matching with reference beat HR. This establishes effective participation of NC signals in majority voting fusion method and contribution of these signals in accurate HR estimation when both ECG and ABP signals are corrupt concurrently. Hence, inclusion of NC signals in fusion of multimodal signals for HR estimation enhances robustness of the system.

7.5 Implementation of algorithms on Single board microcomputer

The proposed algorithms are validated on standard training and test datasets as well as on synthetic noise dataset in previous chapters. With the advancement of mobile technology, portable medical devices have become integral part of modern healthcare systems. The portable medical device software development is significantly becoming more important due to low power consumption, increased wireless connectivity, telemedicine, home-care and remote monitoring. These software programs can be accessed on different platforms to connect many different devices with one another. This facility has made it possible to monitor vital health parameters of body continuously and obtain the doctor's advice in advance for treatment.

We have also implemented our algorithms on single board microcomputer to demonstrate that the algorithms can run on portable devices as well. Different varieties of single board microcomputers are available based on their architecture, connectivity to hardware, size, memory, power consumption and cost. Raspberry Pi is a series of small single-board computers developed in the United Kingdom by the Raspberry Pi foundation and it has numerous advan-

tages over other processors.

RPi uses software programs that are open source and provides direct accessible processor pins as GPIOs. It has very less software glitches and therefore very convenient to use. It is low cost, small in size, portable, consumes less power and uses a SD card for storage, which is fast and has no moving parts. The advantage of SD card storage is that it can be easy to swap data quickly with other SD cards running on other GNU/Linux distributions and it easily changes the functionality of the Pi. The ability to load Linux OS and Windows 10 IoT in RPi has made it versatile for many applications. It is compatible to use with any monitor and input devices.

The Raspberry Pi has two models; model A and model B. The board of model A has no Ethernet port and it's power consumption is low whereas model B has an Ethernet port. It comprises of a program memory (RAM), processor and graphics chip, CPU, GPU, Ethernet port, GPIO pins, Xbee socket, UART, power source connector and various interfaces for other external devices. The Central processing unit processes the instructions of the computer through logical and mathematical operations and the GPU (Graphics Processing Unit) is designed to speed up the operation of image calculations. The Ethernet port is used for communicating with additional devices and the general purpose input & output pins (GPIO) are used to associate with the other electronic components. These pins can accept input & output commands based on programming of raspberry pi. The raspberry pi affords digital GPIO pins. The XBee socket is used for wireless communication and the power source cable enables an external power source. The Universal Asynchronous Receiver/ Transmitter (UART) is a serial input & output port that can be used to transfer the serial data in the form of text and also useful for converting the debugging code. It supports three different O/Ps for display like HDMI video, composite video, and DSI video, where the DSI video needs some specific hardware. Raspberry pi contains SD card as a main storage device and it supports max 64 GB SD card.. The raspberry pi supports Linux, Qtonpi, ARM, Mac operating systems. Disk manager application can select OS to write it to an SD card.

We have chosen Raspberry Pi 3 with 64 bit CPU, single board microcomputer to implement our algorithms. Raspberry Pi 3 is the latest type B model in RPi series. It's Specifications are: 1.2 GHz, 1 GB RAM, BCM 2837 Quad Core ARMv7 processor.

Implementation details: We have implemented our algorithms in Octave using WFDB toolbox. Octave is an open source scientific programming language that is very similar to MATLAB. The WFDB Toolbox for Octave is a collection of functions for reading, writing, and processing physiologic signals and time series in the formats used by PhysioBank databases. In order to port our algorithms to Raspberry Pi, we chose Raspbian OS which is a free operating system based on Debian, optimized for Raspberry Pi hardware and supports octave packages. However, WFDB toolbox could not be installed on Raspberry Pi as the tool-

box requires 64 bit OS and there is no free/open-source 64 bit OS that supports it. Therefore, we converted all the signals in WFDB compatible formats to csv format using wfdb2mat application. This allows our software to easily read signals/records by using octave's native file readers. It removes the dependency of our software on WFDB toolbox for reading and writing data. Furthermore, to improve the run time performance, we vectorized octave code and used C++ implementations for parts of code that could not be vectorized. After installing octave on Raspbian and making modifications to data I/O part of our code as mentioned above, we were able to port our software to Raspberry Pi 3 successfully.

Validation of Run time Performance: The run time performance of MVF algorithm on Raspberry Pi 3 has been analysed using various signals of standard and synthetic noise datasets. Data acquisition and signal conditioning time is assumed to be zero because the datasets used in this study are pre-recorded signals.

(1) We have chosen record no. 100 from Physionet/CinC Challenge 2014 that contains 7 simultaneously recorded signals like ECG, ABP, EEG, SpO2 etc. are of 10 minutes duration. The fusion algorithm was implemented on three signals ECG, ABP, EEG. The signals in record no.100 were converted to csv format using wfdb2mat application. The converted csv files and algorithms in octave files were stored in SD card of Raspberry Pi 3. The algorithm achieved the following performance statistics:

(i) Algorithm run time for computing 693 beat annotations (10 minutes of recorded data) has been reduced to 4.3248 secs

(ii) Time between beats: 10 x 60 / 693 = 0.865 secs

(iii) Average algorithm compute time on Raspberry Pi 3 between beats: 4.3248 / 693 = 0.00624 seconds ~ 6.24 ms.

(iv) Real time constraints for next beat computation < 0.865 sec

Computation time achieved is ~ 138 x faster than required constraints: 0.00624 seconds vis-a-vis 0.865 seconds

The algorithm computation time is 6.24 ms/beat whereas in real hospital environment, computation time up to 865 ms/beat is available.

(2) We have also evaluated computation time on a record no. 113 from PhysioNet/CinC Challenge - 2014 containing seven signals i.e. ECG, ABP, EEG, EOG, EMG etc. The algorithm using five signals of the record in the fusion i.e. ECG, ABP, EEG, EOG and EMG has achieved the following performance statistics:

(i) Algorithm run time for computing 665 beat annotations (10 minutes of recorded data) has been reduced to 8.372 secs

(ii) Time between beats: 10 x 60 / 665 = 0.902 secs

(iii) Average algorithm compute time on Raspberry Pi 3 between beats: 8.372 / 665 =

0.01258 seconds ~ 12.6 ms.

(iv) Real time constraints for next beat computation < 0.902 sec

Computation time achieved is ~ 72 x faster than required constraints: 0.01258 seconds vis-a-vis 0.902 seconds

The algorithm computation time is 12.6 ms/beat whereas in real hospital environment, computation time up to 902 ms/beat is available.

(3) The run time of the proposed HR estimation algorithm has also been measured on the synthetic noise dataset using ECG with 'ma' noise and ABP with 'square wave' noise of -12 dB each mixed in clean ECG and ABP signals of record no. 123 of set-p dataset of Physionet/CinC Challenge - 2014. The record contains seven signals i.e. ECG, ABP, EEG, EOG, EMG etc.

Total number of beats in the signal is 734 and its duration is 10 minutes.

(a) Run time with algorithm using cardiovascular signals only (ECG and ABP): The run time of the algorithm using only cardiovascular signals is 2.3015 seconds with following accuracy: Sensitivity 92.10%, Predictivity 79.34%, F1 score 85.25% and HR rMSE 64.21 bpm.

(i) Algorithm run time for computing 734 beat annotations (10 minutes of recorded data) is 2.3015 seconds.

(ii) Time between beats: 10 x 60 / 734 = 0.817 seconds

(iii) Average algorithm computation time on Raspberry Pi 3 between beats: 2.3015 / 734 = 0.00314 seconds ~ 3.14 ms.

(iv) Real time constraints for next beat computation < 0.817 seconds

Computation time achieved is ~ 260 times faster than required constraints i.e. 0.00314 seconds vis-a-vis 0.817 seconds

The algorithm computation time is 3.14 ms/beat whereas in real hospital environment, computation time up to 817 ms/beat is available.

(b) Run time with algorithm using cardiovascular signals along with EEG, EOG and EMG (5 signals): The run time of the algorithm using cardiovascular signals and non-cardiovascular signals is 7.97 seconds with following accuracy: Sensitivity 99.73%, Predictivity 99.73%, F1 score 99.73% and HR rMSE 0.19 bpm.

(i) Algorithm run time for computing 734 beat annotations (10 minutes of recorded data) is 7.97 seconds.

(ii) Time between beats: 10 x 60 / 734 = 0.817 seconds

(iii) Average algorithm computation time on Raspberry Pi 3 between beats: 7.97 / 734 = 0.01085 seconds ~ 10.85 ms.

(iv) Real time constraints for next beat computation < 0.817 seconds

Computation time achieved is ~ 75 times faster than required constraints i.e. 0.01085

seconds vis-a-vis 0.817 seconds

The algorithm computation time is 10.85 ms/beat whereas in real hospital environment, computation time up to 817 ms/beat is available.

The MVF algorithm using calibrated noisy cardiovascular signals (ECG and ABP) in the fusion process takes computation time of 3.14 ms between i.e. 260 times faster than the real time beat interval (817 ms) but the accuracy of beat detection (F1 score 85.25%) and HR estimation (64.21 bpm) are very low. Whereas the fusion of five signals i.e. noisy cardiovascular along with non-cardiovascular signals significantly increased the accuracy of beat detection (F1 score 99.73%) as well as of HR estimation (0.19 bpm) and the computation time of the algorithm (10.85 ms) is still 75 times faster than the real time constraints.

The results show that as more signals are added (fused together), the rMSE decreases, but the computation time increases. This validates an intuitive notion that computation time is a cost function for increased accuracy, better predictability and sensitivity. The run time analyses on Raspberry Pi show that our algorithms can run on portable devices in real time.

7.6 Computational Complexity

We have performed asymptotic runtime complexity analysis of our algorithm. The algorithm was divided into different stages to calculate time complexity of each stage separately. The analyses of computational complexity of different stages are briefly discussed.

(A) Beat Detector: Three QRS detectors and one ABP pulse detector have been used in our algorithm. Let us suppose that there are total 'N' number of samples in the signal.

(a) 'gqrs': 'gqrs' applies low pass filter on every sample of the signal and tries to find peaks in it. The computational complexity of gqrs therefore becomes proportional to N i.e. O(N).

(b) 'epltd': 'epltd' also checks each sample of the ECG signal, to find the R peaks. Thus, the asymtotic runtime complexity of 'epltd' is proportional to N i.e. O(N)

(c) SSF-TKE: SSF-TKE method first applies low pass filter on the entire signal. It then calculates slope sum and Teager Kaiser Energy for every sample in the signal. The computational complexity of SSF-TKE is also proportional to the number of samples in the signal i.e. O(N)

(d) 'wabp': 'wabp' algorithm applies low pass filter on the signal and calculates slope sum function for every sample of the signal. The asymptotic complexity of 'wabp' is also proportional to the number of samples in signal i.e. O(N).

(B) SQI Calculation: The proposed beat SQI has been used in the algorithm for beat signal quality assessment of NC signals and beats derived from ABP, whereas combination of

beat SQI and KSQI have been used for ECG signal quality assessment. The computational complexity of two SQI assessment methods are:

(a) Beat SQI: The proposed beat SQI considers beat locations and their regularity to determine signal quality. Suppose 'K' is the number of detected beats in the signal. Beat SQI algorithm process every detected beat to compute the quality of the signal, hence the asymptotic time complexity is proportional to 'K' i.e. O(K).

(b) K-SQI (Kurtosis SQI): Kurtosis SQI is calculated using a 10s window around every beat location (5s on either side) and Kurtosis is calculated in that window. Thus, the asymptotic complexity of the algorithm is O(K*S); where 'K' represents the number of detected beats and 'S' denotes the number of samples in 10s.

(C) Voting Fusion: Voting Fusion involves three main substeps:

(a) Generate Reference Signal: For generating reference signal, windows of duration 5s are created with 2s overlap for the entire signal. The reference beats in each window are selected from all available signals in the record. Let us suppose there are 'L' numbers of 5s windows with 2s overlap in the entire signal, and M as the number of beats in each window. Since the mean of beat SQIs are calculated, the complexity for each window is O(M). There are 'L' such windows, so the total complexity of this step is O(L*M).

(b) Match beats of other signals with reference signal beat: For identifying beats of other signals that match reference signal beat, the beats in other signals are sorted within 150 ms of the reference beat and the closest beats are selected. If the number of beats in the reference signal is 'R' then the computational complexity of this step would be O(R*log R).

(c) Generate final votes: In the final voting step, we iterate through the final reference beats set and their matches. Let the number of reference beats is 'R', then this step would take complexity of O(R).

Overall the asymptotic complexity of voting fusion is summation O(L*M) + O(R*log R) + O(R). Since 'R' (number of reference beats) < R*log R << L*M (number of beats in a 5s window * number of windows), we can approximate the computational complexity of voting fusion step to be O(L*M).

The asymptotic complexity of our entire pipeline would be the sum of complexities of all the stages: O(Beat detector) + O(SQI calculator) + O(Voting fusion) = O(N) + O(K) + O(L*M). Since, K (number of beats) < L*M (number of beats in a 5s window * number of windows) << N(number of samples in signal), therefore the asymptotic complexity of our algorithm is O(N), where 'N' is the number of samples in the signal.

7.7 Discussion

The proposed MVF algorithm has achieved accurate heart rate estimation for all types of combination of noisy signals and in worst case also where both cardiovascular signals are simultaneously extremely noisy. To achieve accurate heart rate estimation, the threshold (scaling factor 'C') in MVF algorithm has been set to keep the false beat detection (FP) very low. The method has achieved higher gross positive predictivity on PhysioNet/CinC Challenge 2014 public training dataset (except that of Pangerc et al.) and on MIT-BIH polysomnographic database as compared to that of other studies. The higher positive predictivity with nearly same sensitivity as compared to that of single detector 'gqrs' has substantially improved accuracy of HR estimation and has reduced HR rMSE. In the proposed algorithm, we have adopted window wise approach for selection of reference signal for beat fusion. Window wise approach yields accurate and reliable HR estimation as it allows for dynamic switching of the reference signal based on relative quality of the signals. Beat SQI has enhanced participation of NC signals in the voting fusion process, which is evident from the fact that the beat SQI based voting fusion of multimodal signals has achieved excellent results in HR estimation as compared to that of single ECG detector (gqrs) and also when both ECG and ABP signals in PhysioNet/CinC Challenge 2014 public training dataset and MIT-BIH polysomnographic database are noisy. The method is also able to accurately estimate HR in signals with bradycardia and tachycardia.

To the best of our knowledge, none of the previous studies have reported HR estimation from fusion of cardiovascular and NC signals. Q. Li et al. have obtained robust HR estimation with average rMSE of 1.0 ± 0.8 bpm from fusion of cardiovascular signals (ECG and ABP signals) of MIMIC II database using Kalman filter and signal quality analysis, with the assumption that both ECG and ABP signals are not corrupt simultaneously. However, there is no such constraint in the proposed voting fusion method and it has provided accurate HR estimate from fusion of multimodal physiological signals with average rMSE of 0.84 bpm and 1.80 bpm in PhysioNet/CinC Challenge 2014 training dataset respectively for worst case i.e. when both the cardiovascular signals are simultaneously noisy. The rMSE of HR estimates obtained from majority voting fusion of multimodal physiological signals are within acceptable clinical limits of ± 5 bpm [3].

We have evaluated HR estimation performance of majority voting fusion method on synthetic noisy cardiovascular signals to assess the contribution of NC signals in voting fusion for robust HR estimation when both the cardiovascular signals are concurrently noisy. All the three combinations of voting fusion method have demonstrated robust and accurate HR estimation in ECG 'bw','em' and 'ma' noises with different combinations of six types of ABP noise, except for epltd/SSF-TKE and gqrs/epltd combinations on higher levels of brown noise

(Tables 7.6, 7.7 and 7.8). It has also been observed that for low noise levels (high SNR level i.e. 6 dB, 9 dB and 12 dB) the performance of voting fusion is not better than that of single detectors. However, for noisy signals, all the three combinations have substantially improved accuracy of HR estimation over single detectors. It is evident from the experimental analysis that when both the cardiovascular signals are extremely noisy, NC signals have participated in fusion process and contributed to achieve robust and accurate heart rate within clinical acceptable limits.

We have observed that HR estimation results from fusion of multimodal signals are usually better than those of individual signals; this difference of HR estimation is more pronounced when both cardiovascular signals are noisy. Many studies in past have fused only cardiovascular signals i.e. ECG and ABP and obtained very good results. However, the main advantage of using additional three non-cardiovascular signals in our algorithm is that it has increased robustness of the system. This is because our algorithm uses five multimodal signals in fusion and sources of noise affecting these signals are different, hence the likelihood of simultaneous corruption of all the five signals is very low. The data fusion of ECG and ABP signals with NC signals, containing significant quantum of ECG artifacts, can therefore provide a much improved estimation of HR especially, when ECG and ABP are simultaneously corrupted by severe noise and artifacts.

The MVF algorithms are implemented on various signals and their computation time was estimated by single board microcomputer. The run time of proposed algorithm using calibrated noisy cardiovascular signals (ECG and ABP) in the fusion process takes computation time of 3.14 ms which is very low as compared to real time constraints but the accuracy of beat detection (F1 score 85.25%) and HR estimation (64.21 bpm) are very low. The fusion of five signals have significantly increased the accuracy of beat detection (F1 score 99.73%) and HR estimation (0.19 bpm) but the computation time of the algorithm have comparatively increased to 10.85 ms from 3.14 ms. It is still much faster than the real time constraints. The results show that as more signals are fused together the HR, rMSE decreases, but the computation time increases. This validates that computation time is a cost function for increased accuracy of HR estimation better sensitivity and predictability of beat detection. The run time analyses on raspberry pi show that our algorithms can run on portable devices in real time.

The asymptotic complexity of our algorithm would be the sum of complexities of all the stages: O(Beat detector) + O(SQI calculator) + O(Voting fusion) = O(N) + O(K) + O(L*M). Since, K (number of beats) < L*M (number of beats in a 5s window * number of windows) << N(number of samples in signal), therefore the asymptotic complexity of our algorithm is O(N), where 'N' is the number of samples in the signal.

7.8 Conclusion

The majority voting fusion method has substantially improved accuracy of HR estimates from single well known QRS detectors even at higher noise levels in concurrently noisy ECG and ABP signals. The validation of the algorithm on synthetic noise dataset has demonstrated that fusion of NC signals with cardiovascular signals by majority voting fusion method has substantially reduced the HR rMSE even when both ECG and ABP signals are noisy simultaneously. All the three combinations (gqrs/SSF-TKE, epltd/SSF-TKE and gqrs/epltd) of voting fusion have performed consistently well for all types of ECG and ABP noise for high noise levels (-6 dB to -12 dB). The main advantage of using cardiovascular signals along with additional three non-cardiovascular signals in our algorithm is that it has increased robustness of the system. The rMSE of HR estimates obtained from majority voting fusion of multimodal physiological signals are within acceptable clinical limits of ± 5 bpm. The algorithms are implemented successfully on Raspberry Pi and computation time of proposed algorithm was much faster than real time constraints. These algorithms can be implemented on portable device. The computational complexity of algorithms is simple i.e O(N), where 'N' is the number of samples in the signal.

Chapter 8

Conclusions and Future scope

Many studies have been carried out in the past for heart rate estimation from fusion of cardiovascular signals using different signal processing techniques. Most of these studies have used ECG and ABP signals with the assumption that both the signals are not noisy concurrently. It has been observed that sometimes both ECG and ABP signals are simultaneously noisy and HR estimation from such signals will be erroneous. Some of the studies have used non-cardiovascular signals along with cardiovascular signals for robust heart beat detection, but they have not extended their studies to heart rate estimation. This thesis has endeavored to develop signal processing methods for robust heart rate estimation from fusion of cardiovascular signals with non-cardiovascular signals even when cardiovascular signals are noisy simultaneously or missing.

We have developed a novel SSF-TKE method for ECG artifacts detection in non-cardiovascular signals and extended the method for heart beat detection in ECG signal. The proposed method does not require any additional ECG channel as well as any a priori input for R-peak artifacts detection in NC signals. We have next proposed a new statistical and rhythm based beat SQI method for assessment of signal quality which works on single channel. The beat SQI has enabled effective participation of NC signals in majority voting fusion by assigning proper weights to signal beats depending upon their quality. Fusion of quality signals is the next important step in heart rate estimation. A beat SQI based majority voting fusion method has been developed in this study for robust heart rate estimation from multimodal physiological signals.

Our algorithms have been found to work extremely well on noisy signals. We have evaluated the algorithms on many standard databases and also validated them on a synthetic noise dataset in which we have added various levels of different types of noises in clean ECG and ABP signal of record no. 123 from PhysioNet/CinC Challenge 2014 training dataset. It has been observed that when both ECG and ABP signals are extremely noisy concurrently, NC

signals effectively participates in fusion process and provide accurate HR estimates. Finally, the proposed algorithms have been implemented on Raspberry Pi 3 to determine computation time. Our algorithm is about 72 to 138 times faster than the required constraints (depending upon the no. of signals in the record) for real time applications. This makes our algorithm suitable for implementation in any real time device. Computationally also, the proposed algorithm is simple with asymptotic complexity of O(N), where 'N' is the number of samples in the signal.

Some of the major contributions of thesis are summarized below:

- SSF-TKE method works exceedingly well in ECG artifact detection in NC signals. The method has yielded very high sensitivity and predictivity in NC signals containing good quantum of ECG artifacts.

- The R-peak detection performance of proposed SSF-TKE algorithm in ECG has been excellent across a large number of standard databases with wide variety of signal morphologies. It is also highly resistant against for all types of ECG noises and performed quite well in signals with pacemaker beats. The performance of our algorithm on noisy signals is better than that of 'gqrs' and 'epltd'.

- A novel statistical and rhythm based beat SQI algorithm has been proposed that works on a single QRS detector. The performance of beat SQI in the classification of signal quality has been found to be better than that of bSQI, which is a standard metric for signal quality assessment. The method works satisfactorily on bradycardia, tachycardia and signals with different types of arrhythmias. The algorithm can be implemented on real time data.

- The robust heart beat detection performance of proposed beat SQI based majority voting fusion method has been found excellent in standard databases and it has outperformed other methods in MGH/MF waveform database and MIT-BIH noise stress database. Its performance is comparable to other studies on other databases as well. The fusion method has improved the overall score in beat detection over well known single QRS detectors on standard databases, PhysioNet/CinC Challenge 2014 test dataset and also on concurrently noisy ECG and ABP signals of synthetic noise dataset. The majority voting fusion method with epltd/SSF-TKE combination has achieved score of 91.76% on PhysioNet/CinC Challenge 2014 hidden test dataset and it currently ranks 5th in the results from the 2014 challenge.

- The beat SQI based majority voting fusion method has yielded robust heart rate estimation even in records with concurrent noisy ECG and ABP signals of long duration

standard databases and on synthetic noise dataset containing concurrently extremely noisy cardiovascular signals.

- The run time performance of algorithms on Raspberry Pi 3 have been analysed and observed that it can be implemented in real time.
- The proposed algorithm is computationally simple with asymptotic complexity of O(N), where 'N' is the number of samples in the signal.

8.1 Suggestions for future work

Although we have proposed many new signal processing algorithms for heart rate estimation in the present work, but one may consider the following future directions for further improvements:

- We have used SSF-TKE method for ECG artifacts detection in NC signals. The detected artifacts can be removed by developing new techniques to get clean NC signals for improved clinical uses.
- In SSF-TKE method, we have considered morphological features of only QRS complex and its periodicity for R-peak detection in ECG. Performance of the proposed method can be enhanced further, especially in ECGs with arrhythmias, by incorporating other morphological features of ECG waveform.
- The present SSF-TKE method is limited to R-peak detection; it can be further extended for ECG beat classification.
- In our study, we have used only two cardiovascular signals (ECG and ABP) in majority voting fusion for beat detection and heart rate estimation. The method can be further extended to include other simultaneously recorded pulsatile cardiovascular signals i.e. PPG, stroke volume (SV) etc.
- Machine learning techniques can also be explored out for fusion of multimodal physiological signals.

References

[1] W. H. Organization, "Global status report on non-communicable diseases 2014," 2014.

[2] J. M. Dekker, R. S. Crow, A. R. Folsom, P. J. Hannan, D. Liao, C. A. Swenne, and E. G. Schouten, "Low heart rate variability in a 2-minute rhythm strip predicts risk of coronary heart disease and mortality from several causes: The aric study," *The American Heart Association, 7272 Greenville Avenue, Dallas, TX 75231*, vol. Circulation. 102, no. 11, pp. 1239–1244, 2000. [Online]. Available: http://www.circulationaha.org

[3] J. Feldman, H. M. Ebrahim, and I. Bar-Kana, "Robust sensor fusion improves heart rate estimation: Clinical evaluation," *Journal of Clinical Monitoring and Computing 13*, no. 6, pp. 379–384, 1997.

[4] B. U. Kohler, C. Hennig, and Orglmeister, "The principles of software qrs detection," *IEEE Engineering in Medicine and Biology Magazine 21*, no. 1, pp. 42–57, 2002.

[5] G. M. Friesen, T. C. Jannett, M. A. Jadallah, S. L. Yates, S. R. Quint, and H. T. Nagle, "A comparison of the noise sensitivity of nine qrs detection algorithms," *IEEE Transactions on Biomedical Engineering*, vol. 37, no. 1, pp. 85–98, January 1990.

[6] J. Allen and A. Murray, "Assessing ecg signal quality on a coronary care unit," *Physiological Measurement 17*, vol. 17, no. 4, pp. 249–58, 1996.

[7] S. Jakob, I. Korhonen, E. Ruokonen, T. Virtanen, A. Kogan, J. Takala, J. Kruse, and C. Redmond, "Detection of artifacts in monitored trends in intensive care," *Computer Methods and Programs in Biomedicine 63*, no. 3, pp. 203–209, 2000.

[8] J. Kruse and C. Redmond, "Detecting and distinguishing cardiac pacing artifacts," *Analog Dialogue 46*, no. 11, pp. 1–6, November 2012.

[9] S. T. Lawless, "Crying wolf: false alarms in a pediatric intensive care unit," *Critical Care Medicine 22*, no. 6, pp. 981–985, 1994.

[10] C. L. Tsien and J. C. Fackler, "Poor prognosis for existing monitors in the intensive care unit," *Critical Care Medicine 25*, vol. 4, pp. 614–619, 1997.

[11] A. Aboukhalil, L. Nielsen, M. Saeed, R. G. Mark, and G. D. Clifford, "Reducing false alarm rates for critical arrhythmias using arterial blood pressure waveform," *Journal of Biomedical Informatics 41*, no. 3, pp. 442–451, 2008.

[12] M. C. Chambrin, "Alarms in the intensive care unit: how can the number of false alarms be reduced?" *Critical Care 5*, no. 4, pp. 184–188, 2001.

[13] W. Zong, T. Heldt, G. B. Moody, and R. G. Mark, "An open-source algorithm to detect onset of arterial blood pressure pulses," *Computation in Cardiology*, pp. 259–262, 2003.

[14] A. A. R. Kamal, J. B. Harness, G. Irving, and A. J. Mearns, "Skin photoplethysmography - a review," *Computer Methods and Programs in Biomedicine 28*, no. 4, pp. 257–269, 1989.

[15] J. Allen, "Photoplethysmography and its application in clinical physiological measurement," *Physiological Measurement 28*, no. 3, pp. R1–R39, 2007.

[16] D. J. Meredith, D. Clifton, P. Charlton, J. Brooks, C. W. Pugh, and L. Tarassenko, "Photoplethysmographic derivation of respiratory rate: a review of relevant physiology," *Journal of Medical Engineering & Technology 36*, no. 1, pp. 1–7, 2012.

[17] H.-J. Park, J.-M. Han, D.-U. Jeong, and K.-S. Park, Eds., *A Study on the elimination of the ECG Artifacts in the Polysomnographic EEG and EOG using AR model*, vol. 3. Proceedings of the 20th Annual International Conference of the IEEE Engineering in Medicine and Biology Society, 1998.

[18] A. G. Correa, E. Laciar, H. D. Patino, and M. E. Valentinuzzi, "Artifact removal from eeg signals using adaptive filters in cascade," in *Journal of Physics: Conference Series*, vol. 90, no. 1, 2007, pp. 1–10.

[19] J. Taelman, B. Mijovic, S. V. Huffel, S. Devuyst, and T. Dutoit, "Ecg artifact removal from surface emg signals by combining empirical mode decomposition and independent component analysis," *Biosignals*, pp. 421–424, 2011.

[20] G. D. Clifford, W. J. Long, G. B. Moody, and P. Szolovits, "Robust parameter extraction for decision support using multimodal intensive care data," *Philosophical Transactions of the Royal Society of London: A Mathematical, Physical and Engineering Sciences 367*, no. 1887, pp. 411–429, 2009.

[21] C. L. Tsien, I. S. Kohans, and N. Mclntosh, Eds., *Building ICU artifact detection models with more data in less time*, American Medical Informatics Association. Proceedings of the AMIA Symposium, 2001.

[22] D. F. Sittig and M. Factor, "Physiologic trend detection and artifact rejection: a parallel implementation of a multi-state kalman filtering algorithm," *Computer Methods and Programs in Biomedicine 31*, no. 1, pp. 1–10, 1990.

[23] L. Tarassenko, N. Townsend, and J. D. Price, "Combining measurements from different sensors," U.S. Patent 311 250, 2003. [Online]. Available: http://www.freepatentsonline.com/20030187337.html

[24] Q. Li, R. G. Mark, and G. D. Clifford, "Robust heart rate estimation from multiple asynchronous noisy sources using signal quality indices and a kalman filter," *Physiological Measurement 29*, no. 1, pp. 15–32, 2008.

[25] W. Kaiser and M. Findeis, "Novel signal processing methods for exercise ecg," *Int. J. Bioelectron 2*, pp. 61–65, 2000.

[26] W. Zong, G. B. Moody, and R. G. Mark, "Reduction of false arterial blood pressure alarms using signal quality assessment and relationships between the electrocardiogram and arterial blood pressure," *Medical and Biological Engineering and Computing 42*, no. 5, pp. 698–706, 2004.

[27] L. Chen, T. McKenna, A. Reisner, and J. Reifman, "Algorithms to qualify respiratory data collected during the transport of trauma patients," *Physiological measurement 27*, no. 9, pp. 797–816, 2006.

[28] G. de Morais Borges and V. Brusamarello, Eds., *Bayesian Fusion of Multiple Sensors for Reliable Heart Rate Detection*, 2014 IEEE International. In Instrumentation and Measurement Technology Conference (I2MTC) Proceedings, 2014.

[29] D. L. Hall and J. Llinas, Eds., *An introduction to multisensory data fusion*, no. 1. Proceedings of the IEEE 85, 1997, pp. 6-23.

[30] F. Castanedo, "A review of data fusion techniques," *The Science World Journal 2013*, pp. 1–19, 2013.

[31] B. Zhou and Y. Yao, "Decision-level sensor-fusion based on dtrs," *Springer International Publishing*, pp. 321–332, 2015.

[32] F. Cremer, K. Schutte, J. G. M. Schavemaker, and E. den Breejen, "A comparison of decision level sensor-fusion methods for anti-personnel land mine detection," *Information fusion 2*, no. 3, 2001.

[33] W. Elmenreich, "An introduction to sensor fusion," resreport, Vienna institute of technology, Austria, Nov. 2002, 47/2001.

[34] P. J. Nahin and J. L. Pokoski, "Nctr plus sensor fusion equals iffn or can two plus two equal five?" *IEEE transactions on Aerospace and Electronic systems 3*, pp. 320–337, 1980.

[35] B. V. Dasarathy, "More the merrier ... or is it? - sensor suite augmentation benefits assessment," in *Proceedings of the 3rd International Conference on Information Fusion*, vol. 2. Paris, France: Proceedings of the 3rd International Conference on Information Fusion, Jul. 2000, pp. 20–25.

[36] ——, "Information fusion - what, where, why, when, and how?" *Information Fusion, Editorial, 2001*, no. 2, pp. 75–76, 2001.

[37] S. A. Rankawat and R. Dubey, "Robust heart rate estimation from multimodal physiological signals using beat signal quality index based majority voting fusion method," *Biomedical Signal Processing and Control 33*, pp. 201–212, 2017.

[38] E. L. Reilly, *Electroencephalography: Basic Principles and Clinical Applications and Related Fields*, 4th ed., Williams and Wilkins, Eds. Baltimore: Williams and Wilkins, 1999.

[39] M. Nakamura and H. Shibasaki, "Elimination of ekg artifacts from eeg records: a new method of noncephalic referential eeg recording," *Electroencephalography and Clinical Neurophysiology 66*, no. 1, pp. 89–92, 1987.

[40] S. P. Cho, M. H. Song, Y. C. Park, H. S. Choi, and K. J. Lee, "Adaptive noise canceling of electrocardiogram artifacts in single channel electroencephalogram," in *Engineering in Medicine and Biology Society, 2007. EMBS 2007. 29th Annual International Conference of the IEEE*, 29th Annual International Conference of the IEEE. Engineering in Medicine and Biology Society, 2007, pp. 3278–3281.

[41] J.-A. Jiang, C.-F. Chao, M.-J. Chiub, R.-G. Lee, C.-L. Tseng, and R. Lin, "An automatic analysis method for detecting and eliminating ecg artifacts in eeg," *Computers in Biology and Medicine 37*, no. 11, pp. 1660–1671, 2007.

[42] S. A. Rankawat, M. Rankawat, and R. Dubey, "Ecg artifacts detection in non-cardiovascular signals using slope sum function and teager kaiser energy," in *BioSignal Analysis, Processing and Systems (ICBAPS), 2015 International Conference on. IEEE*. BioSignal Analysis, Processing and Systems (ICBAPS), 2015 International Conference on. IEEE, 2015, pp. 6–10.

[43] M. Elgendi, B. Eskofier, S. Dokos, and D. Abbott, "Revisiting qrs detection methodologies for portable, wearable, battery operated, and wireless ecg systems," *PLoS ONE*, vol. 9, no. e84018, 2014.

[44] R. F. Rushmer, *Cardiovascular Dynamics*, 4th ed., W. Saunders, Ed. Philadelphia, PA: WB Saunders, 1976.

[45] R. M. Rangayyan, *Biomedical Signal Analysis: A case study approach*. Wiley India edition, 2009.

[46] *Virtual labs*, An initiative of MHRD. [Online]. Available: http://bmsp-coep.vlabs.ac.in/AbnormalECG/index.html#

[47] W. J. Tompkins, *Biomedical Digital Signal Processing*, Prentice-Hall, Ed. Upper Saddle River, NJ: Prentice-Hall, 1995.

[48] R. E. Klabunde, "Cardiovascular physiology concepts, arterial blood pressure," Marian University College of Osteopathic Medicine, Indianapolis, Indiana, Tech. Rep., 2016. [Online]. Available: http://www.cvphysiology.com/BloodPressure/BP002

[49] R. S. Khandpur, *Handbook of Biomedical Instrumentation*, 2nd ed., T. M.-H. P. C. Limited, Ed. New Delhi: Tata McGraw-Hill Publishing Company Limited, 2008.

[50] *MEMSCAP Invasive Blood Pressure*, 2012. [Online]. Available: http://memscap.com/applications-and-market-segments/medical-and-biomedical/invasive-blood-pressure

[51] A. E. W. Johnson, J. Behar, F. Andreotti, G. D. Clifford, and J. Oster, "R-peak estimation using multimodal lead switching," in *Computing in Cardiology Conference, 2014*, vol. 41, 2014, pp. 281–284.

[52] H. Chen, Y. Erol, E. Shen, and S. Russell, "Probabilistic model-based approach for heart beat detection," *Physiological Measurement 37*, no. 9, pp. 1404– 1421, 2016.

[53] B. H. McGhee and E. J. Bridges, "Monitoring arterial blood pressure: what you may not know," *Critical Care Nurse*, vol. 22, no. 2, pp. 60–79, 2002.

[54] Q. Li, R. G. Mark, and G. D. Clifford, "Artificial arterial blood pressure artifact models and an evaluation of a robust blood pressure and heart rate estimator," *BioMedical Engineering Online 8*, no. 1, p. 13, 2009.

[55] E. Niedermeyer and F. L. da Silva, *Electroencephalography: Basic Principles, Clinical Applications, and Related Fields*, L. W. . Wilkins, Ed. Lippincott Williams & Wilkins, 2005.

[56] M. Taplan, "Fundamentals of eeg measurement," *Measurement science review*, vol. 2, no. section 2, 2002.

[57] A. E. Kaufman, A. Bandopadhay, and B. D. Shaviv, "An eye tracking computer user interface," in *Proceedings of IEEE Symposium on Research Frontiers*, 1993, pp. 120–121.

[58] J. Malmivuo and R. Plonsey, *Bioelectromagnetism: principles and applications of bioelectric and biomagnetic fields*. USA: Oxford University Press, 1995.

[59] C. H. Morimoto and R. Mimica, "Eye gaze tracking techniques for interactive applications," *Computer vision and image understanding 98*, no. 1, pp. 4–24, 2005.

[60] C. C. Chu and J. D. Bronzino, *The biomedical engineering handbook*, C. Press, Ed. Boca Raton, Florida: CRC Press, 1995.

[61] D. G. Childers and J. G. Webster, *Evoked potentials*, ser. Encyclopedia of Medical Devices and Instrumentation, Wiley, Ed. Wiley, 1988.

[62] B. J. Fisch, Fisch, and Spehlmann's, *EEG primer: basic principles of digital and analog EEG*, E. H. Sciences, Ed. Elsevier Health Sciences, 1999.

[63] M. C. Su, K. C. Wang, and G. D. Chen, "An eye tracking system and its application in aids for people with severe disabilities," *Biomedical Engineering: Applications, Basis and Communications 18*, no. 6, pp. 319–327, 2006.

[64] E. Huigen, A. Peper, and C. A. Grimbergen, "Investigation into the origin of the noise of surface electrodes," *Medical and biological engineering and computing 40*, no. 3, pp. 332–338, 2002.

[65] C. J. D. Luca, L. D. Gilmore, M. Kuznetsov, and S. H. Roy, "Filtering the surface emg signal: Movement artifact and baseline noise contamination," *Journal of biomechanics 43*, no. 8, pp. 1573–1579, 2010.

[66] V. R. Mankar, "Emg signal noise removal using neural netwoks," *Advances in Applied Electromyography, InTech*, 2011.

[67] R. F. Yazicoglu, C. V. Hoof, and R. Puers, *Biopotential Readout Circuits for Portable Acquisition Systems*, S. Science and B. Media, Eds. Springer Science and Business Media, 2009.

[68] A. Banerjee, M. Pal, D. N. Tibarewala, and A. Konar, "Electrooculogram based blink detection to limit the risk of eye dystonia," in *Advances in Pattern Recognition (ICAPR), 2015*. Eighth International Conference on, IEEE, 2015, pp. 1–6.

[69] T. Instruments, *Diagnostic and Patient Monitoring and Therapy Applications Guide*, Texas Instruments. [Online]. Available: http://www.ti.com/general/docs/lit/getliterature.tsp?baseLiteratureNumber=slyb147

[70] *Essentials of Data Quality: Optimizing your range and sampling and filtering settings*. [Online]. Available: https://www.adinstruments.com/tips/data-quality

[71] M. Jones-Parker, *Technical corner: Sampling rates for digital Polysomnography*, Sep. 2009.

[72] S. Mahdiani, V. Jeyhani, M. Peltokangas, and A. Vehkaoja, "Is 50 hz high enough ecg sampling frequency for accurate hrv analysis?" in *Engineering in Medicine and Biology Society (EMBC), 2015*. 37th Annual International Conference of the IEEE, 2015, pp. 5948–5951.

[73] D. J. Creel, *The Electroretinogram and Electro-oculogram: Clinical Applications*, W. T. O. of the Retina and V. SystÃ©m., Eds. Webvision: The Organization of the Retina and Visual SystÃ©m., Jul. 2015.

[74] L. Cromwell, F. J. Weibell, and E. A. Pfeiffer, *Biomedical instrumentation and measurements*, P. Hall, Ed. Prentice Hall, 1980.

[75] R. P. Areny, J. G. Webster, and R. Areny, *Sensors and signal conditioning*, Wiley, Ed. New York: Wiley, 2001.

[76] A. L. Goldberger, L. A. Amaral, L. Glass, J. M. Hausdorff, P. C. Ivanov, R. G. Mark, J. E. Mietus, G. B. Moody, and H. E. Stanley, "Physiobank, physiotoolkit, and physionet components of a new research resource for complex physiological signals," *Circulation 101*, no. 23, pp. e215–e220, 2000.

[77] PhysioNet, "Challenge 2011 training set a." 2011. [Online]. Available: http://www.physionet.org/physiobank/database/challenge/2011/set-a/

[78] ——, "Index of /physiobank/database/challenge/2014/set-p." 2014. [Online]. Available: http://physionet.org/physiobank/database/challenge/2014/set-p/

[79] ——, "Index of /physiobank/database/challenge/2014/set-p2," 2014. [Online]. Available: https://physionet.org/physiobank/database/challenge/2014/set-p2/

[80] Y. Ichimaru and G. B. Moody, "Development of the polysomnographic database on cd-rom," *Psychiatry and Clinical Neuroscience 53*, no. 2, pp. 175–177, 1999.

[81] G. B. Moody and R. G. Mark, "The impact of the mit-bih arrhythmia database," *IEEE Engineering in Medicine and Biology Magazine 20*, vol. 3, pp. 45–50, 2001.

[82] G. B. Moody, W. E. Muldrow, and R. G. Mark, "A noise stress test for arrhythmia detectors," *Computers in Cardiology 11*, no. 3, pp. 381–384, 1984.

[83] J. P. Welch, P. J. Ford, R. S. Teplick, and R. M. Rubsamen, "The massachusetts general hospital marquette foundation hemodynamic and electrocardiographic database â comprehensive collection of critical care waveforms," *Clinical Monitoring 7*, no. 1, pp. 96–97, 1991.

[84] K. T. Sweeney, T. E. Ward, and S. F. M. Loone, "Artifact removal in physiological signals - practices and possibilities," *IEEE Transactions on Information Technology in Biomedicine 16*, no. 3, pp. 918–926, 2012.

[85] S. Devuyst, T. Dutoit, P. Stenuit, M. Kerkhofs, and E. Stanus, "Cancelling ecg artifacts in eeg using a modified independent component analysis approach," *EURASIP Journal of Advanced Signal Processing 2008*, no. 1, pp. 1–13, 2008.

[86] Z. Sahul, J. Black, B. Widrow, and C. Guilleminault, "Ekg artifact cancellation from sleep eeg using adaptive filtering," *Sleep research A*, p. 486, 1995.

[87] P. Strobach, K. Fuchs, and W. Harer, "Event-synchronous cancellation of the heart interference," *IEEE Transactions on Biomedical Engineering 41*, no. 4, pp. 343–350, 1994.

[88] T. Benesty and J. Gansler, "New insights into the rls algorithm," *EURASIP Journal on Applied Signal Processing*, p. 331â339, 2004.

[89] R. Everson and S. J. Roberts, "Independent components analysis," *Artificial Neural Networks in Biomedicine*, pp. 153–168, 2000.

[90] A. Hyvarinen and E. Oja, "Independent component analysis: algorithms and applications," *Neural networks 13*, no. 4, pp. 411–430, 2000.

[91] R. Vigario, J. Sarela, V. Jousmiki, M. Hamalainen, and E. Oja, "Independent component approach to the analysis of eeg and meg recordings," *IEEE transactions on biomedical engineering 47*, no. 5, pp. 589–593, 2000.

[92] W. Zhou, "Removal of ecg artifacts from eeg using ica," in *Proceedings of the 2nd Joint Engineering in Medicine and Biology*, vol. 1. 24th Annual Conference and the Annual Fall Meeting of the Biomedical Engineering Society BMES / EMBS Conference 2002,, 2002, p. 206â207.

[93] J. Iriarte, E. Urrestarazu, M. Valencia, M. Alegre, A. Malanda, C. Viteri, and J. Artieda, "Independent component analysis as a tool to eliminate artifacts in eeg: a quantitative study," *Journal of Clinical Neurophysiology 20*, no. 4, p. 249â257, 2003.

[94] C. J. James and C. W. Hesse, "Independent component analysis for biomedical signals," *Physiological Measurement 26*, no. 1, p. 15â39, 2004.

[95] M. B. Hamaneh, N. Chitravas, K. Kaiboriboon, S. D. Lhatoo, and K. A. Loparo, "Automated removal of ekg artifact from eeg data using independent component analysis and continuous wavelet transformation," *IEEE Transactions on Biomedical Engineering 61*, no. 6, pp. 1634–1641, 2014.

[96] C. J. James and O. J. Gibson, "Temporally constrained ica: an application to artifact rejection in electromagnetic brain signal analysis," *Transactions on Biomedical Engineering 50*, no. 9, pp. 1108–1116, 2003.

[97] M. A. A. Dewan, M. J. Hossain, M. M. Haque, and O. Chae, "Contaminated ecg artifact detection and elimination from eeg using energy function based transformation," in *International Conference on Information and Communication Technology 2007*, 2007, pp. 52–56.

[98] J. P. Lanquart, M. Dumont, and P. Linkowski, "Qrs artifact elimination on full night sleep eeg," in *Medical engineering & physics 28*, no. 2, 2006, pp. 156–165.

[99] G. Inuso, F. L. Foresta, N. Mammone, and F. C. Morabito, "Wavelet-ica methodology for efficient artifact removal from electroencephalographic recordings," in *Neural Networks*. International Joint Conference on, IEEE, 2007, pp. 1524–1529.

[100] Y. B. Zhou, S. M. Cai, T. Zhou, and P. L. Zhou, "Mp-based method on detecting and eliminating the synchronous ecg artifacts in the eeg signals," in *Bioinformatics and Biomedical Engineering (iCBBE)*. 4th International Conference on, IEEE, 2010, pp. 1–4.

[101] X. Navarro, F. Poree, and G. Carrault, "Ecg removal in preterm eeg combining empirical mode decomposition and adaptive filtering," in *Acoustics, Speech and Signal Processing (ICASSP), 2012*. IEEE International Conference on, IEEE, 2012, pp. 661–664.

[102] K. S. Vijila, P. Kanagasabapathy, S. Johnson, and V. Ewards, "Artifacts removal in eeg signal using adaptive neuro fuzzy inference system," in *Signal Processing, Communications and Networking, 2007*. International Conference on, IEEE, 2007, pp. 589–591.

[103] A. Jafarifarmand and M. A. Badamchizadeh, "Artifacts removal in eeg signal using a new neural network enhanced adaptive filter," *eurocomputing 103*, pp. 222–231, 2013.

[104] S. F. Sheniha, S. S. Priyadharsini, and S. E. Rajan, "Removal of artifact from eeg signal using differential evolution algorithm," in *Communications and Signal Processing (ICCSP)*. International Conference on, IEEE, 2013, pp. 134–138.

[105] S. Mukhopadhyay and G. C. Ray, "A new interpretation of non-linear energy operator and its efficacy in spike detection," *IEEE transactions on Bio-medical Engineering 45*, no. 2, p. 180 â 187, 1998.

[106] L. Galeotti, C. G. Scully, J. Vicente, L. Johannesen, and D. G. Strauss, "Robust algorithm to locate heart beats from multiple physiological waveforms by individual signal detector voting," *Physiological Measurement 36*, no. 8, p. 1705 â 1716, 2015.

[107] J. M. Stern, *Atlas of EEG patterns*, 2nd ed., L. W. . Wilkins, Ed. Philadelphia: Lippincott Williams & Wilkins, 2013.

[108] U. R. Acharya, K. P. Joseph, N. Kannathal, C. M. Lim, and J. S. Suri, "Heart rate variability: a review," *Medical and biological engineering and computing 44*, no. 12, pp. 1031–1051, 2006.

[109] Elgendi, B. Eskofier, S. Dokos, and D. Abbott, "Revisiting qrs detection methodologies for portable, wearable, battery-operated, and wireless ecg systems," *PLOS 9*, no. 1, p. e84018, 2014.

[110] J. Fraden and M. Neumann, "Qrs wave detection," *Medical and Biological Engineering and Computing 18*, no. 2, pp. 125–132, 1980.

[111] P. Morizet-Mahoudeaux, C. Moreau, D. Moreau, and J. J. Quarante, "Simple microprocessor based system for on-line ecg arrhythmia analysis," *Medical and Biological Engineering and Computing 19*, no. 4, p. 497â500, 1981.

[112] D. Gustafson, "Automated vcg interpretation studies using signal analysis technique," *R-1044 Charles Stark Drape Lab*, p. 30, 1977.

[113] M. Okada, "A digital filter for the qrs complex detection," *IEEE Transactions on Biomedical Engineering 12*, p. 700â703, 1979.

[114] J. Pan and W. Tompkins, "A real-time qrs detection algorithm," *IEEE Transactions on Biomedical Engineering 3*, p. 230â236, 1985.

[115] N. M. Arzeno, Z. D. Deng, and C. S. Poon, "Analysis of first-derivative based qrs detection algorithms," *IEEE Transactions on Biomedical Engineering 55*, no. 2, p. 478â484, 2008.

[116] D. S. Benitez, P. A. Gaydecki, A. Zaidi, and A. P. Fitzpatrick, "A new qrs detection algorithm based on the hilbert transform," *Computers in Cardiology 2000*, p. 379â382, 2000.

[117] F. Zhang and Y. Lian, "Wavelet and hilbert transforms based qrs complexes detection algorithm for wearable ecg devices in wireless body sensor networks," in *Biomedical Circuits and Systems Conference, 2009*. IEEE, 2009, p. 225â228.

[118] R. A. Balda, "Trends in computer-processed electrocardiograms," Amsterdam: North Holland, Amsterdam: North Holland, Tech. Rep., 1977.

[119] M. L. Ahlstrom and W. J. Tompkins, "Automated high-speed analysis of holter tapes with microcomputers," *IEEE Transactions on Biomedical Engineering 10*, p. 651â657, 1983.

[120] W. Engelse and C. Zeelenberg, "A single scan algorithm for qrs-detection and feature extraction," *Computers in Cardiology 6*, p. 37â42, 1979.

[121] U. D. Ulusar, R. B. Govindan, J. D. Wilson, C. L. Lowery, H. Preissl, and H. Eswaran, "Adaptive rule based fetal qrs complex detection using hilbert transform," *Engineering in Medicine and Biology Society (EMBC)*, p. 4666â4669, 2009.

[122] P. E. Trahanias, "An approach to qrs complex detection using mathematical morphology," *IEEE Transactions on Biomedical Engineering 40*, no. 2, pp. 201–205, 1993.

[123] Y. Chen and H. Duan, "A qrs complex detection algorithm based on mathematical morphology and envelope," in *27th Annual International Conference of the Engineering in Medicine and Biology Society 2005*, 2005, p. 4654â4657.

[124] F. Zhang and Y. Lian, "Electrocardiogram qrs detection using multiscale filtering based on mathematical morphology," in *29th Annual International Conference of the IEEE Engineering in Medicine and Biology Society 2007*, 2007, p. 3196â3199.

[125] H. Xing and M. Huang, "A new qrs detection algorithm based on empirical mode decomposition," in *2nd International Conference on Bioinformatics and Biomedical Engineering, 2008*, 2008, p. 693â696.

[126] M. A. Arafat and M. K. Hasan, "Automatic detection of ecg wave boundaries using empirical mode decomposition," in *IEEE International Conference on Acoustics, Speech and Signal Processing*, 2009, p. 461â464.

[127] S. K. Zhou, J. T. Wang, and J. R. Xu, "The real-time detection of qrs-complex using the envelope of ecg," in *Annual International Conference of the IEEE Engineering in Medicine and Biology Society*, 1988, p. 38.

[128] M. E. Nygards and L. Sornmo, "Delineation of the qrs complex using the envelope of the ecg," *Medical and Biological Engineering and Computing 21*, no. 5, p. 538â547, 1983.

[129] H. Y. Zhou and K. M. Hou, "Embedded real-time qrs detection algorithm for pervasive cardiac care system," in *9th International Conference on Signal Processing 2008*, 2008, p. 2150â2153.

[130] W. T. Cheng and K. L. Chan, "Classification of electrocardiogram using hidden markov models," in *Engineering in Medicine and Biology Society, 1998.* 20th Annual International Conference of the IEEE, 1998, p. 143â146.

[131] V. X. Afonso, W. J. Tompkins, T. Q. Nguyen, and S. Luo, "Ecg beat detection using filter banks," *IEEE Transactions on Biomedical Engineering 46*, no. 2, p. 192â202, 1999.

[132] F. Zhang, Y. Wei, and Y. Lian, "Frequency-response masking based filter bank for qrs dection in wearable biomedical devices," *IEEE International Symposium on Circuits and Systems, 2009*, p. 1473â1476, 2009.

[133] V. X. Afonso, W. J. Tompkins, T. Q. Nguyen, S. Trautmann, and S. Luo, "Filter bank-based processing of the stress ecg," in *17th IEEE Annual Engineering Conference in Medicine and Biology Society, 1995*, vol. 2, 1995, p. 887â888.

[134] H. A. N. Dinh, D. K. Kumar, N. D. Pah, and P. Burton, "Wavelets for qrs detection," in *23rd Annual International Conference of the IEEE Engineering in Medicine and Biology Society, 2001*, vol. 2, 2001, p. 1883â1887.

[135] L. Szilagyi, "Wavelet-transform-based qrs complex detection in on-line holter systems," in *Proceedings of First Joint 21st Annual Conference and the 1999 Annual Fall Meeting of the Biomedical Engineering Society (BMES/EMBS)*, vol. 1, 1999, p. 271.

[136] S. Liang-Yu, W. Ying-Hsuan, and W. Hu, "Using wavelet transform and fuzzy neural network for vpc detection from the holter ecg," *IEEE Transactions on Biomedical Engineering 51*, no. 7, p. 1269â1273, 2004.

[137] X. Zheng, Z. Li, L. L. Shen, and Z. Ji, "Detection of qrs complexes based on biorthogonal spline wavelet," *International Symposium on Information Science and Engineering, 2008*, vol. 2, p. 502â506, 2008.

[138] A. Alesanco, S. Olmos, R. Istepanian, and J. Garcia, "A novel real-time multilead ecg compression and de-noising method based on the wavelet transform," *Computers in Cardiology, 2003, IEEE*, 2003.

[139] S. M. Szilagyi and L. Szilagyi, "Wavelet transform and neural-network-based adaptive filtering for qrs detection," in *Proceedings of the 22nd Annual International Conference IEEE on Engineering in Medicine and Biology Society*, vol. 2, 2000, p. 1267â1270.

[140] X. Xu and Y. Liu, "Adaptive threshold for qrs complex detection based on wavelet transform," in *27th Annual International Conference of the Engineering in Medicine and Biology Society, 2005*, 2005, p. 7281â7284.

[141] J. P. Martinez, R. Almeida, S. Olmos, A. P. Rocha, and P. Laguna, "A wavelet based ecg delineator: evaluation on standard databases," *IEEE Transactions on Biomedical Engineering 51*, no. 4, p. 570â581, 2004.

[142] Q. Xue, Y. Hu, and W. J. Tompkins, "Neural-network-based adaptive matched filtering for qrs detection," *IEEE Transactions on Biomedical Engineering 39*, p. 317â329, 1992.

[143] G. D. Clifford, F. Azuaje, and P. McSharry, "Advanced methods and tools for ecg data analysis," USA: Artech House, Norwood, MA, Tech. Rep., 2006.

[144] Y. H. Hu, W. J. Tompkins, J. L. Urrusti, and V. X. Afonso, "Applications of artificial neural networks for ecg signal detection and classification," *Journal of Electrocardiology 26*, pp. 66–73, 1992.

[145] G. Vijaya, V. Kumar, and H. K. Verma, "Ann-based qrs-complex analysis of ecg," *Journal of Medical Engineering & Technology 22*, no. 4, pp. 160–167, 1998.

[146] D. T. Kaplan, "Simultaneous qrs detection and feature extraction using simple matched filter basis functions," in *Proceedings, IEEE*, C. in Cardiology 1990, Ed. Proceedings, IEEE, 1990.

[147] A. Ruha, S. Sallinen, S. Nissila, A. Ruha, S. Sallinen, and S. Nissila, "A real-time microprocessor qrs detector system with a 1-ms timing accuracy for the measurement of ambulatory hrv," *IEEE Transactions on Biomedical Engineering 44*, no. 3, p. 159â167, 1997.

[148] P. S. Hamilton and W. J. Tompkins, "Adaptive matched filtering for qrs detection," in *Proceedings of the Annual International Conference of IEEE on Engineering in Medicine and Biology Society*, 1998, pp. 147–148.

[149] Y. Lu, Y. Xian, J. Chen, and Z. Zheng, "A comparative study to extract the diaphragmatic electromyogram signal," in *IEEE International Conference on BioMedical Engineering and Informatics 2008*, vol. 2, 2008, p. 315â319.

[150] G. Belforte, R. D. Mori, and F. Ferraris, "A contribution to the automatic processing of electrocardiograms using syntactic methods," *IEEE Transactions on Biomedical Engineering 3*, p. 125â136, 1979.

[151] E. J. Ciaccio, S. M. Dunn, and M. Akay, "Biosignal pattern recognition and interpretation systems," *IEEE Engineering in Medicine and Biology Magazine 12*, no. 3, p. 106â113, 1993.

[152] P. Trahanias and E. Skordalakis, "Syntactic pattern recognition of the ecg," *IEEE Transactions on Pattern Analysis and Machine Intelligence 12*, no. 7, p. 648â657, 1990.

[153] S. Mallat and W. L. Hwang, "Singularity detection and processing with wavelets," *IEEE Transactions on Information Theory 38*, no. 2, p. 617â643, 1992.

[154] R. Poli, S. Cagnoni, and G. Valli, "Genetic design of optimum linear and nonlinear qrs detectors," *IEEE Transactions on Biomedical Engineering 42*, no. 11, pp. 1137–1141, 1995.

[155] F. Gritzali, "Towards a generalized scheme for qrs detection in ecg waveforms," *Signal Processing 15*, no. 2, pp. 183–192, 1988.

[156] R. S. Anand and V. Kumar, "Efficient and reliable detection of qrs-segment in ecg signals," in *Engineering in Medicine and Biology Society, 1995 and 14th Conference of the Biomedical Engineering Society of India*. An International Meeting, Proceedings of the First Regional Conference, IEEE, 1995.

[157] P. Gosse, R. Lasserre, C. Minifie, P. Lemetayer, J. Clementry, and Philippe, "Blood pressure surge on rising," *Journal of hypertension 22*, no. 6, pp. 1113– 1118, 2004.

[158] D. Franchi, R. Bedini, F. Manfrendi, S. Berti, G. Palagi, S. Ghione, and A. Ripoli, "Blood pressure evaluation based on arterial pulse wave velocity," *Computers in Cardiology, 1996, IEEE*, pp. 397–400, 1996.

[159] T. He, G. Clifford, and L. Tarassenko, "Application of independent component analysis in removing artefacts from the electrocardiogram," *Neural Computing & Applications 15*, no. 2, pp. 105–116, 2006.

[160] G. B. Moody and R. G. Mark, "Qrs morphology representation and noise estimation using the karhunen-loeve transform," in *Computers in Cardiology 1989, Proceedings*, 1989, pp. 269–272.

[161] B. E. Moody, "Rule-based methods for ecg quality control," *Computing in Cardiology, 2011*, pp. 361–363, 2011.

[162] V. Chudacek, L. Zach, J. Kuzilek, J. Spilka, and L. Lhotska, "Simple scoring system for ecg quality assessment on android platform," *Computing in Cardiology 2011*, pp. 449–451, 2011.

[163] H. Xia, G. A. Garcia, J. C. McBride, A. Sullivan, T. D. Bock, J. Bains, D. C.Wortham, and X. Zhao, "Computer algorithms for evaluating the quality of ecgs in real time," *Computing in Cardiology, 2011*, pp. 369–372, 2011.

[164] D. Hayn, B. Jammerbund, and G. Schreier, "Ecg quality assessment for patient empowerment in mhealth applications," *Computing in Cardiology, 2011*, pp. 353–356, 2011.

[165] G. D. Clifford, D. Lopez, Q. Li, and I. Rezek, "Signal quality indices and data fusion for determining acceptability of electrocardiograms collected in noisy ambulatory environments," *Computres in Cardiology*, vol. 38, pp. 285–288, 2011.

[166] J. Y. Wang, "A new method for evaluating ecg signal quality for multi-lead arrhythmia analysis," *Computers in Cardiology, 2002*, pp. 85–88, 2002.

[167] A. Bartolo, B. D. Clymer, R. C. Burgess, J. P. Turnbull, J. A. Golish, and M. C. Perry, "An arrhythmia detector and heart rate estimator for overnight polysomnography studies," *IEEE Trans. Biomed. Eng.*, vol. 48, no. 5, pp. 513–521, May 2001.

[168] I. Silva, J. Lee, and R. G. Mark, "Signal quality estimation with multichannel adaptive filtering in intensive care settings," *Transactions on Biomedical Engineering*, vol. 59, no. 9, pp. 2476–2485, 2012.

[169] G. Clifford, J. Behar, Q. Li, and I. Rezek, "Signal quality indices and data fusion for determining clinical acceptability of electrocardiograms," *Physiol. Meas. 33*, pp. 1419–1433, 2012.

[170] J. Behar, J. Oster, Q. Li, and G. D. Clifford, "Ecg signal quality during arrhythmia and its application to false alarm reduction," *IEEE Trans. on Biomed. Eng 60*, pp. 1660–1666., 2013.

[171] P. S. Hamilton and W. J. Tompkins, "Quantitative investigation of qrs detection rules using the mit/bih arrhythmia database," *IEEE Trans. Biomed. Eng. 33*, p. 1157â65, 1986.

[172] W. Zong, G. Moody, and D. Jiang, "A robust open-source algorithm to detect onset and duration of qrs complexes," *Computers in Cardiology 2003*, vol. 30, pp. 737–740, 2003.

[173] J. Behar, J. Oster, Q. Li, and G. D. Clifford, "A single channel ecg quality metric," *Comput. Cardiol.*, vol. 39, p. 381â384, 2012.

[174] M. A. Pimentel, M. D. Santos, D. B. Springer, and G. B. Clifford, "Heart beat detection in multimodal physiological data using a hidden semi-markov model and signal quality indices," *Physiol. Meas. 36*, 2015.

[175] M. Vollmer, "Robust detection of heart beats using dynamic thresholds and moving windows," *Comput. Cardiol. 41*, p. 569â72, 2014. [Online]. Available: www.cinc.org/archives/2014/pdf/0569.pdf

[176] L. Johannesen, J. Vicente, C. G. Scully, L. Galeotti, and D. G. Strauss, "Robust algorithm to locate heart beats from multiple physiological waveforms," *Comput. Cardiol., 2014*, p. 277â80, 2014. [Online]. Available: www.cinc.org/archives/2014/pdf/0277.pdf

[177] D. T. Cooman, G. Goovaerts, C. Varon, D. Widjaja, and S. V. Huffel, "Heart beat detection in multimodal data using signal recognition and beat location estimation," *Comput. Cardiol. 41*, p. 257â 60, 2014. [Online]. Available: www.cinc.org/archives/2014/pdf/0257.pdf[

[178] J. H. Estrada, E. Cano-Plata, C. Younes, C. Velosa, and C. Cortes, "Entropy and coefficient of variation (cv) as tools for assessing power quality," *Ingen. e Invest. 31*, pp. 45–50, 2011.

[179] *Testing and Reporting Performance Results of Cardiac Rhythm and ST Segment Measurement Algorithms*, American National Standards Institute âANSI/AAMIEC57", 1998.

[180] M. G. Terzano, D. Mancia, M. R. Salati, G. Costani, A. Decembrino, and L. Parrino, "The cyclic alternating pattern as a physiologic component of normal nrem sleep," *Sleep. 1985*, no. 8(2), pp. 137–45, Jun. 1985.

[181] M. Saeed, M. Villarroel, A. T. Reisner, G. Clifford, L. W. Lehman, G. Moody, T. Heldt, T. H. Kyaw, B. Moody, and R. G. Mark, "Multiparameter intelligent monitoring in intensive care ii (mimic-ii): a public-access intensive care unit database," *Critical care medicine 39*, no. 5, pp. 1–9, 2011.

[182] S. Bhanot, B. Singh, and K. Singh, "Issues in multisensor fusion technology," in *National conference in Trends in Industrial Electronics, Transducers, Controls and Communication, 2000*. Thapar Institute of Engineering & Technology,, 2000, pp. 72–76.

[183] J. Gieraltowski, K. Ciuchcinski, I. Grzegorczyk, K. Kosna, M. Solinski, and P. Podziemski, "Rs slope detection algorithm for extraction of heart rate from noisy, multimodal recordings," *Physiol. Meas. 36*, p. 1743 â 1761, 2015.

[184] J. Yu, T. Jeon, and M. Jeon, "Heart beat detection method with estimation of regular intervals between ecg and blood pressure," *Comp. in Cardio. 41*, p. 561 â 564, 2014.

[185] Q. Ding, Y. Bai, Y. B. Erol, R. Salas-Boni, X. Zhang, L. Li, and X. Hu, "Multimodal information fusion for robust heart beat detection," *Comp. in Cardio. 41*, pp. 261–264, 2014.

[186] R. Schulte, J. Krug, and G. Rose, "Identification of a signal for an optimal heart beat detection in multimodal physiological datasets," *Comp. in Cardio.*, pp. 273–276, 2014.

[187] U. Pangerc and F. Jager, "Robust detection of heart beats in multimodal records using slope- and peak-sensitive band-pass filters,," *Physiol. Meas. 36*, pp. 1645–1664, 2015.

[188] I. Silva, B. Moody, J. Behar, A. Johnson, J. Oster, G. D. Clifford, and G. B. Moody, "Robust detection of heart beats in multimodal data," *Physiol. Meas. 36*, pp. 1629–1644, 2015.

[189] R. B. Pachori, P. Avinash, K. Shashank, R. Sharma, and U. R. Acharya, "Application of empirical mode decomposition for analysis of normal and diabetic rr-interval signals," *Expert Systems with Applications 42*, no. 9, pp. 4567–4581, 2015.

[190] M. H. Ebrahim, M. F. Jeffrey, and I. Bar-Kana, "A robust sensor fusion method for heart rate estimation," *Journal of clinical monitoring 13.6*, pp. 385–393, 1997.

[191] Y. Mendelson, "Pulse oximetry: theory and applications for noninvasive monitoring," *Clin. Chem. 38*, p. 1601â7, 1992.

[192] Gribok, V. Andrei, C. Xiaoxiao, and J. Reifman, "A robust method to estimate instantaneous heart rate from noisy electrocardiogram waveforms," *Annals of biomedical engineering 39.2*, pp. 824–834, 2011.

[193] "Matlab source code for generating artifacts in abp." [Online]. Available: https://www.ncbi.nlm.nih.gov/pmc/articles/PMC2728101/bin/1475-925X-8-13-S1.zip

PUBLICATIONS

- **International Conferences**

1. S. A. Rankawat, M. Rankawat, and R. Dubey, “ECG Artifacts detection in Non-cardiovascular Signals using Slope Sum Function and Teager Kaiser Energy”, IEEE International Conference on BioSignal Analysis, Processing and Systems (ICBAPS), pp. 6-10, 2015.
2. S. A. Rankawat, M. Rankawat, and R. Dubey, “Heart rate estimation from non-cardiovascular signals using Slope Sum function and Teager Energy”, IEEE International Conference on Industrial Instrumentation and Control (ICIC), pp. 1534-1539. 2015.

- **International Journals**

1. S. A. Rankawat and R. Dubey, “Robust heart rate estimation from multimodal physiological signals using beat signal quality index based majority voting fusion method”, Biomedical Signal Processing and Control 33, pp. 201-212, 2017.
2. “Evaluation of Beat SQI based majority voting fusion algorithm on noisy multi-modal Signals”: manuscript under preparation.

Appendix A

Detailed results of ECG artifacts detection, R-peak detection and majority voting fusion

Table A.1: R-peak artifacts detection performance of SSF-TKE method on EEG, EOG and EMG signals of PhysioNet/CinC Challenge 2014 training dataset

Signal No.	Total No. of beats	EEG		EOG		EMG	
		Sensitivity (%)	Predictivity (%)	Sensitivity (%)	Predictivity (%)	Sensitivity (%)	Predictivity (%)
100	693	39.54	37.90				
101	797	67.38	75.00				
102	685	98.25	98.83				
103	707	67.47	67.66	96.75	97.02	49.79	49.37
104	720	52.64	54.53				
105	724	55.11	55.80				
106	888	79.62	85.70	86.04	93.17	47.64	59.08
107	757	53.63	58.25				
108	907	88.75	92.74	74.42	81.13	47.08	57.62
109	655	39.08	36.06				
110	735	53.61	54.95				
111	690	82.90	79.33	96.67	95.83	88.26	86.75

112	707	41.87	42.65	90.66	90.66	59.26	57.63
113	665	56.69	54.64	83.61	80.81	56.24	50.54
114	631	100.00	99.68				
115	648	70.52	65.57				
116	169	48.52	61.65				
117	868	60.14	69.32	86.52	92.03	51.38	59.31
118	551	66.24	53.76	75.86	66.35	68.6	56.67
119	741	97.57	97.97	99.87	99.73	97.98	97.98
120	722	50.97	52.12				
121	883	83.81	88.94	57.64	69.54	45.3	55.17
122	631	92.71	93.30				
123	734	99.46	98.38	99.59	98.65	99.05	98.78
124	787	79.92	87.60	91.11	93.12	73.57	78.14
125	721	44.24	44.99				
126	635	68.50	63.04	81.57	78.13	69.61	67.79
127	738	49.73	51.62				
128	800	39.88	45.64				
129	685	84.82	84.20				
130	838	92.00	94.83				
131	693	56.71	56.38				
132	869	78.25	86.96	94.59	96.37	52.01	61.58
133	792	34.85	40.59				
134	757	68.69	74.29				
135	661	50.98	48.07				
136	695	94.10	96.04				
137	728	37.23	38.28				
138	740	74.32	76.50	97.7	98.1	93.92	95.73
139	601	67.05	60.97				
140	715	37.90	39.68				
141	702	93.30	92.78				
142	600	66.50	57.74				
143	920	76.85	83.38	73.37	81.33	42.61	52.83
144	527	61.29	69.46	99.24	99.43	71.54	75.1
145	708	86.30	88.94	63.7	65.65	50.14	47.59

146	794	74.94	81.96	93.07	94.99	82.49	84.63
147	872	98.05	99.07				
148	728	39.01	40.40				
149	727	97.39	97.93	84.59	85.42	74.69	73.98
150	811	42.05	47.76				
151	806	92.93	95.54				
152	595	42.86	35.61				
153	566	67.84	57.57	74.38	63.69	75.44	68.1
154	920	85.00	92.11				
155	745	75.57	80.20	95.03	97.12	81.48	84.42
156	882	35.94	47.46				
157	717	40.73	43.20				
158	838	64.68	71.88				
159	710	89.44	87.95				
160	659	49.32	45.26				
161	670	72.24	67.41	86.57	82.5	96.87	95.3
162	690	64.78	64.22	81.16	82.23	48.55	46.02
163	884	89.37	93.71	61.2	72.04	46.95	53.97
164	872	87.61	92.83	79.24	84.06	50.11	57.12
165	646	41.33	37.77				
166	684	43.71	43.08				
167	736	13.18	42.73				
168	860	37.21	44.82				
169	785	48.15	52.87				
170	738	74.66	76.74				
171	665	40.60	38.24				
172	880	71.59	80.77				
173	728	59.07	59.89				
174	805	60.37	66.03				
175	723	63.35	62.48	95.99	95.99	73.58	72.98
176	688	55.23	54.60	77.03	76.7	41.72	38.89
177	689	51.67	50.14	87.23	85.37	55.88	52.96
178	774	78.94	81.47	98.84	99.09	97.55	98.05
179	861	57.14	68.81	87.46	91.83	57.03	67.26

180	884	83.03	91.18				
181	655	44.89	39.89	82.6	78.98	41.53	37.47
182	791	92.54	94.09	54.87	59.21	76.99	78.89
183	697	63.41	61.30	99.71	99.14	82.07	78.46
184	602	63.12	56.97	73.42	66.27	40.37	33.33
185	729	44.86	44.31				
186	726	61.57	61.83				
187	592	40.03	33.15	54.9	46.63	43.92	35.09
188	841	62.31	69.96				
189	721	38.83	39.44	89.04	91.32	52.98	51.48
190	698	39.83	37.37	89.4	88.76	49.71	46.45
191	460	44.78	46.82				
192	721	49.51	50.00				
193	597	97.99	96.69				
194	841	35.20	44.78				
195	717	40.45	41.19				
196	527	62.24	69.49				
197	681	97.21	95.94	56.83	54.35	44.2	41.12
198	699	43.78	41.46	91.27	92.2	45.35	40.43
199	666	96.47	96.34				
1020	600	47.50	40.25				
1023	635	68.50	63.04	81.57	78.13	69.61	67.79
1032	799	44.31	52.52				
1069	738	64.09	66.90				
1073	602	63.12	56.97	73.42	66.27	40.37	33.33
1503	751	57.66	63.40	87.35	89.86	60.85	62.43
2283	784	39.29	45.43				
2527	701	38.37	42.23	56.49	56.9	53.35	51.44
2800	752	41.22	45.59				
3188	822	39.17	49.77				
Total	79597						
Average		62.74	64.52	82.76	83.09	62.45	62.71
Gross		63.17	65.25	82.73	83.40	62.15	62.54

Gross F1 Score (%)		64.19		83.06		62.34	
Overall Score (%)		63.92		83.00		62.46	

Table A.2: R-peak artifacts detection performance of SSF-TKE method on EEG, EOG and EMG signals of MIT-BIH Polysomnographic database

Signal No.	Total number of beats	EEG		EOG		EMG	
		Sensitivity (%)	Predictivity (%)	Sensitivity (%)	Predictivity (%)	Sensitivity (%)	Predictivity (%)
slp 01a	7806	98.73	98.72				
slp 01b	11467	95.26	94.72				
slp 02a	16145	89.03	94.24				
slp02b	11317	81.86	89.08				
slp 03	24917	42.42	41.98				
slp 04	27029	52.07	54.86				
slp 14	22920	49.92	45.85				
slp 16	27604	39.74	44.23				
slp 32	21718	41.08	40.37	79.14	77.82	51.72	47.55
slp 37	30611	74.76	84.19	71.46	80.67	49.82	58.17
slp 41	25884	67.12	64.20	82.10	80.52	70.41	67.40
slp 45	27686	82.36	83.92	94.21	94.92	87.43	87.76
slp 48	24711	59.69	55.70	78.56	74.38	48.48	43.30
slp 59	16901	39.53	39.68				
slp 60	25017	45.51	63.28				
slp 61	25482	54.69	54.13				
slp 66	15775	72.29	73.77				
slp 67x	5374	82.88	84.13				
Total	368364						
Average		64.94	67.06	81.10	81.66	61.57	60.83
Gross		60.79	62.74	81.01	81.91	61.94	61.22

Gross F1 Score (%)		61.75		81.46		61.58	
Overall Score (%)		63.88		81.42		61.39	

Table A.3: R-peak detection performance of SSF-TKE method on ECG signal of PhysioNet/CinC Challenge 2014 training dataset

Signal No.	Total number of beats	Sensitivity (%)	Predictivity (%)	F1 score
100	693	100	100	100.00
101	797	99.12	100	99.56
102	685	100	100	100.00
103	707	100	100	100.00
104	720	100	100	100.00
105	724	100	100	100.00
106	888	100	100	100.00
107	757	100	100	100.00
108	907	100	100	100.00
109	655	100	100	100.00
110	735	100	100	100.00
111	690	100	100	100.00
112	707	99.72	99.72	99.72
113	665	100	99.85	99.92
114	631	100	100	100.00
115	648	100	100	100.00
116	169	100	100	100.00
117	868	100	100	100.00
118	551	100	99.46	99.73
119	741	100	100	100.00

120	722	100	100	100.00
121	883	100	100	100.00
122	631	100	100	100.00
123	734	100	100	100.00
124	787	99.87	99.87	99.87
125	721	100	100	100.00
126	635	100	100	100.00
127	738	99.59	99.73	99.66
128	800	100	100	100.00
129	685	100	100	100.00
130	838	99.76	99.76	99.76
131	693	99.86	99.86	99.86
132	869	100	100	100.00
133	792	98.23	98.86	98.54
134	757	100	100	100.00
135	661	100	100	100.00
136	695	100	100	100.00
137	728	100	100	100.00
138	740	100	100	100.00
139	601	100	100	100.00
140	715	100	100	100.00
141	702	100	100	100.00
142	600	100	100	100.00
143	920	100	100	100.00
144	527	100	100	100.00
145	708	100	99.86	99.93
146	794	99.24	99.49	99.36
147	872	100	100	100.00
148	728	100	100	100.00
149	727	100	100	100.00
150	811	100	100	100.00
151	806	100	99.88	99.94
152	595	100	100	100.00
153	566	100	99.82	99.91

154	920	99.13	100	99.56
155	745	100	100	100.00
156	882	100	100	100.00
157	717	100	100	100.00
158	838	100	100	100.00
159	710	100	100	100.00
160	659	99.7	99.85	99.77
161	670	100	100	100.00
162	690	100	100	100.00
163	884	100	100	100.00
164	872	100	100	100.00
165	646	100	100	100.00
166	684	100	100	100.00
167	736	100	100	100.00
168	860	100	100	100.00
169	785	100	100	100.00
170	738	100	100	100.00
171	665	100	100	100.00
172	880	98.86	99.54	99.20
173	728	100	100	100.00
174	805	100	100	100.00
175	723	100	100	100.00
176	688	100	100	100.00
177	689	100	100	100.00
178	774	100	100	100.00
179	861	100	99.88	99.94
180	884	99.89	100	99.94
181	655	100	100	100.00
182	791	100	100	100.00
183	697	100	100	100.00
184	602	100	100	100.00
185	729	100	100	100.00
186	726	100	100	100.00
187	592	100	100	100.00

188	841	98.22	98.69	98.45
189	721	99.45	99.58	99.51
190	698	100	100	100.00
191	460	100	99.78	99.89
192	721	100	100	100.00
193	597	100	100	100.00
194	841	100	100	100.00
195	717	100	100	100.00
196	527	100	100	100.00
197	681	100	100	100.00
198	699	100	100	100.00
199	666	100	100	100.00
1003	957	100	100	100.00
1009	1330	54.29	98.9	70.10
1016	806	100	100	100.00
1019	254	98.03	83.28	90.06
1020	600	100	99.67	99.83
1022	873	99.77	100	99.88
1023	635	100	100	100.00
1028	572	66.96	59.47	62.99
1032	799	95.62	96.95	96.28
1033	744	98.92	98.92	98.92
1036	1139	64.79	100	78.63
1043	857	100	100	100.00
1069	738	100	100	100.00
1071	604	99.17	99.5	99.33
1073	602	100	100	100.00
1077	997	99.3	100	99.65
1169	1013	78.38	88.42	83.10
1195	819	2.56	2.56	2.56
1242	844	7.46	8.55	7.97
1284	649	96.3	96.3	96.30
1354	894	37.7	50.15	43.04
1376	1580	51.39	98.19	67.47

1388	1002	98.7	100	99.35
1447	583	78.56	64.69	70.95
1456	967	98.55	99.79	99.17
1485	942	88	98.93	93.15
1503	751	100	100	100.00
1522	746	68.5	69.34	68.92
1565	715	99.58	99.44	99.51
1584	1208	54.55	99.85	70.55
1683	653	64.62	76.59	70.10
1686	786	83.21	82.26	82.73
1715	1130	63.36	93.47	75.52
1742	1000	99.9	100	99.95
1774	1139	55.66	97.84	70.95
1804	520	69.62	57.92	63.23
1807	766	83.42	87.41	85.37
1821	1111	79.66	98.99	88.28
1858	783	21.07	22.98	21.98
1866	764	97.64	99.73	98.67
1900	986	97.06	99.69	98.36
1906	643	83.36	81.21	82.27
1954	748	100	99.87	99.93
1993	724	99.72	99.59	99.65
1998	1222	53.6	99.7	69.72
2041	16	100	72.73	84.21
2063	639	88.42	87.06	87.73
2132	864	81.13	97.77	88.68
2164	1068	88.48	94.88	91.57
2174	883	93.2	99.04	96.03
2201	1130	60	95.22	73.61
2203	682	80.94	78.97	79.94
2209	677	99.85	99.56	99.70
2247	914	86.87	98.51	92.32
2277	942	63.91	73.5	68.37
2279	147	51.02	74.26	60.48

2283	784	60.2	63.27	61.70
2296	732	100	100	100.00
2327	546	92.12	86.13	89.02
2370	449	71.49	55.63	62.57
2384	1636	52.87	100	69.17
2397	940	98.94	99.36	99.15
2469	962	99.38	99.58	99.48
2527	701	99.43	99.57	99.50
2552	1004	98.71	99.7	99.20
2556	990	98.99	100	99.49
2602	573	82.9	76.37	79.50
2639	963	99.38	99.58	99.48
2664	1126	58.44	86.13	69.63
2714	864	88.77	98.21	93.25
2728	104	100	89.66	94.55
2732	1010	94.55	97.75	96.12
2733	522	75.1	69.5	72.19
2798	833	100	99.4	99.70
2800	752	80.32	85.55	82.85
2812	980	83.78	88.28	85.97
2839	1611	50.71	99.51	67.18
2850	561	82	72.56	76.99
2879	620	95.81	92.81	94.29
2885	930	87.85	98.67	92.95
2886	149	100	100	100.00
2907	722	91.69	89.1	90.38
2923	1084	91.42	100	95.52
2970	940	91.38	99.65	95.34
3188	822	100	99.76	99.88
3266	982	82.38	99.14	89.99
41024	86	100	100	100.00
41025	622	99.04	99.04	99.04
41081	729	51.85	96.92	67.56
41164	631	95.09	98.68	96.85

41173	982	97.45	97.95	97.70
41180	680	86.76	86.76	86.76
41566	168	95.24	81.63	87.91
41778	87	77.01	72.83	74.86
41951	254	59.06	98.68	73.89
42228	866	92.84	97.57	95.15
42511	173	37.57	48.51	42.34
42878*	929			
42961	614	49.67	99.67	66.30
43247	748	51.47	99.48	67.84
Total	151031			
Average		90.83	94.46	92.65
Gross		89.62	95.21	
Gross F1 Score (%)		92.33		
Overall Score (%)		92.53		

* Record no. 42878 of PhysioNet/CinC Challenge 2014 training dataset does not have ECG signal, hence total no. of ECG beats in the dataset is 150102

Table A.4: R-peak detection performance of gqrs, SSF-TKE method and epltd on ECG signals of MIT-BIH Polysomnographic database

Signal No.	Total number of beats	gqrs		SSF-TKE		epltd	
		Sensitivity (%)	Predictivity (%)	Sensitivity (%)	Predictivity (%)	Sensitivity (%)	Predictivity (%)
slp 01a	7806	99.96	99.94	100	99.99	99.99	99.96
slp 01b	11467	99.95	99.91	99.97	99.97	99.97	99.83
slp 02a	16145	99.8	99.46	99.54	99.90	99.86	99.50
slp02b	11317	99.78	99.01	99.43	99.67	99.85	99.04
slp 03	24917	99.97	96.15	99.97	97.83	99.99	95.80

slp 04	27029	99.96	99.18	99.72	99.84	99.93	99.44
slp 14	22920	99.91	99.73	99.75	99.79	99.94	99.42
slp 16	27604	99.89	98.71	99.64	99.87	99.91	99.17
slp 32	21718	99.94	99.11	99.88	99.91	99.96	99.25
slp 37	30611	99.92	99.93	100	100	99.98	99.90
slp 41	25884	99.95	99.84	99.93	99.85	99.99	99.86
slp 45	27686	99.96	99.6	99.94	99.96	99.97	99.66
slp 48	24711	99.96	99.73	99.99	99.98	99.99	99.79
slp 59	16901	100	99.99	99.99	99.99	99.99	100.00
slp 60	25017	100	99.98	99.97	98.88	100.00	94.51
slp 61	25482	99.96	99.97	99.75	99.80	100.00	99.96
slp 66	15775	100	100	99.96	99.99	99.99	100.00
slp 67x	5374	100	99.98	100	100	99.98	100.00
Total	368364						
Average		99.94	99.46	99.86	99.74	99.96	99.17
Gross		99.94	99.38	99.86	99.69	99.96	99.02
Gross F1 Score (%)		99.66		99.77		99.49	
Overall Score (%)		99.68		99.79		99.53	

Table A.5: R-peak detection performance of gqrs and SSF-TKE method ECG signals of MIT-BIH Arrhythmia database

Signal No.	Total number of beats	gqrs		SSF-TKE method	
		Sensitivity (%)	Predictivity (%)	Sensitivity (%)	Predictivity (%)
100	2273	99.87	100.00	100.00	100.00
101	1865	99.87	100.00	100.00	99.95
102	2187	100.00	100.00	100.00	100.00
103	2084	98.13	90.48	99.95	100.00
104	2229	98.61	97.69	99.78	99.73
105	2572	95.72	94.19	99.92	99.77

106	2027	98.13	92.51	95.12	96.79
107	2137	97.94	99.90	99.86	99.81
108	1763	99.32	92.79	96.94	94.00
109	2532	99.37	99.92	99.64	99.76
111	2124	99.86	99.86	99.76	99.44
112	2539	99.53	99.92	100.00	100.00
113	1795	99.94	100.00	100.00	100.00
114	1879	100.00	100.00	99.79	98.63
115	1953	99.69	99.44	100.00	100.00
116	2412	99.75	100.00	99.92	99.96
117	1535	100.00	100.00	100.00	100.00
118	2278	100.00	100.00	100.00	99.65
119	1987	100.00	99.85	99.95	99.80
121	1863	99.95	99.89	100.00	99.95
122	2476	99.84	100.00	100.00	100.00
123	1518	99.93	100.00	99.60	97.67
124	1619	99.88	100.00	100.00	99.39
200	2601	52.15	90.76	99.23	99.69
201	1963	97.66	100.00	94.80	93.75
202	2136	99.72	100.00	92.93	99.20
203	2980	99.09	94.50	79.90	98.55
205	2656	98.83	99.81	99.17	100.00
207	1860	99.57	99.89	96.94	97.99
208	2955	82.33	91.19	88.16	99.69
209	3005	97.90	96.36	94.74	100.00
210	2650	98.34	99.24	97.25	99.61
212	2748	98.22	98.76	100.00	99.96
213	3251	100.00	100.00	91.88	99.97
214	2262	99.51	99.65	99.51	99.47
215	3363	99.46	99.97	73.60	100.00
217	2208	98.19	99.86	98.28	98.73
219	2154	99.95	99.86	98.56	94.86
220	2048	99.95	100.00	99.12	100.00
221	2427	99.09	98.40	99.01	99.22

222	2483	99.80	100.00	89.29	99.91
223	2605	99.16	99.96	99.88	99.88
228	2053	99.95	99.56	99.51	99.03
230	2256	100.00	99.96	100.00	100.00
231	1571	99.94	99.94	90.58	84.05
232	1780	100.00	97.37	98.99	77.66
233	3079	99.45	99.84	91.39	99.93
234	2753	99.96	100.00	99.64	100.00
Total	109494				
Average		97.99	98.57	97.14	98.45
Gross		97.71	98.55	96.63	98.59
Gross F1 Score (%)		98.12		97.60	
Overall Score (%)		98.20		97.70	

Table A.6: R-peak detection performance of SSF-TKE method and epltd algorithm on ECG signals of MGH/MF Waveform database

Signal No.	Total number of beats	SSF-TKE method		epltd	
		Sensitivity (%)	Predictivity (%)	Sensitivity (%)	Predictivity (%)
1	2628	76.45	65.35	94.06	94.32
2	6652	95.60	99.22	99.20	99.80
3	7042	53.49	99.63	99.33	99.93
4	3317	98.34	94.94	98.46	96.37
5	8284	99.13	99.87	99.18	99.94
6	7600	99.14	99.42	95.76	85.02
7	5598	98.48	99.89	98.95	99.78
8	5006	98.62	99.82	96.38	91.24
9	9374	73.85	99.58	99.15	99.03
10	9511	76.86	99.93	98.93	99.37

11	6663	97.76	98.49	97.01	99.69
12	6326	83.70	99.25	87.46	91.32
13	6663	99.62	99.82	99.43	98.87
14	7741	99.50	98.15	99.08	83.69
15	6714	98.78	99.80	98.66	94.41
16	3906	99.10	99.79	99.10	97.04
17	8170	99.39	99.72	99.39	99.22
18	7267	89.51	99.68	98.07	99.12
19	5730	95.92	99.53	95.72	99.93
20	6492	90.28	98.16	99.52	99.69
21	5041	94.35	99.79	98.81	99.82
22	6762	96.69	98.04	98.55	97.50
23	7165	94.45	97.83	98.42	98.62
24	7390	99.16	99.54	99.31	99.90
25	4160	96.42	95.52	96.56	67.02
26	7984	45.93	47.95	47.22	47.84
27	5474	93.90	98.79	99.36	99.05
28	5094	96.25	96.10	99.35	99.37
29	7894	98.66	99.30	99.46	99.75
30	7098	97.56	99.17	99.28	98.11
31	7369	55.19	77.20	95.16	94.64
32	6812	95.05	99.55	97.87	97.31
33	8872	99.32	99.56	99.20	90.62
34	5061	99.21	100.00	98.66	90.93
35	4110	99.54	99.95	99.54	99.98
36	5873	99.34	99.34	99.34	99.68
37	5657	98.78	99.48	98.92	99.26
38	4697	99.08	99.23	99.13	97.47
39	5798	99.67	99.78	98.48	84.61
40	3947	91.26	71.81	0.00	0.00
41	503	87.28	24.02	0.00	0.00
42	4585	48.46	88.49	73.96	97.81
43	7692	82.58	99.65	98.69	99.78
44	5371	83.82	96.18	97.56	99.85

45	10340	51.75	99.65	97.48	99.79
46	5876	88.02	99.14	95.49	99.57
47	11378	52.74	98.34	97.87	99.31
48	2928	97.58	99.51	99.76	99.32
49	9242	56.17	99.06	94.70	98.73
50	11130	48.39	98.93	97.06	99.73
51	5355	99.29	95.70	99.18	99.36
52	6455	87.11	99.47	98.81	95.64
53	5859	99.25	99.97	99.23	99.81
54	6718	99.58	99.96	99.60	99.94
55	5693	99.07	98.57	59.51	59.64
56	5116	99.30	99.74	99.71	99.38
57	5811	74.15	75.07	75.34	42.67
58	4027	95.43	99.87	99.60	99.88
59	6828	96.49	99.88	99.55	99.72
60	2793	99.86	99.96	99.53	98.86
61	6842	67.41	66.61	99.09	97.19
62	5036	99.70	99.07	99.31	99.92
63	6661	99.34	99.91	94.82	79.24
64	7629	99.36	99.24	98.66	95.33
65	7019	99.39	99.03	99.39	99.71
66	2423	97.32	91.29	95.87	90.04
67	6571	94.61	96.58	97.57	97.82
68	4750	98.08	99.32	97.71	89.47
69	8173	69.94	93.72	69.50	100.00
70	9809	63.18	99.69	72.60	98.29
71	5717	99.28	98.82	99.32	98.35
72	6552	74.94	74.72	99.11	70.18
73	11641	52.13	98.20	99.52	99.76
74	6653	24.44	28.31	0.00	0.00
75	1762	65.66	63.26	99.04	99.54
76	9663	52.75	98.87	94.91	91.90
77	7173	86.42	99.95	99.78	99.99
78	7914	99.42	99.81	93.04	82.67

79	5031	99.54	99.62	99.58	99.90
80	4326	99.28	100.00	99.28	99.84
81	7467	0.00	0.00	99.30	99.64
82	7332	58.93	99.72	98.62	99.72
83	5683	99.28	99.98	99.28	99.98
84	3923	96.56	87.40	99.06	97.08
85	9790	54.99	99.94	99.64	99.91
86	9811	71.31	98.98	97.91	98.24
87	4383	99.16	96.84	99.18	98.71
88	5982	99.38	99.71	99.38	99.80
89	8154	93.21	99.92	98.61	96.26
90	4197	99.36	99.33	99.38	99.78
91	5739	99.60	99.97	99.29	99.37
92	6427	98.51	99.26	95.66	65.82
93	7131	90.87	99.98	99.44	99.90
94	5734	99.48	99.74	99.55	99.83
95	8405	53.53	83.45	98.88	94.96
96	4817	98.96	99.87	98.92	99.81
97	6934	99.44	99.96	98.79	97.19
98	6341	97.97	99.63	99.40	99.78
99	7915	99.46	100.00	99.33	99.65
100	4222	99.48	99.76	99.62	99.86
101	4711	98.26	98.80	99.04	97.59
102	4212	98.84	95.99	98.93	99.36
103	6358	96.84	97.82	97.88	98.73
104	6544	99.19	99.04	98.81	99.16
105	7777	84.63	99.22	98.56	92.97
106	6797	94.78	99.91	96.51	92.23
107	4512	98.83	99.82	98.56	99.17
108	8364	96.34	99.88	99.63	99.90
109	8841	74.01	94.95	99.59	99.92
110	6057	99.36	99.78	99.27	99.60
111	6782	99.19	99.93	98.29	98.92
112	6536	98.59	99.32	99.01	96.78

113	6851	99.39	100.00	99.37	99.63
114	7384	98.71	99.95	98.56	98.70
115	8166	89.76	99.99	98.27	99.31
116	5189	97.75	80.25	99.02	99.50
117	8229	65.85	97.31	98.12	96.37
118	9544	79.35	99.71	97.55	93.73
119	5742	81.19	99.74	96.69	92.01
120	5613	97.97	99.12	99.39	98.12
121	8481	99.39	99.48	99.56	99.38
122	660	48.18	17.25	65.00	18.46
123	6257	97.57	98.06	86.32	55.15
124	9359	51.48	99.90	89.62	95.30
125	9262	85.36	99.82	99.31	99.56
126	4302	95.49	93.90	97.88	89.20
127	4072	65.79	64.68	95.95	74.45
128	8583	92.47	99.75	93.22	96.99
129	11053	56.85	99.51	98.13	98.89
130	4013	75.08	73.01	70.52	70.91
131	5976	98.64	99.83	98.69	99.73
132	7937	73.16	99.83	99.51	99.48
133	4390	99.93	76.59	99.36	92.77
134	6441	99.21	99.98	99.38	99.88
135	4777	81.43	99.79	99.41	99.77
136	7358	55.26	99.98	99.31	99.92
137	6480	97.64	99.72	99.04	99.64
138	3933	99.26	99.31	99.24	98.76
139	7823	84.39	98.74	99.09	98.92
140	7955	98.98	99.76	99.33	98.60
141	6432	96.02	99.63	99.18	99.52
142	7639	97.37	99.95	99.27	99.58
143	5334	98.71	99.12	99.12	96.65
144	4407	98.41	99.63	98.46	95.28
145	8751	93.72	99.93	98.02	96.50
146	6655	97.40	99.36	99.11	99.74

147	9399	71.79	99.91	99.55	98.55
148	8265	97.94	99.91	99.33	99.50
149	7120	99.28	99.48	99.10	98.33
150	7283	69.05	99.66	98.81	97.07
151	7247	52.86	97.41	99.13	99.87
152	4261	99.32	96.62	99.34	99.44
153	3592	98.69	97.77	98.89	99.75
154	6053	98.91	99.98	98.98	99.83
155	7330	91.62	99.97	99.24	99.86
156	6192	99.18	99.22	99.22	99.92
157	9102	69.59	99.06	99.45	99.93
158	9557	54.89	98.31	99.33	99.05
159	7872	53.26	83.43	99.52	99.86
160	6430	99.21	99.35	99.14	99.47
161	6516	99.05	98.43	98.39	95.06
162	5461	99.21	99.16	98.90	98.47
163	4962	96.27	98.17	94.46	99.64
164	5880	99.10	100.00	97.93	99.74
165	6583	99.06	99.98	98.95	99.21
166	9322	54.05	99.82	99.59	99.96
167	4891	99.63	95.32	99.69	99.67
168	6360	99.80	99.13	99.86	99.44
169	7780	99.31	99.83	99.28	99.10
170	894	99.89	100.00	99.66	99.78
171	7710	99.73	99.66	99.83	99.81
172	3681	86.36	72.07	99.65	98.55
173	9819	61.02	99.87	85.33	86.38
174	9277	91.89	99.95	99.07	99.71
175	7384	53.35	99.95	98.97	99.25
176	3871	98.92	96.09	93.65	72.85
177	5842	99.25	98.42	99.26	99.06
178	5219	92.12	97.31	98.37	96.05
179	4290	98.79	95.49	71.89	88.39
180	6934	96.96	99.54	99.11	99.68

181	6633	98.99	98.50	94.95	78.39
182	6960	97.30	98.92	98.59	97.25
183	5133	100.00	99.04	99.96	99.75
184	6273	99.92	99.68	99.68	97.67
185	5326	99.91	98.48	99.14	96.30
186	7708	90.74	98.77	96.25	99.12
187	7566	95.32	99.85	99.52	99.85
188	6501	96.74	98.93	95.39	94.37
189	10885	53.84	99.02	87.10	92.46
190	6904	95.13	98.69	96.18	95.37
191	7314	58.57	99.24	99.22	98.45
192	7280	98.82	99.49	99.52	98.93
193	7539	97.67	98.57	99.77	99.21
194	4632	98.55	80.58	98.68	96.99
195	6131	99.25	99.57	99.14	99.48
196	6693	99.93	99.97	99.88	99.39
197	7679	99.67	99.26	99.93	99.13
198	9747	53.65	99.34	99.79	99.94
199	3917	98.90	99.59	99.08	99.54
200	5668	99.42	99.86	99.61	99.65
201	5623	99.20	98.92	99.25	99.43
202	4152	99.08	100.00	99.08	99.81
203	6136	99.01	99.74	99.15	99.80
204	6060	91.80	90.96	27.05	99.76
205	2816	99.57	86.04	0.04	10.00
206	999	98.60	80.94	98.00	89.08
207	4710	95.65	84.74	97.64	88.17
208	2956	97.87	98.91	99.42	98.39
209	1949	98.05	93.95	69.01	55.44
210	6460	89.21	97.00	90.36	98.18
211	2766	97.69	93.82	99.17	98.07
212	9806	49.14	98.65	96.16	99.19
213	7187	88.08	96.66	96.15	98.90
214	4325	95.08	92.74	99.38	98.92

215	7067	94.20	94.91	99.14	98.91
216	3723	51.92	49.39	93.02	97.88
217	6738	50.58	97.85	97.63	99.37
218	4606	79.05	94.11	21.30	82.09
219	6781	51.05	90.63	96.89	99.49
220	6348	40.12	98.38	71.77	98.51
221	4858	51.32	94.90	95.16	99.66
222	7898	48.67	98.06	91.43	99.68
223	5182	64.42	95.29	99.59	99.83
224	4171	95.68	99.68	99.14	99.69
225	2441	73.74	84.27	96.11	95.37
226	7520	99.52	99.44	99.53	100.00
227	9384	57.03	99.78	99.29	99.81
228	3942	91.40	71.35	0.00	0.00
229	3620	96.91	69.94	0.00	0.00
230	0				
231	3969	76.95	67.14	0.03	50.00
232	3999	99.32	97.33	0.03	25.00
233	3717	96.34	75.72	0.00	0.00
234	5227	92.31	90.70	0.02	50.00
235	0				
236	5969	94.14	98.35	98.96	99.24
237	5989	96.46	95.02	0.02	20.00
238	5332	79.73	78.58	0.00	0.00
239	4782	95.32	81.63	0.00	0.00
240	5523	87.09	77.73	0.00	0.00
241	5119	20.10	19.50	0.02	50.00
242	5806	68.41	68.36	0.02	50.00
243	6435	48.95	48.25	0.00	0.00
244	3856	64.55	90.21	82.86	98.70
245	4865	94.04	95.79	99.38	99.57
246	1784	98.77	92.30	99.55	94.02
247	6435	95.35	96.42	94.56	98.45
248	5609	97.18	98.04	100.00	97.09

249	5749	99.93	99.57	99.95	99.88
250	2103	99.48	99.81	99.86	99.90
Total	1542273				
Average		86.76	93.75	89.46	90.06
Gross		84.61	95.06	91.44	95.59
Gross F1 Score (%)		89.53		93.47	
Overall Score (%)		90.05		91.64	

Table A.7: R-peak detection performance of gqrs, SSF-TKE method and epltd algorithm on ECG signals with paced beats in PhysioNet/CinC Challenge 2014 training dataset

Signal No.	Total number of beats	gqrs		SSF-TKE method		epltd	
		Sensitivity (%)	Predictivity (%)	Sensitivity (%)	Predictivity (%)	Sensitivity (%)	Predictivity (%)
2469	962	100	49.97	99.38	99.58	99.9	49.97
2639	963	99.9	49.97	99.38	99.58	99.9	50
2812	980	99.9	50	83.78	88.28	99.9	50.03
41173	982	100	50.03	97.45	97.95	93.48	86.04
Total	3887						
Average	3887	99.95	49.99	95.00	96.35	98.30	59.01
Gross		99.95	49.99	94.96	96.42	98.28	55.60
Gross F1 Score (%)		66.65		95.67		71.02	
Overall Score (%)		74.97		95.67		77.79	

Table A.8: Heart beat detection performance of majority voting fusion method with different combinations of QRS detectors on PhysioNet/CinC Challenge 2014 training dataset

Signal No.	Total number of beats	Voting fusion (gqrs/SSF-TKE)		Voting fusion (epltd/SSF-TKE)		Voting fusion (gqrs/epltd)	
		Sensitivity (%)	Predictivity (%)	Sensitivity (%)	Predictivity (%)	Sensitivity (%)	Predictivity (%)
100	693	100.00	100.00	100.00	100.00	100.00	100.00
101	797	100.00	100.00	99.87	100.00	100.00	100.00
102	685	100.00	100.00	100.00	100.00	100.00	100.00
103	707	99.86	100.00	99.86	100.00	99.86	100.00
104	720	100.00	100.00	99.86	100.00	100.00	100.00
105	724	100.00	100.00	100.00	100.00	100.00	100.00
106	888	100.00	100.00	99.89	100.00	99.89	100.00
107	757	99.87	100.00	100.00	100.00	99.87	99.87
108	907	100.00	100.00	99.89	100.00	99.89	100.00
109	655	100.00	100.00	99.85	100.00	99.85	100.00
110	735	99.86	100.00	99.86	100.00	99.73	100.00
111	690	99.71	100.00	99.71	100.00	99.57	100.00
112	707	100.00	100.00	100.00	100.00	100.00	100.00
113	665	99.85	99.85	100.00	100.00	99.40	99.10
114	631	100.00	100.00	100.00	100.00	100.00	100.00
115	648	100.00	100.00	100.00	100.00	100.00	100.00
116	169	99.41	100.00	99.41	100.00	99.41	100.00
117	868	100.00	100.00	100.00	100.00	100.00	100.00
118	551	100.00	100.00	99.82	100.00	99.82	100.00
119	741	100.00	100.00	99.87	100.00	100.00	100.00
120	722	100.00	100.00	100.00	100.00	100.00	100.00
121	883	100.00	100.00	100.00	100.00	100.00	100.00
122	631	99.84	100.00	100.00	100.00	99.84	99.84
123	734	100.00	100.00	100.00	100.00	100.00	100.00
124	787	99.87	99.87	100.00	99.87	99.87	99.75

125	721	100.00	100.00	100.00	100.00	100.00	100.00
126	635	100.00	100.00	100.00	100.00	99.84	100.00
127	738	99.59	99.73	99.73	99.86	99.86	100.00
128	800	100.00	100.00	99.88	100.00	99.88	100.00
129	685	100.00	100.00	100.00	100.00	100.00	100.00
130	838	100.00	100.00	100.00	100.00	99.88	100.00
131	693	99.86	99.86	99.71	99.86	99.86	97.88
132	869	99.88	100.00	99.88	100.00	99.88	100.00
133	792	99.62	99.50	99.87	99.37	99.75	99.37
134	757	100.00	100.00	100.00	100.00	100.00	100.00
135	661	100.00	100.00	100.00	100.00	100.00	100.00
136	695	100.00	100.00	100.00	100.00	100.00	100.00
137	728	100.00	100.00	99.86	100.00	99.86	100.00
138	740	99.86	100.00	99.86	100.00	99.86	100.00
139	601	99.83	100.00	99.83	100.00	99.67	100.00
140	715	99.86	100.00	100.00	100.00	99.86	100.00
141	702	100.00	100.00	100.00	100.00	100.00	100.00
142	600	100.00	100.00	99.83	100.00	99.83	100.00
143	920	100.00	100.00	100.00	100.00	100.00	100.00
144	527	99.81	100.00	100.00	100.00	99.62	100.00
145	708	100.00	100.00	100.00	100.00	100.00	100.00
146	794	100.00	100.00	99.87	100.00	100.00	100.00
147	872	100.00	100.00	99.89	100.00	100.00	100.00
148	728	100.00	100.00	100.00	100.00	100.00	100.00
149	727	100.00	100.00	100.00	100.00	100.00	100.00
150	811	100.00	100.00	100.00	100.00	100.00	100.00
151	806	99.88	100.00	99.88	100.00	99.88	100.00
152	595	100.00	100.00	100.00	100.00	100.00	100.00
153	566	99.82	100.00	99.82	100.00	99.82	100.00
154	920	100.00	100.00	100.00	100.00	99.78	99.78
155	745	100.00	100.00	100.00	100.00	100.00	100.00
156	882	100.00	100.00	100.00	100.00	100.00	100.00
157	717	100.00	100.00	100.00	100.00	100.00	100.00
158	838	99.88	100.00	100.00	100.00	99.88	100.00

159	710	100.00	100.00	99.86	100.00	99.86	100.00
160	659	99.85	100.00	100.00	100.00	99.70	100.00
161	670	99.70	99.70	100.00	100.00	99.70	99.70
162	690	100.00	100.00	99.86	100.00	99.86	100.00
163	884	100.00	100.00	99.89	100.00	99.89	100.00
164	872	100.00	100.00	100.00	100.00	100.00	100.00
165	646	99.85	100.00	100.00	100.00	99.85	100.00
166	684	100.00	100.00	100.00	100.00	100.00	100.00
167	736	100.00	100.00	99.86	100.00	100.00	100.00
168	860	100.00	100.00	100.00	100.00	99.88	100.00
169	785	100.00	100.00	100.00	100.00	100.00	100.00
170	738	100.00	100.00	99.86	100.00	99.86	100.00
171	665	100.00	100.00	100.00	100.00	100.00	100.00
172	880	99.43	99.66	99.66	99.89	99.66	99.66
173	728	99.86	100.00	99.86	100.00	99.86	100.00
174	805	100.00	100.00	100.00	100.00	99.88	100.00
175	723	100.00	100.00	99.86	100.00	99.72	100.00
176	688	100.00	100.00	100.00	100.00	100.00	100.00
177	689	99.71	100.00	99.71	100.00	99.71	100.00
178	774	100.00	100.00	100.00	100.00	100.00	100.00
179	861	100.00	100.00	100.00	100.00	99.88	100.00
180	884	99.89	100.00	100.00	100.00	100.00	99.89
181	655	100.00	100.00	100.00	100.00	100.00	100.00
182	791	100.00	100.00	100.00	100.00	100.00	100.00
183	697	100.00	100.00	100.00	100.00	100.00	100.00
184	602	100.00	100.00	100.00	100.00	99.83	100.00
185	729	100.00	100.00	100.00	100.00	99.86	100.00
186	726	100.00	100.00	100.00	100.00	100.00	100.00
187	592	100.00	100.00	100.00	100.00	100.00	100.00
188	841	99.64	99.64	99.64	99.64	99.64	99.76
189	721	99.72	99.72	99.86	99.86	99.86	99.72
190	698	100.00	100.00	99.86	100.00	99.86	100.00
191	460	100.00	100.00	99.78	100.00	100.00	100.00
192	721	100.00	100.00	99.86	100.00	99.86	100.00

193	597	100.00	100.00	100.00	100.00	100.00	100.00
194	841	100.00	100.00	99.88	100.00	99.88	100.00
195	717	99.86	100.00	99.86	100.00	99.72	100.00
196	527	99.81	100.00	100.00	100.00	99.62	100.00
197	681	99.71	100.00	99.85	100.00	99.71	100.00
198	699	100.00	100.00	100.00	100.00	100.00	100.00
199	666	100.00	100.00	100.00	100.00	100.00	100.00
1003	957	99.69	100.00	100.00	100.00	99.90	100.00
1009	1330	99.92	99.92	99.92	99.92	99.92	99.92
1016	806	100.00	100.00	100.00	100.00	100.00	100.00
1019	254	68.90	77.78	100.00	81.94	99.61	93.36
1020	600	100.00	99.83	100.00	100.00	100.00	99.83
1022	873	99.77	100.00	99.77	100.00	100.00	100.00
1023	635	100.00	100.00	100.00	100.00	99.84	100.00
1028	572	81.99	56.92	83.22	58.77	80.24	55.64
1032	799	97.00	97.00	97.50	97.50	99.87	99.87
1033	744	0.00	0.00	0.00	0.00	0.00	0.00
1036	1139	100.00	100.00	99.39	100.00	99.82	100.00
1043	857	100.00	100.00	100.00	100.00	99.88	100.00
1069	738	100.00	100.00	99.86	100.00	100.00	100.00
1071	604	96.19	99.15	97.85	99.16	96.19	99.15
1073	602	100.00	100.00	100.00	100.00	99.83	100.00
1077	997	99.50	99.90	99.50	99.90	99.50	99.90
1169	1013	99.41	97.48	99.90	97.50	99.41	97.48
1195	819	3.66	4.52	53.48	52.77	35.16	34.99
1242	844	44.67	44.46	74.17	78.64	44.67	44.46
1284	649	99.69	99.85	99.69	99.85	99.69	99.85
1354	894	95.30	89.12	90.49	94.62	95.30	88.38
1376	1580	91.01	99.38	97.72	99.61	91.90	99.32
1388	1002	96.21	99.90	96.21	99.90	96.11	99.90
1447	583	71.53	78.38	95.88	75.13	90.05	90.05
1456	967	99.79	99.69	99.79	99.69	99.90	99.79
1485	942	91.51	98.97	88.00	98.81	97.98	98.40
1503	751	99.87	99.87	100.00	100.00	99.20	99.87

1522	746	33.38	25.94	32.84	25.31	33.51	25.43
1565	715	99.16	99.16	99.30	99.16	98.60	96.84
1584	1208	99.92	99.92	99.09	99.17	99.34	99.26
1683	653	70.90	71.22	96.94	97.38	70.60	69.85
1686	786	95.42	99.21	96.06	99.34	95.42	99.21
1715	1130	99.56	100.00	99.56	100.00	99.56	100.00
1742	1000	99.70	100.00	99.80	100.00	99.60	99.80
1774	1139	91.04	98.11	89.99	96.70	93.94	90.30
1804	520	90.38	88.35	95.58	93.42	90.38	88.35
1807	766	83.29	82.86	83.81	83.05	83.29	82.86
1821	1111	99.01	99.46	99.19	99.55	99.73	99.73
1858	783	85.19	87.53	82.38	87.52	82.63	88.15
1866	764	96.07	99.73	96.07	99.73	98.17	99.34
1900	986	99.09	99.39	99.29	99.80	99.80	99.29
1906	643	77.29	36.95	78.85	37.67	77.92	36.95
1954	748	96.39	99.86	99.87	98.94	96.26	99.86
1993	724	98.90	99.31	99.72	99.45	98.90	99.31
1998	1222	97.55	98.92	98.28	99.75	98.28	99.75
2041	16	93.75	100.00	100.00	94.12	93.75	100.00
2063	639	62.44	64.04	84.51	88.24	86.85	88.94
2132	864	98.15	98.83	98.61	98.61	97.92	97.80
2164	1068	94.66	93.78	95.60	94.36	99.34	91.70
2174	883	72.71	93.31	73.95	90.07	72.71	93.31
2201	1130	85.22	95.73	83.01	95.62	87.26	94.26
2203	682	98.83	87.53	98.39	86.47	97.36	87.60
2209	677	99.70	99.56	99.70	99.70	99.70	99.41
2247	914	90.81	98.22	90.92	98.46	98.03	97.71
2277	942	93.95	93.85	100.00	99.05	94.16	92.40
2279	147	100.00	98.66	100.00	98.66	100.00	98.66
2283	784	40.69	36.50	40.94	36.85	40.94	36.77
2296	732	100.00	100.00	100.00	100.00	99.73	99.46
2327	546	96.52	93.77	96.52	92.62	98.17	93.22
2370	449	99.78	99.12	99.78	99.12	99.78	99.12
2384	1636	99.88	99.94	99.88	100.00	99.88	99.94

2397	940	99.79	98.74	99.79	98.84	99.47	95.41
2469	962	99.79	99.17	99.79	99.17	99.90	49.97
2527	701	99.71	99.86	100.00	100.00	99.71	99.86
2552	1004	99.40	99.20	99.10	98.81	99.10	98.91
2556	990	99.49	99.49	99.60	99.50	99.49	99.49
2602	573	91.45	89.73	92.32	90.74	91.10	89.54
2639	963	99.79	99.17	99.79	99.17	99.90	50.00
2664	1126	99.56	98.33	99.56	98.33	99.56	98.33
2714	864	91.32	98.50	90.28	98.48	96.41	98.23
2728	104	99.04	89.57	99.04	89.57	99.04	100.00
2732	1010	99.31	99.70	99.80	99.70	99.80	99.70
2733	522	78.74	73.52	78.16	74.32	80.08	73.72
2798	833	99.52	99.52	99.88	99.40	99.52	99.52
2800	752	74.47	74.17	74.47	72.45	75.00	71.76
2812	980	90.92	80.05	88.37	85.40	99.80	52.75
2839	1611	96.15	99.74	95.84	99.94	97.64	99.68
2850	561	98.22	93.71	98.22	91.83	99.11	91.00
2879	620	96.61	87.57	96.45	83.99	95.48	85.92
2885	930	90.43	98.71	87.96	98.44	96.24	98.68
2886	149	99.33	100.00	99.33	100.00	98.66	100.00
2907	722	97.37	99.72	97.23	99.72	97.37	99.72
2923	1084	98.43	100.00	98.25	100.00	98.43	100.00
2970	940	98.09	99.78	99.04	99.79	98.62	99.68
3188	822	99.88	99.64	100.00	100.00	100.00	100.00
3266	982	95.52	98.84	96.03	98.85	99.39	99.29
41024	86	96.51	100.00	97.67	100.00	96.51	100.00
41025	622	99.36	99.52	99.36	99.68	99.36	99.52
41081	729	99.45	98.37	99.45	99.32	99.86	98.64
41164	631	97.78	97.01	96.51	97.13	97.15	95.63
41173	982	97.45	97.95	98.68	98.68	92.57	78.77
41180	680	37.35	37.35	78.24	78.24	37.21	37.21
41566	168	74.40	52.97	79.76	51.15	77.98	53.91
41778	87	85.06	72.55	88.51	63.11	86.21	66.96
41951	254	100.00	99.61	100.00	100.00	100.00	99.61

42228	866	95.50	98.22	97.58	99.18	96.65	99.05
42511	173	17.34	16.04	19.08	14.29	19.08	15.94
42878	929	99.78	100.00	99.78	100.00	99.78	100.00
42961	614	97.56	100.00	97.39	100.00	98.86	99.35
43247	748	94.39	99.02	93.85	99.72	97.99	99.73
Total	151031						
Average		94.76	94.62	96.04	95.48	95.56	94.17
Gross		95.28	95.04	96.35	95.83	96.01	93.36
Gross F1 Score (%)		95.16		96.09		94.66	
Overall Score (%)		94.93		95.93		94.78	

Table A.9: Heart beat detection performance of majority voting fusion method with different combinations of QRS detectors on MIT-BIH Polysomnographic database

Signal No.	Total number of beats	Voting Fusion (gqrs/SSF-TKE)		Voting Fusion (epltd/SSF-TKE)		Voting Fusion (gqrs/epltd)	
		Sensitivity (%)	Predictivity (%)	Sensitivity (%)	Predictivity (%)	Sensitivity (%)	Predictivity (%)
slp 01a	7806	100.00	99.99	99.99	100.00	99.99	99.99
slp 01b	11467	99.91	99.92	99.50	99.95	99.49	99.92
slp 02a	16145	99.61	99.87	99.93	99.94	99.88	99.81
slp02b	11317	99.45	99.64	99.86	99.92	99.87	99.78
slp 03	24917	99.97	97.76	99.98	97.06	99.99	96.87
slp 04	27029	99.77	99.85	99.91	99.93	99.94	99.93
slp 14	22920	99.77	99.74	99.87	99.89	99.91	99.82

slp 16	27604	99.65	99.83	99.96	99.94	99.98	99.92
slp 32	21718	99.85	99.88	99.96	99.99	99.94	99.95
slp 37	30611	100.00	100.00	100.00	99.99	99.99	99.99
slp 41	25884	99.95	99.86	99.95	99.96	99.97	99.97
slp 45	27686	99.94	99.96	99.98	99.96	99.95	99.94
slp 48	24711	99.96	99.94	99.99	100.00	99.97	99.98
slp 59	16901	99.96	99.99	100.00	99.99	100.00	100.00
slp 60	25017	99.37	99.96	100.00	99.88	99.97	99.94
slp 61	25482	99.75	99.80	99.83	99.84	100.00	99.98
slp 66	15775	99.96	99.99	100.00	99.99	99.99	100.00
slp 67x	5374	100.00	100.00	100.00	100.00	100.00	100.00
Total	368364						
Average		99.83	99.78	99.93	99.79	99.93	99.77
Gross		99.82	99.74	99.94	99.75	99.95	99.72
Gross F1 Score (%)		99.78		99.84		99.84	
Overall Score (%)		99.79		99.85		99.84	

Table A.10: Heart beat detection performance of majority voting fusion method with different combinations of QRS detectors on MGH/MF Waveform database

Signal No.	Total number of beats	Voting fusion (gqrs/SSF-TKE)		Voting fusion (gqrs/epltd)		Voting fusion (epltd/SSF-TKE)	
		Sensitivity (%)	Predictivity (%)	Sensitivity (%)	Predictivity (%)	Sensitivity (%)	Predictivity (%)
1	2628	96.23	99.37	97.30	99.38	93.91	97.98
2	6652	98.20	99.32	98.38	99.73	98.41	99.32
3	7042	97.71	99.93	97.71	99.94	97.69	99.93
4	3317	97.86	95.75	98.07	98.04	97.26	94.19
5	8284	99.13	99.87	99.14	99.95	98.93	99.98
6	7600	99.26	99.63	99.26	99.91	98.86	95.83
7	5598	98.77	99.89	98.71	99.89	98.70	99.86
8	5006	98.56	99.82	98.48	99.64	94.39	98.13
9	9374	99.08	99.72	99.15	99.82	99.00	99.60
10	9511	98.91	99.96	99.22	99.88	98.48	99.68
11	6663	97.63	98.55	97.82	99.80	96.02	96.85
12	6326	96.46	99.71	98.23	99.68	93.16	97.32
13	6663	99.56	99.36	99.52	99.31	99.31	99.25
14	7741	99.50	99.44	99.60	99.63	98.59	97.14
15	6714	98.59	99.35	98.44	98.80	71.86	96.17
16	3906	99.13	99.87	99.13	99.79	93.86	99.08
17	8170	99.40	99.83	99.39	99.98	62.97	51.15
18	7267	97.52	99.58	97.81	99.75	91.23	97.40
19	5730	95.46	99.51	95.46	99.91	95.45	99.36
20	6492	94.49	98.68	99.49	99.28	92.41	91.10
21	5041	98.29	99.74	98.67	99.88	98.43	99.68
22	6762	97.57	98.60	96.97	99.57	88.11	98.30
23	7165	98.72	98.51	98.91	99.80	96.82	99.61
24	7390	99.27	99.55	99.28	99.92	99.20	99.57
25	4160	92.55	98.52	93.05	99.28	94.09	88.47

26	7984	46.56	46.80	46.53	46.77	46.67	47.37
27	5474	96.49	98.99	99.14	99.40	95.78	98.55
28	5094	92.70	92.43	93.78	95.83	91.77	90.95
29	7894	99.40	99.48	99.42	99.85	95.83	99.34
30	7098	97.58	99.80	98.00	99.64	96.17	99.71
31	7369	94.86	96.83	95.70	97.48	93.50	92.97
32	6812	97.77	99.51	97.78	99.43	77.89	95.35
33	8872	99.33	99.51	99.35	99.95	99.12	99.83
34	5061	99.15	99.96	99.15	99.86	97.85	97.85
35	4110	99.54	100.00	99.54	100.00	99.54	99.98
36	5873	99.35	99.37	99.39	99.95	91.79	99.37
37	5657	97.37	98.87	97.60	98.82	97.68	98.84
38	4697	98.89	99.66	98.87	99.81	71.34	96.77
39	5798	99.55	99.86	99.57	99.98	98.09	94.45
40	3947	96.45	62.72	96.38	62.70	96.63	59.48
41	503	91.05	23.51	91.05	22.32	92.05	19.31
42	4585	79.19	96.21	72.91	99.46	71.15	91.50
43	7692	96.44	96.13	97.93	97.07	97.57	96.89
44	5371	81.70	94.67	85.50	95.79	96.15	98.59
45	10340	93.87	99.48	96.41	99.61	81.19	99.85
46	5876	90.37	98.96	95.68	99.07	88.05	96.80
47	11378	97.21	96.98	97.81	98.33	95.80	99.39
48	2928	95.49	97.83	95.56	96.58	95.63	97.56
49	9242	97.72	99.66	98.43	99.38	91.81	98.84
50	11130	74.11	97.16	76.89	99.25	88.62	99.81
51	5355	92.32	94.66	91.02	95.64	95.01	97.19
52	6455	99.60	99.06	99.64	99.08	86.32	55.69
53	5859	99.11	99.93	99.15	99.93	99.03	99.88
54	6718	99.58	99.96	99.58	99.96	99.58	99.96
55	5693	99.58	98.57	77.45	77.77	59.76	58.97
56	5116	99.30	99.47	99.34	99.49	99.65	98.95
57	5811	74.86	74.44	75.32	38.87	74.38	43.73
58	4027	99.45	99.85	99.50	99.83	99.58	99.98
59	6828	99.63	99.90	99.65	99.97	86.32	95.20

60	2793	99.79	99.96	99.79	99.96	99.82	90.52
61	6842	32.96	51.74	32.96	51.74	59.28	70.43
62	5036	99.70	99.07	99.70	99.88	99.62	99.07
63	6661	99.31	99.94	99.35	99.92	76.46	56.70
64	7629	99.41	99.28	99.42	98.76	99.08	98.44
65	7019	98.56	99.84	98.56	99.84	82.21	97.66
66	2423	97.69	91.07	97.73	93.93	87.91	86.44
67	6571	99.24	98.05	99.10	97.95	98.39	97.81
68	4750	98.57	99.49	98.86	99.77	96.67	96.84
69	8173	97.74	99.63	98.12	99.98	94.10	99.41
70	9809	98.04	99.95	98.57	99.94	91.98	99.61
71	5717	98.44	98.96	98.34	98.13	98.99	98.67
72	6552	87.79	87.92	99.25	99.09	92.19	69.47
73	11641	99.17	98.56	99.66	99.96	97.59	96.11
74	6653	49.92	50.27	50.64	48.96	50.53	51.92
75	1762	90.35	96.48	99.49	99.66	64.25	73.36
76	9663	97.86	97.16	97.88	97.21	92.01	93.17
77	7173	99.57	99.87	99.64	99.87	99.68	99.99
78	7914	99.43	99.97	99.44	99.90	90.06	98.41
79	5031	99.54	99.60	99.54	99.98	99.52	99.54
80	4326	99.21	99.95	99.19	99.74	99.19	99.93
81	7467	81.85	97.36	81.85	97.36	81.85	97.36
82	7332	99.58	100.00	99.58	100.00	98.68	100.00
83	5683	99.28	99.98	99.26	99.96	99.28	99.98
84	3923	98.22	85.39	98.24	85.53	99.01	85.91
85	9790	99.43	99.94	99.54	99.93	99.47	99.92
86	9811	96.94	99.94	97.32	99.92	79.67	81.78
87	4383	99.11	96.83	99.11	100.00	98.88	96.78
88	5982	99.40	99.73	99.40	99.92	99.31	99.68
89	8154	99.58	99.88	99.58	99.88	83.92	98.36
90	4197	93.26	98.61	93.30	98.47	76.24	94.28
91	5739	99.58	99.95	99.58	99.90	84.28	98.33
92	6427	99.24	99.69	99.25	99.36	97.03	91.73
93	7131	99.06	99.99	99.40	99.96	98.89	99.96

94	5734	99.46	99.93	99.51	99.89	96.42	99.71
95	8405	99.12	94.89	99.26	94.39	98.47	96.49
96	4817	98.92	99.83	98.88	99.83	98.86	99.81
97	6934	99.42	99.94	99.34	99.88	82.97	99.22
98	6341	96.12	98.98	96.23	98.91	81.25	98.68
99	7915	99.42	99.99	99.42	99.91	99.33	99.89
100	4222	99.50	99.83	99.50	99.83	99.31	99.79
101	4711	96.20	98.78	96.75	99.85	82.70	99.21
102	4212	90.98	97.11	90.88	99.71	91.00	96.87
103	6358	95.91	97.65	96.85	98.69	95.19	97.60
104	6544	97.85	99.75	97.57	99.87	74.39	97.71
105	7777	94.02	99.40	97.18	97.88	77.88	97.21
106	6797	97.68	99.91	98.31	99.58	94.79	96.58
107	4512	98.69	99.82	98.71	99.73	98.76	99.80
108	8364	99.57	99.82	99.57	99.94	99.59	99.82
109	8841	99.56	96.13	99.68	98.99	99.46	97.83
110	6057	98.73	99.77	98.88	99.85	82.07	98.71
111	6782	99.01	99.66	99.01	99.60	71.68	85.58
112	6536	98.59	99.34	98.97	99.92	92.84	98.43
113	6851	99.34	99.99	99.33	99.90	99.10	99.57
114	7384	99.01	99.96	99.01	99.88	98.63	99.51
115	8166	99.35	99.96	99.38	99.95	90.11	99.50
116	5189	83.14	92.04	83.10	93.29	83.20	92.09
117	8229	86.81	99.76	99.03	99.67	97.07	97.55
118	9544	99.74	99.57	99.74	99.72	99.16	98.32
119	5742	99.67	99.84	99.67	99.84	99.39	98.72
120	5613	98.29	99.14	99.16	99.71	97.59	98.58
121	8481	99.49	99.45	99.53	99.42	92.81	98.88
122	660	60.61	15.88	73.64	17.23	67.42	20.67
123	6257	97.92	98.60	98.00	98.76	88.22	77.45
124	9359	90.55	99.84	98.20	99.69	91.07	98.58
125	9262	93.86	99.87	99.51	99.79	77.48	99.13
126	4302	96.51	96.85	96.61	97.58	96.37	95.11
127	4072	81.11	95.30	81.11	93.12	85.14	91.60

128	8583	97.68	99.82	97.59	99.75	93.25	98.78
129	11053	85.19	99.59	98.84	99.66	84.25	99.08
130	4013	56.34	54.96	55.97	56.39	70.27	68.80
131	5976	98.76	99.86	98.78	99.90	92.52	99.28
132	7937	95.26	99.95	99.21	99.87	94.71	99.68
133	4390	99.93	88.63	99.77	99.73	83.44	91.83
134	6441	99.25	99.98	99.35	99.92	99.36	99.97
135	4777	97.07	99.81	99.00	99.85	97.22	99.85
136	7358	99.51	99.92	99.51	99.92	78.57	98.25
137	6480	98.07	99.48	99.10	99.61	62.85	97.56
138	3933	99.21	99.31	99.19	99.85	99.11	99.21
139	7823	95.33	99.22	98.24	99.34	95.23	99.10
140	7955	99.30	99.75	99.35	99.75	98.92	99.42
141	6432	89.96	99.09	91.00	99.12	87.78	98.35
142	7639	99.28	99.89	99.27	99.84	98.86	99.60
143	5334	95.18	97.94	95.16	97.71	92.61	96.47
144	4407	98.48	99.63	98.84	99.73	70.18	96.00
145	8751	99.45	99.93	99.27	99.79	98.32	98.91
146	6655	98.87	99.76	98.93	99.85	99.29	99.74
147	9399	95.05	99.96	99.32	99.74	91.24	99.10
148	8265	98.14	99.88	98.39	99.80	98.05	99.69
149	7120	99.21	99.73	99.20	99.76	98.68	99.20
150	7283	97.38	99.94	98.89	99.90	97.67	99.37
151	7247	97.70	99.97	97.71	99.97	98.01	98.64
152	4261	99.34	96.64	99.30	99.11	99.37	96.60
153	3592	82.24	96.07	82.24	96.13	98.78	97.63
154	6053	99.06	99.98	99.06	99.97	98.58	99.40
155	7330	98.20	99.70	98.32	99.67	98.92	99.92
156	6192	99.05	99.95	99.03	99.84	99.05	99.22
157	9102	99.19	99.76	99.36	99.94	99.03	99.79
158	9557	99.37	99.27	99.37	99.29	98.92	99.38
159	7872	95.48	88.15	95.48	88.15	99.28	88.75
160	6430	98.41	99.33	98.41	99.98	99.10	99.18
161	6516	97.34	99.06	97.18	99.86	98.50	98.63

162	5461	99.23	98.96	99.23	99.60	99.14	98.44
163	4962	96.27	98.17	94.60	99.75	95.71	97.88
164	5880	99.10	100.00	99.08	99.91	98.20	99.62
165	6583	98.97	99.97	98.94	99.82	98.85	99.92
166	9322	99.52	99.88	99.53	99.96	99.53	99.88
167	4891	99.67	95.63	99.65	97.66	99.69	95.72
168	6360	99.80	99.30	99.78	99.87	99.73	99.03
169	7780	99.37	99.83	99.38	99.82	99.07	99.52
170	894	99.89	100.00	99.78	100.00	99.89	100.00
171	7710	90.73	90.83	90.77	90.85	94.28	94.22
172	3681	99.10	99.00	99.10	99.00	97.31	99.11
173	9819	99.30	99.94	98.85	99.22	66.68	66.89
174	9277	99.16	99.80	99.11	99.73	99.04	96.96
175	7384	99.36	99.88	99.40	99.95	96.93	99.10
176	3871	97.88	96.05	97.91	99.79	89.77	93.01
177	5842	99.20	98.39	99.20	99.95	98.94	98.25
178	5219	98.79	99.40	98.79	99.88	98.14	97.15
179	4290	96.76	96.69	96.64	99.50	86.90	94.48
180	6934	98.38	99.10	98.44	99.56	98.21	99.40
181	6633	98.94	99.51	98.94	99.48	91.65	95.97
182	6960	98.53	98.96	99.20	98.21	98.58	96.80
183	5133	100.00	99.00	99.98	99.04	100.00	98.98
184	6273	99.84	99.89	99.89	99.86	99.16	98.00
185	5326	99.87	98.70	99.92	99.37	99.27	98.14
186	7708	92.85	98.94	95.04	99.35	91.61	98.88
187	7566	99.37	99.84	99.50	99.93	99.33	99.81
188	6501	98.14	99.07	98.34	98.70	96.65	97.25
189	10885	98.02	99.92	99.72	99.93	91.70	98.68
190	6904	97.58	97.78	98.09	96.66	93.13	97.75
191	7314	98.92	96.71	99.70	96.84	98.74	79.04
192	7280	99.35	99.48	99.35	99.57	99.44	99.49
193	7539	91.86	98.84	91.84	99.30	99.92	98.59
194	4632	98.58	91.78	98.64	96.84	98.53	81.50
195	6131	99.09	99.57	99.17	99.56	99.07	99.59

196	6693	99.91	99.97	99.96	99.79	99.85	99.93
197	7679	99.86	99.26	99.90	99.20	99.91	99.19
198	9747	99.72	99.76	99.72	99.82	99.83	99.68
199	3917	99.00	99.90	99.03	99.85	98.98	99.85
200	5668	99.40	99.79	99.47	99.75	99.61	99.88
201	5623	99.00	98.88	98.86	99.93	99.11	98.85
202	4152	99.06	99.95	99.04	99.76	97.78	99.95
203	6136	97.96	99.68	98.01	99.83	99.09	99.77
204	6060	89.83	99.54	90.53	99.84	13.86	49.12
205	2816	91.80	89.88	93.29	99.77	14.60	30.49
206	999	98.50	90.03	98.50	98.11	97.90	87.01
207	4710	66.28	74.02	66.45	73.35	95.33	86.00
208	2956	97.43	99.31	98.14	99.49	98.21	98.78
209	1949	97.23	94.66	97.59	93.01	58.65	58.20
210	6460	91.15	93.15	91.16	98.02	90.43	94.95
211	2766	97.90	85.43	98.84	89.96	97.69	93.40
212	9806	79.99	92.09	85.80	93.03	88.10	99.47
213	7187	90.87	97.16	95.91	98.97	92.00	97.28
214	4325	97.94	89.52	98.17	95.59	98.94	89.74
215	7067	82.81	90.57	85.06	92.75	95.78	95.82
216	3723	88.61	96.12	92.18	98.73	90.46	62.73
217	6738	79.56	87.74	77.68	96.11	92.05	99.41
218	4606	95.57	96.05	96.44	96.29	37.00	66.07
219	6781	91.49	99.22	92.83	95.39	88.81	99.55
220	6348	52.49	86.66	77.85	89.81	68.21	86.74
221	4858	44.42	95.36	51.71	94.22	78.24	81.72
222	7898	88.53	97.14	89.11	88.00	56.77	61.22
223	5182	91.91	97.26	97.72	97.25	99.15	99.92
224	4171	97.96	98.84	98.87	99.11	98.11	99.27
225	2441	95.58	88.71	96.03	88.96	95.45	97.20
226	7520	99.52	99.44	99.52	100.00	98.32	99.50
227	9384	99.39	99.82	99.42	99.90	96.24	99.79
228	3942	98.35	77.05	98.55	76.00	93.66	73.04
229	3620	96.57	57.59	96.57	57.62	96.52	54.45

230	0						
231	3969	96.62	96.99	98.39	95.31	98.56	94.33
232	3999	99.52	97.60	99.75	97.67	99.10	95.96
233	3717	84.50	52.99	84.37	49.06	87.06	38.14
234	5227	95.89	92.51	97.17	92.65	97.17	91.23
235	0						
236	5969	94.49	98.31	97.79	98.90	95.43	98.72
237	5989	94.17	98.26	94.07	97.93	79.21	85.65
238	5332	96.14	84.35	96.34	82.17	97.34	75.95
239	4782	96.01	65.73	95.80	65.62	95.90	65.47
240	5523	95.18	73.14	95.51	72.32	95.71	70.56
241	5119	29.89	28.30	29.73	29.56	31.82	28.73
242	5806	82.33	77.31	83.33	74.63	85.29	56.93
243	6435	74.89	71.74	82.08	78.45	98.06	93.73
244	3856	74.77	99.38	75.60	98.91	86.41	93.41
245	4865	92.39	97.57	92.62	98.34	98.71	96.97
246	1784	96.86	93.56	96.75	94.16	98.93	93.49
247	6435	90.13	93.94	90.33	93.08	93.50	96.58
248	5609	99.70	99.40	99.66	99.10	99.68	99.34
249	5749	99.95	99.65	99.95	99.91	99.93	99.67
250	2103	99.90	99.95	99.90	99.95	99.90	99.95
Total	1542273						
Average		94.61	95.22	95.35	95.47	91.31	92.22
Gross		94.87	95.99	95.68	95.89	91.60	92.65
Gross F1 Score (%)		95.42		95.78		92.12	
Overall Score (%)		95.17		95.60		91.94	

Table A.11: Heart beat detection performance of majority voting fusion method with different combinations of QRS detectors on MIT-BIH noise stress database

Signal No.	Total number of beats	Voting fusion (gqrs/SSF-TKE)		Voting fusion (gqrs/epltd)		Voting fusion (epltd/SSF-TKE)	
		Sensitivity (%)	Predictivity (%)	Sensitivity (%)	Predictivity (%)	Sensitivity (%)	Predictivity (%)
118 e24	2301	99.00	99.61	99.00	99.96	99.00	99.65
118 e18	2301	99.00	99.61	99.00	99.91	99.00	99.65
118 e12	2301	99.00	99.48	99.00	99.61	98.96	99.13
118 e06	2301	98.96	98.57	98.48	89.42	98.91	98.87
118 e00	2301	96.35	90.86	97.04	67.98	96.31	96.22
118 e-06	2301	90.57	78.32	95.87	58.67	87.22	87.72
119 e24	2094	94.51	98.07	94.84	100	94.51	98.36
119 e18	2094	94.46	98.02	94.84	99.8	94.46	98.12
119 e12	2094	94.32	97.58	94.79	95.62	94.32	95.09
119 e06	2094	90.11	92.05	94.41	87.36	90.26	89.15
119 e00	2094	85.96	84.43	92.55	72.07	85.34	84.49
119 e-06	2094	82.23	72.69	91.26	59.24	78.75	78.98
Total	26370						
Average		93.71	92.44	95.92	85.80	93.09	93.79
Gross		93.87	92.07	96.03	82.60	93.25	93.89
Gross F1 Score (%)		92.96		88.81		93.57	
Overall Score (%)		93.02		90.09		93.50	

Table A.12: Heart beat detection performance of majority voting fusion method with different combinations of QRS detectors on MIT-BIH Arrhtyhmia database

Signal No.	Total number of beats	Voting fusion (gqrs/SSF-TKE)		Voting fusion (gqrs/epltd)		Voting fusion (epltd/SSF-TKE)	
		Sensitivity (%)	Predictivity (%)	Sensitivity (%)	Predictivity (%)	Sensitivity (%)	Predictivity (%)
100	2273	100	100	100	100	100	100
101	1865	99.95	99.89	99.09	99.78	99.95	99.79
102	2187	100	100	100	100	100	100
103	2084	99.95	100	99.86	99.43	100	100
104	2229	99.87	99.73	99.87	99.60	99.91	99.73
105	2572	99.92	99.3	98.83	97.73	98.52	98.56
106	2027	95.12	96.79	99.65	98.25	93.73	96.50
107	2137	97.94	99.9	99.72	100	99.91	99.95
108	1763	97.45	97.56	99.49	97.88	99.38	98.82
109	2532	99.64	99.76	100	99.96	99.84	99.84
111	2124	99.95	99.91	99.95	99.95	100	100
112	2539	100	100	99.92	100	100	100
113	1795	100	100	100	100	100	100
114	1879	99.79	99.15	99.31	99.89	99.73	99.10
115	1953	100	100	100	99.95	100	100
116	2412	99.79	100	99.79	100	99.92	99.96
117	1535	100	100	100	100	100	100
118	2278	99.96	99.65	100	100	100	99.65
119	1987	99.95	99.8	99.95	100	99.6	98.65
121	1863	99.95	99.9	100	100	100	100
122	2476	100	100	100	100	100	100
123	1518	99.8	99.47	99.74	100	99.8	99.67
124	1619	99.94	99.75	99.94	100	99.63	99.57
200	2601	99.54	99.85	94.5	99.88	99.88	99.88
201	1963	95.67	96.31	97.66	100	95.72	96.26

202	2136	98.55	99.67	99.67	100	98.50	99.67
203	2980	82.95	98.37	98.89	97.07	78.62	94.94
205	2656	99.21	100	99.55	99.85	99.47	100
207	1860	99.14	98.14	99.89	100	99.30	98.14
208	2955	98.85	99.73	98.78	99.42	99.26	99.86
209	3005	99.33	100	99.47	99.1	98.47	99.40
210	2650	97.85	99.65	99.47	99.92	98.49	99.43
212	2748	100	100	99.82	99.75	100	100
213	3251	99.48	100	99.97	100	99.69	100
214	2262	99.56	99.65	99.56	99.65	99.91	99.96
215	3363	99.41	100	99.67	100	99.38	100
217	2208	98.37	99.82	98.41	99.86	99.95	99.95
219	2154	99.26	96.22	99.91	100	99.21	96.83
220	2048	99.07	100	99.95	100	99.12	100
221	2427	99.3	99.22	99.79	99.84	98.52	98.31
222	2483	91.1	99.96	99.80	99.60	91.06	99.69
223	2605	99.88	99.88	99.54	100	99.96	99.96
228	2053	99.46	98.98	100	99.81	99.51	99.03
230	2256	100	100	100	99.96	100	100
231	1571	99.94	99.56	100	100	99.94	99.56
232	1780	99.16	80.23	100	98.13	99.04	80.17
233	3079	98.64	99.9	99.55	99.9	98.67	100
234	2753	99.96	100	99.96	100	100	100
Total	109494						
Average		98.81	99.08	99.56	99.67	98.78	98.98
Gross		99.44	99.18	99.54	99.65	98.63	99.02
Gross F1 (%)		99.31		99.60		98.82	
Overall Sc. (%)		99.12		99.61		98.85	

Table A.13: Heart beat detection performance of majority voting fusion method on ECG 'bw' noise and different types of ABP noises of synthetic noise dataset

ABP noise	Noise in ECG & ABP (dB)	F1 Score (%)							Improvement in F1 score due to voting over gqrs/epltd (%)		
		gqrs	epltd	SSF-TKE	ABP	Voting			Voting		
						gq/ST*	ep/ST*	gq/ep*	gq/ST*	ep/ST*	gq/ep*
a_{smax}	0	99.86	100.0	100.0	75.00	99.73	99.86	99.86	-0.13	-0.14	-0.14
	-3	99.59	100.0	100.0	75.00	99.86	99.86	99.86	0.27	-0.14	-0.14
	-6	98.99	100.0	100.0	75.00	99.86	99.86	99.86	0.87	-0.14	-0.14
	-9	96.96	99.86	100.0	74.74	99.73	99.86	99.73	2.77	0.00	-0.13
	-12	93.27	99.59	100.0	74.49	99.73	99.86	99.73	6.46	0.27	0.14
a_{smin}	0	99.86	100.0	100.0	82.57	99.73	99.86	99.86	-0.13	-0.14	-0.14
	-3	99.59	100.0	100.0	82.35	99.86	99.86	99.86	0.27	-0.14	-0.14
	-6	98.99	100.0	100.0	82.29	99.86	99.86	99.86	0.87	-0.14	-0.14
	-9	96.96	99.86	100.0	81.61	99.73	99.86	99.73	2.77	0.00	-0.13
	-12	93.27	99.59	100.0	79.81	99.73	99.86	99.73	6.46	0.27	0.14
a_{lamean}	0	99.86	100.0	100.0	99.73	99.73	99.86	99.86	-0.13	-0.14	-0.14
	-3	99.59	100.0	100.0	99.59	99.86	99.86	99.86	0.27	-0.14	-0.14
	-6	98.99	100.0	100.0	99.46	99.86	99.86	99.86	0.87	-0.14	-0.14
	-9	96.96	99.86	100.0	75.00	99.73	99.86	99.73	2.77	0.00	-0.13
	-12	93.27	99.59	100.0	75.00	99.73	99.86	99.73	6.46	0.27	0.14
a_{sw}	0	99.86	100.0	100.0	74.33	99.73	99.86	99.86	-0.13	-0.14	-0.14
	-3	99.59	100.0	100.0	74.26	99.86	99.86	99.86	0.27	-0.14	-0.14
	-6	98.99	100.0	100.0	73.92	99.86	99.86	99.86	0.87	-0.14	-0.14
	-9	96.96	99.86	100.0	68.50	99.73	99.86	99.73	2.77	0.00	-0.13
	-12	93.27	99.59	100.0	65.97	99.73	99.86	99.73	6.46	0.27	0.14
a_{hf}	0	99.86	100.0	100.0	71.79	99.73	99.86	99.86	-0.13	-0.14	-0.14
	-3	99.59	100.0	100.0	71.44	99.86	99.86	99.86	0.27	-0.14	-0.14
	-6	98.99	100.0	100.0	70.90	99.73	99.86	99.73	0.74	-0.14	-0.27
	-9	96.96	99.86	100.0	70.75	99.73	99.86	98.99	2.77	0.00	-0.88
	-12	93.27	99.59	100.0	70.36	99.73	99.86	99.73	6.46	0.27	0.14

* Abbreviations:- a_{smax}: Exponential saturation to BP maxm. noise, a_{smin}: Exponential saturation to BP minm. noise, a_{lamean}: Linear saturation to BP mean noise, a_{sw}: Square wave noise, a_{hf}: High frequency noise, gq/ST: gqrs/SSF-TKE, ep/ST: epltd/SSF-TKE and gq/ep: gqrs/epltd.

Table A.14: Heart beat detection performance of majority voting fusion method on ECG 'em' noise and different types of ABP noises of synthetic noise dataset

ABP noise	Noise in ECG & ABP (dB)	F1 Score (%)							Improvement in F1 score due to voting over gqrs/epltd (%)		
		gqrs	epltd	SSF-TKE	ABP	Voting			Voting		
						gq/ST*	ep/ST*	gq/ep*	gq/ST*	ep/ST*	gq/ep*
a_{smax}	0	91.28	99.79	100.0	75.00	99.73	99.73	99.66	8.45	-0.06	-0.13
	-3	85.54	98.33	100.0	75.00	99.73	99.66	99.66	14.19	1.33	1.33
	-6	83.02	93.73	99.93	75.00	99.73	99.66	99.66	16.71	5.93	5.93
	-9	79.98	87.05	99.79	74.74	99.73	99.66	99.66	19.75	12.61	12.61
	-12	77.47	85.37	98.57	74.49	99.73	99.66	99.66	22.26	14.29	14.29
a_{smin}	0	91.28	99.79	100.0	82.57	99.73	99.73	99.66	8.45	-0.06	-0.13
	-3	85.54	98.33	100.0	82.35	99.73	99.66	99.66	14.19	1.33	1.33
	-6	83.02	93.73	99.93	82.29	99.73	99.66	99.66	16.71	5.93	5.93
	-9	79.98	87.05	99.79	81.61	99.73	99.66	99.66	19.75	12.61	12.61
	-12	77.47	85.37	98.57	79.81	99.73	99.66	99.66	22.26	14.29	14.29
a_{lamean}	0	91.28	99.79	100.0	99.73	99.73	99.73	99.73	8.45	-0.06	-0.06
	-3	85.54	98.33	100.0	99.59	99.73	99.73	99.73	14.19	1.40	1.40
	-6	83.02	93.73	99.93	99.46	99.73	99.73	99.73	16.71	6.00	6.00
	-9	79.98	87.05	99.79	75.00	99.73	99.73	99.73	19.75	12.68	12.68
	-12	77.47	85.37	98.57	75.00	99.73	99.73	99.73	22.26	14.36	14.36

a_{sw}	0	91.28	99.79	100.0	74.33	99.73	99.73	99.66	8.45	-0.06	-0.13
	-3	85.54	98.33	100.0	74.26	99.73	99.66	99.66	14.19	1.33	1.33
	-6	83.02	93.73	99.93	73.92	99.73	99.66	99.66	16.71	5.93	5.93
	-9	79.98	87.05	99.79	68.50	99.73	99.66	99.66	19.75	12.61	12.61
	-12	77.47	85.37	98.57	65.97	99.73	99.66	99.66	22.26	14.29	14.29
a_{hf}	0	91.28	99.79	100.0	71.79	99.73	99.73	98.92	8.45	-0.06	-0.88
	-3	85.54	98.33	100.0	71.44	99.73	98.85	98.85	14.19	0.52	0.52
	-6	83.02	93.73	99.93	70.75	99.73	98.19	98.19	16.71	4.46	4.46
	-9	79.98	87.05	99.79	70.90	98.85	98.79	98.79	18.87	11.73	11.73
	-12	77.47	85.37	98.57	70.36	99.73	99.66	99.66	22.26	14.29	14.29

* Abbreviations:- a_{smax}: Exponential saturation to BP maxm. noise, a_{smin}: Exponential saturation to BP minm. noise, a_{lamean}: Linear saturation to BP mean noise, a_{sw}: Square wave noise, a_{hf}: High frequency noise, gq/ST: gqrs/SSF-TKE, ep/ST: epltd/SSF-TKE and gq/ep: gqrs/epltd.

Table A.15: Heart beat detection performance of majority voting fusion method on ECG 'ma' noise and different types of ABP noises of synthetic noise dataset

ABP Noise	Noise in ECG & ABP (dB)	F1 Score (%)							Improvement in F1 score due to voting over gqrs/epltd (%)		
		gqrs	epltd	SSF-TKE	ABP	Voting			Voting		
						gqrs/SSF-TKE	epltd/SSF-TKE	gqrs/epltd	gqrs/SSF-TKE	epltd/SSF-TKE	gqrs/epltd
a_{smax}	0	88.14	97.73	99.79	75.00	99.73	99.73	99.73	11.59	2.00	2.00
	-3	84.89	93.81	99.79	75.00	99.73	99.73	99.66	14.84	5.92	5.85
	-6	81.11	91.71	98.71	75.00	99.73	99.66	99.66	18.62	7.95	7.95
	-9	78.80	88.17	96.54	74.74	99.73	99.66	99.66	20.93	11.49	11.49
	-12	76.57	85.60	89.51	74.49	99.73	99.66	99.66	23.16	14.06	14.06

a_{smin}	0	88.14	97.73	99.79	82.57	99.73	99.73	99.73	11.59	2.00	2.00
	-3	84.89	93.81	99.79	82.35	99.73	99.73	99.66	14.84	5.92	5.85
	-6	81.11	91.71	98.71	82.29	99.73	99.66	99.66	18.62	7.95	7.95
	-9	78.80	88.17	96.54	81.61	99.73	99.66	99.66	20.93	11.49	11.49
	-12	76.57	85.60	89.51	79.81	99.73	99.66	99.66	23.16	14.06	14.06
a_{lamean}	0	88.14	97.73	99.79	99.73	99.73	99.73	99.73	11.59	2.00	2.00
	-3	84.89	93.81	99.79	99.59	99.73	99.73	99.73	14.84	5.92	5.92
	-6	81.11	91.71	98.71	99.46	99.73	99.73	99.73	18.62	8.02	8.02
	-9	78.80	88.17	96.54	75.00	99.73	99.73	99.73	20.93	11.56	11.56
	-12	76.57	85.60	89.51	75.00	99.73	99.73	99.73	23.16	14.13	14.13
a_{sw}	0	88.14	97.73	99.79	74.33	99.73	99.73	99.73	11.59	2.00	2.00
	-3	84.89	93.81	99.79	74.26	99.73	99.73	99.66	14.84	5.92	5.85
	-6	81.11	91.71	98.71	73.92	99.73	99.66	99.66	18.62	7.95	7.95
	-9	78.80	88.17	96.54	68.50	99.73	99.66	99.66	20.93	11.49	11.49
	-12	76.57	85.60	89.51	65.97	99.73	99.66	99.66	23.16	14.06	14.06
a_{hf}	0	88.14	97.73	99.79	71.79	99.73	99.86	98.98	11.59	2.13	1.25
	-3	84.89	93.81	99.79	71.44	99.86	99.06	97.99	14.97	5.24	4.18
	-6	81.11	91.71	98.71	70.75	99.12	98.39	97.67	18.01	6.67	5.95
	-9	78.80	88.17	96.54	70.90	99.73	98.78	98.85	20.93	10.61	10.68
	-12	76.57	85.60	89.51	70.36	99.73	98.92	98.99	23.16	13.32	13.39

Table A.16: HR estimation performance of majority voting fusion method with gqrs/SSF-TKE combination on PhysioNet/CinC Challenge 2014 training dataset

Signal No.	Total number of beats	HR rMSE (bpm)					
		ECG (gqrs)	ABP	EEG	EOG	EMG	Voting (gqrs/SSF-TKE)
100	693	0.02	12.75	7.81			0.05
101	797	0.02	3.42	11.64			0.10
102	685	0.96	0.06	4.11			0.07
103	707	0.17	0.09	7.99	9.56	13.78	0.21
104	720	0.02	1.17	9.42			0.05
105	724	0.03	2.04	11.49			0.07
106	888	1.99	1.31	14.73	11.87	22.02	0.17
107	757	2.99	1.60	12.76			1.34
108	907	0.06	0.21	12.06	14.80	17.22	0.09
109	655	1.32	0.91	12.19			0.05
110	735	1.10	0.11	8.18			1.12
111	690	0.64	0.85	6.39	2.32	4.46	1.05
112	707	19.52	0.86	7.40	2.69	6.95	0.14
113	665	4.98	27.90	9.16	8.24	10.86	0.16
114	631	0.95	2.77	2.12			0.08
115	648	0.03	0.11	13.46			0.21
116	169	0.14	0.56	26.87			0.13
117	868	1.24	5.51	17.73	11.93	16.79	0.17
118	551	0.04	5.47	17.11	14.73	15.66	0.06
119	741	0.56	0.09	3.03	1.07	1.76	0.12
120	722	0.02	1.38	9.42			0.09
121	883	0.06	0.23	13.40	17.35	20.31	0.14
122	631	1.84	3.75	4.88			0.18
123	734	0.04	0.08	1.71	1.21	1.11	0.07
124	787	18.08	8.70	11.20	5.81	9.36	0.25
125	721	0.03	0.07	6.26			0.03
126	635	0.05	0.04	10.54	10.13	9.96	0.07

127	738	1.09	1.42	10.10			0.22
128	800	0.02	0.10	9.72			0.03
129	685	0.01	0.10	7.55			0.07
130	838	0.17	1.07	7.04			0.27
131	693	12.08	37.32	9.47			0.24
132	869	1.81	3.52	12.43	7.34	16.67	0.15
133	792	26.66	2.76	14.22			1.89
134	757	0.84	0.10	7.55			0.09
135	661	0.07	0.14	8.97			0.09
136	695	0.02	0.06	6.66			0.03
137	728	0.02	0.08	7.34			0.09
138	740	0.05	1.25	9.40	4.54	5.16	0.06
139	601	0.65	1.07	12.33			0.64
140	715	0.82	0.09	13.96			0.82
141	702	0.02	0.10	4.19			0.04
142	600	0.02	0.53	11.95			0.02
143	920	1.50	2.94	9.55	13.36	16.23	0.10
144	527	0.98	0.21	9.24	0.38	8.81	0.99
145	708	1.15	2.99	3.31	7.99	9.94	0.04
146	794	22.53	0.08	9.22	6.20	7.99	0.15
147	872	0.17	0.12	5.33			0.26
148	728	18.26	0.06	10.59			0.08
149	727	0.04	1.46	1.61	5.97	4.98	0.07
150	811	0.04	1.06	12.35			0.04
151	806	0.09	0.85	8.43			0.09
152	595	0.02	0.32	14.02			0.01
153	566	3.80	7.90	15.21	12.96	12.18	1.04
154	920	5.20	11.88	14.30			0.45
155	745	0.20	0.09	8.91	3.34	7.99	0.28
156	882	8.88	1.74	19.58			0.08
157	717	0.06	0.08	11.70			0.11
158	838	1.12	0.15	11.33			1.16
159	710	0.75	0.07	3.39			0.10
160	659	2.34	0.13	5.43			2.49

161	670	0.05	0.05	9.48	6.55	5.23	0.12
162	690	0.03	3.49	8.77	6.56	8.75	0.09
163	884	0.06	0.24	10.82	14.51	16.54	0.15
164	872	1.09	0.93	6.83	9.49	13.31	0.12
165	646	1.39	0.10	10.43			1.42
166	684	2.53	2.48	12.08			0.21
167	736	0.55	0.07	6.42			0.03
168	860	15.68	0.90	18.77			0.08
169	785	30.39	0.14	13.25			0.25
170	738	0.02	0.07	5.51			0.02
171	665	0.04	0.10	12.49			0.17
172	880	8.65	0.85	14.98			2.24
173	728	1.04	0.11	9.82			1.04
174	805	0.05	0.12	11.03			0.08
175	723	6.24	0.09	11.35	2.30	8.44	0.28
176	688	2.45	2.31	8.35	6.18	9.12	0.17
177	689	6.92	2.20	7.80	7.30	8.25	1.88
178	774	1.25	0.73	7.57	2.06	4.45	0.08
179	861	0.07	8.56	15.44	14.08	17.41	0.14
180	884	4.02	1.31	10.96			1.11
181	655	0.02	0.05	9.89	4.838	9.14	0.04
182	791	0.07	0.05	6.16	7.73	4.93	0.07
183	697	0.03	0.52	6.93	1.40	6.13	0.03
184	602	0.08	1.56	13.66	12.65	15.89	0.08
185	729	0.46	0.08	6.60			0.13
186	726	0.01	0.73	5.48			0.03
187	592	1.06	0.05	14.04	14.41	15.27	0.05
188	841	35.10	1.67	13.88			1.58
189	721	20.01	0.96	7.83	6.37	7.55	0.34
190	698	4.28	0.05	7.48	4.69	9.16	0.10
191	460	5.68	0.13	10.06			0.15
192	721	4.14	0.44	6.32			0.04
193	597	0.02	0.77	4.38			0.05
194	841	0.04	1.45	24.34			0.09

195	717	2.93	0.11	11.55			1.47
196	527	0.73	1.96	13.22			0.74
197	681	0.54	16.28	1.80	7.19	9.87	0.56
198	699	19.71	0.96	8.26	3.53	9.61	0.14
199	666	0.04	1.01	6.35			0.04
1020	600	5.10	0.57	13.42			0.07
1023	635	0.05	0.04	10.54	10.13	9.96	0.07
1032	799	0.16	4.40	19.38			0.74
1069	738	0.02	1.24	10.18			0.06
1073	602	0.08	1.56	13.66	12.98	15.89	0.08
1503	751	19.79	3.22	10.54	7.25	9.68	0.25
2283	784	68.29	10.88	25.43			4.87
2527	701	17.55	0.12	14.12	8.42	8.87	0.11
2800	752	41.87	16.78	13.41			4.02
3188	822	39.78	14.76	18.16			1.48
Total	79597						
Average HR rMSE (bpm)		4.90	2.46	10.35	7.83	10.54	0.42

Table A.17: HR estimation performance of majority voting fusion method with combination of QRS detectors on MIT-BIH Polysomnographic database

Signal No.	Total number of beats	HR (rMSE)							
		ECG (gqrs)	ABP	EEG	EOG	EMG	Voting (gqrs/SSF-TKE)	Voting (epltd/SSF-TKE)	Voting (gqrs/epltd)
slp 01a	7806	0.57	1.02	2.82			0.56	0.07	0.45
slp 01b	11467	1.00	4.57	5.07			0.67	1.84	2.19
slp 02a	16145	4.65	5.90	9.79			3.14	0.88	2.66
slp02b	11317	6.78	4.33	12.90			4.56	1.74	1.54
slp 03	24917	4.28	2.11	10.79			1.23	1.67	2.71
slp 04	27029	6.57	4.18	11.13			1.27	1.01	0.92
slp 14	22920	2.07	6.98	12.17			1.77	0.83	2.27
slp 16	27604	7.20	1.98	14.83			1.68	0.84	1.39
slp 32	21718	5.08	1.30	10.70	6.71	9.98	1.01	0.48	0.71
slp 37	30611	1.78	3.69	13.85	14.59	17.33	0.49	0.41	0.36
slp 41	25884	1.44	7.62	9.80	8.61	9.11	0.75	0.45	0.96
slp 45	27686	3.12	1.28	7.75	4.78	5.90	0.77	0.56	0.83
slp 48	24711	1.91	1.13	10.73	9.00	11.70	0.28	0.24	0.52
slp 59	16901	0.12	1.84	10.81			0.20	0.16	0.05
slp 60	25017	0.25	1.82	22.34			0.51	0.54	0.51
slp 61	25482	0.53	1.35	11.86			0.63	0.35	0.39
slp 66	15775	0.01	1.34	8.26			0.11	0.24	0.05
slp 67x	5374	0.02	0.85	8.37			0.19	0.06	0.05
Total	368364								
Average HR rMSE (bpm)		2.63	2.96	10.78	8.74	10.80	1.10	0.69	1.03

Appendix B

Results From the 2014 Challenge

RESULTS FROM THE 2014 CHALLENGE

- * User Home
- Login / Create an Account
- * Works in Progress
- PhysioNetWorks Project Guide
- Data Sharing
- PhysioNetWorks Help
- About PhysioNetWorks

TOP RESULTS

Overall score	Participant	Entry
93.64	urska.pangerc	420
92.24	sachinvernekar50	407
91.54	shalinirankawat	470
91.50	alistairewj	425
90.80	joachim.behar	413
90.70	hoog.antink	407
90.02	thomas.decooman	420
89.73	lj	405
89.55	marcus.vollmer	402
88.85	abbasatyabi	428
88.66	quan.ding	458
88.57	bschandra	402
88.34	krug.johannes	402
88.07	podziemski	403
87.50	shalinirankawat	403
87.38	[sample entry in Octave]	405

On this page:
- Top results

Figure B.1: Snapshot of PhysioNet website showing results from the 2014 challenge on 29-12-2016

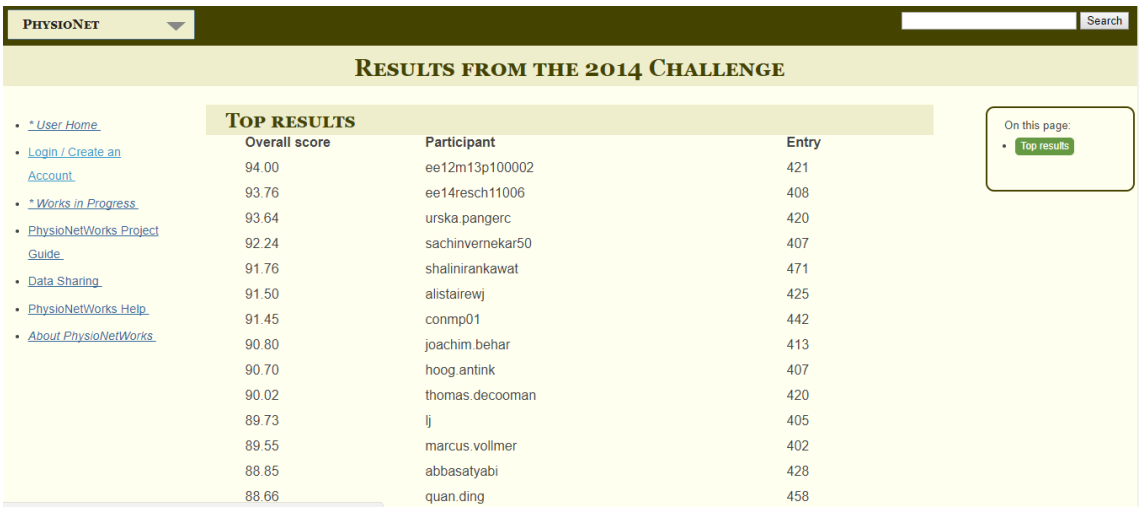

PHYSIONET

Search

RESULTS FROM THE 2014 CHALLENGE

- * User Home
- Login / Create an Account
- * Works in Progress
- PhysioNetWorks Project Guide
- Data Sharing
- PhysioNetWorks Help
- About PhysioNetWorks

TOP RESULTS

Overall score	Participant	Entry
94.00	ee12m13p100002	421
93.76	ee14resch11006	408
93.64	urska.pangerc	420
92.24	sachinvernekar50	407
91.76	shalinirankawat	471
91.50	alistairewj	425
91.45	conmp01	442
90.80	joachim.behar	413
90.70	hoog.antink	407
90.02	thomas.decooman	420
89.73	lj	405
89.55	marcus.vollmer	402
88.85	abbasatyabi	428
88.66	quan.ding	458

On this page:
- Top results

Figure B.2: Snapshot of PhysioNet website showing results from the 2014 challenge on 14-08-2017